Ground vibration measurements with special reference to pile driving

Uromeihy, Ali

Volume Two

Chapter Six
6. Data Analyses and Discussions

6.1 Introduction

In the preceding chapter, a number of ground vibration records which were taken from various sites were displayed and information about the site conditions and the vibration levels was given. Here, the main consideration is focused on the analysis techniques that can be employed to predict, describe and control the effects of ground vibration caused by civil engineering construction, mainly those associated with pile driving activities. Although the vibration from such construction sources has a temporary duration, the disturbance may result in permanent damage to nearby structures and in nuisance to the local population.

Different methods used in the prediction of the ground vibration are discussed in section (6.2). The methods include the inverse linear relation between the distance and the recorded velocity, and the non-uniform distribution of wave generation around the pile-toe. A method is also proposed based on the calculation of arrival time of body and surface waves at a vibration detector. The effect of different variables on the ground vibration attenuation is discussed in section (6.3). These variables include the magnitude of the input energy, the radial and the horizontal distance of the vibration detector from the source, the depth of the pile-toe and the conditions of the ground.

Use of the hemispherical projection in presenting and appraising the ground vibration records is explained in section (6.4). This method is used to present in a two dimensional plane the three dimensional information on ground vibrations taken along three orthogonal axes. The effect of ground vibration components with respect to the orientation of a building is discussed in section (6.5). Some information about the classification of the vibration records using a data-base program is given in section (6.6) and finally some conclusions obtained from this chapter are included in section (6.7).

6.2 Methods of Evaluation of the Vibration Amplitude

The amplitude of the ground vibration is controlled by a number of factors such as the source of vibration, the ground conditions and the distance of the detector from the source. In the case of pile driving activity, the source of vibration is defined by the magnitude of the input energy, by the driving hammer and the type of the driven pile with respect to its length, weight and dimensions. The geological conditions of the ground and the horizontal and the radial distance from the source are also main variables in the evaluation of ground vibration amplitude.

Some of the methods used in the prediction of vibration amplitude and attenuation are reviewed and others are suggested in the following sections.

6.2.1 Method (1)

The simplest estimate of attenuation is based on an inverse linear relation between the level of vibration and distance from the source. In an elastic half-space, the *body-waves* propagate radially outward from an assumed point source along a spherical wave front while a *Rayleigh-style surface wave* propagates radially outwards along a shallow cylindrical wave front. The density of the input energy decreases with distance in each wave front due to the radial expansion from the source. This dilution of energy is called *geometrical damping*. It has been shown (for example, Richart, Hall & Woods (1970) and Das (1983)) that the amplitude of the body waves and surface waves decreases in proportion to the ratio of $1/r$ and $1/\sqrt{r}$, respectively.

Attewell (1985) suggested that the amplitude of the vibration at ground surface is mainly affected by the propagation of the waves from the shaft and from the toe of a pile. As shown in figure (6.1), the energy generated along the pile shaft propagates radially outwards producing a cylindrical wave front♣ around the pile, while the energy transmitted from the pile-toe propagates radially outwards in sensibly spherical wave fronts. He also analysed the development of the dynamic energies

---

♣ This wave front actually has an inverted conical form as described in section (2.6.3), but in this report (Attewell 1985), it was assumed to be cylindrical due to the steepness of the conical surface, the inclination of which is a function of the relative wave velocities in steel and soil.

introduced in the pile-soil system after each hammer blow as follows:

W_o : the notional input energy of the hammer/blow

W_i : the actual input energy of the hammer/blow

W_{fv} : the shaft vertical friction wave energy

W_{fh} : the shaft flexural (whip) wave energy

W_{sv} : the vertical shear wave energy at pile-toe

W_{ps} : the combined spherical body and shear waves at the pile toe

W_w : the energy used in pile penetration

W_r : the energy reflected in the pile from its toe

The actual energy W_i introduced to the pile by the hammer at impact can be related to the nominal input energy W_o of the hammer by the following expression

$$W_i = kW_o$$

where k is the fraction of W_o going to W_i.

The actual input energy is approximately the sum of the energies mentioned above

$$W_i = W_{fv} + W_{fh} + W_{sv} + W_{ps} + W_w + W_r$$

By a process of analysis he derived an equation for evaluating the amplitude of the shaft-generated shear waves as a function of transmission distance, taking account of energy densities reduction in the wavefront as a result of geometrical divergence:

$$\frac{v_n}{v_1} = \frac{\sqrt{r_1}}{\sqrt{r_n}}. \tag{6.1}$$

The following equation may be used to evaluate the amplitude of the body-waves:

$$\frac{v_n}{v_1} = \frac{r_1}{r_n} \tag{6.2}$$

where v_1 and v_n are the vibration amplitudes (in term of peak particle velocity) at stand-offs r_1 and r_n, respectively.

In addition, the amplitude of the ground vibration will also be affected by frictional ground losses. This form of attenuation is known as *material damping.* The variables which control the ground material losses include the degree of saturation, density and particle size distribution. Bornitz (1931)† combined the effect of geometrical and material damping and introduced the following equation for the calculation of the vibration amplitude at the ground surface.

$$\frac{v_n}{v_1} = \frac{\sqrt{r_1}}{\sqrt{r_n}} exp[-\beta(r_n - r_1)] \tag{6.3}$$

where β is the material damping coefficient. Typical values are presented in table (T6-1).

Table (T6-1)

Values of *absorption coefficient* (β)

No	Soil type	$\beta(m^{-1})$
1	Saturated fine grained sand	0.10
2	Saturated fine grained sand in a frozen state	0.06
3	Saturated sand with laminae of peat and organic silt	0.04
4	Clayey sands with laminae of sand and silt above water level	0.04
5	Heavy water saturated brown clays with some sand silt	0.04-0.12
6	Marly chalk	0.10
7	Loess and loessal soil	0.10

The above table shows that the material damping values are in the range of 0.04 to $0.1m^{-1}$. Attewell & Farmer (1976) suggested that in the case of the lower values, the vibration attenuation due to material damping is insignificant compared with the geometrical losses. Even in the case of organic clay with a higher value of $\beta = 0.2m^{-1}$, material damping is only of the order of 20% of geometrical damping.

Finally, a reduction in the amplitude of the vibration may be caused by *structural geological damping.* Attention should be given to a study of the structure of the

† See Das (1983)

ground and in particular the presence of faults, cracks and gaps in the soil or rock and to ground strata having different acoustic impedance zones which control the reflection and refraction of waves in the soil media.

6.2.2 Method (2)

Another technique of prediction was proposed by Selby (1986). The idea was based on the suggestion of non-uniform distribution of the energy transmitted to the surrounding soil around the pile-toe during pile driving. Figure (6.2) shows maximum and minimum concentrations of energy vertically below and above the pile-toe. Consequently, the amplitude of surface vibration recorded at locations close to the pile may be less than that recorded at some distance. This argument is mainly proposed to explain the behaviour of the radial-wave records which in many cases showed some increase in magnitude with horizontal distance from the pile and then decreased as the distance increased.

The following equation was introduced as a modification of Eq(6.2).

$$v_n = v_1 \alpha . exp[-\beta r_n/2] . \frac{\sqrt{4\pi r_1^2}}{\sqrt{4\pi r_n^2}}$$

The above equation can also be written as:

$$\frac{v_n}{v_1} = \frac{r_1}{r_n} \alpha . exp[-\beta r_n/2] \qquad (6.3)$$

where $\alpha = \sqrt{sin(\theta/2)}$

θ = the expansion angle (see figure (6.2))

$$tan\theta = \frac{\text{horizontal distance}}{\text{toe-depth}} \quad .$$

This equation may be used to calculate the level of the ground vibration at any radial distance from the pile. In the example below, the level of ground surface vibration (v_n) is calculated and compared to the measured vibration taken at **Blaydon**. The pile had penetrated 20m into the ground and the geophone sets were located 4, 8, 17, 27 & 37m from the pile. The site information, vibration results and

the calculation based on equation (6.3) are shown in table (T6-2). Also, the data of the above example is plotted, for comparison, in figure (6.3). It is assumed that $\beta = 0.1$, $r_1 = 1.0m$ and $v_1 = 2000mm/s$[Θ].

Table (T6-2)

Calculation of ppv at the ground surface, using method-2

Date	Site	File
28.06.1988	Blaydon	BLN2
Pile		
Type	Size	Depth
H-pile	356 × 368 × 152kg/m	20.0m
Hammer		
Weight	Type & Model	Drop-height
5000kg	Hydraulic-hammer (BSP357)	800mm

x	r_n	θ	$\sqrt{sin(\theta/2)}$	$exp[-\beta r_n/2]$	r_1/r_n	$v_n(mm/s)$	
m	m	deg.				Calculated	Measured
4	20.39	11.31	0.314	0.361	0.049	11.11	9.36
8	21.54	21.80	0.435	0.341	0.046	13.65	11.15
17	26.25	40.36	0.587	0.269	0.038	12.00	14.48
27	33.60	53.47	0.671	0.186	0.029	7.24	4.69
37	42.06	61.60	0.716	0.122	0.024	4.19	3.40

The above example should not be treated as a serious technique for estimation of particle velocity at the ground surface but rather as a possible way to explain the phenomenon of some of the vibration plots, and in particular the frequently observed maximum ppv at some 12-15m from the pile.

Θ The assumption of the v_1 is based on the measurements of strain in a steel pile during driving (see section 7.7.6) which gives a typical value of $400\mu\epsilon$, and with wave velocity c of $5000m/s$, an estimate value of particle velocity in the steel pile of $ppv = \epsilon \times c = 2000mm/s$ is used.

6.2.3 Method (3)

Another method is proposed in this section for the evaluation of the ground vibration at different stations from the driven pile. This method is based on the calculation of the arrival time of the wave-fronts, at different stations on the ground surface, from the shaft and from the toe of the pile (see figure (6.4)). When these two arrival times coincide, a maximum vibration level may be expected at that position. This method is useful for explaining the vibration records measured in the radial direction, but could be modified and could be applied to other senses of vibration. Four records of vibration taken at different sites are examined in the following sections with satisfactory conclusions. The following procedures should be followed in the calculation:

1. **Calculation of the P-wave**

Calculation of the **P-wave** velocity in the ground can be achieved from the time history records of the vibration data. Diagrams which display five sets of data recorded simultaneously at five different stations from the pile are more useful in this calculation since the occurrence of the peak particle velocity at two different stations can easily be picked up. Examples of such diagrams were shown in the previous chapter.

To calculate the **P-wave** velocity, the arrival time of the wave at station one and at station two should be calculated (see figure (6.4)):

$$t_1 - t_0 = \frac{r_1}{c_p} \tag{6.4}$$

$$t_2 - t_0 = \frac{r_2}{c_p} \tag{6.5}$$

Subtract Eq(6.4) from Eq(6.5), then the calculation of c_p can be obtained from the following equation:

$$t_2 - t_1 = \frac{(r_2 - r_1)}{c_p}$$

or

$$c_p = \frac{(r_2 - r_1)}{(t_2 - t_1)} \tag{6.6}$$

where c_p : velocity of the P-wave in the ground

t_0 : transmission time of the waves from pile to ground

t_1 : arrival time of the P-wave at station one

t_2 : arrival time of the P-wave at station two

r_1 : radial distance between station one and pile-toe

r_2 : radial distance between station two and pile-toe

2. Calculation of the Surface-wave

Since the velocity of the P-wave in the ground is approximately twice as fast as that of the surface-wave (*Attewell and Farmer, 1973*), it is considered in the following calculations that $c_r = \frac{1}{2}c_p$, where c_r is the velocity of the surface-wave.

3. Measurements of x and r

The measurement of the horizontal and the radial distances of a vibration detected at the ground surface is needed for the calculation of the arrival time of the surface-wave and the p-wave at that particular station, respectively.

The horizontal distance (x) of the geophone from the location of the pile is usually measured on the site.

The radial distance (r) of the geophones from the pile-toe can be calculated by:

$$r = \sqrt{x^2 + d^2}$$

where d is the depth of the pile-toe from the ground surface.

4. Calculation of the arrival time

The arrival time of the wave-front of the surface-wave and of the body-wave at the ground surface can be obtained from the following equations:

$$t_r = \frac{x}{c_r} \tag{6.8}$$

and

$$t_p = \frac{r}{c_p} + \frac{d}{c_s} \tag{6.9}$$

where t_p : arrival of P-wave at a specified station

t_r : arrival of surface-wave at the same station

c_s : velocity of a P-wave in a steel pile($c_s = 5000m/s$)

d : depth of the pile-toe.

6. Discussion and analysis

The calculated figures can then be tabulated or plotted on diagrams for an easy comparison of the arrival time of both waves at different stations. When these arrival times coincide at an specified point, then this shows the highest level of vibration.

Example (1)

Consider the ground vibration record taken from a site in Blaydon during the driving of a 25m long steel H-pile by a 5000kg hydraulic-hammer. The vibration amplitudes as a function of time for all fifteen channels were presented in figure (5.22). The figure showed some increment in radial wave magnitudes as the distance from the pile location increased (for example, a maximum ppv of 14.48mm/s was recorded at 17m stand-off distance from the pile), and then decreased at further distance. The above method of analysis was used to interpret this form of attenuation.

First the P-wave velocity in the ground was calculated from the traces recorded by geophone-sets A & C at horizontal distances of 4m and 37m from the pile, respectively.

$$\textit{velocity of P-wave} \quad c_p = \frac{r_2 - r_1}{t_2 - t_1} = \frac{42 - 20}{0.225 - 0.06} = 134m/s$$

$$\textit{velocity of the surface wave is} \quad c_r = c_p/2 = 67m/s.$$

The arrival times of the wave-fronts at station three which was located some 17m from the pile are:

$$t_p = \frac{26.2}{134} + \frac{20}{5000} = 0.156sec$$

$$t_r = 17 \div 67 = 0.25sec.$$

A similar procedure is followed for the calculation of arrival time of the wave-fronts at different stations. The results are listed in table (T6-3). The table also includes other relevant information about the site, pile, and hammer.

Figure (6.5) displays plots of the field measurement of the radial ppv and the calculated arrival times of the waves with respect to geophone stand-off. From the above table and the figure a maximum particle velocity could be expected at a horizontal distance of 12m from the pile where the arrival of the wave-fronts from the shaft and from the toe coincide. By comparing the above calculation of time-dependent arrivals with the records taken from the site, quite close agreement can be found.

Example (2)

A site at Keighley is selected to reinforce the above suggestion for predicting the attenuation of the induced vibration in the ground. Measurements of the ground vibration were recorded during the operation of a three tonne hydraulic-hammer driving a steel H-pile 32m into the ground. Five sets of vibration records taken in the radial direction were displayed in figure (5.50b). From the figure, the approximate value of the body-wave velocity $c_p \approx 422m/s$, and the surface-wave velocity $c_r \approx 211m/s$ was calculated. The calculation of the arrival time for the wave fronts from the toe and the pile shaft, together with information on the site are shown in table (T6-4). The above calculations are graphically plotted in figure (6.6). Referring to the figure and the table, a highest level of vibration could be expected at 12m horizontal distance from the pile.

Example (3)

Another set of ground vibration records from the Keighley site is examined below. Records of radial waves taken simultaneously at five different stations were displayed in figure (5.55b). The records were taken during the driving of a steel H-pile 15m into the ground by a diesel-hammer(DE50c). The velocity of the wave propagation is calculated from the figure and gives an approximate value of $c_p =$

$96m/s$ and $c_r = c_p/2 = 48m/s$. Site information and the calculation of the time arrival of the body and the surface waves at different stations are listed in table (T6-5). Graphical presentation of these calculations is shown in figure (6.7). In this example, the highest level of vibration is expected at about 10m from the pile position.

Example (4)

A data file taken in St.Annes is examined in this example. The data were recorded during the driving of 15m long sheet-piles using a seven tonne hydraulic-hammer. An example of radial waves recorded at five stations was displayed in figure (5.88b). An approximate calculation of the wave velocity of $c_p \approx 120m/s$ was calculated from the above figure. This gives the surface velocity of $c_r \approx 60m/s$. The calculation of arrival time of the waves at the location of different geophones together with the site information is listed in table (T6-6). The plot of radial ppv with respect to geophone stand-off and the plot of the time arrival at the geophone location are shown in figure (6.8). The table and the figure suggest a maximum vibration amplitude at some 8m horizontal distance from the pile.

Table (T6-3)

Calculation of arrival time, example one

Date	Site	File
28.06.1988	Blaydon	BLN2
Pile		
Type	Size	Depth
H-pile	356 × 368 × 152kg/m	20.0m
Hammer		
Weight	Type & Model	Drop-height
5000kg	Hydraulic-hammer (BSP357)	800mm

Geophone set	Distance		Arrival Time		Vibration Records
	horizontal (x) m	radial (r) m	$t_r = x/c_r$ sec	$t_p = r/c_p$ sec	mm/s
A	4.0	20.39	0.060	0.156	9.36
B	8.0	21.54	0.119	0.165	11.15
D	17.0	26.25	0.254	0.199	14.48
E	27.0	33.60	0.403	0.255	4.69
C	37.0	42.06	0.552	0.318	3.49

Table (T6-4)

Calculation of arrival time, example two

Date	Site	File
02.03.1987	Keighley	ELY4
Pile		
Type	Size	Depth
H-pile	305 × 305 × 126kg/m	32.0m
Hammer		
Weight	Type & Model	Drop-height
3000kg	Hydraulic-hammer (BSP357)	800mm

Geophone set	Distance		Arrival Time		Vibration records
	horizontal (x) m	radial (r) m	$t_r = x/c_r$ sec	$t_p = r/c_p$ sec	mm/s
A	4.0	20.39	0.025	0.055	10.35
B	7.0	21.19	0.039	0.057	10.51
C	10.0	22.36	0.054	0.059	10.95
D	15.0	25.00	0.077	0.066	9.92
E	20.0	28.28	0.101	0.073	8.99

Table (T6-5)

Calculation of arrival time, example three

Date	Site	File
21.05.1987	Keighley	KDH4
Pile		
Type	Size	Depth
H-pile	356 × 368 × 134kg/m	15.0m
Hammer		
Energy/blow	Type & Model	Strike-rate
61.0kJ	Diesel-hammer (BSP-DE50c)	47 bl/min

Geophone set	Distance		Arrival Time		Vibration Records
	horizontal (x) m	radial (r) m	$t_r = x/c_r$ sec	$t_p = r/c_p$ sec	mm/s
A	2.0	15.13	0.042	0.161	10.08
B	5.0	15.81	0.104	0.168	7.04
C	7.0	16.55	0.146	0.175	7.33
D	11.0	18.60	0.226	0.197	10.51
E	15.0	21.21	0.312	0.224	9.93

Table (T6-6)

Calculation of arrival time, example four

Date	Site	File
01.12.1987	St.Annes	ANS-12
Pile		
Type	Size	Depth
Sheet-pile	Larssen(32W)	10.65m
Hammer		
Weight	Type & Model	Drop-height
7000kg	Hydraulic(BSP.357)	800mm

Geophone set	Distance		Arrival Time		Vibration Records
	horizontal (x) m	radial (r) m	$t_r = x/c_r$ sec	$t_p = r/c_p$ sec	mm/s
A	2.0	12.81	0.034	0.092	21.78
B	5.0	13.60	0.083	0.100	16.44
C	8.0	14.97	0.134	0.113	22.21
D	12.0	17.44	0.200	0.136	10.01
E	18.0	22.00	0.300	0.176	5.12

6.3 Analysis of Ground Vibration Attenuation

The magnitude of the vibration at a given distance is a function of the energy at the source. This principle is adopted and used for estimating the amplitude of ground vibration at any distance from the source (see, for example, Attewell & Farmer, 1973 and Wiss, 1981). The relationship between the three main variables may be expressed as

$$v = kW_o{}^{\alpha} r^{\beta} \tag{6.5}$$

where	v	: peak particle velocity	mm/s
	W_o	: input energy in joules	N.m
	r	: distance from source	m
	k, α, β	: constants related to the site conditions.	

The most commonly used forms of the above equation are broadly expressed as

square root scaling

$$v = k\left(\frac{r}{W_o{}^{\frac{1}{2}}}\right)^{-n} \tag{6.6}$$

cube root scaling

$$v = k\left(\frac{r}{W_o{}^{\frac{1}{3}}}\right)^{-n} \tag{6.7}$$

where k and n are empirical constants. The above equations allow simple graphical presentation of the field data as a straight line on a log-log plot using a linear regression analysis of the given data, where k defines the intercept (mm/s) and $-n$ defines the gradient of the line. It is noted that the dimensional balance of the above equations is satisfied only if a force unit (eg. kN) rather than an energy unit (eg kN.m) is used. This is why these prediction equations are used in connection with blasting, where W defines the weight of explosive. Nevertheless, for this thesis it is necessary to use the energy parameter for pile driving.

Many independent variables also have some influence in controlling the ground vibration. These include the density ρ and the wave velocity c of the transmission medium. However, the variations of density and wave velocity for different types of soils and rocks are relatively small in comparison to the variation of W_o and r, and their effects are usually neglected (Dowding (1985)).

Based on field measurements of civil engineering vibration, Attewell and Farmer (1973) obtained the following relations to predict the amplitude of ground vibration for the best fit and upper bound line, respectively:

$$v = 0.76\left(\frac{\sqrt{W_o}}{r}\right)^{0.87} \quad and \quad v = 1.5\left(\frac{\sqrt{W_o}}{r}\right) \tag{6.8}$$

where W_o in J, r in m and v in mm/s. These equations can be rewritten as follows:

$$v = 15\left(\frac{r}{\sqrt{W_o}}\right)^{-0.87} \quad and \quad v = 42\left(\frac{r}{\sqrt{W_o}}\right)^{-1} \tag{6.9}$$

where W_o in kJ, r in m and v in mm/s. The above attenuation equations are widely used in predicting the amplitude of the ground vibration from civil engineering activities, particularly those associated with pile driving.

6.3.1 Regression Analysis of Vibration Records

Several groups of the site records were analysed using the general square root scaling equation† $v = k(r/\sqrt{W_o})^{-n}$, where r is the direct transmission distance measured from the pile-toe to geophone position on the ground surface, W_o is the manufacturer's figure of the hammer notional input energy⊕ (where W_o (kJ)=ram weight (kN) × drop height(m)), and the values of the empirical constant k (the ordinate intercept mm/s) and n (the slope) are dependent on the conditions of the site, such as type of hammer, type of pile, the ground conditions and the distance of recording equipment from the source. Although in practice the above equation will not give the best prediction of the vibration amplitude because of the presence of a number of factors, for example, the variation at the ground conditions in different depths and the complicated mechanism of wave transmission, it is the most widely used equation for the prediction of vibration attenuation.

---

† It has been suggested that the square root equation in the form of Eq.(6.9) should be used for graphical presentation since the magnitude of $r/\sqrt{W_o}$ increases with reduction of ppv amplitudes as the distance from the source increases (negative slope regression line), and that the form of Eq.(6.8) (positive slope regression line) be used for vibration prediction (see New (1984)).

⊕ The nominal energy has been used throughout the following sections as W_o since reliable estimate of energy transferred into the pile can be made.

6.3.1.1 Vibrodriver

Vibrodrivers are widely used for driving different types of piles in granular ground. A study of the ground vibrations recorded during the operation of this type of hammer shows different forms of attenuation according to the type of driven pile and the depth of toe penetration.

a. Vibrodriver, End-bearing Piles

Figures (6.9a) and (6.9b) show the least squares regression analyses of ground vibration records for toe depths of less than and greater than five metres, respectively. Because the data were taken from several sites having different environmental conditions, each record is analysed individually. The attenuation equations of each line are included on the figures and are listed in the table below.

toe-depth less than 5m					
file name	HOW-5	RAK-7	RIV-7	KVH-1	FV-6
equations	$v = 46.6\left(\frac{r}{\sqrt{W}}\right)^{-1.8}$	$v = 19.4\left(\frac{r}{\sqrt{W}}\right)^{-2.0}$	$v = 143\left(\frac{r}{\sqrt{W}}\right)^{-1.8}$	$v = 26.1\left(\frac{r}{\sqrt{W}}\right)^{-1.5}$	$v = 247\left(\frac{r}{\sqrt{W}}\right)^{-1.9}$
Corr.Coef	r=-0.97	r=-0.96	r=-0.98	r=-0.99	r=-0.95
toe-depth greater than 5m					
file name	HOW-13	RAK-11	RIV-10	KVH-5	FV-3
equations	$v = 17318\left(\frac{r}{\sqrt{W}}\right)^{-5.1}$	$v = 897\left(\frac{r}{\sqrt{W}}\right)^{-3.5}$	$v = 2388\left(\frac{r}{\sqrt{W}}\right)^{-2.9}$	$v = 1189\left(\frac{r}{\sqrt{W}}\right)^{-3.7}$	$v = 229\left(\frac{r}{\sqrt{W}}\right)^{-1.5}$
Corr.Coef	r=-0.97	r=-0.80	r=-0.96	r=-0.96	r=-0.86

The figures show that the attenuation of vibration for shallower toe-depths is less than that for deeper penetration. The average gradients of the attenuation line for figures (6.9a) and (6.9b) are -60° and -70°, respectively.

b. Vibrodriver, sheet piles

The ground vibration data recorded during the driving of sheet piles using a vibrodriver has been analysed with respect to pile toe-depth less than and greater than 5m. The plots are displayed in figures (6.10a) and (6.10b), respectively. For

the shallower toe-depths, the use of standard and a high frequency vibrodriver[⊘] showed two forms of attenuation lines defined by the following equations:

toe-depth less than 5m, standard vibrodriver

$$v = 53\left(\frac{r}{\sqrt{W_o}}\right)^{-2.01}$$

toe-depth less than 5m, high frequency vibrodriver

$$v = 280\left(\frac{r}{\sqrt{W_o}}\right)^{-2.11}$$

Finally, the attenuation equation for greater toe-depths is:

toe-depth greater than 5m

$$v = 106\left(\frac{r}{\sqrt{W_o}}\right)^{-1.99}$$

The correlation coefficients (r) of the above equations are r=-0.95, r=-0.91 and r=-0.87, respectively. The figures show similar attenuation lines for different depths of penetration, with gradients of -63° to -65°.

A comparison of the above records shows that the vibration attenuation during the operation of vibrodrivers in driving end-bearing piles is greater than when driving sheet-piles and is greater for deeper penetration than for shallower toe-depths.

6.3.1.2 Diesel-hammer, H-pile Records

Several sets of ground vibration data recorded during the operation of diesel-hammers were analysed by least squares regression. The form of vibration attenuation varied according to the depth of pile penetration. An example of an attenuation line of four records taken in Sheffield for depths less than ten metres is shown in figure (6.11a). The general equation of the line is:

$$v = 21\left(\frac{r}{W_o}\right)^{-1.85}$$

The best fit line has a slope of $-62°$ and a correlation coefficient of r = -0.896.

⊘ The operational frequencies of standard and high frequency vibrodrivers are in the order of 25-35Hz and 40-60Hz, respectively (see table (T3-5)).

For a pile-toe depth of more than 15m, the attenuation line of the recorded data showed rather a complicated form. Thus, each set of the record is analysed separately, as shown in figure (6.11b). The correlation coefficients of these analyses are very small and so indicate a lack of correlation and unreliability of the constant in the equations. The derived attenuation equations and their correlation coefficients at different toe-depths are listed in the following table:

List of vibration attenuation equations *recorded from diesel-hammers, depth more than 15m*					
file name	FAR-7	DIS-11	DIS-4	RAK-17	KDH-13
depths	25.0m	23.0m	22.2m	17.0m	24.3m
equations	$v = 7.84\left(\frac{r}{\sqrt{W}}\right)^{-0.35}$	$v = 96\left(\frac{r}{\sqrt{W}}\right)^{-1.89}$	$v = 18.7\left(\frac{r}{\sqrt{W}}\right)^{-0.56}$	$v = 171\left(\frac{r}{\sqrt{W}}\right)^{-3.62}$	$v = 240\left(\frac{r}{\sqrt{W}}\right)^{-3.13}$
correl.co.	r=-0.69	r=-0.83	r=-0.39	r=-0.74	r=-0.40

The above table and the figure show that some of the attenuation lines, for example those belonging to files FAR-7 and DIS-4, have rather flat lines with an average gradient of -22^{o}. The other three sets showed much steeper lines with an average gradient of -68^{o}.

6.3.1.3 Air-hammer Records

Analyses of air-hammer records taken from five different sites are shown in figure (6.12). Referring to the figure, clear differences between two sets of records can be observed. The data recorded at St.Helens and Scarborough showed a great difference in amplitudes of vibration captured by geophones close to the pile as also did those at some distances, due mainly to the topography of the construction sites⊙. The regression analysis of the data recorded at remote distances from the piles at these two sites gives the general equation of attenuation as follows:

$$v = 3.82\left(\frac{r}{\sqrt{W_o}}\right)^{-1.02}$$

⊙ More information on the conditions of the above sites is given in sections 5.4.15 and 5.4.17, respectively.

Regression analyses of the other three records taken in Blaydon during the driving of H-section and sheet-piles is summarized in the following table:

Summary of attenuation equations recorded from air-hammers, differnt toe-depths			
File name	BAH-6	BSA-14	BSA-6
Depths	12.0m	7.2m	2.4m
Pile-type	H-pile	sheet-pile	sheet-pile
Equations	$v = 301\left(\frac{r}{\sqrt{W}}\right)^{-2.76}$	$v = 70\left(\frac{r}{\sqrt{W}}\right)^{-1.44}$	$v = 27\left(\frac{r}{\sqrt{W}}\right)^{-0.86}$
Slopes	$-70°$	$-55°$	$-41°$
Correl.Co.	r=-0.89	r=-0.96	r=-0.93

Referring to figure (6.12) and the above table it can be noted that the steepness of the best fit line increases with increase of toe-depth. This means that attenuation of the ground vibration caused by the operation of the air-hammer is more rapid for a deeply penetrated pile than for a shallower toe-depth.

6.3.1.4 Drop-hammer Records, Bearing-piles

Least squares regression analysis is used on a number of ground vibration records taken from the operation of a winch-drop-hammer during the driving of steel H-section and concrete piles. The plots of the data are shown in figure (6.13) together with file names and pile toe-depths. The general equation for the best fit line is :

$$v = 45\left(\frac{r}{\sqrt{W_o}}\right)^{-2.17}$$

The correlation coefficient of the above equation is r = -0.87 and the line has a gradient of $-65°$.

6.3.1.5 Impact-hammers, Sheet-pile

Examples of regression analyses of vibration records taken at different sites from impact-hammers of various types driving sheet-piles is displayed in figure (6.14). The line represents the regression analysis of four sets of data recorded in Edinburgh,

Waltham Cross and Grimsby. The geology of the ground at the depth of the pile-toe comprises silty clay deposits. The line has a correlation coefficient of r=-0.84, a gradient of -72^{o} and the following attenuation equation:

$$v = 113\left(\frac{r}{\sqrt{W_o}}\right)^{-3.14}.$$

The data recorded in St.Annes during the driving of sheet-piles in dense sand by a seven tonne hydraulic-hammer showed a shallower attenuation line, a correlation coefficient of r=-0.98 and a gradient of -53^{o}, as expressed in the following equation:

$$v = 31.66\left(\frac{r}{\sqrt{W_o}}\right)^{-1.33}$$

Referring to the records of the ground vibration measured at this site[⊘], the amplitude of the radial wave increased as the distance from the source increased and then attenuated with the increase of distance from the pile. An explanation was suggested for this form of attenuation in the previous section (see method three).

6.3.1.6 Hydraulic-hammer, H-pile

The attenuation of ground vibrations recorded from the driving of H-piles by hydraulic-hammer at two different sites in Blaydon and Keighley are analysed in the following sections:

a. Blaydon, H-pile, Hydraulic-hammer

Seven sets of vibration records taken at different sites are analaysed by least squares regression. A hydraulic-hammer (BSP-357, 5000kg) was the source of the input energy for driving steel H-section piles. The data are analysed with respect to the pile toe-depths and the plots of these analyses are shown in figure (6.15). A summary of the derived attenuation equations with other relevant information is listed in the following table:

⊘ See table (T5-64) for more information.

List of Attenuation Equations *Blaydon, H-pile, Hydraulic-hammers*				
file-name	depth	attenuation equations	Corr.Coe.	slope
BRH-5	33.0m	$v = 17042\left(\frac{r}{W_o}\right)^{-4.67}$	r=-0.89	-78^o
BHC-7	33.0m	$v = 8176759\left(\frac{r}{W_o}\right)^{-8.91}$	r=-0.92	-83^o
BHH-6	21.0m	$v = 114\left(\frac{r}{W_o}\right)^{-1.90}$	r=-0.74	-62^o
BLH-12	21.0m	$v = 900\left(\frac{r}{W_o}\right)^{-3.12}$	r=-0.95	-72^o
BLN-2	19.8m	$v = 401\left(\frac{r}{W_o}\right)^{-2.51}$	r=-0.93	-68^o
BLH-2	10.0m	$v = 22.77\left(\frac{r}{W_o}\right)^{-1.41}$	r=-0.99	-55^o
GHH-6	12.0m	$v = 21.6\left(\frac{r}{W_o}\right)^{-1.53}$	r=-0.99	-57^o

From the above table and figure (6.15), the following suggestion can be made:

1. The gradient of the attenuation line increased with an increase of toe-depths
2. At shallower pile-toe depths, the vibration attenuation occurs over a wide area around the pile, while for a deeper penetrated pile, a higher level of vibration was recorded around the location of the pile than at a remote distance.
3. As the soil resistance to driving increased with the increase of toe-depth, a higher level of vibration was recorded at ground surface and around the pile location. Attenuation was rapid with distance. This may be due to the eccentric movement of the upper part of the pile on impact in comparison to the rigid lower part. There is the generation of more surface wave energy around the pile and close to the ground surface.

b. Keighley, H-pile, Hydraulic-hammer

The plots of the data recorded in Keighley are displayed in figure (6.16). Because the depths of pile-toe for most of the plotted data were over 20m and only a very small variation in ppv amplitudes was recorded at the ground surface, most of the plots are concentrated in the centre of the diagram. Obviously, no best fit regression line could be drawn for these records.

6.3.1.7 Summary

A review of the ground vibration data discussed in the preceding sections indicates that as the density of granular soil and the stiffness of cohesive soil increases with depth the amplitude of vibration increases close to the pile, but the gradient of the attenuation line increases. This characteristic behaviour has been noticed in a number of records taken in different sites, for example, Blaydon, Keighley and Sheffield during driving different types of pile by different hammers. The gradients of the regression lines varied between -40° and -75° for toe-depths of 5m to 22m, respectively. The value of correlation coefficient indicating a less monotonic attenuation. Indeed, when driving piles with deep toe penetration into dense sand or stiff clay, the graphs of vibration against stand-off distance often showed a plateau, with maximum vibrations being recorded at some 10m-15m from the pile. In such cases, a linear regression of `log(v)` against `log(x)` gives a poor representation of behaviour, with low values of correlation coefficient. This behaviour was also observed when piling through very soft soil into very dense sand as in St.Annes and Whalley.

In comparison to Attewell and Farmer best fit line, the regression analysis of the ground vibration data presented in preceding sections showed relatively steeper attenuation gradients and the plotted data are concentrated above the line.

6.3.2 Discussion of the Regression Analyses

In preceding section, several sets of ground vibration records were analysed using the standard least sequares regression analysis. In this section, the above analysis of vibration attenuation at the ground surface is compared to the plot of vibration amplitudes with respect to stand-off distance from the pile. It has been observed from a number of site records that the vibration amplitude did not follow a monotonic decay and that the attenuation curve is affected by the type of the ground and the depth of the pile-toe. For example, consider the following two records taken in Blaydon and Sheffield:

Example One, Blaydon

Three sets of data recorded in Blaydon during the driving of a steel H-pile by a five tonne hydraulic-hammer to different toe-depth are examined. The plots of vibration amplitude with respect to $r/\sqrt{W_o}$ and related to stand-off distance are shown in figure (6.17) and the relevant information is listed in the following table:

Blaydon records			
file-names	BLH-1	BLH-7	BLH-13
toe-depth	9.5m	17.0m	21.0m
ground con.	alluvial clay and sand	glacial soft clay and silt	glacial stiff clay with cobbles
equations	$v = 50\left(\frac{r}{\sqrt{W_o}}\right)^{-3.36}$	$v = 757\left(\frac{r}{\sqrt{W_o}}\right)^{-3.43}$	$v = 1229\left(\frac{r}{\sqrt{W_o}}\right)^{-3.37}$
corr.coeff.	r=-0.906	r=-0.982	r=-0.926
gradient	-73°	-74°	-73°

The regression analysis shows parallel attenuation lines for the vibration records of different depths but with different intercept values which increased as the toe-depths increased. On the other hand, the plot of the attenuation curve of vibration taken at 9.5m toe-depth when the pile was driven into loose deposits of alluvial clay and sand shows a monotonic decay of vibration amplitude with distance. However, for further toe-depths of 17 and 21m, driving respectively in soft glacial clay and

silt, and stiff glacial clay with cobbles, the attenuation curve is not linear and the records show some increment in amplitudes which then decreased with the increase of distance from the pile location.

Example Two, Sheffield

A similar case is considered by analysing the vibration records taken in Sheffield. A diesel-hammer (BSP-B15) was used for trial driving a single 12m long steel H-section pile. Records of ground vibration taken at three different toe-depths are analysed using the regression analysis equation and also are plotted against the horizontal stand-off, as shown in figure (6.18). A summary of relevant information is listed in the table below:

Sheffield records			
file-names	FDH-1	FDH-7	FDH-8
toe-depth	5.0m	7.6m	8.2m
ground con.	loose coarse grained clayey Sand	very dense brown sandy Gravel	grey laminated Sandstone interbeded with siltstone
equations	$v = 12.6\left(\frac{r}{\sqrt{W_e}}\right)^{-2.03}$	$v = 29.7\left(\frac{r}{\sqrt{W_e}}\right)^{-2.58}$	$v = 36.7\left(\frac{r}{\sqrt{W_e}}\right)^{-2.43}$
corr.coeff.	r=-0.95	r=-0.98	r=-0.93
gradient	-64°	-69°	-68°

The regression analysis shows reasonably parallel attenuation lines for the vibration records taken at different depths, and having an average gradient of 67°. However, the attenuation of vibration with respect to stand-off distance is non-uniform as function of toe-depth increase.

The above examples show that the regression analysis cannot be used to fully describe the attenuation of the ground vibration with respect to the increase of depth of penetration. Although the attenuation lines for different toe-depths were derived to be parallel, the vibration amplitudes with respect to stand-off distance, varied with different toe-depths.

6.3.3 Vibration Attenuation with respect to Energy Source

The propagation of the ground vibration, recorded from several different sources, in terms of peak particle velocity and assessed with respect to horizontal distance, is analysed and discussed in this section. The data are plotted on a logarithmic scale using the general transmission equation

$$v = k(D)^{-n}$$

where D is the horizontal distance from the source, and k & n are constant and can be found from regression analysis of the field measurements of the ground vibration.

The results are shown in figure (6.19). The figure displays four general bands of vibrations: *explosive demolition, pile-driving, rail-traffic* and *road-traffic*. The figure also provides some general guidance of the level of vibrations recorded from these sources. It can be seen that the vibration generated by demolition blasting produced the highest levels while road traffic caused the lowest values. The propagation of vibration associated with pile driving showed that at 1m from the pile the levels of vibration introduced by the hammer were ranked as follows:

1.Vibrodriver, 2.Drop-hammer, 3. Diesel-hammer, 4.Hydraulic-hammer & 5.Air-hammer

The figure also shows that the attenuation of vibration at some 10m horizontal distance from the pile showed the slowest and fastest by the sequences of the following hammers, respectively:

1.Diesel-hammer, 2.Hydraulic-hammer, 3.Drop-hammer, 4.Vibrodriver & 5.Air-hammer

From the above explanation it can be concluded that the air hammer produces a low level of vibrations, but on the site, they are very noisy and are more suitable for driving in granular soil. The vibrodriver causes a high amplitude of vibration in the ground close the pile but the induced vibration attenuates rapidly with distance. The rapid attenuation of vibration and the low level of noise are two advantages of using this hammer in urban areas when driving in granular soil. When driving in hard and dense ground is considered, the hydraulic hammers are a good choice, and in addition they offer a highly controllable energy input both from variable drop height and often by variable ram weight. This controllability may be of advantage

when starting to drive piles close to a sensitive structure. Also, when driving in very dense ground or into the bedrock the height of drop can be reduced to avoid any possible damage to either the pile head or the pile toe. The adjustable drop height is also available with the employment of a drop-hammer, But they operate at a lower rates of blows per minute. The use of diesel-hammer offers a fast rate of ram strike per minute to the pile but the hammer input energy is a function of soil stiffness.

In general, the weight of a drop-hammer varies from 0.5 to 2 times the pile weight, with a height of drop in the range of 0.2m to 2m. For effective pile driving, the weight of the hammer should be at least the same as that of the pile (BSC (1986)). Research by Packshaw (1951) of driving a 15.2m long, 355mm square-section concrete pile by a 4.7 tonne drop-hammer showed that the hammer efficiency varied from less than 5% for a ratio of $\frac{\text{hammer weight}}{\text{pile weight}} = 0.32$ to almost 50% at a ratio of 1.06 (see Fleming *et al* (1985)). The above reference also suggested that some increase in hammer drop is required for a raking pile where the input energy is reduced by approximately 10% for a 1/3 rake. Studies carried out by Storey and Ellery (1985) from BSP concluded that a hydraulic-hammer having a heavier ram and lower impact velocity showed a higher driving efficiency than was the case with the high impact force and velocity of a diesel-hammer even within conditions of dense soil.

6.3.4 Analysis of Vibration with respect to Toe-depth and Soil-type

Several records are analysed to examine the effect of pile-toe depth on the amplitude of the measured ground surface vibration. Generally, there is an inverse relation between the increase of pile depth and the amplitude of surface vibration. This is because the radial distance which defines the expansion of wave-fronts increases for deeper penetration. However, although the potential reduction in vibration at ground surface increases as the pile toe advances more deeply (as a result of the layer transmission pattern and the effect of both geometrical divergence and material friction upon the energy density in the wavefront), in the case of layered ground where the acoustic impedance ρc of the layers decreases towards ground surface there is some indication that the vibration amplification (as the waves travel upwards) due to progressively reducing ρc exceeds the path-length-attenuation reduction. The following expression can be used to describe the above discussion:

$$\sigma = \rho c \frac{\partial u}{\partial t} \quad and \quad \frac{\partial u}{\partial t} = \frac{\sigma}{\rho c}$$

where $\partial u/\partial t$ represents the particle velocity at the ground surface. As ρc decreases faster than the decrease of σ along the different layers, a larger amplitude of vibration can be expected at the ground surface.

The vibration amplitude at the ground surface may also be increased due to the following causes:

- When driving in dense or stiff soil a larger portion of vibration energy tends to be transmitted from the-pile toe into the surrounding medium (see the phenomena of reflection and refraction, Appendix A1.2).
- The dense ground shows more resistance to the driven pile so more energy will be transmitted from shaft of the pile as well as the toe.
- The energy from the pile toe will be transferred to the ground surface with a smaller degree of material friction losses than is the case with a less dense ground medium.

Typical levels of peak particle velocity measured at the ground surface at some 5m stand-off distance during pile driving in different types of ground are listed in the following table:

Peak particle velocity values (mm/s)			
Non-cohesive deposit			
Toe-depth	Loose	Medium dense	Dense
less than 15m	12-40	20-50	25-85
greater than 15m	—	10-22	7-15
Cohesive deposit			
Toe-depth	Soft	Firm	Stiff
less than 15m	15-30	20-35	35-60
greater than 15m	—	10-18	5-10

The above values of peak particle resultant velocities were extracted from the field measurements of the ground vibration associated with pile driving from different sites. The wide range of the given values is mainly caused by the effect of different variables on the generation of vibration. These variables include the types of hammer, pile, toe-depth, distance from the source and the density of the ground. A complete set of ppv values with respect to the above variables was presented in table (T5-70) of chapter five.

An attempt is also made to define the range of the dominant frequency in different types of ground generated from pile driving operation. Again, the type of the operating hammer controls the magnitude of the frequency induced in the ground. For example, a high frequency vibrodriver generates more frequency in the ground than does a drop-hammer. However, the type and density of the ground also has a great influence on the frequency magnitude. A more dense ground produces a higher vibration frequency than does a loose ground. A summary of the derived dominant frequencies in different types of ground is listed in the following table:

Dominant Frequency Hz		
Non-cohesive deposit		
Loose	Medium dense	Dense
18-25	20-52	40-110
Cohesive deposit		
Soft	Firm	Stiff
15-20	20 34	30-65

The measurement of vibration at the ground surface with respect to pile toe depth is explained in the following examples:

Example (1)

The decrease of vibration amplitude with an increase of pile-toe depth is considered in the following two cases of field records shown in figure (6.20). The records were taken in Blaydon during the operation of a vibrodriver (PTC-50c) and the use of a five tonne ram hydraulic-hammer (BSP-357) in driving a 20m long steel H-pile 356 × 368 × 152kg/m. The amplitudes of the peak particle resultant velocity at different toe-depths and different stand-off distances are listed in table (T6-7A)†.

Example (2)

Two cases showing an increase of vibration amplitude recorded at the ground surface with the increase of pile toe depths are demonstrated in figure (6.21). The plots of ppv/stand-off are displayed for ground vibrations recorded in Sheffield and Newark during the driving of steel H-piles using a diesel-hammer (BSP-15B) and a 5000kg ram drop-hammer, respectively. The amplitudes of the peak particle resultant velocity of these records are listed in table (T6-7B)⊘.

---

† the details of these records are displayed in tables (T5-6) and (T5-26), respectively

⊘ see tables (5-61) and (5-45) for more information.

Table (T6-7A)

Decrease of vibration amplitude with depth in terms of ppv ($mm.s^{-1}$)						
vibrodriver records						
File names	Toe-depth (m)	Distance from pile (m)				
		2.0	5.0	8.0	12.0	18.0
RAK-5	1.0	49.50	28.81	13.44	4.78	2.00
RAK-13	15.0	8.34	4.50	2.47	3.05	1.08
hydraulic-hammer records						
File names	Toe-depth (m)	Distance from pile (m)				
		2.0	9.0	15.0	17.0	21.0
GHH-1	3.7	51.42	20.80	9.27	7.04	4.61
GHH-7	13.5	17.50	8.48	6.13	5.21	2.91

Table (T6-7B)

Increase of vibration amplitude with depth in terms of ppv ($mm.s^{-1}$)					
diesel-hammer records					
File names	Toe-depth (m)	Distance from pile (m)			
		2.0	5.0	8.0	12.0
SDH-2	6.0	17.87	9.09	11.10	4.74
SDH-10	8.35	49.24	44.77	20.82	28.61
drop-hammer records					
File names	Toe-depth (m)	Distance from pile (m)			
		4.0	7.0	10.0	14.0	22.0
NEW-1	5.0	13.55	5.04	5.65	2.06	1.14
NEW-6	17.0	21.25	8.89	11.66	5.92	3.86

6.3.5 Effects of Pile-geophone Orientation on Vibration Records

The effects of pile position on the generation of vibration at the ground surface are considered in this section. It was noted by reviewing the vibration records listed in the previous chapter that the amplitudes of the vibration in the radial, transverse and vertical directions varied according to the positions and the orientations of the geophones to the driven pile. The driving of two types of steel sheet-pile and H-pile is examined in the following sections.

a. Sheet-pile

When the geophone sets were placed normal to the width of a sheet-pile (or a series of sheet-piles), the amplitudes of vibration recorded by both the radial and vertical geophones were higher than that of the transverse geophone. The vibration records taken in Edinburgh (table (T5-29)), Grimsby (tables (T5-32) & (T5-33)) and Waltham Cross (table (T5-67)) provide some examples of the above observation.

However, when the geophones were located parallel to the width of the sheet-pile, the vibrations recorded by the transverse geophone showed a similar or even a higher amplitude than those recorded by the radial and vertical geophones. It is suggested that during the impact, the hammer causes some lateral movement or whip in the direction of the wider side of the sheet-pile, so increasing the generation of a 'Love-style' wave$^{\diamond}$ motion at the ground surface. This phenomena is demonstrated in figure (6.22a). The following cases of the site measurements of the ground vibration, give some reinforcement to the above discussion:

Consider the data recorded at St.Annes (see tables (T5-63) & (T5-64)). At this site the geophones were placed 2, 5, 8, 12 & 18m from the pile and along the axis of the wall (see figure (5.75)). The piles were Larssen (32W) and were driven by a vibrodriver (PTC-50H3) to 10m depth and then by a seven tonne ram hydraulic-hammer (BSP-357) to deeper penetration. The percentages of the vibra-

---

$^{\diamond}$ This is a type of surface wave which causes horizontal particle motion perpendicular to the direction of wave propagation.

tion recorded by the three orthogonal geophones at 5m stand-off are listed in the table below:

Depth (m)	Percentage of Vibration Components		
	Radial	*Transverse*	*Vertical*
1.0	37	40	23
3.0	52	33	15
7.0	34	48	18
10.0	37	38	23

A similar case was also observed in Grimsby. The ground vibrations were measured during trial driving of single and pairs of interlocked sheet piles by a diesel-hammer (BSP-B15) having a maximum nominal input energy of 37.2kJ. The geophones were located in a radial arrangement around the pile at different stand-off distances (see figure (5.45)). The figure shows that the orientation of transverse geophones in sets C and B is parallel to the direction of the possible 'Love-style', motion. The recorded field data are displayed in table (T5-31). By comparing the amplitudes of vibration in relation to their orientation with the pile it can be noted that geophone sets C and B showed a higher level of transverse vibration than did the other sets.

b. H-pile

Based on field measurent of the ground vibration, it was found that driving a raked H-pile causes the generation of a higher level of transverse wave on the ground surface close to the pile location than does the driving of a vertical H-pile. This was especially observed when the geophones were positioned normal to the raking direction. Figure (6.22b) shows that the impact force along the length of the pile can be resolved to two vertical and horizontal components. The horizontal component induces a lateral movement in the ground in the form of 'Love-style' wave. As described above, this particle movement coincides with the axial movement of a transverse geophone; consequently a large amplitude of ground vibration in the direction of the transverse geophone can be recorded.

This characteristic behaviour of the ground vibrations was noted in reviewing the data recorded at Blaydon (see tables (T5-6), (T5-7) & (T5-21)), Newark (see table (T5-44)) and Sheffield (see table (T5-62)).

6.4 The Use of Hemispherical Projection Method

6.4.1 Applications

The hemispherical projection is a method of data represention which visualises three-dimensional geometrical information on a two-dimensional diagram. The method was originally used in different fields of geological science, for example in structural geology to study the geological features and the orientation of lines and planes such as beddings, folds, faults, discontinuities (see Davis (1984) and Phillips (1978)), and in mineralogy for determining the angular relations of crystal faces, edges and axes (for example see Correns (1969)). The method has also gained wide acceptance in solving rock engineering problems, as in the analysis and study of the discontinuties and interangular relations within rock masses, and for determination of the direction of the active forces, to support the design of engineering structures such as tunnels, ground excavation and road cuttings (see Hoek & Brown (1980), Hoek & Bray (1981), Priest (1985) and Goodman (1980)). More recently, the method has been adopted for bioengineering studies of lower spine and hip joint movements by Jones *et al* (1987), in order to assist the clinical diagnosis of many human joint diseases.

It is proposed in this section that the ground vibration data measured in three orthognal directions (*radial, transverse & vertical*) together with their sense of motion along each axis, can be projected on to an upper or a lower hemisphere (as a function of directional sense) representing the direction of the vector of resultant velocities of the ground. This form of analysis can be used in evaluation of the stability of block foundations in relation to the applied vibration forces. Application of the method is explained in the following sections. Some examples of plotting and analysing ground vibrations measured during pile driving are given.

Note that some of the symbols used in this section may look similar to those used in preceding section but they have different meaning. The definitions of the symbols are given within the text and in the diagrams.

6.4.2 The Principle of Hemispherical Projection

The principle of hemispherical projection is described in many books on the subject of structural geology, mineralogy, rock mechanics and engineering geology. Much useful information on the method is provided by Priest (1985).

As the name implies, the method is based on the projection of any point or line of a three-dimensional reference sphere onto a two-dimensional reference plane which passes horizontally through the centre of the reference sphere and cuts the sphere into an upper and a lower hemisphere. The reference plane is also known as *projection plane.*

Several types of spherical projection are in use for different purposes. The most common ones are the *polar* and *equatorial* projections. Figure (6.23) illustrates a simplified form of polar and equatorial projection of a sphere.

There are two main methods of construction of the polar and equatorial nets. These are called *equal-angle* and *equal-area* projections, and also are known as *Wulf* and *Schmidt* nets. The method of construction of the nets are fully detailed by Priest (1985) while a brief description is given below.

Figure (6.24) illustrates the construction of polar projection of an inclined line of maximum dip of θ. The line intersects the reference sphere at point p. The equal-angle projection of this point can be achieved by drawing a straight line from p to M which is located at distance R vertically above the sphere centre O (see figure (21a)). The line cuts the projection plane at point p_1 which has a radius r_1 from the centre O. By a simple geometery, the radius r_1 can be expressed as

$$r_1 = R \quad \tan\left(\frac{90^o - \theta}{2}\right)$$

When $\theta = 0^o$ then $r_1 = R$ and the projection of the point will be on the perimeter of the reference plane, and when $\theta = 90^o$ then $r_{=}0$ and projection of the point will be at the centre of the reference plane.

The equal-area projection of the point p on a horizontal plane can be made by drawing a circular arc centred at point N, which is at distance R vertically below the centre O, from point p and intersects the horizontal plane at point p_2 which is

at distance r_2 from the centre N.

$$r_2 = 2R\cos\left(\frac{90^\circ + \theta}{2}\right)$$

When $\theta = 0^\circ$ then $r_2 = \sqrt{2}R$. This means that the radius of the projected point is larger, by a factor of $\sqrt{2}$, than the radius of the reference sphere, and in order to reduce its diameter to that of the sphere, r_2 should be divided by $\sqrt{2}$. The relation between r_1 and r_2 is expressed as follows:

$$r_1 = r_2/\sqrt{2}$$

The construction of equatorial projections is similar in principle of those described for the polar projection. The polar projection is usually used for plotting points which may need to be contoured while the equatorial projection is preferable for planes and lines of various orientations (Priest (1985)).

The equal area projection is preferred by geologists for statistical analysis of the geological data while engineers prefer the equal-angle projection because the net provides accurate geometrical construction. Throughout this section, both the upper and lower hemisphere projections of equal-angle nets are used for the plotting the ground vibration data.

6.4.3 Directional Sense of Vibration

The three-dimensional orientation of the ground vibration components which are usually expressed as *radial, transverse & vertical* axes can be represented as the three constitutives axes on the projection net. To identify the location of the vibration components on lower or upper hemisphere, it is necessary to determine the directional sense of the vibratory motion. A *right-hand-rule* convention is adopted to define the sense of vibration for each individual component. Plate (6-1) illustrates the orthogonal orientation of a right hand (thumb, forefinger and middle finger) in combination with a set of three perpendicular geophones. The source of vibration lies in the same direction of radial axis (location of the body in the above photograph). The directional sense of vibration components is positive when the right-hand fingers have the positions indicated in table (T6-8)

Table (T6-8)

Right hand fingers	Direction from the source	Sense	Wave axes orientation
Thumb	upwards	positive	Vertical
Forefinger	outwards	positive	Radial
Middlefinger	to the left	positive	Transverse

The directional sense of each individual geophone was checked and an arrow was painted on each set of geophones to indicate the location of the vibration source (the peak of the arrow is directed toward the source of vibration). The procedure was achieved by applying an impulse vibration, in the direction of radial axes, to a set of three orthogonal geophones. The applied vibrations to the geophones were recorded by the PDR-2 unit and the time-based trace for each geophone was then monitored on the screen to identify positive directions corresponding to the *right-hand-rule.*

6.4.4 Projection of the Vibration Components

In order to clarify the method of plotting vibration data on a hemispherical projection, some useful definitions are given in the following paragraphs.

An example of hemispherical projection of ground vibrations is shown in Figure (6.25), where the radial axis (+R), (-R) is aligned with the 3-9 o'clock diameter of the circle, the transverse axis (+T), (-T) is aligned with the 12-6 o'clock diameter of the circle respectively, and the vertical axis is located at the centre of the circle ((+V) in the centre of an upper hemisphere projection and (-V) in the lower hemisphereical projection). Three forms of vector motion could be represented on a stereonet as shown below:

1. *Radial Motion Only*: when *radial wave* is the maximum while transverse and vertical waves are zero. The radial motion, regarding the sense of vibration, causes forwards and backwards movement of the ground particles.

$$\pm R = \text{max.} \quad T = 0, V = 0$$

2. *Transverse Motion Only*: when *transverse* wave is the maximum while radial and vertical waves are zero.

$$\pm T = \text{max.} \quad R = 0, V = 0$$

3. *Vertical Motion Only*: when *vertical* wave is the maximum while transverse and

radial waves are zero.

$$\pm V = \max. \quad R = 0, T = 0$$

Concerning the directional sense of the vibration, radial, transverse and vertical motions cause forward-backward, left-right and up-down movements of the ground particles respectively. The vertically downward movement of free ground, if ascribed to the foundation response, implies a small temporary reduction in the foundation net weight. If followed rapidly by sensibly horizontal shear this could imply some soil-foundation relative movement, depending upon the type of foundation and the shear strength parameters for the soil-foundation interface (Attewell *et al* (1989)).

When the three components of the ground vibration have the same amplitude (as a function of time), there will be four positions of the resultant vector in the upper hemisphere where the vertical wave has a positive sense (`+V`), and four positions on the lower hemisphere where the vertical wave has a negative sense (`-V`), see figure (6.26). The lower and upper hemispherical plots are shown by solid and open circles respectively.

6.4.5 The Plotting Technique

To simplify the plotting technique for a vibration record taken in three orthogonal directions, consider the example shown in figure (6.27). A Cartesian method of plotting the three orthogonal components of the ground vibration is shown in figure (6.27a) where α is defined as the angle of rotation around the centre of the sphere of a horizontal plane which contains both radial and transverse motions (also see figure (6.27b)). The value of α can be obtained as follows:

$$tan\alpha = T/R$$

$\alpha = 0^o$ when $R = 0$ and $T = maximum$ and its direction aligns in the direction of the `R-axis`. $\alpha = 90^o$ when $T = 0$, and $R = maximum$ and aligns with the direction of the `T-axis`. The direction of the angle α represents the resultant vector of both radial and transverse components V_{rt}, which can be derived as

$$V_{rt} = \sqrt{(R^2 + T^2)}$$

θ defines the angle of the resultant vector with respect to the equatorial projection plane plane containing both the vertical component and the resultant vector V_{rt}, see figure (6.27c).

$$tan\theta = V/V_{rt}$$

The direction of the angle θ represents the direction of the resultant vector of the three components of the vibration V_{res}, and can be obtained from the following equation

$$V_{res} = \sqrt{(V^2 + V_{rt}^2)}$$

When $V = 0$ then $\theta = 0$ and V_{res} will locate on the perimeter of the reference plane. When both R & T are zero, V_{res} will be in the centre of the reference plane.

The spherical presentation of the above example is shown in figure (6.27d) while the hemispherical projection of the same point is shown in figure (6.27e).

The example displayed in table (T6-9) will be used to demonstrate the different stages of the plotting technique.

Table (T6-9)

Vibration Components (mm/s)			Resultants (mm/s)		Vector Angles (degrees)	
Radial	Transverse	Vertical	V_{rt}	V_{res}	α	θ
16.46	10.50	14.32	19.52	24.21	32.53°	36.26°

Several ways are available for plotting the above example manually on a stereonet (see for example, Brady and Brown (1985) (*using fixed stereonet*), Uromeihy (1988) (*using rotated stereonet*)). The different stages of plotting are shown below:

1. Calculate the values of the angle α and θ as described above.
2. Mark the angle α on the perimeter of an equal angle equatorial net (note the sense of R and T values).
3. Align the marked point with the E-W diameter of the stereonet and measure the angle θ along that diameter towards the centre of the net.
4. The point represents the vector resultant of the vibration components.

A computer program was written and used in this work for the plotting procedure. The program is listed in Appendix (A4)

6.4.6 Projection of Pile-driving Records

A number of ground vibration records taken during pile driving from two types of impact and vibrodriver hammers are presented using the hemispherical projection technique. The data points are sampled at 5 ms intervals and are distributed over lower and upper hemispheres of projection. The projections shown in figures (6.29), (6.32) and (6.33) are computer generated and the projection of the points on the lower hemisphere are shown as crosses (the tail of an arrow) while those of the upper hemisphere are shown by open circles (the point of an arrow). Because the projection technique accommodates angles and angular differences only, the magnitudes of the velocity vector components are numbered and listed on the right-hand side of each projection plane and related to the 5ms time steppings numbers projected on the hemisphere. Eight projection planes are plotted in each figure in a form of two columns. The left and right hand side columns represent respectively the lower and upper hemisphere projected points.

6.4.6.1 Vibrodriver Records

Typical plots of ground vibration caused by a vibrodriver are illustrated in figure (6.28), where the three components of vibration, *radial, transverse* & *vertical* are shown in colour as *pink, red* & *green* respectively. The record was taken in Flitwick during the driving of a 12m long H-pile by a high-frequency vibrodriver (model PTC-13HFI), 7m deep into ground comprising a uniform dense sand.

The record shows a typical periodic type of vibration where a sequence of repeatable vibration is induced into the ground. Vibration in the radial direction was dominant and in the range of 23mm/s, while it was of the order of 2-3mm/s along both transverse and vertical directions.

A hemispherical projection of the above record is illustrated in figure (6.29). Since the induced vibration was in this case dominated by the radial wave, the

projection of the vector points are concentrated around the E-W perimeter of the both upper and lower hemispheres. When the source of vibration, which is located to left hand side (-R) of the figure, is related to the orientation of a structure, the imposed vibrational-motion of that structure can be defined. Development of *Rayleigh-type*◇ surface wave motion may also be indicated by the projected vector points. The records show a very flat retrograde orbit motion of the ground, with an R:V axis ratio of about 10:1. It is noted that the style of vibration is controlled mainly by the type of the hammer, type of pile and the ground conditions.

6.4.6.2 Impact-hammer Records

Two sets of ground vibration records taken at 3 and 18m stand-off during the driving of a 35m long H-pile($356 \times 386 \times 152$kg/m) by a five tonnes hydraulic-hammer (BSP-357) are shown in figures (6.30a) and (6.30b) respectively. The pile was driven 19m into silty sand/gravelly deposits in a site at Blaydon for the construction of viaduct foundations as part of the extension of a new western-by-pass at Newcastle upon Tyne. The original peak particle velocity data were first integrated (see figures (6.31a) and (6.31b)), and the relevant peak particle acceleration vector points were then projected on to lower and upper hemispheres as shown in figures (6.32) and (6.33).

The projection of vector points on figure (6.32) show some shear motion in the radial and vertical directions, then there is some more random vector motion, particularly in the downward and transverse directions.

Now consider figure (6.33) which projects the resultant vector of the same blow but taken at a horizontal distance of 18m. The low amplitudes of the early points are not projected in the figure. The generation of a retrograde orbit, mainly in the R-V plane, can be detected. Subsequently, the projected points indicate ground motion in a substantially transversely-downward direction.

◇ The term 'Rayleigh-type' is used because although the motions are shown to have developed as surface waves in many cases they do not necessarily exhibit the characteristics of Rayleigh seismic waves.

Finally, from these observations it may be concluded that careful analysis of a large number of resultant vector points can promote identification of the applied vibration character, thereby assisting its interpretation in the context of applied dynamic forces and their directions with respect to a building in the vicinity.

6.5 Analysis of Vibration Vectors on Building

The dynamic character of a structure can be described by its natural modes of vibration, natural frequencies and damping factors. A structure may experience up to six components of ground vibration. Three are translational as in *radial, transverse* and *vertical* movements and three are rotational as in *pitching, rocking* and *yawing* motion around the x, y and z axes respectively, In reality, the combination of different modes of vibration of a structure causes a soil-structure system to vibrate in manner compatible with an infinite number of degrees of freedom (White 1982).

For each possible mode of vibration in a given direction, there will be a corresponding natural resonant frequency. Any possible failure of a building (or structural component of the building) is likely to occur only when its natural frequency is approximately of the same order as the applied frequency of the forcing vibration (and perhaps a higher harmonic frequency). The natural frequency of a two storey domestic building is in the range of 3-7Hz and the induced frequency from pile driving activities is in the range of 15-65Hz. Vibration at high frequency has a short wave-length and period where $f = \frac{1}{T}$ and $\lambda = \frac{c}{f}$. Das (1983) concluded the following points for the safety of a structural foundation:

1. The natural frequency of a foundation-soil system should be at least twice the applied frequency.
2. The resonant frequency decreases as the foundation weight increases.
3. The resonant frequency increases as the shear modulus of soil increases.

The effects of vibration having different frequencies (or wave-lengths) on the sides of a simple rectangular structure are shown in figure (6.31). Vertical vibration has greatest effect on the horizontal components of a building such as some roofs and slabs, while the horizontal vibrations (radial and transverse) have a greater effect

on vertical elements such as walls and columns of a building.

The presence of damping factors in the soil-structure system has some effects on controlling the levels of vibration and in reducing the natural frequencies of the system. Usually a low rise structure having a larger foundation plan has a higher level of damping than a taller structure.

6.6 The Use of a Data-base Program

A database program is used to store a substantial amount of ground vibration data recorded at different sites, and to provide an easy and quick means of analysing and interpreting the recorded data. Recently, Walton (1990) used the method to investigate cases of structural damage in relation with different sources and amplitudes of induced vibrations.

At Durham University, a commercially available program package SmartWare-II has been employed for the construction of the database files. An IBM, PC compatible computer RM Nimbus-286 was used to run the Smart-II program. The system was supplied with a colour EGA monitor and was connected to a HP LaserJetSeries-IIP printer.

The database system consists of alpha-numeric fields which allow storage of different site measurement information on specially created files. Each file includes the general information on the site, hammer, pile and the relevant ground vibration records in terms of peak particle velocity, acceleration and displacement taken in three orthogonal directions plus their resultant vectors. The vibration records are stored in the form of cubic equations and can be plotted as a function of distance to display the vibration attenuation (see Oliver (1989)).

Any specific queries can be obtained by viewing the database files on the screen. A support program is written to provide easy access to the required information. The information is divided in the following categories:

1. *hammer type*
2. *pile type*

3. *ground type*
4. *toe depth*
5. *record number*

Such a facility was requested by the *Piling Technical Services* at `British Steel`, and most of the work in this field has been done by A.Oliver†. A full description of the program can be found in a number of internal reports and manuals presented by Oliver (1990), and Attewell *et al* (1989).

6.7 Conclusions

This chapter has described some methods of analysing ground vibrations associated with pile driving operations. Three methods of analysis for describing vibration attenuation were discussed. The third method which is based on calculating the arrival time of surface and body waves at the ground surface showed a close agreement with field data.

Employment of least squares regression analysis for log(velocity) against log(stand-off) on a number of ground vibration records with respect to different types of hammer, pile, toe-depth and the ground conditions showed that the steepness of the attenuation line increased with the increase of pile toe-depth. This behaviour was observed in most of the sites where the stiffness of the ground increased gradually with depth. However, the regression analysis of data recorded for toe-depths over 25m in very dense ground showed a shallower form of attenuation line.

The use of vibrodrivers in driving of end-bearing piles caused a steeper attenuation line than when driving sheet-pile.

For comparable toe-depths, vibration caused by vibrodrivers showed steeper attenuation lines than impact hammers.

Compared with other types of hammer, the operation of vibrodrivers caused large vibration amplitudes close to the location of the pile, but these attenuated

---

† A Research Assistant in the Applied Mechanic Group, Durham University

rapidly with distance.

Use of the hemispherical projection method in presenting the resultant vector orientations was found to be helpful in defining the directions and senses of the applied forced vibrations on buildings and structures.

Use of a database program provides a quick and an easy access for case history reference and matching of site specific data to stored data.

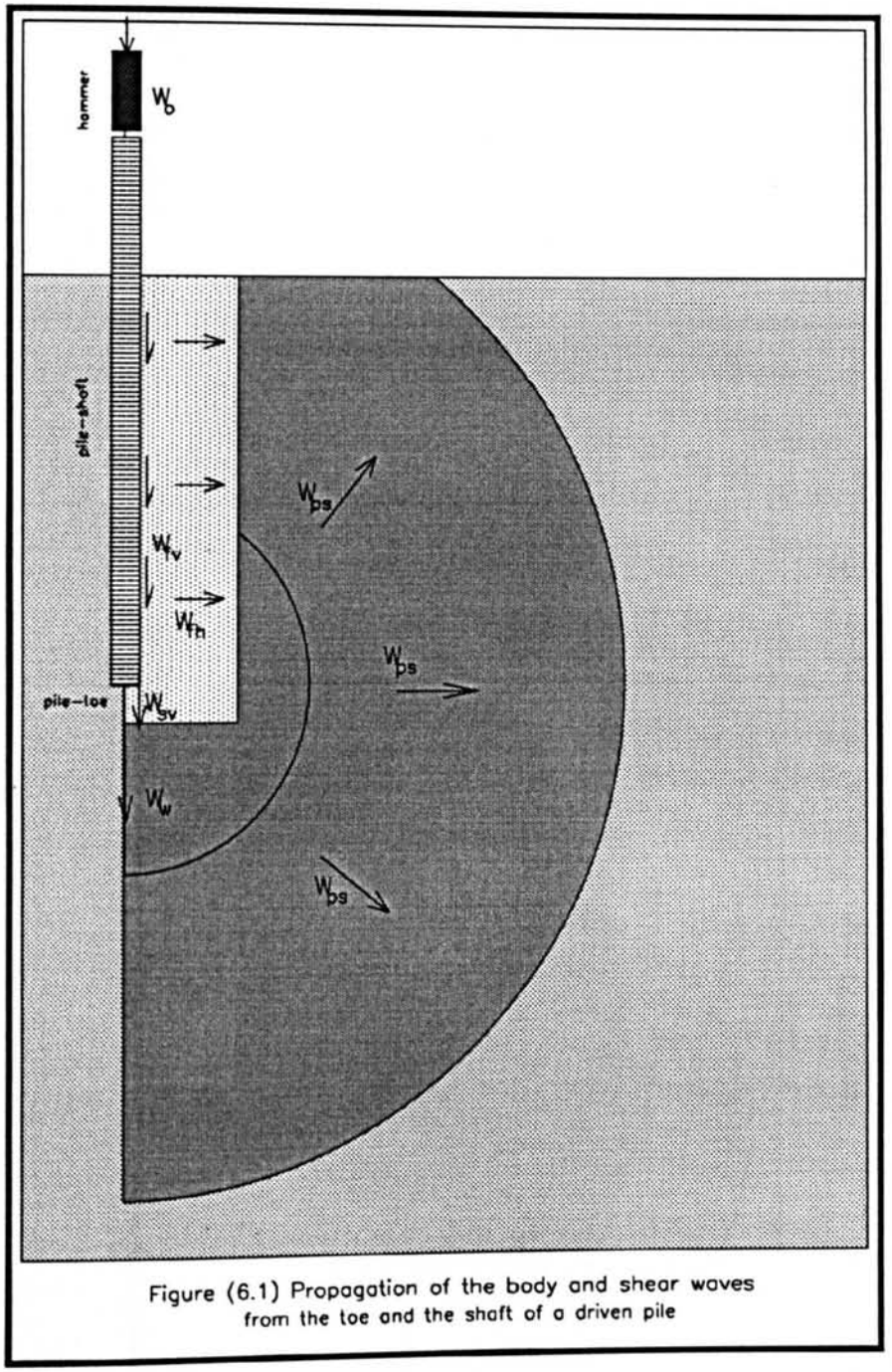

Figure (6.1) Propagation of the body and shear waves from the toe and the shaft of a driven pile

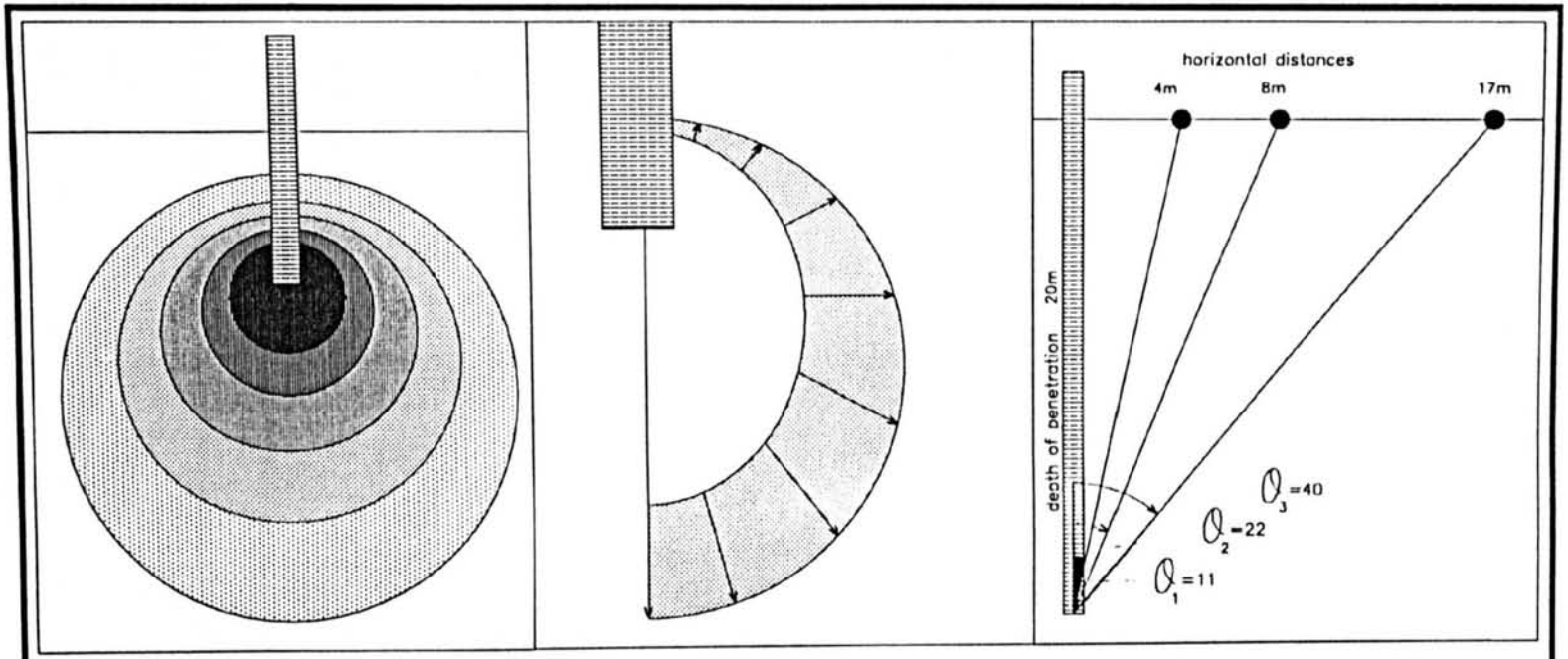

Figure (6.2) presentation of non-uniform distribution of energy around the pile-toe

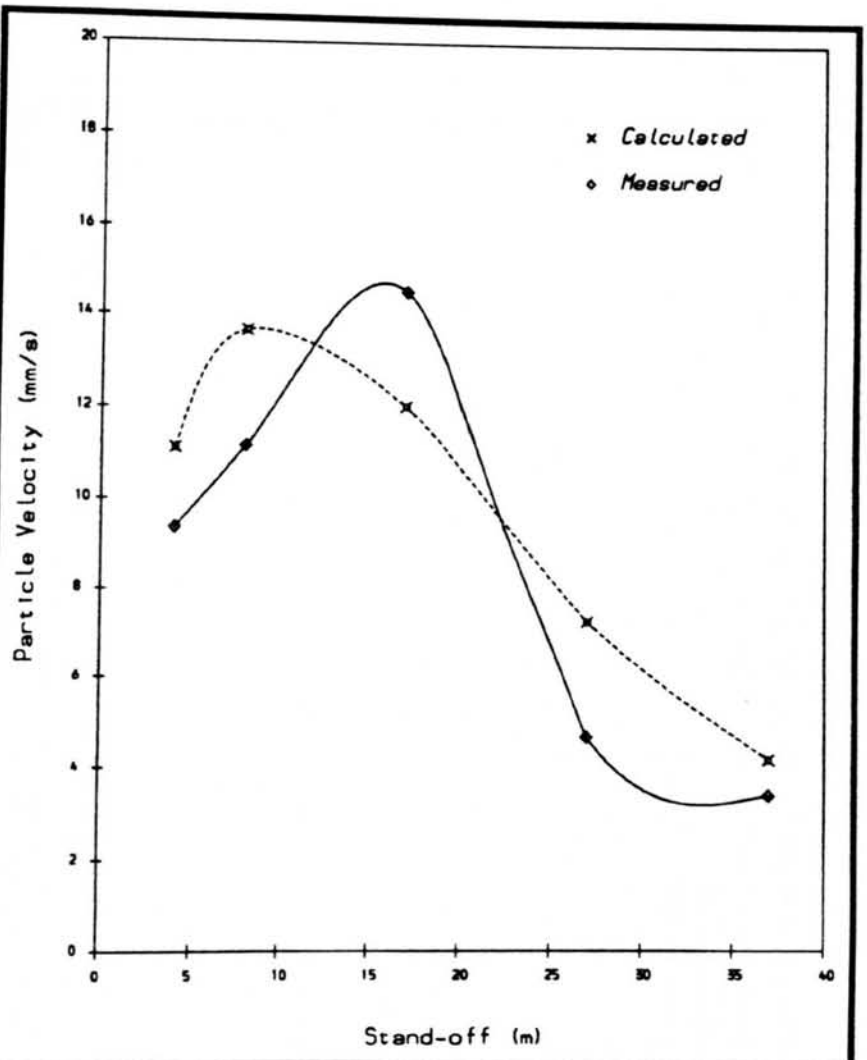

Figure (6.3) Display of measured and calculated vibration using method 2 of analysis

Hydraulic-hammer, H-pile, Toe-depth=19.8m, Radial-wave
Blaydon, File:[BLN-2]

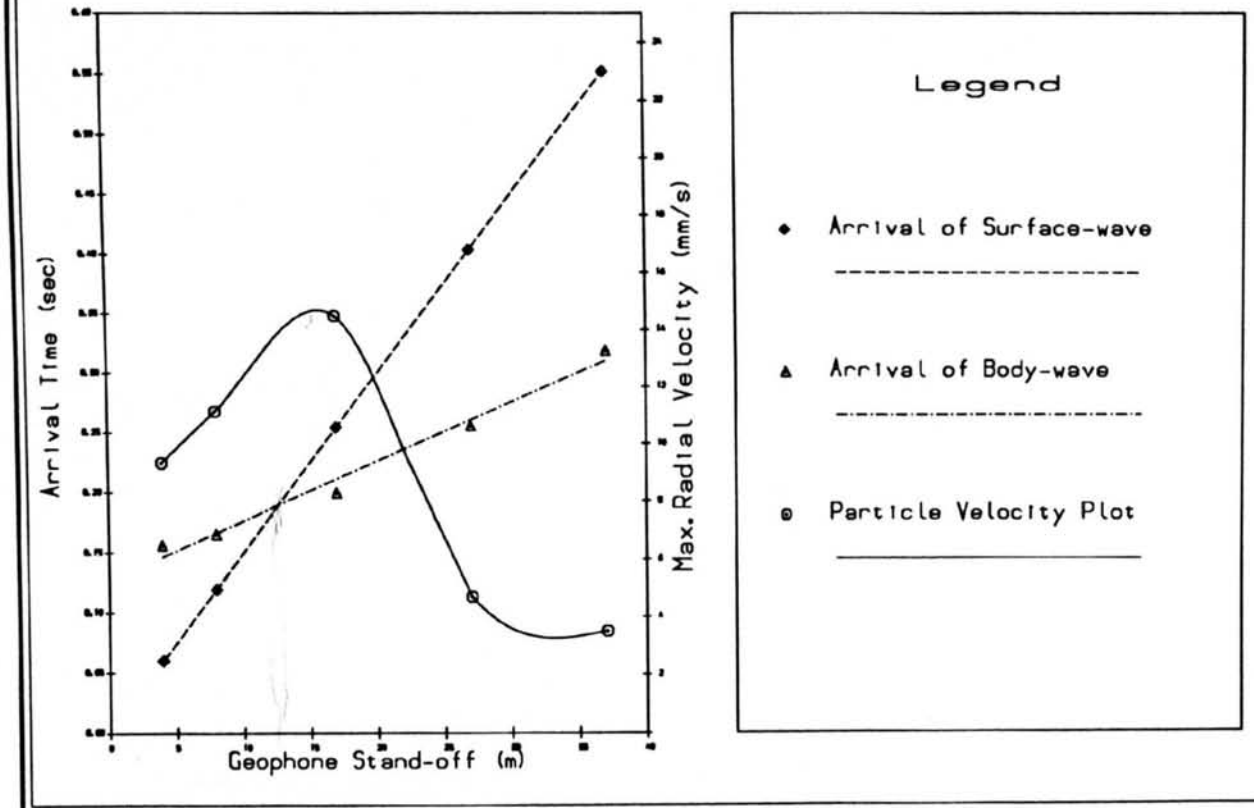

Figure (6.5) Prediction of Vibration Attenuation,
Blaydon, File BLN-2, Example (1)

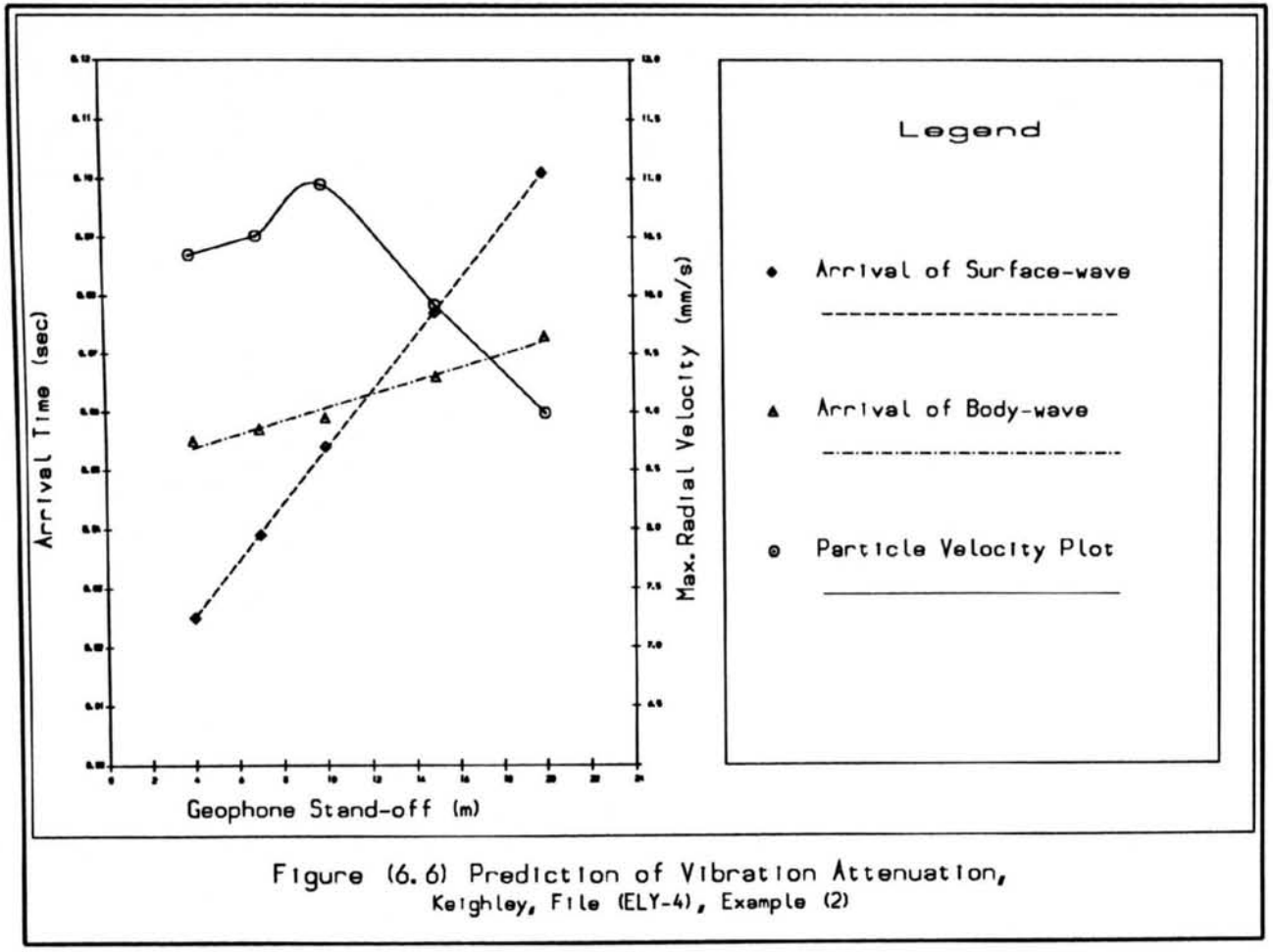

Figure (6.6) Prediction of Vibration Attenuation,
Keighley, File (ELY-4), Example (2)

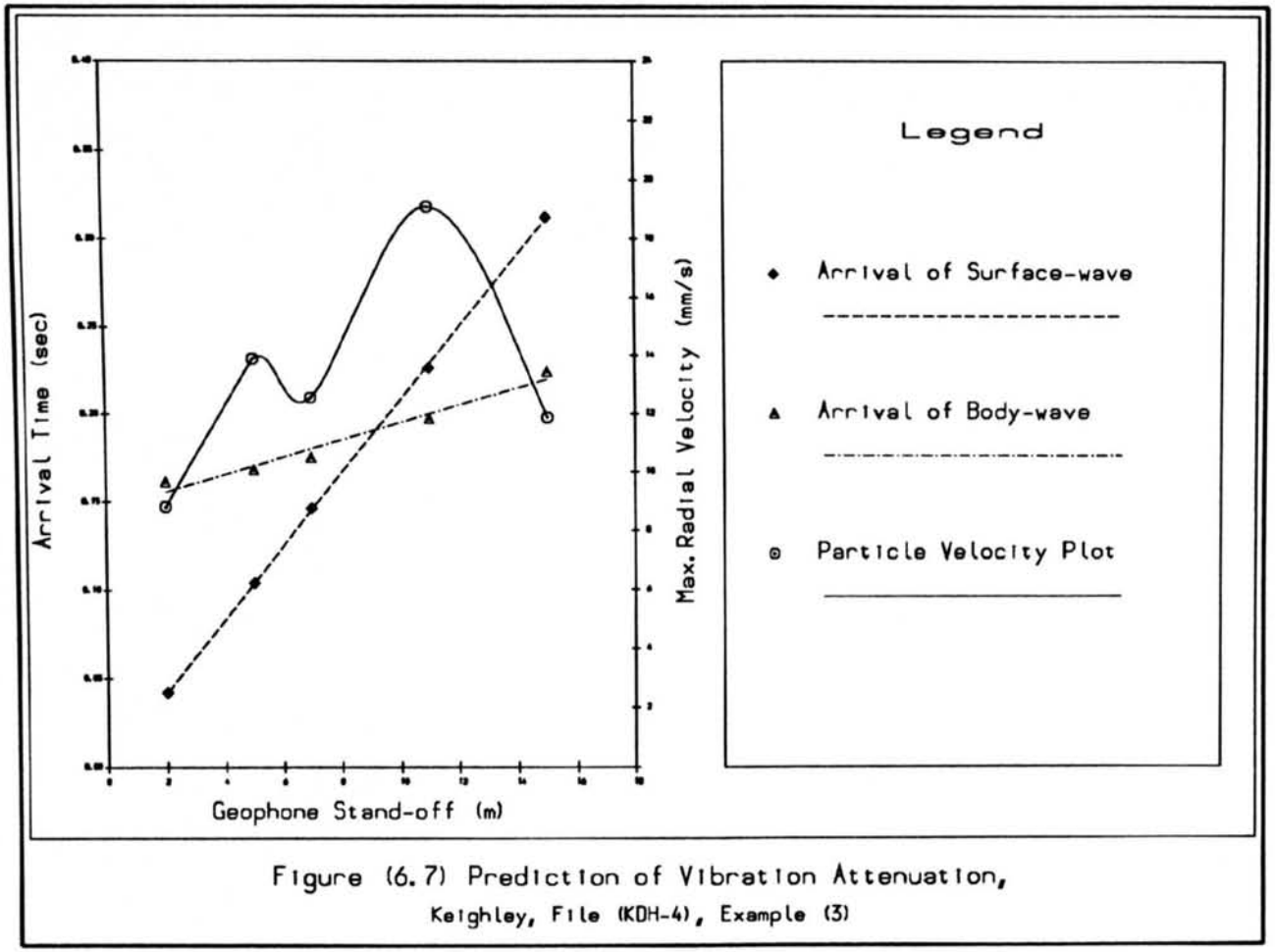

Figure (6.7) Prediction of Vibration Attenuation,
Keighley, File (KDH-4), Example (3)

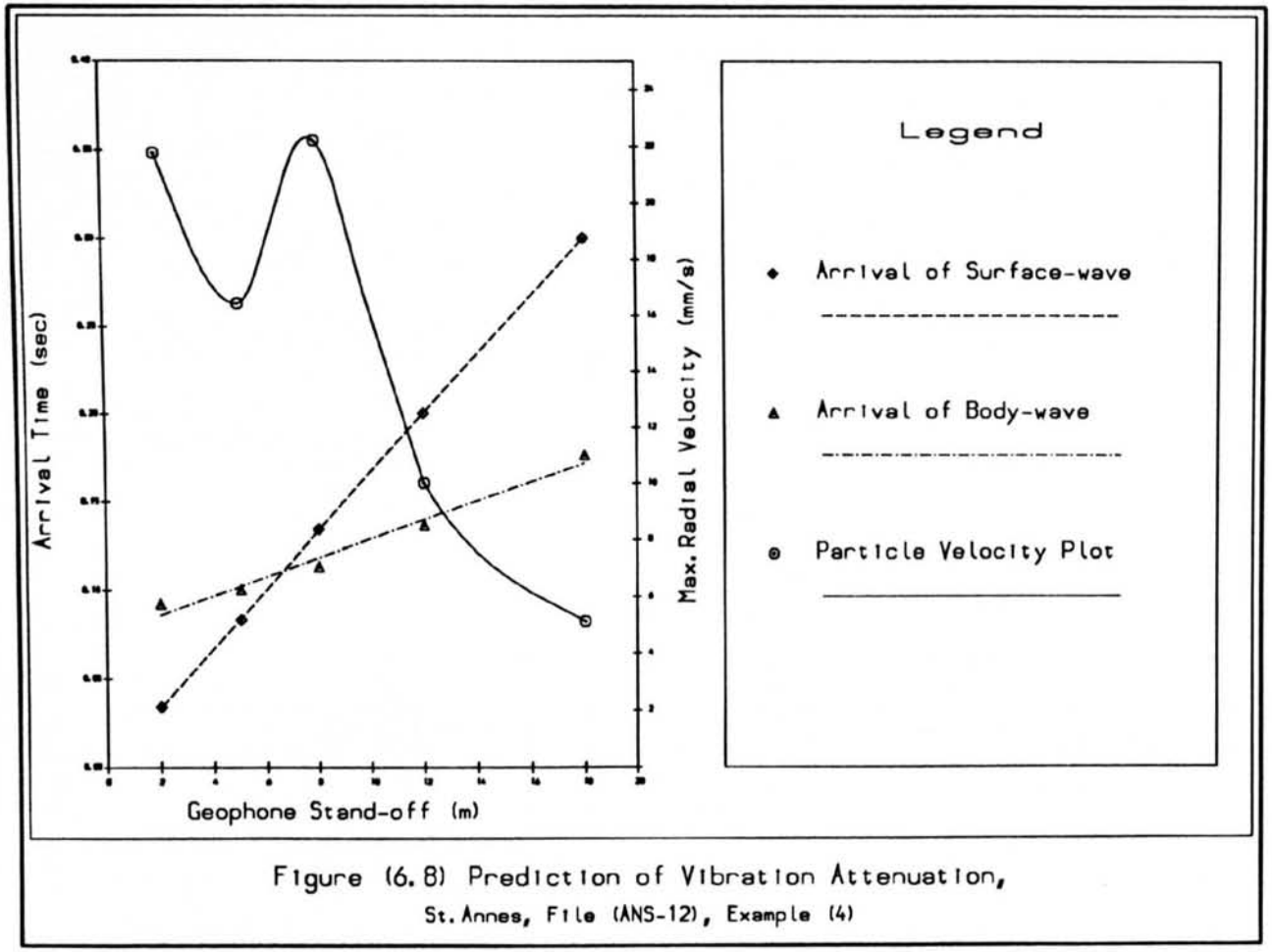

Figure (6.8) Prediction of Vibration Attenuation,
St. Annes, File (ANS-12), Example (4)

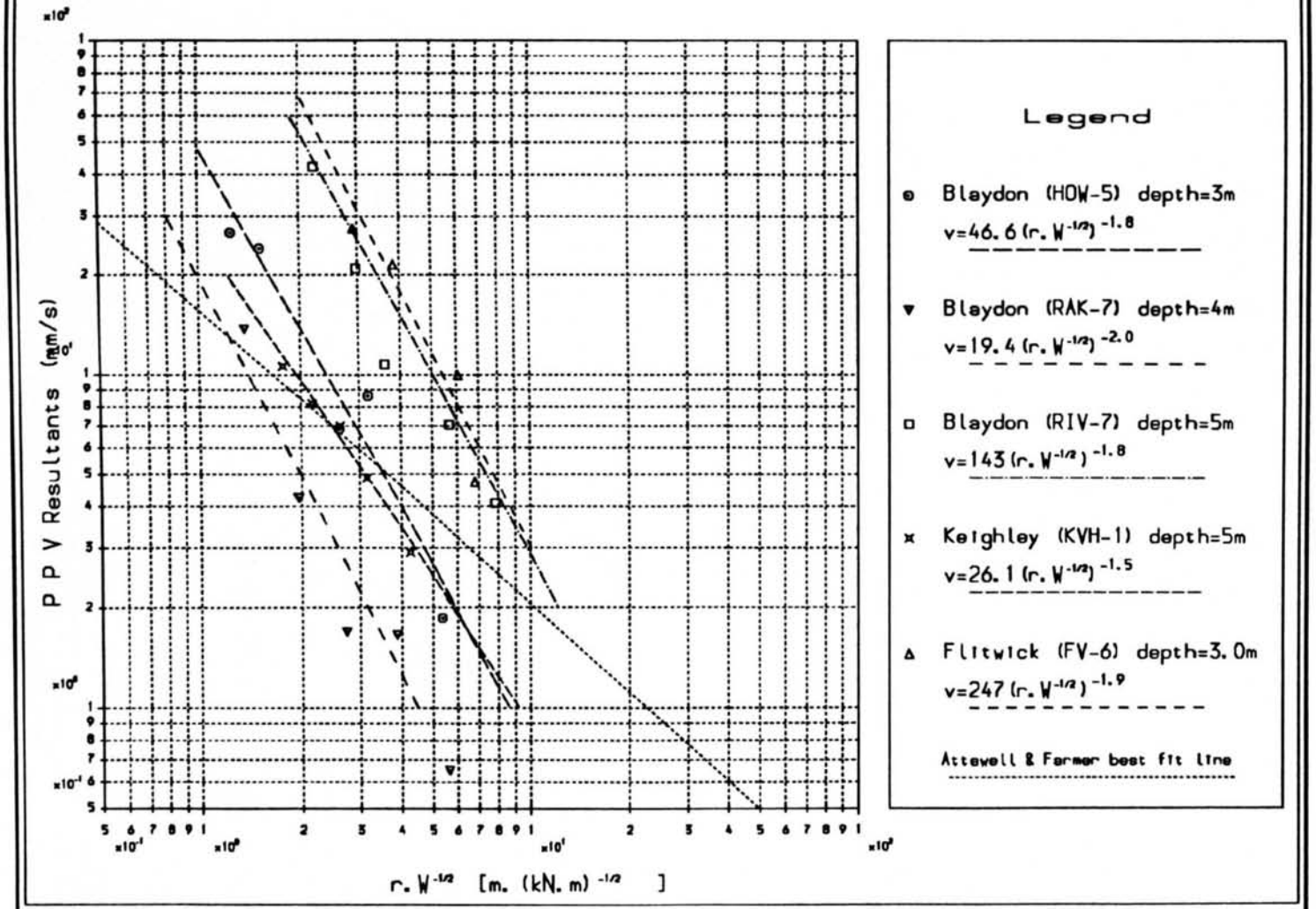

Figure (6.9a) Vibrodriver End-bearing-piles Depth < 5m

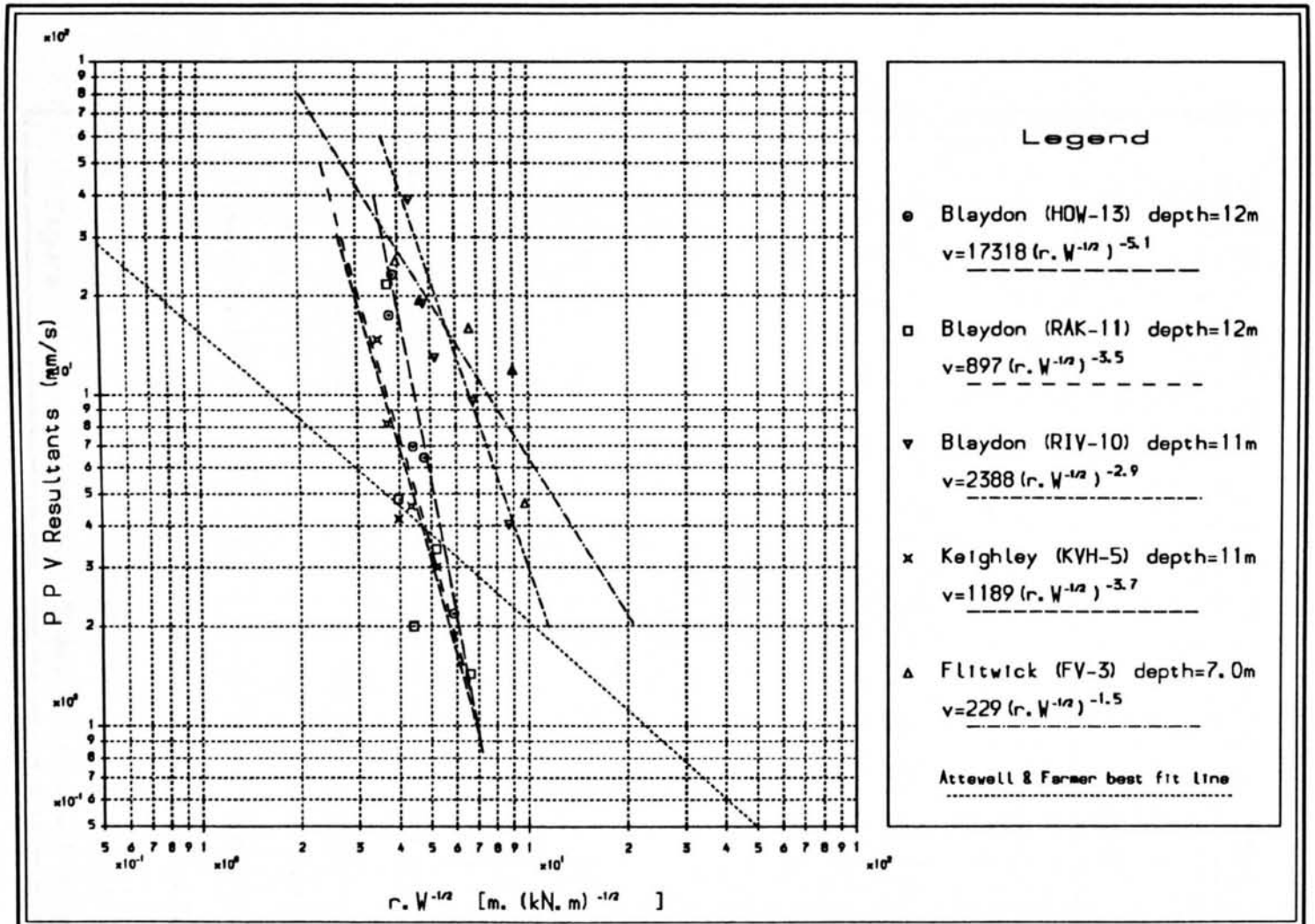

Figure (6.9b) Vibrodriver End-bearing-piles Depth > 5m

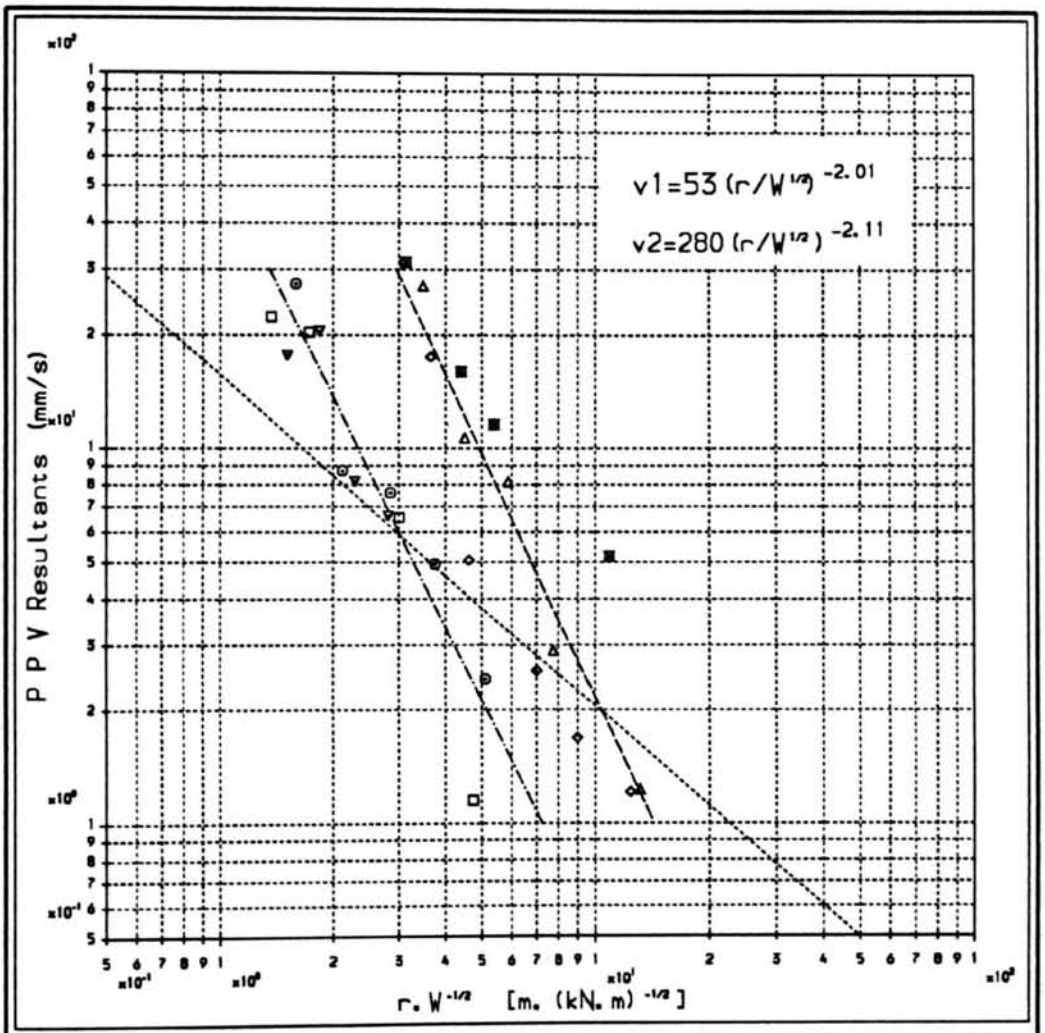

Legend

Standard Vibrodriver

- Keighley (KVS-2), Depth=4.8m
- Rotherhithe (RLM-3), Depth=4.0m
- Rotherhithe (RLV-4), Depth=4.5m

High-frequency Vibrodriver

- Newbiggin (NVS-5), Depth=4.5m
- Reston (RSV-2), Depth=4.2m
- Newark (NSV-8) Depth=4.5m

Attewell & Farmer best fit line

Figure (6.10a) Vibrodriver Sheet-piles Depth < 5m

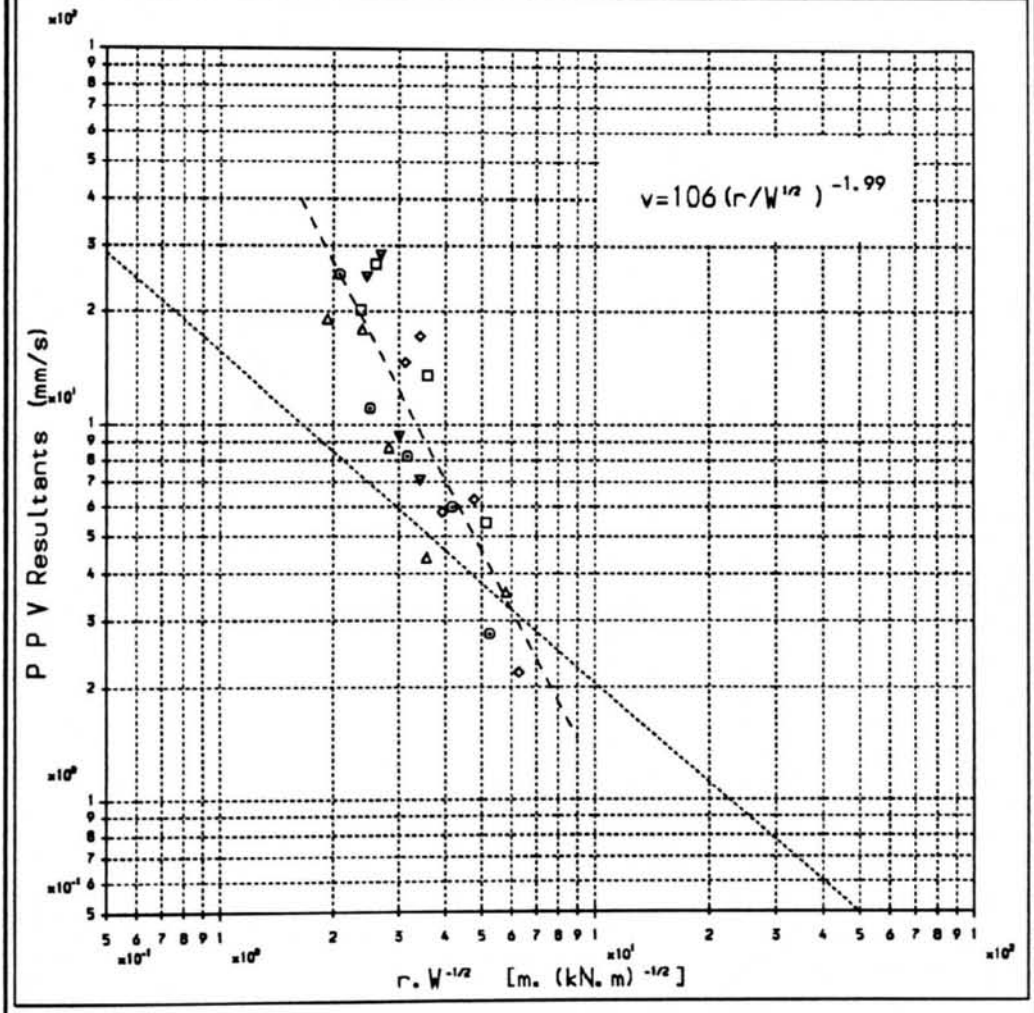

Legend

- ● Keighley (KVS-8) Depth=6.5m
- □ Rotherhithe (RLM-7) Depth=7.5m
- ▼ Rotherhithe (RLV-10) Depth=7.8m
- △ St. Annes (POL-10) Depth=10m
- ◇ St. Annes (POL-7) Depth=6.0m

Attewell & Farmer best fit line

Figure (6.10b) Vibrodriver Sheet-piles Depth > 5m

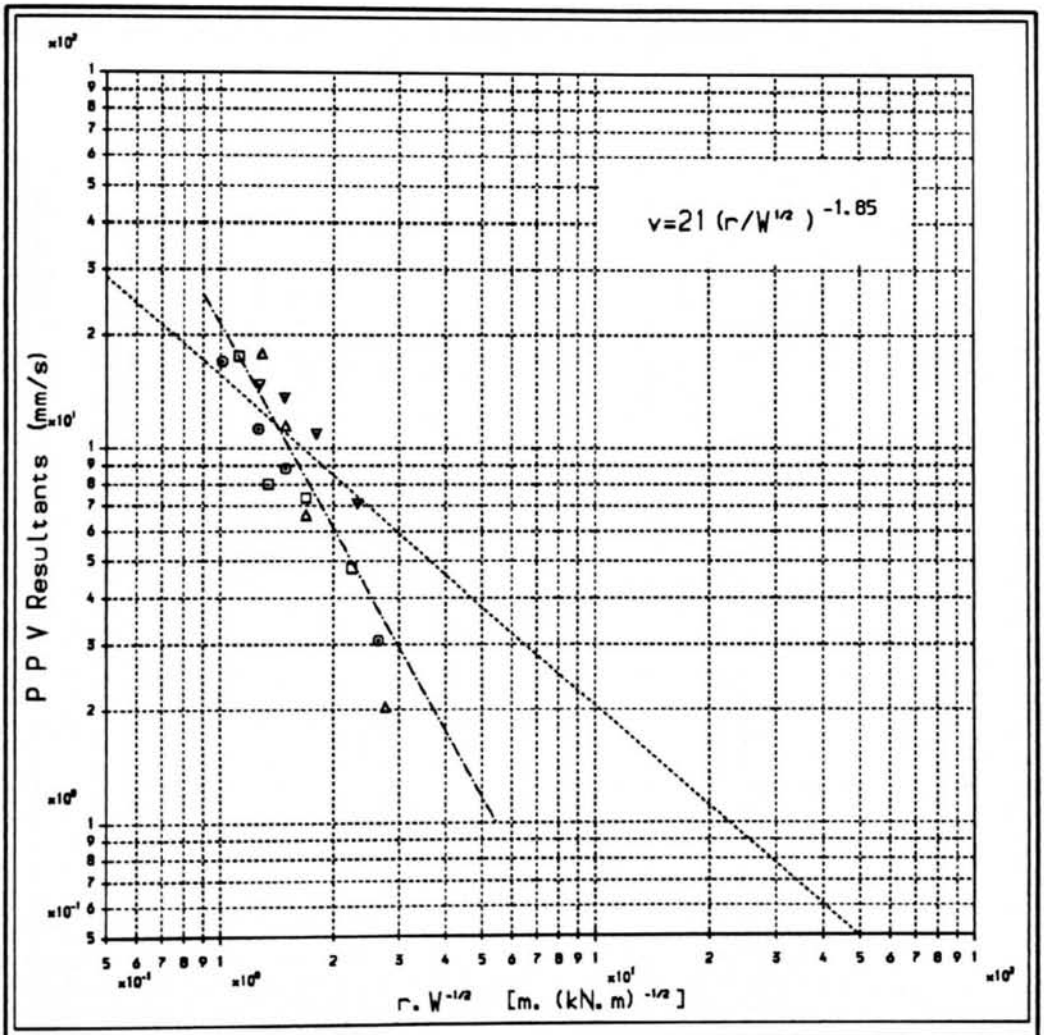

Legend

- Sheffield (FDH-2) Depth=5.8m
- Sheffield (SDH-3) Depth=6.5m
- Sheffield (SDH-5) Depth=7.5m
- Sheffield (FDH-5) Depth=7.6m

Attewell & Farmer best fit line

Figure (6.11a) Diesel-hammer, H-pile, Depth < 10m

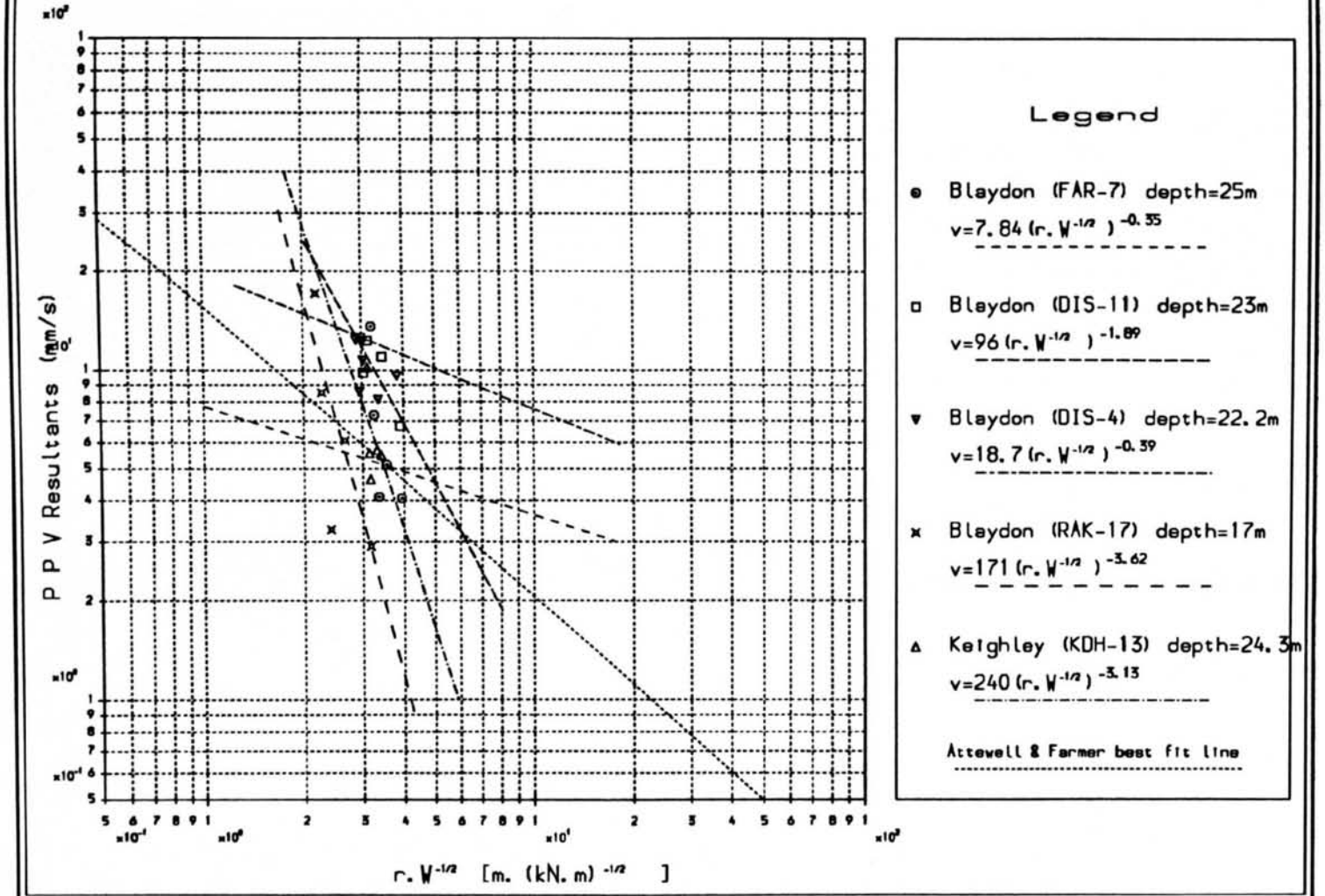

Figure (6.11b) Diesel-hammer, H-pile, Depth > 15m

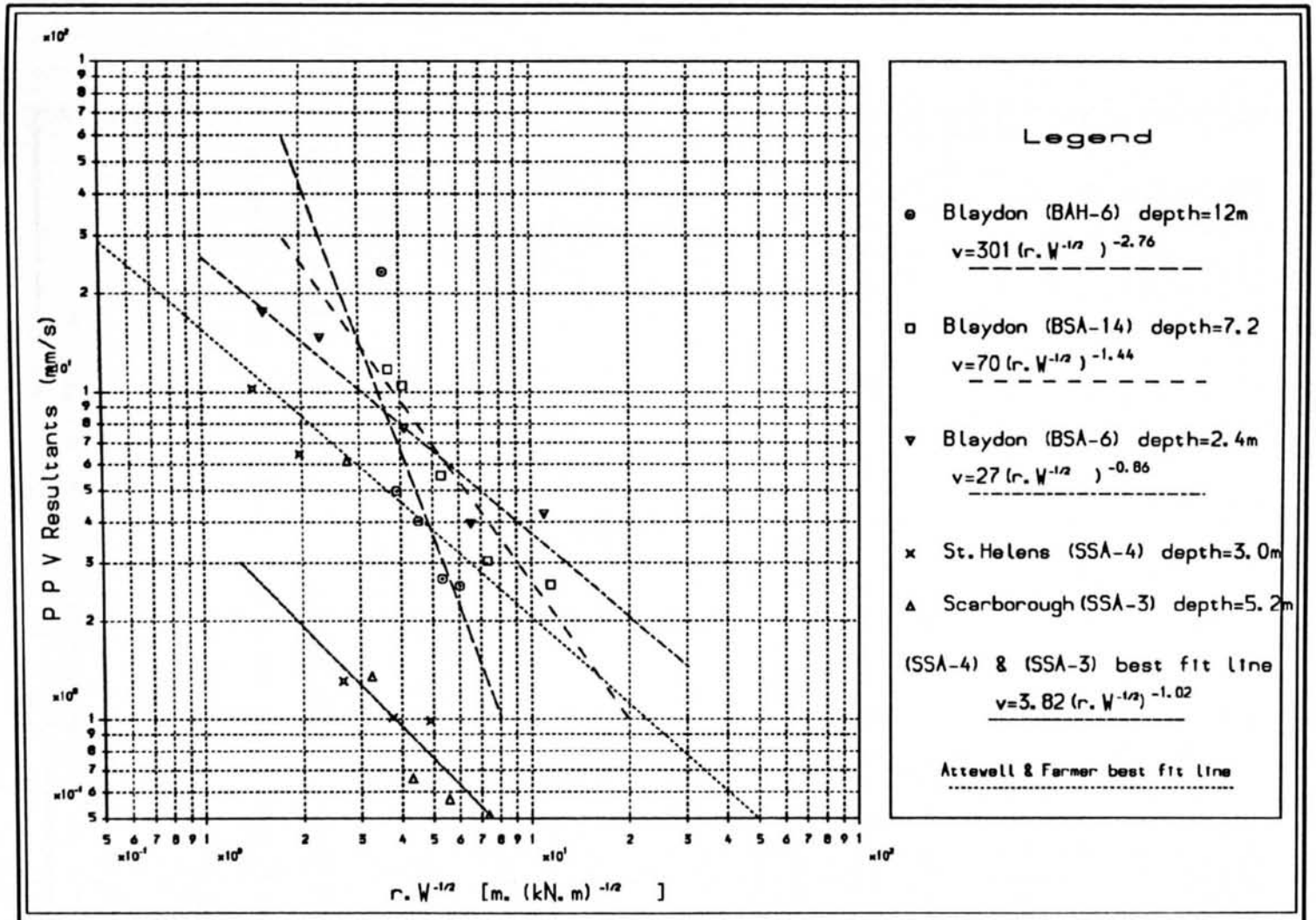

Figure (6.12) Air-hammer, Steel-piles

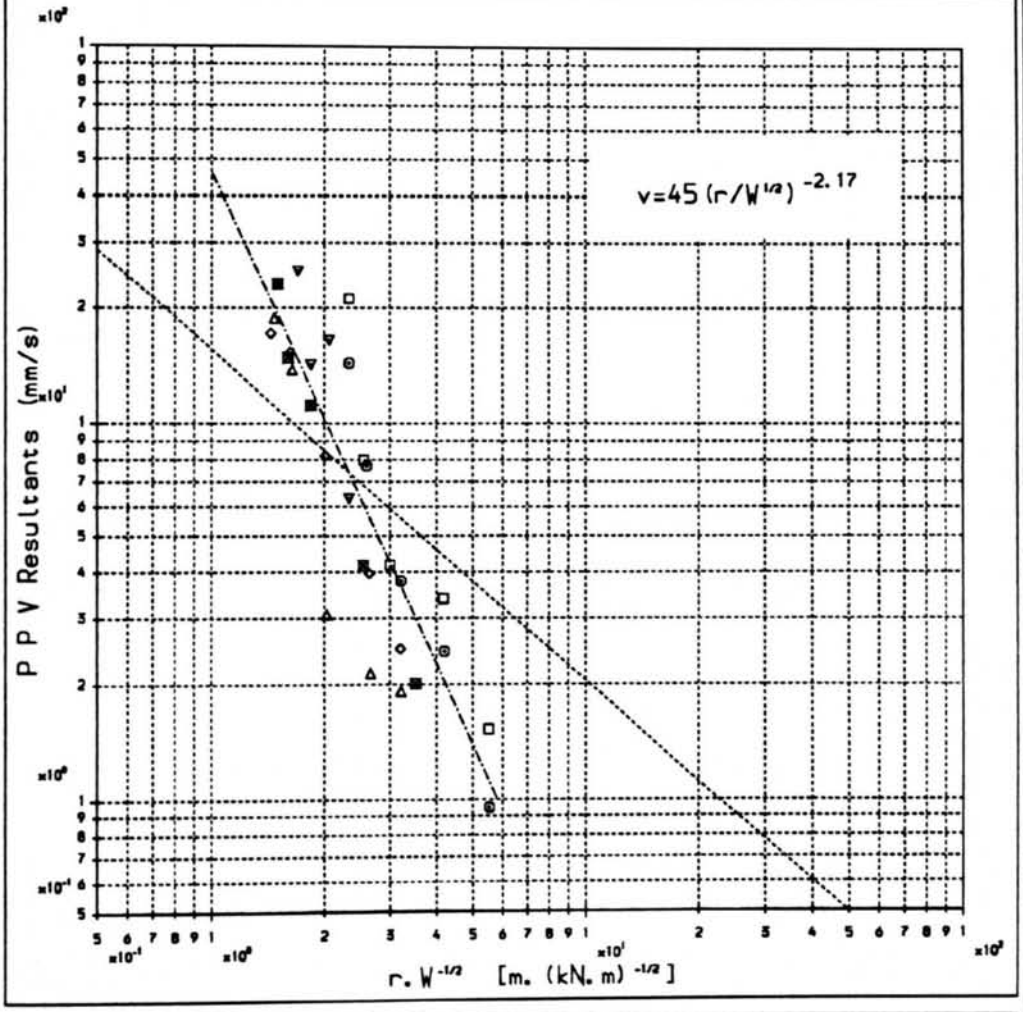

Legend

- Selby (SCD-4) depth=9.0m
- Selby (MCD-6) depth=8.8m
- Whalley (WAL-11) depth=8.0m
- Newark (NDH-6) depth=9.0m
- Newark (WDH-12) depth=8.8m
- Newark (NHD-6) depth=9.2m

Attewell & Farmer best fit line

Figure (6.13) Drop-hammer Records

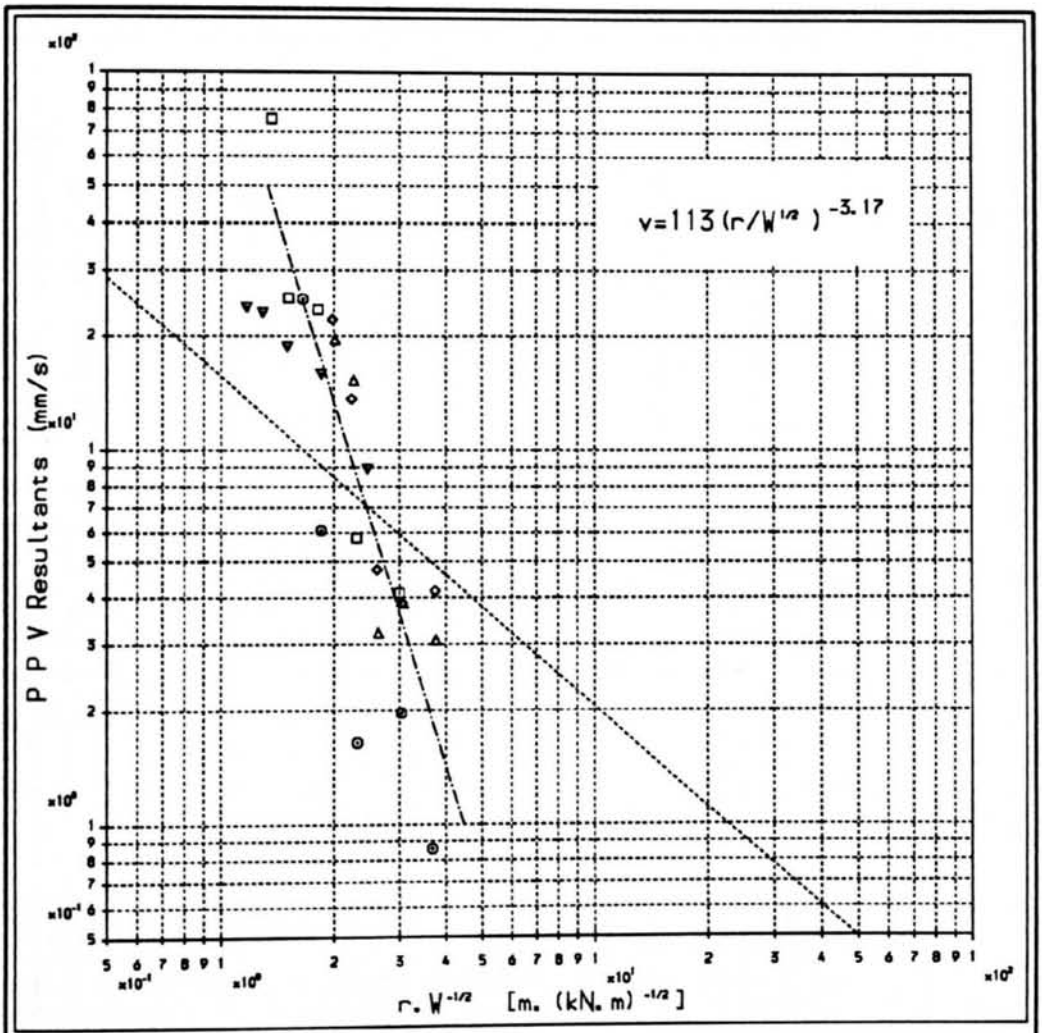

Legend

- Edinburgh (ESH-8) Hydraulic-hammer depth=8.7m
- Waltham Cross (WSH-11) Hydraulic-hammer depth=8.0m
- St. Annes (ANS-5) Hydraulic-hammer depth=9.5m
- Grimsby (GRD-2) Diesel-hammer depth=11.2m
- Grimsby (GRS-6) Diesel-hammer depth=11.0m

Attewell & Farmer best fit line

Figure (6.14) Impact-hammers, Sheet-piles

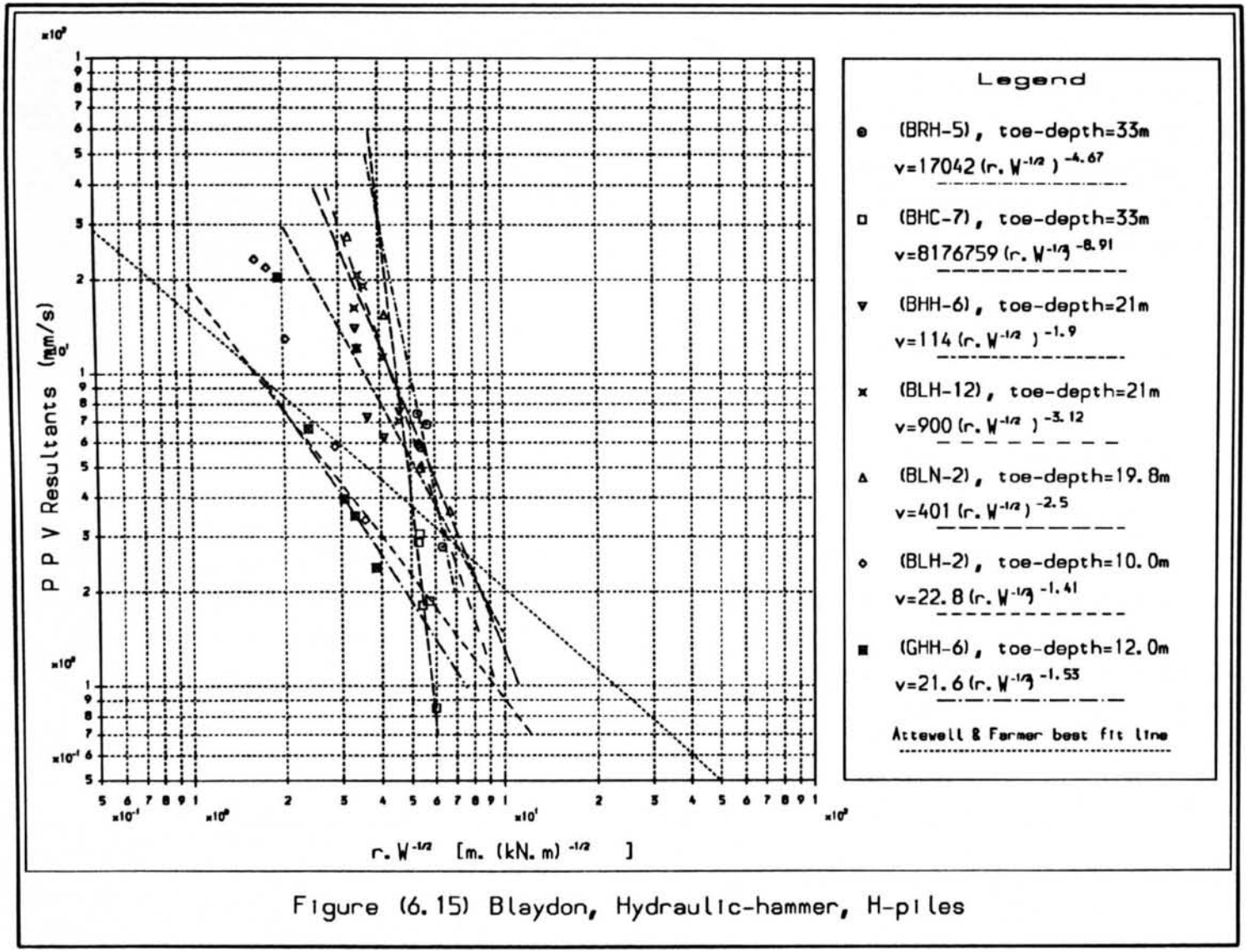

Figure (6.15) Blaydon, Hydraulic-hammer, H-piles

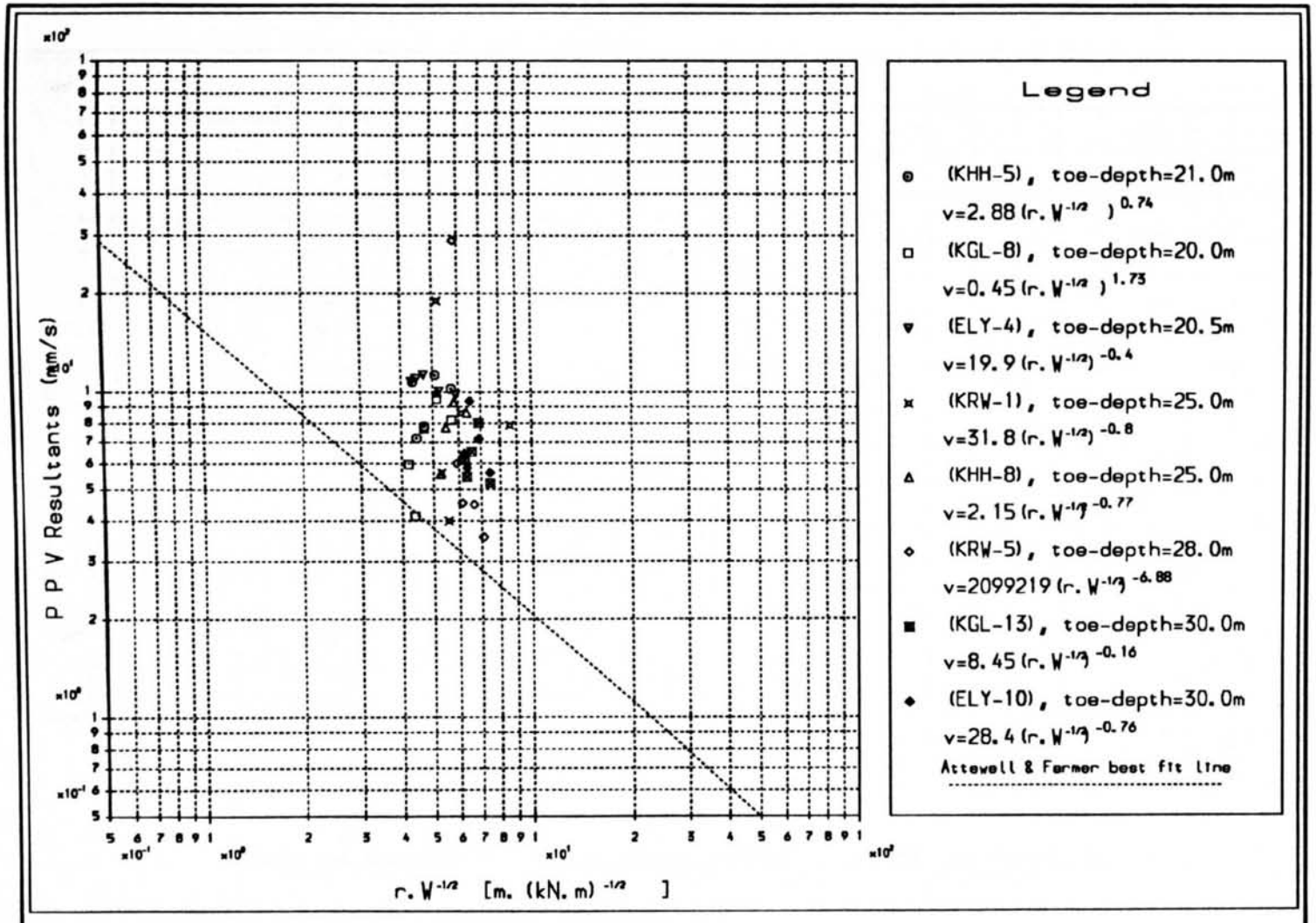

Figure (6.16) Keighley Hydraulic-hammer, H-piles

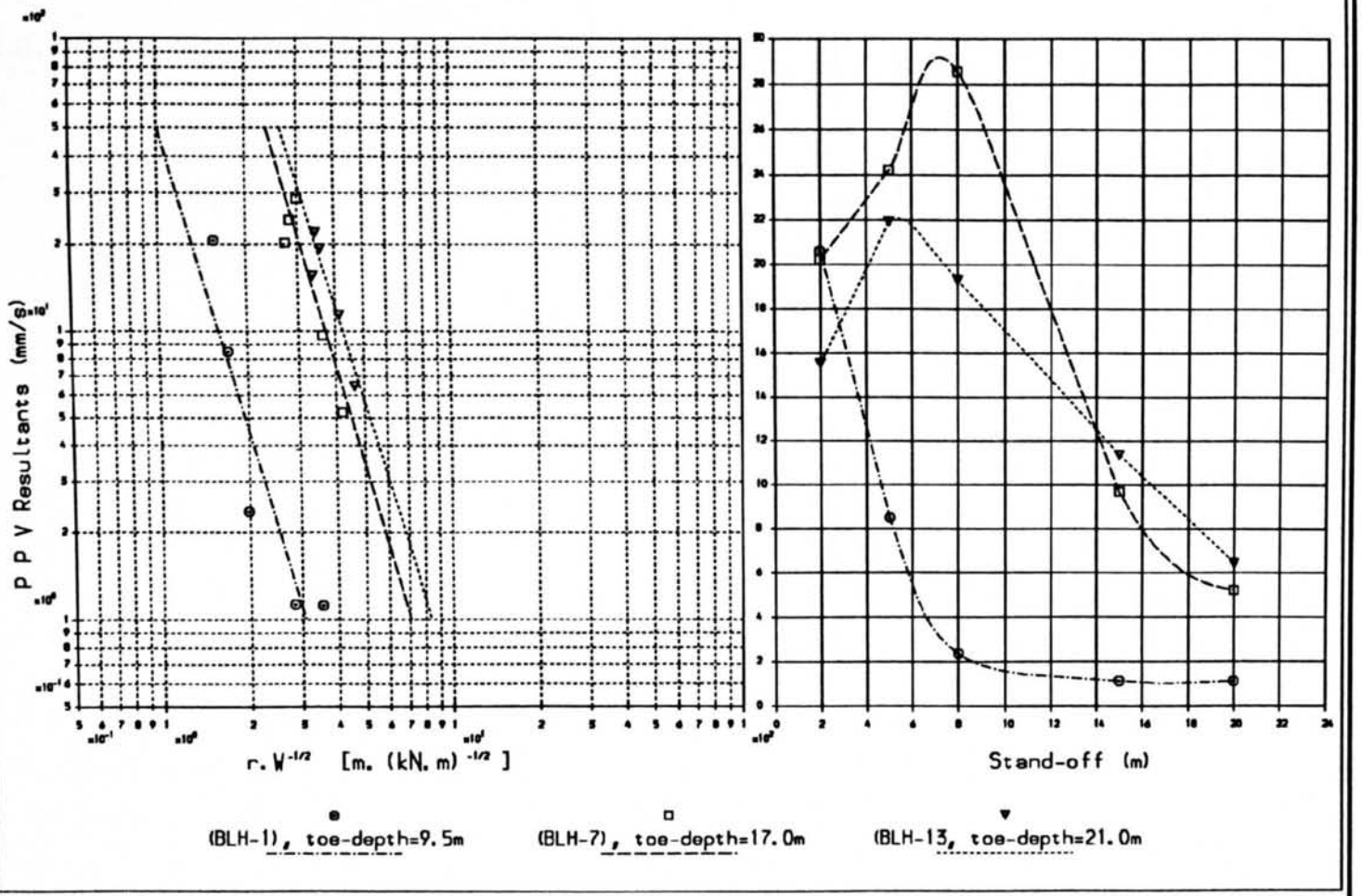

Figure (6.17) Blaydon, Hydraulic-hammer, H-pile

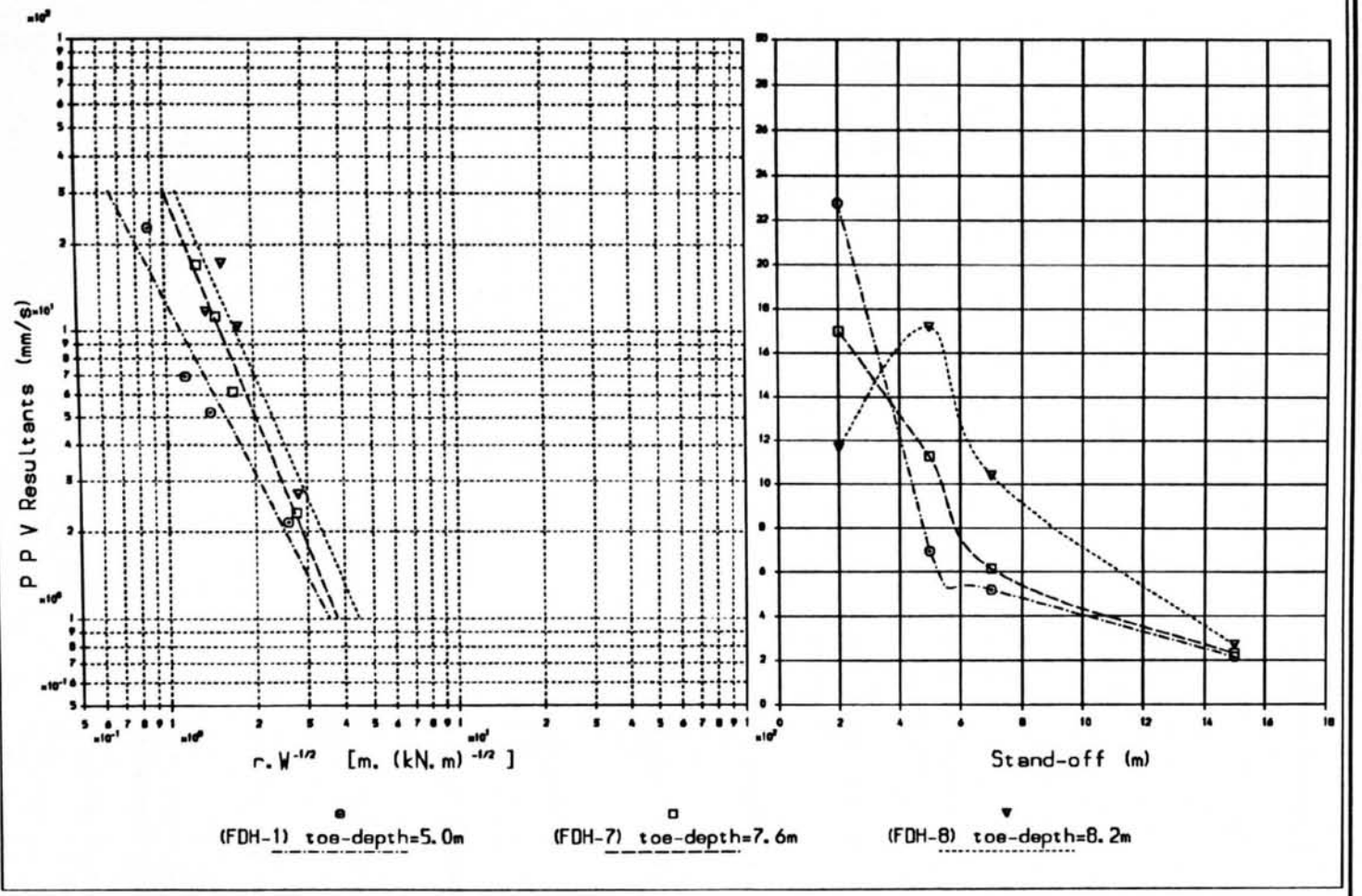

Figure (6.18) Sheffield Diesel-hammer, H-pile

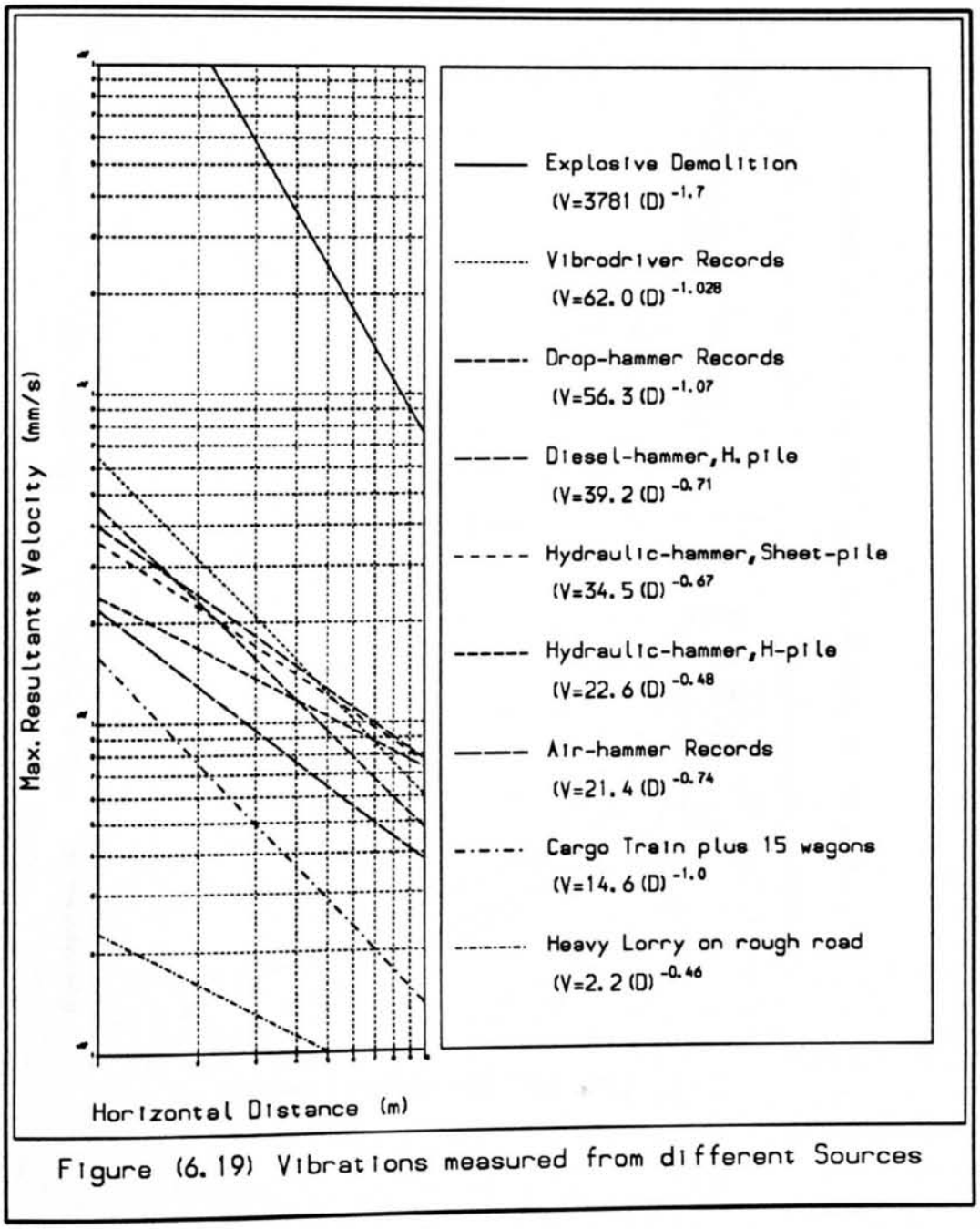

Figure (6.19) Vibrations measured from different Sources

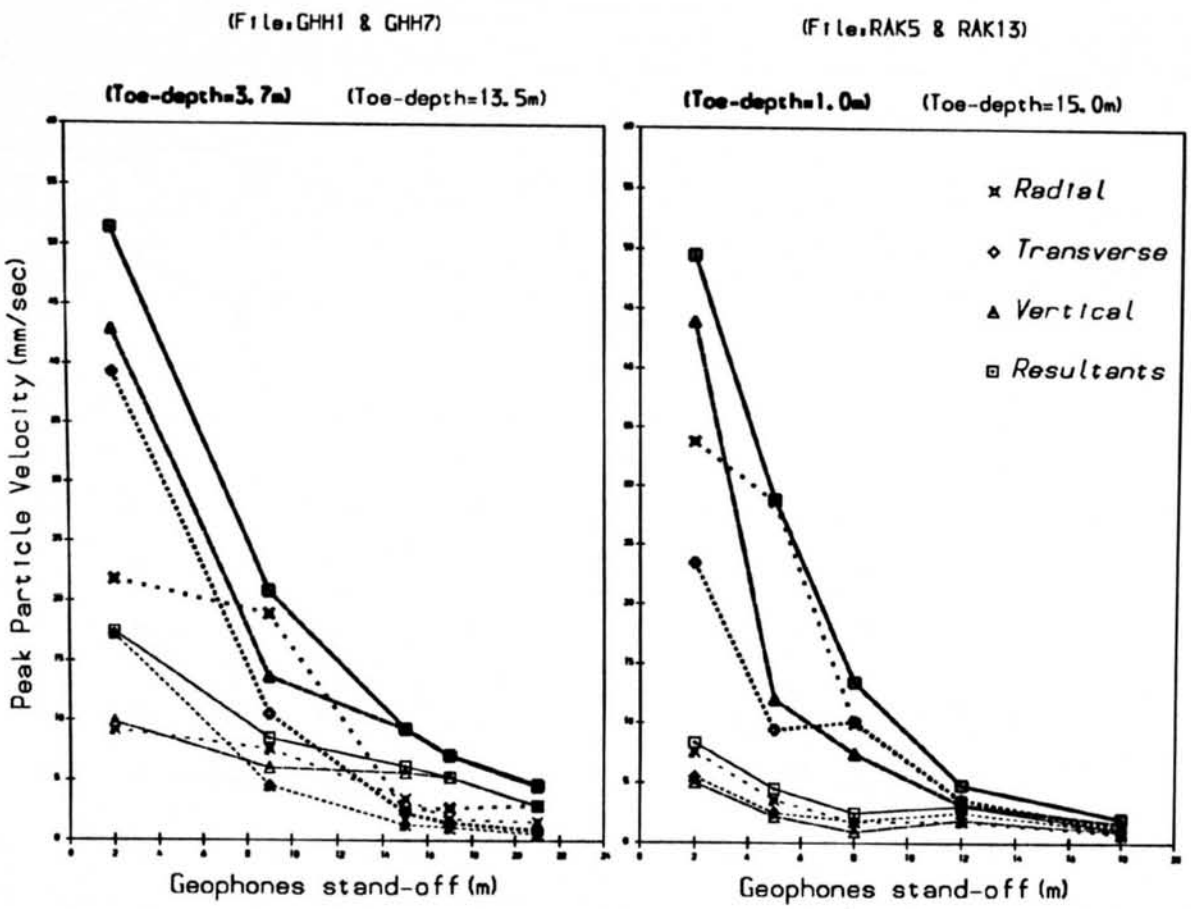

Figure (6.20) Vibration decrement with toe-depth

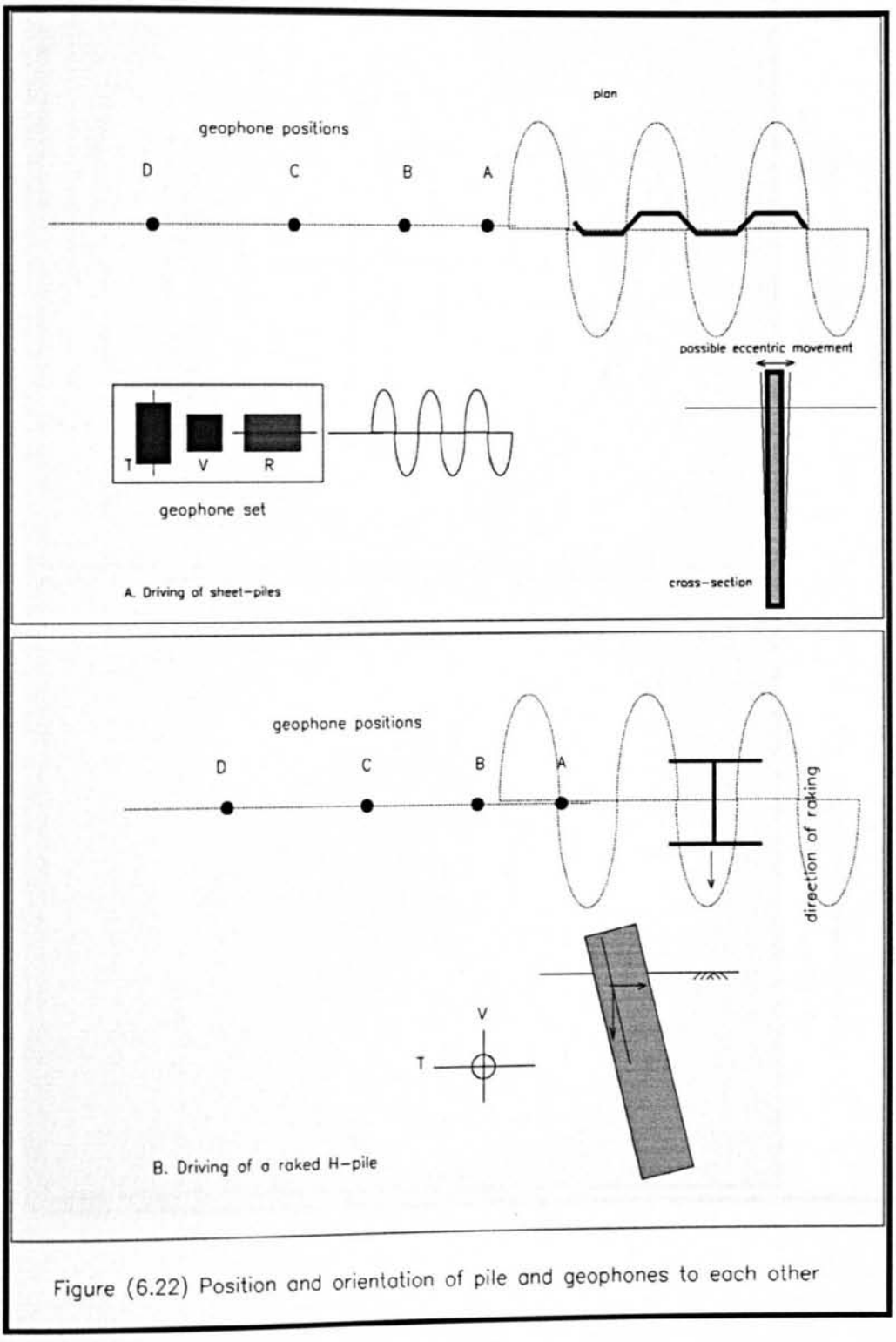

Figure (6.22) Position and orientation of pile and geophones to each other

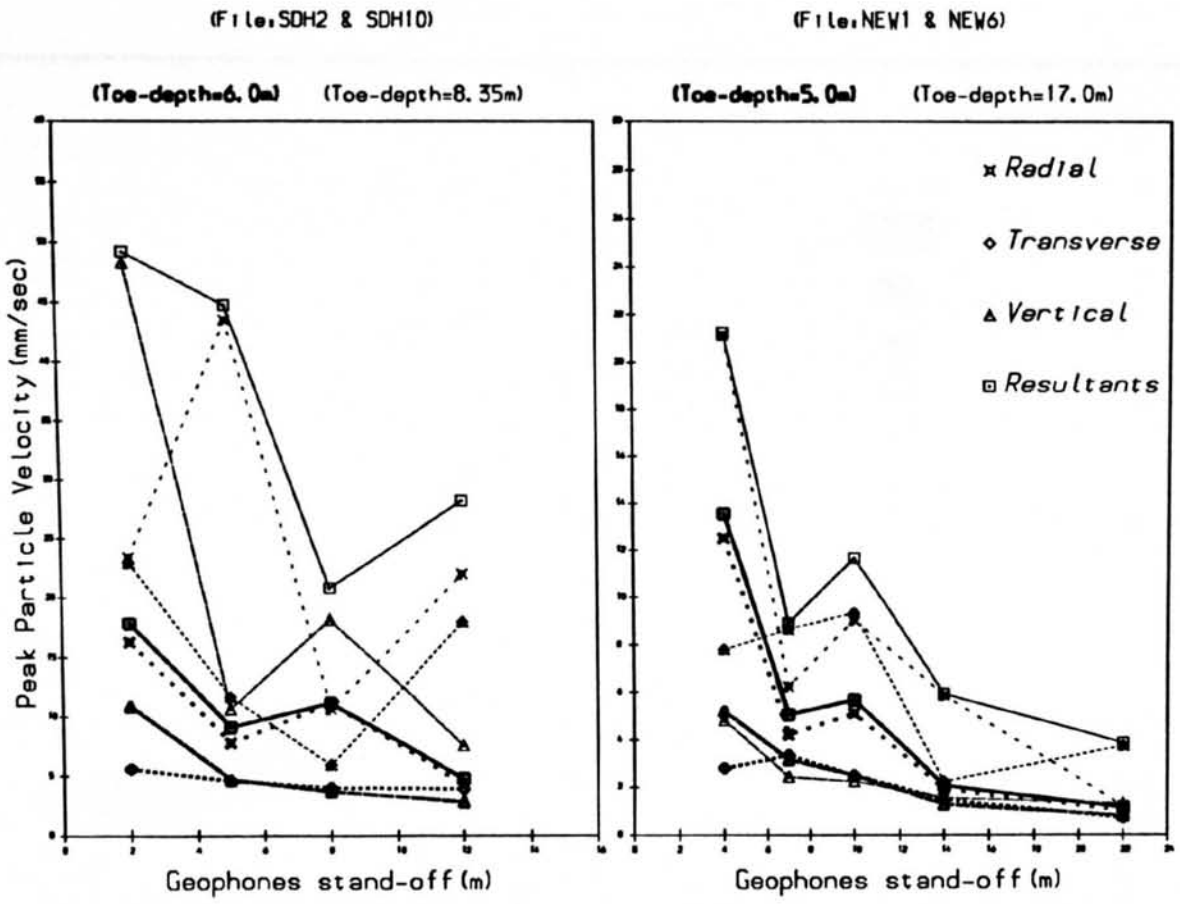

Figure (6.21) Vibration increment with toe-depth

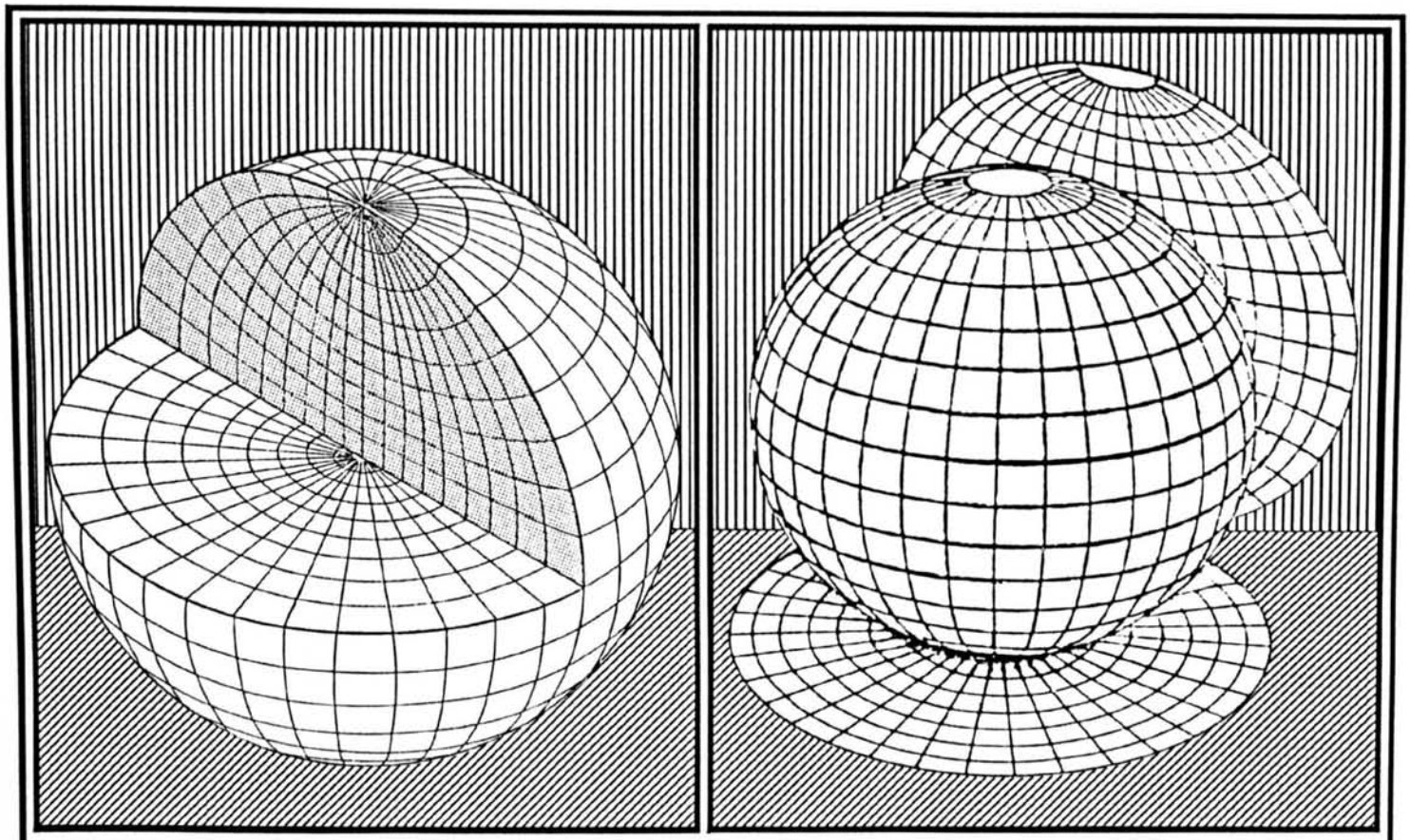

a. Equal–angle projection
after Hoek & Brown (1980)

b. Equal–area projection
after Hoek & Bray (1981)

Figure (6.23) Polar and Equatorial projection of sphere

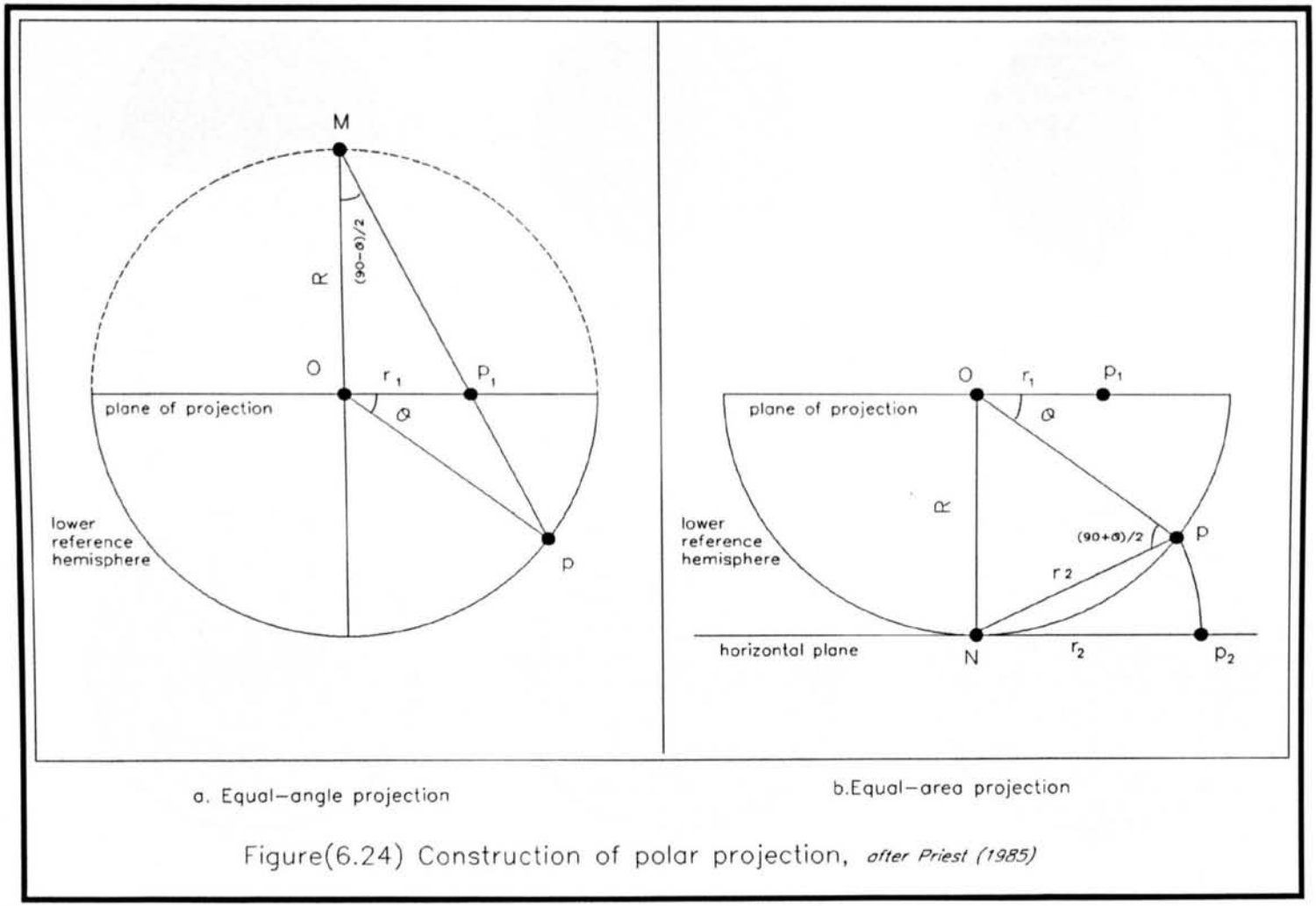

a. Equal–angle projection

b.Equal–area projection

Figure(6.24) Construction of polar projection, *after Priest (1985)*

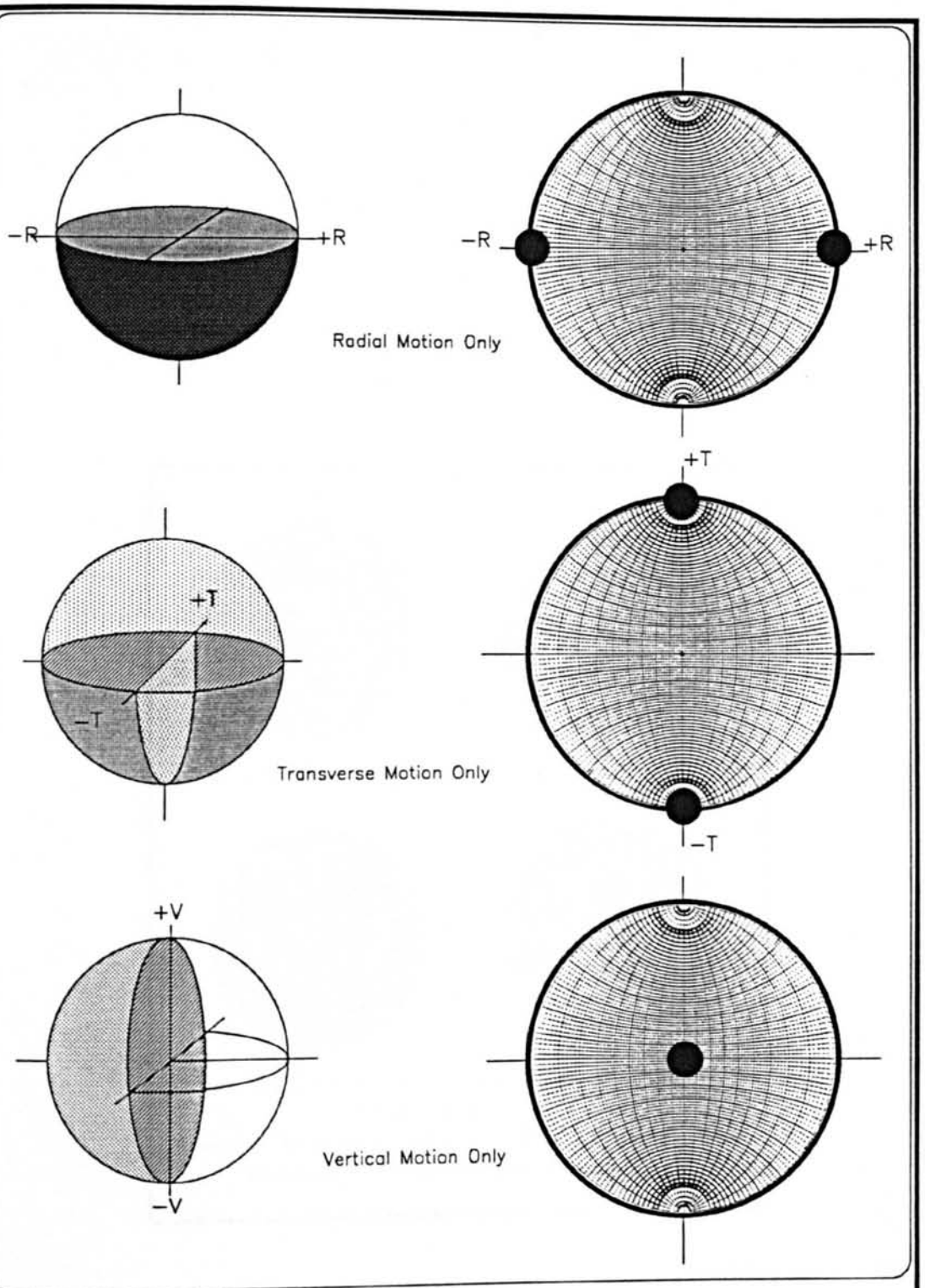

Figure (6.25) Directional motions of vibration components

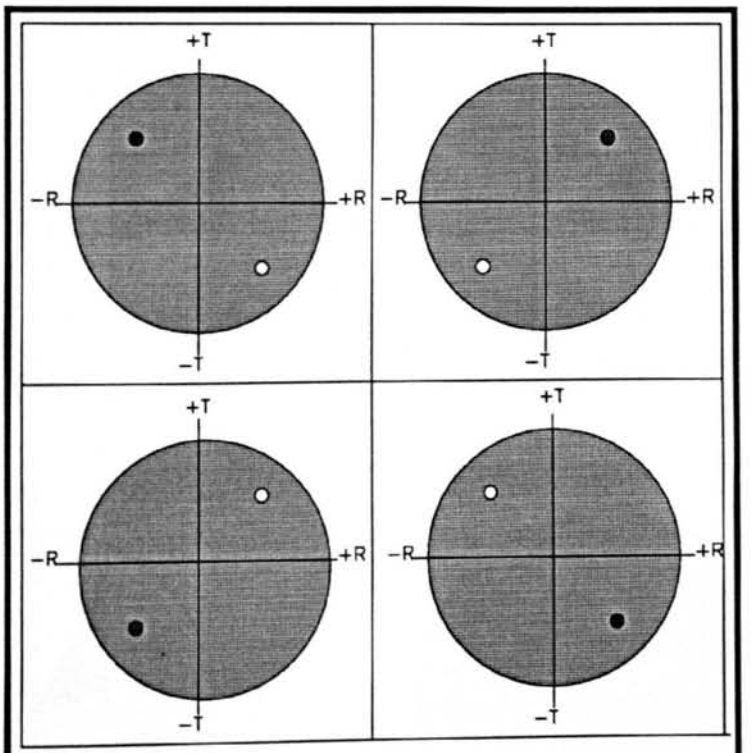

Figure (6.26)

Projection of resultant vector of equal amplitude orthogonal components of a pure sinusoidal vibration.

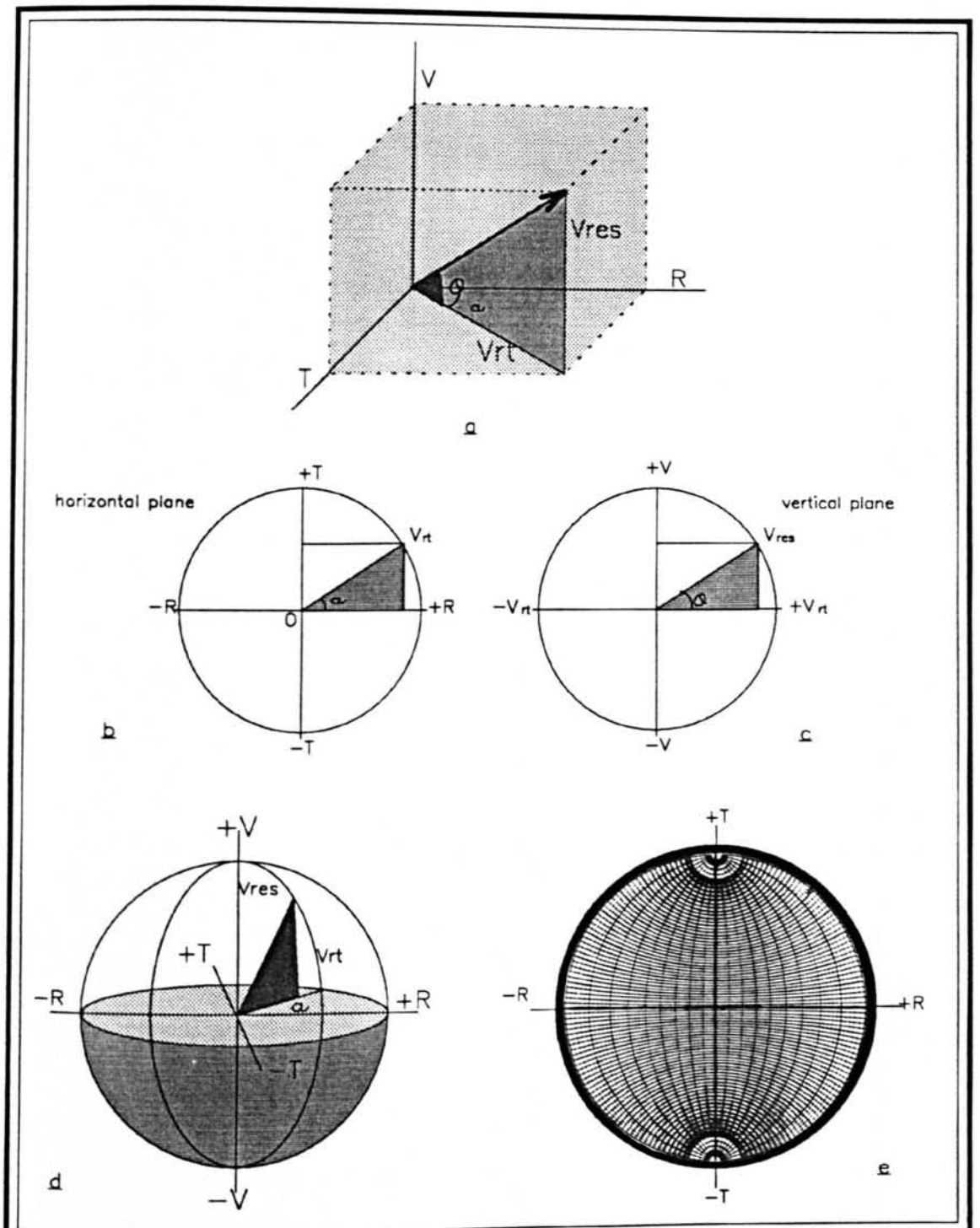

Figure (6.27) Plotting of ground vibration components

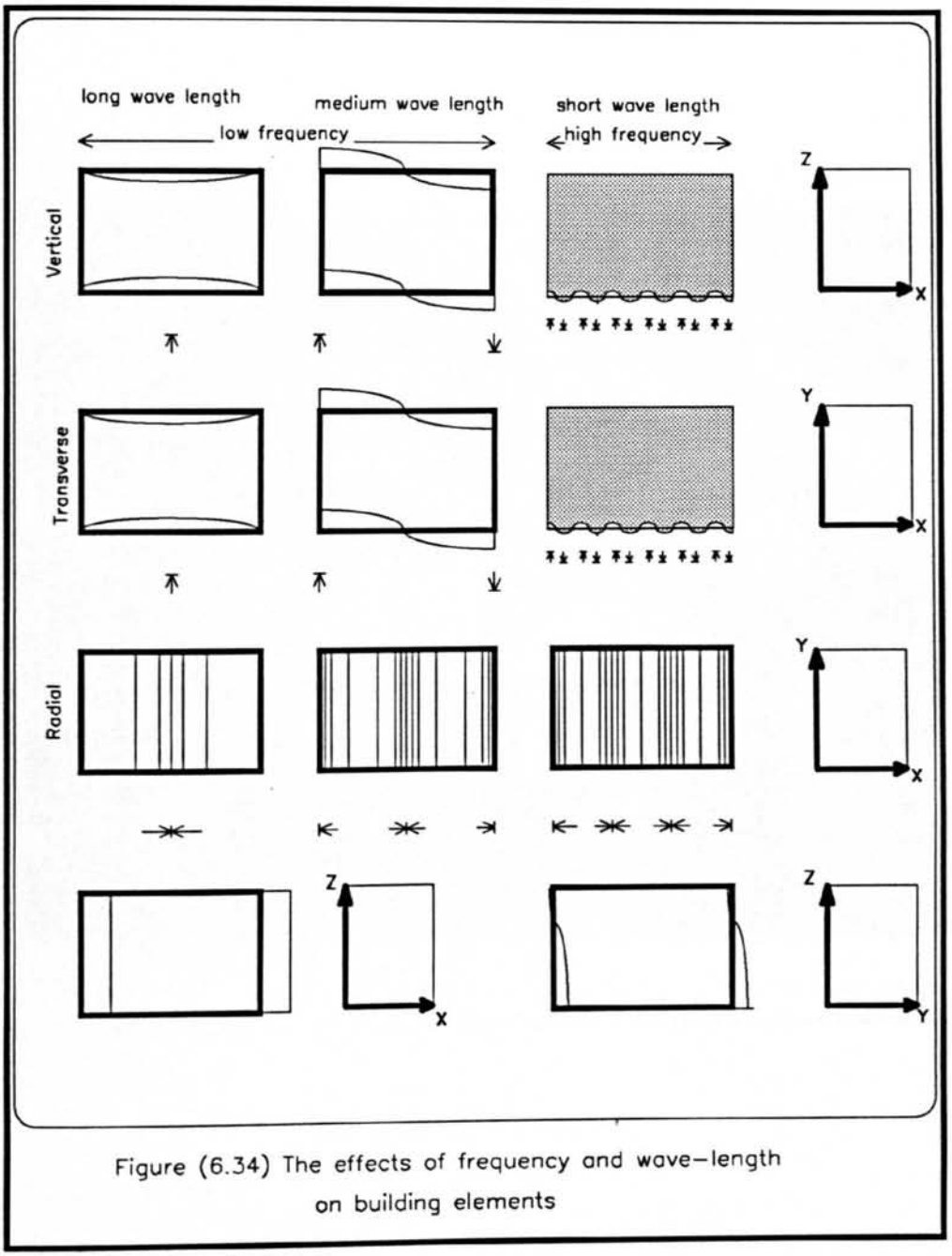

Figure (6.34) The effects of frequency and wave-length on building elements

Plate (6–1)
Right–hand rule for sense of vibration in connection with geophone positions

Chapter Seven

7. Study of Brick Wall Response to Dynamic Forces

7.1 Introduction

In order to investigate the effects of ground vibration caused by pile driving on brickwork structures, a series of field tests were carried out on brickwork walls in a site near Flitwick in Bedfordshire. The main objectives were to derive empirical relations of peak particle velocities at ground surface for a range of stand-off distances, to measure the dynamic strains on the walls, and consequently, to evaluate a safe level of vibration with respect to the risk of damage to surrounding buildings in relation to transferred energy during pile driving.

Four L-shape brickwork walls were constructed and were then instrumented with a number of:

- electrical resistance strain gauges for measuring the induced dynamic strains in the brick walls.
- glass telltales to indicate very high transient strain.
- buttons for demec† gauge readings, for indicating possible residual strain imposed in the walls.

The ground surface vibration was measured simultaneously at different horizontal stand-off distances from the pile by 15 geophones used in all other sites. The multichannel portable digital recorder PDR-2 was employed to record, store and process the captured data. A strain gauge amplifier (SGA) was specifically designed for this project and used to transfer the records of the dynamic strains from the gauges into the PDR-2 unit.

Two types of hammer, a simple winch drop-hammer and a high frequency vibrodriver, were used to drive two types of steel H-pile and sheet-pile in the ground at

---

† Demountable mechanical gauges.

different locations from the walls, to different depths of penetration and under controlled conditions. The procedure of pile driving and data recording was completed within a week.

This chapter represents the details of the programme including the site work, instrument installation, data recording and processing, analysis and discussions of the results and drawing of final conclusions. A complete set of diagrams, tables and some photographs are included at the end of the chapter. More information on soil mechanics tests are presented in Appendix(A5).

7.2 The Site

7.2.1 Site Location

A site of approximately 24m by 20m, was loaned by Dawson Construction Plant, (DCP) near Flitwick in Bedfordshire. This particular site was chosen because of its ground conditions and the easy access to the pile driving equipment including the steel piles, hammers and labourer available within the DCP yard. A schematic layout of the site is illustrated in figure (7.1).

The area was first cleared, the topsoil was stripped out and the soft subsoil was trimmed level in July 1988.

7.2.2 Ground Conditions

On 7th and 8th of August 1988, a site investigation was carried out by *Ian Farmer Associates*. The investigation comprised drilling of three boreholes to a maximum depth of 9m. The locations of the boreholes are indicated in figure (7.1b). Simplified geological conditions of the ground are shown in figure (7.2). The details of the boreholes logs are included in Appendix (A5.1) (also see Selby (1989)). The ground contains three main deposits as follows:

- soft grey-brown silty sandy clay which extends to a maximum depth of 3.0m below the ground surface.

- loose to medium yellow sand and gravel with flints and cobbles occasionally, and becoming more sandy with depth; maximum depth is about 5.6m from the ground level.
- dense light grey sand with bands of silt.

The boreholes terminate at a depth of 9m. The water table was at 2.7 to 3.0m from the ground surface.

7.2.3 Soil Mechanics Tests

A number of tests, including particle size distribution analyses, undrained triaxial tests and consolidated shear box tests, were carried out on selected samples. The soft clay near the ground surface showed quick undrained cohesions $c = 10 - 34$kPa. The uniform dense sand below the depth of 5m had a friction angle $\phi = 36^{o} - 55^{o}$ and the standard penetration tests (SPT) of this deposit gave values in the order of 80-110 blows per 270mm. Details of these tests are shown in tables (TA5-1) to (TA5-4) of Appendix (A5.1).

7.3 The Walls

7.3.1 Wall Construction

Four brick-wall units (L-shaped) were constructed on unreinforced concrete strip footings between 16th and 24th August 1988. The walls were 1.5m in height above the ground level with side dimensions of 2.0 and 1.5m (see figure (7.1b)). The strip footings were made of concrete (L30) and founded 500mm below the ground surface with dimensions of 300mm wide and 200mm deep.

Walls A and B were laid in stretcher-bond‡, using common bricks of half-brick construction, 115mm thick and with no dpc *(damp proof course)*. Wall C was bonded in similar form as in A & B, but contained a dpc at 150mm above ground level.

---

‡ Bonding is a form of alignment of bricks on-each-other in order to distribute vertical and horizontal loads over a larger area and number of bricks. Various methods of bonding are used giving special names to bond patterns (Knight (1975)).

Additionally, the vertical joints between the bricks were left open, as potential crack initiators at the dpc layer and in a layer located at 1.2m above ground level. Wall D was of single-brick construction, English bond, 230mm thick, and contained a dpc at 150mm above the ground level.

The bricks were **Bedford commons**, with a standard frog indentation, and a rather shiny dense texture to the side faces. The mortar was a nominal 3:1 mixture of soft sand to masonry cement and above the ground contained some plasticiser. The bonding strength of the brickwork was tested in the laboratory, failure being shown at a strain of approximately 30×10^{-6} under static test. The dynamic strain capacity would be expected to be higher. Details of this test is included in Appendix (A5.2).

7.3.2 Wall Instrumentation

The walls were instrumented with a number of strain gauge units, glass telltales and buttons for **demec** *(demountable mechanical)* gauges readings (see plate (P7-1)).

Each strain gauge unit consisted of a 10mm electrical resistance strain gauge, type (FLA-10-11), which was glued on to a light aluminium alloy angle and attached to a three core screened cable. The units were pre-assembled and tested in the laboratory, and on the site these were glued on to the walls. The positions of the strain gauge units on the walls were at 300mm in and down from the top corners and 300mm in and above the bottom corners above ground level, in both horizontal and vertical axes on to the wider face of the wall, and only along the horizontal axis onto the smaller face of the wall. The locations of the strain gauge units were numbered and were orientated towards the directions of the orthogonal components of the vibration axes, where gauges 1, 3, 5 & 7 were parallel to the transverse direction, gauges 2, 4, 6 & 8 in the same direction as the vertical and gauges 9, 10, 11 & 12 were in the direction of the radial axis (see figure (7.3)).

The demec-gauge buttons were glued on to the brickwork at 16 points, where each points contains two buttons glued 50mm apart on either sides of mortar joints. The positions and numbers of the points are also shown in figure (7.3).

The glass telltales were again glued on to the brickwork straddling mortar joints in locations close to the demec-gauge points (see plate (7-1)). The glass slips were 50mm long and 150mm wide and a three point bending test indicated strain capacity of some 1000×10^{-6}. Thus a single crack of 0.05mm width would be sufficient to achieve the failure strain in the glass.

The type of glue used on the wall was a metal loaded epoxy putty giving good adhesion and filling, while providing the necessary viscosity during fixing to the vertical brickwork face of the walls.

7.4 Measuring Equipment

The vibrations induced by pile driving into the ground, walls and pile were recorded by the portable digital recorder (PDR-2) unit, the data being then stored and later processed by the unit. The different stages of recording and processing the data were described in chapter four section 4.3.

The ground vibrations were measured simultaneously by five sets of geophones which were placed at different horizontal stand-offs from the driven pile. Each set included three geophone units which were oriented orthogonally for measuring the three components of vibration along the radial, transverse and vertical axes.

The dynamic strains induced in the wall during the pile driving were also recorded by the PDR-2 unit via the use of a strain gauge amplifier SGA†. The SGA was used to enlarge the output voltage of the electrical resistance strain gauges and to provide a high stability of the energising voltage. The twelve strain gauge units mounted on the wall were connected individually to the twelve channels of the amplifier which were balanced prior to each set of records. A separate 23 way 'D' connector was used to connect the output from the SGA to the PDR-2 unit. The strain signals in the SGA had already been calibrated so that the reading on the PDR-2 showed the direct strain records.

Using a pair of accelerometers and a pair of strain gauges, an attempt was

---

† The features and the operation of the SGA have been explained in section (4.2.3)

made to measure the input energy to the pile by the hammer during driving. These instruments were attached near the top of the steel H-pile some 1.5m from the pile-head. The output of the accelerometers was sent to a charge amplifier and then to the PDR2 unit while the SGA was used to transfer the signals from the strain gauges to the PDR-2 unit.

7.5 Driving Equipment

7.5.1 Driven Piles

Two types of steel pile, an H-pile and a sheet-pile, were driven during the test procedure to different depths and at different stand-off from the walls. The H-section pile was of $305 \times 305 \times 89 kg/m$, 12m long and was driven to a maximum depth of 7.0m and then extracted for the next driving. The sheet-pile was a Frodingham 3N-section 10m long and was driven to a maximum depth of 5.0m and extracted.

Location and vertical alignment of the pile was achieved by the use of a DCP guide frame which was mounted on steel beams, resting in turn on Rendhex sections lying on prepared ground.

7.5.2 Driving Hammers

An impact hammer and a vibrodriver were used throughout the work. The impact hammer was a simple drop-hammer consisting of a 3200 kg falling weight within a guide frame, and a formed steel cap capable of accepting either the above pile-section or a hardwood dolly. The hammer was suspended from the crane rig by means of steel cables and was operated directly by the crane driver in the cabin.

The drop weight was some 3 times the weight of the H-pile, and was effective in driving the pile to different depth levels. The nominal energy of the hammer was 31.4kJ for 1.0 m drop and 15.7kJ for 0.5m drop.

The vibrodriver was a high frequency type, PTC model 13HF1, powered hydraulically, with a nominal power rating of 112HP, at a maximum frequency of 38Hz. The vibrodriver achieved the desired 7.0m penetration, but only with difficulty in the denser sand. The vibrodriver was very effective in extracting the piles.

7.6 Test Procedure

The walls were tested individually in turn with a number of tests. Each test began by driving an H-pile at 15m distance from the wall corner by a drop-hammer (or vibrodriver). The measurement of the ground surface vibrations together with the dynamic strains of the wall were taken when the penetration of the pile was 3, 5 & 7m into the ground. The pile was then extracted by a vibrodriver, when the ground vibration and the dynamic strains were also measured during the early part of extraction. The tests were repeated for pile stand-offs 10, 5, 2 & 0.5m distance from the wall. Additional tests were carried out driving the sheet-pile in front of walls D & C. Figure (7.4) illustrates a complete set of the test procedure including the type of driven piles, locations of the piles from the walls, and the depth of penetration.

Wall [A] was tested during driving a 12m long H-pile by a drop-hammer. The pile was setup at 15m distance from the wall corner and the geophones were positioned on the ground surface at 2, 7, 12, 15 & 16.5m from the pile (see figure (7.5)). The pile was driven to a depth of 3.0m. Then a single 1.0m hammer drop was imparted, during which the ground particle velocities and wall strains were recorded together with pile-set per blow. A single blow of 0.5m drop was then delivered and similar records were taken. The wall was then inspected for signs of damage, either of visible cracking or of cracking of the glass telltales (laboratory tests showed that the glass had a tensile strain capacity of about 1000×10^{-6}, so that a single crack in the brickwork of some 0.05mm would cause failure of the glass slip). The Demec-gauge points were recorded periodically before and after each set of driving. The pile was then driven on to 5.0m depth and single blows of 1.0m and then 0.5m drops were delivered with measurements as before. The pile was driven to 7.0m depth and again the 1.0m and 0.5m drops were given. Finally the vibrodriver was used to extract the pile, and ground particle velocities and wall strains were recorded during the early part of the extraction.

The pile was then set up at 10m from the wall, and the geophone sets were

repositioned where a set was placed on the wall. The whole driving procedure was then repeated, and then the pile was extracted. The above procedure was repeated with the pile driven at 5.0m, 2.0m & 0.5m from the wall corner.

Wall [B] was tested following a similar procedure as described for wall [A], but with driving of the H-pile by vibrodriver. Readings were taken at 3, 5 & 7m penetration, in the normal driving mode. The reading of pile-set was taken in seconds per 0.5m penetration.

Wall [C], which contained the dpc and the deliberate gaps in perpends of two courses, was tested in the same way as wall [A], with the drop-hammer for the driving and the vibrodriver for extraction, except that the 15m distant pile drive was omitted because of the site geometry. In addition, a 10m long sheet-pile (Frodingham (3N)) was driven at 0.5m from the wall by drop-hammer where the measurements of the ground vibration and the wall strains were taken at 3m and 5m penetration depth. Plate (7-2) shows the process of extracting the H-pile by the vibrodriver.

Wall [D] was tested in a similar way to the tests carried out on wall [A], but the most distant drive was at 12.5m (rather than 15m) because of site constriction. Again Wall [D] was retested in response to driving of the 10m long sheet-pile (Frodingham, 3N). The pile was as in previous test at locations of 9.8, 5.0, 2.0 & 0.5m from the wall, and was driven by the drop-hammer to a maximum penetration depth of 5m. Figure (7.6) illustrates the geometery of the site where the pile is located 2m from the wall and positions of the geophones. Plate (7-3) also illustrates the use of a drop-hammer in driving a sheet-pile.

One additional drive of an 8m length of H-pile section was undertaken, with a pile head transducer attached. The intention was to derive an indication of energy partition in the pile, following the CASE/CAPWAP method.

7.7 Results and Discussions

The site work records, taken from the ground vibration, dynamic strains of the walls, demec-gauges, pile-set readings and pile-head measurements, are summarized and presented in tables, plots and traces, and some examples are included at the end of the chapter. Presentation of the data and discussion of the results are given in the following sections.

7.7.1 Ground Vibration Measurements

The measurements of the ground vibrations, which were taken by geophones, are expressed in terms of peak particle velocity ($mm.s^{-1}$). The data were integrated and differentiated to obtain the peak particle displacements (mm) and acceleration ($mm.s^{-2}$), respectively. The frequency dependent records (in Hz) were also derived from the relevant output traces.

As described before, the ground surface vibrations were measured during the procedure of driving piles by either drop-hammer or vibrodriver and during extracting the piles by vibrodriver. The pile was driven at five different distances from the wall, and vibration records were taken when the pile penetrated 3, 5 and 7m into the ground. When the drop-hammer was used, the height of the falling weight was adjusted to 1.0 and 0.5m drop which corresponded to nominal input energy of 31.4kJ and 15.7kJ, respectively.

a. Wall [A]

Figure (7.7a) displays three typical components of ground vibration records caused by driving a 12m long H-pile with a drop-hammer. The pile was located 15m horizontal distance from wall A and the pile toe was at 6.7m penetration. The peak particle velocity (ppv) at the ground surface was recorded simultaneously by 15 geophones which were positioned in five stations at 2, 7, 12, 15 & 16.5m from the pile (see figure (7.5)). The displays of the five sets of vibration traces taken in the radial direction of the same file are shown in figure (7.7b). The figure shows that the highest level of vibration (48.44mm/s) was recorded not by the geophone close

to the pile but by the one placed at 7m from the pile. This radial velocity peak is often observed in different sites, and a full discussion of this matter was given in section (6.2)♠. Figure (7.8) illustrates the attenuation of peak particle velocity with respect to the horizontal stand-off for three sets of records taken at different penetration depths of 3, 5 & 7m. It can be seen that, for the shallower depth, the attenuation of the ppv's has a more uniform curve in which the amplitude of vibration decreased with the increase of distance from the source. However, when the pile penetrates deeper (eg. 7m), a non-uniform attenuation could be observed in the vibration records taken in the radial direction.

Some of the recorded peak particle velocities and of derived peak particle displacements and accelerations are displayed in tables (T7-6) to (T7-14). In addition, a complete set of ppv records together with the wall dynamic strain measurements for wall A, at a maximum penetration depth of 7m, are given in tables (T7-15) to (T7-19).

b. Wall [B]

The vibrodriver was used to drive the 12m long H-pile in the selected distance (as before) from the wall B. Figure (7.9a) displays three sets of typical sinusodial characters of vibration traces caused by the vibrodriver. Again the radial wave record shows the largest magnitude of vibration in comparison to the vertical and the transverse waves. A display of four sets of vibration taken in the radial direction is illustrated in figure (7.9b). The figure shows a uniform decrement in vibration amplitudes with respect to the increase of the horizontal distance from the pile location. A comparison of vibation attenuation of three records taken at 3, 5 & 7m is displayed in figure (7.10). As before, the attenuation was more uniform at a shallower pile penetration than at a deeper pile penetration.

Summaries of the peak particle velocities, accelerations and displacements are listed in tables (T7-20) to (T7-24). Also, records of ppv's together with strains

---

♠ Employment of method-3 of that section can give a reasonable answer to the above behaviour of the vibration

measured for 7m penetration depth for all five driving locations are displayed in tables (T7-25) to (T7-29).

c. Wall [C]

Some of the results recorded during driving an H-pile by the drop-hammer close to wall C are shown in tables (T7-30) to (T7-33). Two examples of the ground vibration traces are shown in figures (7.11a) and (7.11b). It can be noted that the vibration was dominated by the radial wave where a maximum of 43mm/s was recorded by a geophone located 5m from the pile position. Examples of attenuation curves of ppv's versus horizontal stand-off for different depths of penetration are shown in figure (7.12). Again, the attenuation curve follows the same patterns as described for wall A.

The ground vibration was also measured during driving a 10m long sheet-pile (3N), 0.5m from wall C by the drop-hammer. The recorded results are summarised in table (T7-43). Transverse waves were the dominant vibration with a largest level of 47.7mm/s.

d. Wall [D]

Finally, the ground vibration was measured during driving both H-pile and sheet-pile at selected distances from wall D. Some the results are displayed in tables (T7-34) to (T7-42). Examples of three and five sets of vibration plots are shown in figures (7.13) and (7.14), respectively. As in other records, the vibration was dominated by the radial wave, and the overall levels of vibrations were similar to those recorded in front of other walls. The attenuation of vibration with respect to horizontal distance for three records taken at different depths of penetration is displayed in figure (7.15) which shows a rather flat attenuation over a narrow stand-off band.

Examples of vibration plots caused by driving a Frodingham 3N sheet-pile by a drop-hammer are shown in figures (7.16a) and (7.16b). The records showed similar features to those obtained from the driving the H-piles.

e. Summary of the vibration results

By reviewing the ground vibration results discussed above and presented in tables and graphs, the following topics are considered below:

Drop-height

A summary of vibration data recorded at different toe-depths by different drop heights is displayed in table (T7-44). The pile was located 10m from wall A. The following points can be derived from the table and which could also be implied from other drop-hammer records.

- Despite the difference in the falling height of the drop-hammer in which the nominal input energy was varied from 31.4kJ for 1.0m drop to 15.7kJ for a 0.5m drop, the recorded peak particle velocities showed little difference in magnitude.
- The magnitude of the propagation energy in the ground, in terms of $\sqrt{W}/r$ for the 0.5m drop was in the order 72% of that generated by the 1.0m drop.
- The ppv amplitudes recorded at shallower penetration depths were almost the same for both drop heights, but at 7m toe depth with a dense sand deposit and where the soil resistance to driving increased, the vibrations recorded by the 1.0m drop showed a larger amplitude.
- The speed of driving was faster with the 1.0m drop, where the pile-set per blow was double that achieved by the 0.5m drop. This could suggest that the drop-hammer was more efficient at a 1.0m drop.

Ground conditions

There was a general trend of increasing the magnitude of peak particle velocities as a function of pile toe-depth with the largest ppvs occurring when the pile toe was at 7m and reduced as the depth was at 5m and 3m. This trend is not universal, when the geometric damping is considered in which a higher amplitude of ppvs would be expected at a shallower toe-depth. The main factor which may affect this

trend is the ground conditions. The density and stiffness of the ground increased rapidly with depth[⊘]. This was also indicated by the pile-set per blow, so that a higher proportion of energy was transmitted into the ground from the deeper pile penetrations. Referring to table (T7-44) the maximum amplitude of particle velocity recorded at 5m stand-off, by a 1.0m drop and at different pile-toe depths of 3, 5 & 7m were 10.7, 36.0 & 58.3mm/s, respectively. The records taken during the operation of the vibrodriver showed a smaller differences in ppvs amplitude (see table (T7-45)). It can be assumed that the vibrodriver caused some liquefaction in the ground which reduced the strength of the stiffer deposites.

Analysing the vibration records according to method-3, discussed in section (6.2), helps to estimate the vibration amplitude at the ground surface. A list of calculations of the time arrivals for both the surface and the body waves is presented in the table (T7-1). The velocity of the body wave, $c = 350m/s$, is obtained from figure (7.8).

Table (T7-1)

Horizontal distance (m)	Arrival time			
	R-wave (sec)	Body-waves (sec)		
		d=3m	d=5m	d=7m
2.0	0.087	0.097	0.065	0.048
5.0	0.035	0.060	0.050	0.040
10.0	0.017	0.033	0.031	0.029
11.5	0.015	0.029	0.028	0.026

The above table suggests that a maximum vibration amplitude can be expected at 2-4m horizontal distance when the pile toe is at 3m and 5m depths and at 5-7m when the pile toe is 7m deep. The above table should be used with table (T7-44) to compare and study the vibration data recorded at different stations.

[⊘] According to the borehole logs (fig.7.2), the ground consisted of soft silty sandy clay (0-2.5m), medium dense sand and gravel (2.5-5.5m), and dense uniform sand (below 5.5m)

Evaluation of vibration attenuation

The logarthmic least squares regression analysis is used for the evaluation of the ground vibration attenuation. The following form of analysis was required by British Steel who financially supported this series of tests. The variables considered in this analysis are the nominal input energy of the hammer, the pile-toe depth and the locations of the geophones from the pile. The general attenuation equation is expressed in the following form:

$$v = k\left(\frac{\sqrt{W}}{r}\right)^n$$

where	v	: peak particle velocity	mm/s
	W	: the nominal hammer input energy	N.m
	r	: radial distance from the pile-toe to the geophone	m
	k	: intercept of the regression line	mm/s
	n	: slope of the regression line	

Many sets of ground vibration data recorded during the operation of the drop-hammer and the vibrodriver are analysed by the above equation.

The regression analysis of vibration data recorded from the driving of an H-pile by the vibrodriver, some 10m from wall B and at different toe-depths of 3, 5 and 7m, gives the following attenuation equation:

$$v = 1.48\left(\frac{\sqrt{W}}{r}\right)^{1.10}$$

The gradient of the line is 47°. The graphical presentation of the above equation is displayed in figure (7.17). The figure shows a uniform vibration attenuation with respect to different toe-depths. The line coincided with the Attewell and Farmer$^{\odot}$ upper bound line and plots well above their best fit line.

$^{\odot}$ Attewell and Farmer (1973) defined the following emperical attenuation equations:

best fit line $v = 0.75(\sqrt{W}/r)$

upper limit line $v = 1.5(\sqrt{W}/r)$.

The least squares regression method is also used to analyse the ground vibration data recorded from the driving of an H-pile by a three tonne drop-hammer. The pile was located 10m from wall A and the results of the regression analyses with respect to different toe-depths and different drop heights are presented graphically in figure (7.18) and a summary of the results are also listed in the following table:

Drop-hammer Operation Ram weight (3200kg), H-pile (305 × 305 × 89kg/m)			
Drop-height=0.5m			
toe-depths	attenuation equations	correlation coefficients	gradients
3.0	$v = 0.09\left(\frac{\sqrt{W}}{r}\right)^{1.63}$	r=0.99	58°
5.0	$v = 0.95\left(\frac{\sqrt{W}}{r}\right)^{1.26}$	r=0.96	52°
7.0	$v = 9.13\left(\frac{\sqrt{W}}{r}\right)^{0.53}$	r=0.59	28°
Drop-height=1.0m			
toe-depths	attenuation equations	correlation coefficients	gradients
3.0	$v = 0.04\left(\frac{\sqrt{W}}{r}\right)^{1.65}$	r=0.99	59°
5.0	$v = 0.59\left(\frac{\sqrt{W}}{r}\right)^{1.23}$	r=0.96	51°
7.0	$v = 4.45\left(\frac{\sqrt{W}}{r}\right)^{0.76}$	r=0.69	37°

The above table and the plotted data in figure (7.18) show a rapid vibration attenuation for shallow pile-toe penetration and a slower attenuation for deeper penetration. This indicates a prediction of a higher level of vibration amplitude with greater distance for deeper toe-depths than for shallower toe-depths. The above information also show that the variation of drop-height increased the values of the intercepts but the gradient lines were almost the same. The regression lines of the 3m and over 5m toe-depths were plotted below and above Attewell and Farmer best fit line, respectively.

The vibrations caused by the vibrodriver were smaller than those of the drop-hammer. This is mainly because the nominal input energy of the vibrodriver is relatively small in the order of 3.4kJ/cycle in comparison to 31.4kJ of the drop-

hammer at 1.0m drop-height.

The vibration amplitudes recorded on top of the walls were large in amplitude but unreliable because the geophone sets were not securely clamped to the brick-works and started to 'chatter'. Figure (7.19) shows an example of such recorded vibration.

7.7.2 Wall Dynamic Strain Measures

As described before, twelve strain gauges were glued on each wall, but because of failure in channel eight of the strain gauge amplifier (SGA), only eleven gauges were used and the faulty channel was connected to strain gauge number 12 and 3 in walls A, B & C and wall D, respectively, where the readings from those channels were ignored. The location of the strain gauge positions and numbers have already been shown in figure (7.3).

a. Wall A

The pattern of wall dynamic strains records, taken during piling in front of wall A, is displayed in figure (7.20). The results of the strain measurements taken at different locations of pile driving from wall A, at a maximum toe-depth of 7m, are summarised in tables (T7-15) to (T7-19). It can be seen that gauge number 9 showed the largest strain of 107$\mu\epsilon$. Only very small levels of strain were observed in the front panel especially in the far end of the wall (strain gauge numbers 1-4). This indicates that very little 'plate' bending was occurring. However, the top of the wall was vibrating significantly, so that it was deduced that considerable rigid body motion was occuring, primarily in a radial direction with some rocking.

A comparison of the dominant frequency in the radial direction, measured by geophones and by strain gauge number 9 (the gauge which showed the largest strain), is given in table (T7-2). It can be noticed that the frequency obtained from the strains showed a lower magnitude than those from the ground vibration. This is consistent with the behaviour of a damped single degree of freedom system, comprising the mass of the wall, some of the surrounding soil, the stiffness of the soil

beneath and around the foundation, and some associated damping.

Table (T7-2)

Stand-off (m)	Frequency (Hz)	
pile-to-wall	*radial-wave*	*Sg.n. 9*
15.0	32.0	21.7
10.0	36.0	19.6
5.0	40.0	19.6
2.0	30.0	18.5
0.5	55.0	17.5

It is relevant to consider the relative dimensions of the wall and half wave length of the ground disturbance. If the radial wave propagation velocity is from figure (7.8) about $c = 350m/s$ and the dominant frequency of some $f = 25\text{Hz}$, then the wavelength is around $\lambda = c/f = 14m$, which is large in comparison with the wall leaf dimension of 1.5m. It also exceeds the largest dimension of most domestic structures, implying that they might '`ride`' the wave disturbances with relatively low induced strains. This argument is clearer with respect to vertical vibrations (see figure (7.21a)), when short structures fare better than long elements.

Dowding (1985) stated that, if a wave length is longer than the size of a structure, the entire structure tends to move in one direction, and when the wave length is only twice the size of the structure, the two sides of the structure move in opposite directions. He introduced the following expression to calculate the phase difference between the two sides of a structure when exposed to a sinusoidal vibration:

$$\phi = \frac{2\pi f b}{c_s}$$

Where ϕ : the phase angle difference

f : the vibration frequency

b : the building length

c_s : the shear wave velocity

According to the above reference the wave length is considered to be long when $\phi < \pi/8$ and short when $\phi = \pi$. When the above equation is used to evaluate the phase difference across the walls, ϕ is found to be equal to $\phi = \pi/5$.

The effects of wave length of vibration in increasing the risk of damage to a structure was also considered by Massarsch (1983), who expected that the most critical conditions exist when the wave length is twice the length of structure (see figure (7.21b)). He proposed the following equation to calculate the critical vibration velocity that may cause damage to structural foundations.

$$v = \frac{1.6u\lambda c_r}{b^2}$$

Where v : the maximum allowable vibration velocity

u : the critical deflection below foundation

λ : the wave length

b : the building length

c_r : the surface wave velocity

The above reference suggests $u = 5 \times 10^{-4}m$[†]; from the previous example the magnitude of the surface wave[⊙] $c_r = c_s/2 = 175m/s$, the wave length can be calculated from $\lambda = c_r/f = 7m$, and length of the wall $b = 1.5m$. Introducing these values into the above equation gives a maximum allowable vibration velocity of over 400mm/s[⊕]. This indicates a safe pile driving procedure with respect to a structure of these dimensions.

A plot of peak wall strains, in radial, vertical and transverse senses, corresponding to gauge numbers 9, 8 and 5, respectively, together with the resolved and the peak particle velocities in the above directions, are shown in figure (7.22). Some correlation is clear between strain and the ppv's.

It is significant that some very large strains of over 100×10^{-6} were observed in the wall, as a result of hard driving, and yet the demec readings and glass tell-tales did not show any cracking.

---

† This figure was obtained empirically from the failure of sensitive structures subjected to static loadings.

⊙ According to Attewell & Farmer (1973), the velocity of the surface wave is half of that of the body-wave.

⊕ This shows unreasonable value of ground vibration which is equivalent to about three times the ground gravity (g).

b. Wall B

The 12m long H-pile was driven in front of Wall-B by the vibrodriver, and, as was noticed in previous section, the magnitudes of the ground vibrations were much smaller than the ppv's observed in response to the drop-hammer.

Figure (7.23) shows the dynamic strain records taken at 2m stand-off from the wall B. The largest strain was recorded by gauge number 5, which was located in the transverse direction on the top corner of the wall. This may indicate some plate-like bending of the front leaf. A summary of the wall strain records taken at different distance from wall B are displayed in tables (T7-25) to (T7-29).

The radial peak particle velocities, at the wall base, which showed the highest amplitude, are tabulated with strains in gauge 5, and with the frequency of the signals which were closely locked to the frequency of the vibrodriver at the time of recording, in table (T7-3a).

Table (T7-3a)

Stand-off (m) *pile-to-wall*	PPV (mm/s) *radial wave*	Strain *for gauge 5*	Frequency (Hz) *w*
15.0	11.0	8.0	19.0
10.0	18.0	3.0	20.0
5.00	18.0	9.0	26.0
2.00	19.0	13.0	25.0
0.53	14.0	6.0	30.0

No clear pattern emerges as a function of stand-off distance, until evaluation of the vibration of the frequency of the excitation signal is incorporated.

If it is assumed that wall B acts as a damped single degree of freedom system, the differential dynamic strain of the ground and the wall can be calculated from:

$$\frac{\delta}{u_o} = \frac{1}{\sqrt{[(1 - w^2/w_n^2)^2 + 4\gamma^2 w^2/w_n^2]}}$$

Where u_o = maximum strain of the ground

δ = relative strain in the wall

γ =damping ratio

w =frequency of the excitation

w_n =natural frequency

If the damping ratio $\gamma = 0.2$ and the natural frequency $w_n = 20\text{Hz}$, then the modified strain gauge response in column 4 of table (T7-3b) is deduced. When these values are plotted with radial ppv's, figure (7.24), a clearer pattern emerges. As before, a plateau of strain and of ppv can be seen for driving at some 2-4m from the wall.

Table (T7-3b)

Stand-off (m) *pile-to-wall*	w/w_n	δ/u_o	$\epsilon_5/\frac{\delta}{u_o}$
15.0	0.95	2.55	3×10^{-6}
10.0	1.00	2.50	1×10^{-6}
5.00	1.30	1.16	8×10^{-6}
2.00	1.25	1.33	10×10^{-6}
0.53	1.50	0.72	9×10^{-6}

The process emphasises the importance of comparing excitation frequency with the major natural or resonant frequencies of the structure and structural elements under test.

c. Wall C

Wall C was constructed with a damp-proof-course (dpc) and, in addition, two courses of bricks were laid with open perpends. The gauges were attached across these lines of weakness. Whilst the distribution of strain around the wall panel was different from that in wall A, the maximum values of the recorded strain were not significantly larger, and in some cases were reduced. The gauge showing largest strain was now number 4, a vertical gauge spanning the dpc, located at the bottom corner of the front wall (see figure (7.3)).

Figure (7.25) illustrates some of the dynamic strain measurements recorded during the operation of drop-hammer in driving the H-pile 5m from the wall. A

maximum of $90\mu\epsilon$ was recorded by strain gauge number 4, which showed a dominant frequency of 13Hz. Again, some correlation of the ppv's records with strain are shown in figure (7.26). Also, the strains and the ppv results are tabulated in tables (T7-30) to (T7-33) and (T7-43), respectively, for the driving of the H-pile and the sheet-pile.

d. Wall D

Wall D was a single-brick construction, and was thus considerably stiffer and heavier than the other walls. The ground vibrations incident upon the wall were slightly lower than those upon wall A, but the strains were clearly smaller, showing a maximum of $30\mu\epsilon$ recorded by both gauges 8 and 9 and dominant frequency in the order of 20Hz. An example of dynamic strain measurement caused by the drop-hammer is shown in figure (7.27). A general trend of vibration attenuation in three orthogonal directions together with their relevant strain measures is presented in figure (7.28). A complete set of strain measurements of both H-pile and sheet-pile driving is displayed in tables (T7-34) to (T7-42).

e. Summary

A summary of the strain gauge measurements for all walls is shown in figure (7.29). In this figure, the maximum strain magnitudes in the radial direction of the walls are plotted against the peak particle velocities in the same direction. The figure shows that the largest strain and vibration was recorded by wall A, The vibration in terms of particle velocities recorded in front of walls C & D was smaller in magnitude than for wall A. The dynamic strain on wall C was large, while on wall D it was relatively smaller. Finally, the vibration and strain measurements recorded in front of wall B caused by the operation of the vibrodriver showed much smaller magnitudes in comparison to other walls.

7.7.3 Demec-gauge Reading

The demountable mechanical 'demec' gauge had a gauge length of 50mm and

a single division on the dial indicated a strain of 19.8×10^{-6}. Whilst the gauge is a robust and reliable instrument when used by one person, it must be recognised that site conditions do reduce the reliability of reading, and one common error when access is difficult is to misread the small $\times 100$ reading by one digit. Any varation in reading of less than 10 can probably be ignored, and changes very close to 100 should also be received with suspicion. Some of the recorded values are summarised in table (T7-4). In terms of magnitude, an observed change in gauge reading of 100 is equivalent to a residual movement of a single crack of 0.1mm.

During testing of wall A, the largest reliable change in demec-gauge reading before and after the pile driving procedure was 20 units, equivalent to a single crack of width 0.02mm or a residual strain of 430×10^{-6} (in compression). The largest strain was observed in gauge numbers 3, 5 & 16, corresponding to areas of potentially large bending strain. However, the difficulty in obtaining reliable reading gives rise to doubt that any clear indication of cracking was obtained.

Wall B was tested for its responses to vibrodriving of the H-pile. The largest reliable change in demec-gauge reading was 21 divisions, observed by gauge number 2 when the pile was driven 0.5m from the wall. The reading is equivalent to a single crack of 0.02mm width or a residual strain of 400×10^{-6}. Again, because of less reliability of the readings, no clear indication of cracking can be deduced.

Wall C which contained a dpc and, deliberately, some open perpend joints across which the gauges were mounted, was vibrated by driving of the H-pile by drop-hammer. The largest observed change in demec reading was 8 divisions, equivalent to a change in joint width of 0.008mm, an insignificant value.

Demec gauge records from wall D were generally less than 5 divisions in response to driving of the H-pile, but after driving of the sheet pile at 0.5m distance, there were indications of some possible cracking of around 0.06mm at two gauge positions. No visible evidence was observed to corroborate these suggested cracks.

In summary, the demec readings taken throughout the test programme gave little evidence of cracking. Conversely, they offered considerable evidence of absence of cracking, which is consistent with both the visual observations and with the return

to zero of the transient strain signals.

7.7.4 Glass slip (tell-tales) Observations

The use of tell-tales glasses over existing cracks can give an early warning of any possible structural movements. In this project glass slips of 150mm long and 50mm width were glued on to the brickwork straddling mortar joints to monitor any formation of strain in the wall during the pile driving procedure.

Despite strong vibrations imposed to the brick walls, no glass slip was cracked or broken throughout the driving procedure. The strain capacity of the glass slips was found in the laboratory by three point bending test to be some 1000×10^{-6}.

7.7.5 Pile-set Records

Records of pile-set were taken manually during the pile-driving procedure. The records were in mm/blow for the drop-hammer and in second/0.5m penetration for the vibrodriver. A complete set of the readings is presented in table (T7-5). Also, the pile-set records taken during pile driving in front of wall A are plotted in figure 7.30).

The table and the figure show a linear relation between the pile-set records and the toe-depth in which was reflected the conditions of the ground (see figure (7.2)). The driving was faster in soft top soil with a record of 98mm pile-set per blow and slower in stiff ground at only 8mm per blow.

The direct relation also was indicated by the pile-set records with respect to drop height. The magnitudes of the peak particle velocities were in very close range for both 1.0m and 0.5m drops. The records suggested that driving with a 1.0m drop could be more efficient because the driving operation would be faster.

7.7.6 Pile-head Measurements

An attempt was made to measure the precise amount of energy delivered to the pile head at the hammer impact by measuring the induced force and velocity

at the pile head. The magnitude of the applied force can be deduced from strain gauge reading as $F = \frac{E}{A\epsilon}$, and the proportional velocity from the differentiation of the accelerometer reading. This method which is known CASE/CAPWAP and was introduced by Smith (1960) is widely used in dynamic analysis of pile driving (see Gravare *et al* (1980) and Kightley (1980)).

A maximum strain of $380\mu\epsilon$ was recorded by a pair of electrical resistance strain gauges attached on both sides of pile web some 1.0m below the pile head. If the wave velocity in steel is 5200m/s the particle velocity in the steel can be calculated as $v = \epsilon c = 2000mm/s$.

7.8 Conclusions

Records from two different types of pile driving using two types of hammer, and the vibration effects in the ground and on instrumented brick walls, have been discussed in preceding sections. The main conclusions which were extracted from the results are summarized below:

A maximum particle velocity of 75mm/s was recorded at the ground surface close to the wall location when the pile was driven at 10m from the wall by the drop-hammer. The largest vibrations were recorded in the radial direction while those recorded in the vertical and transverse directions showed relatively smaller amplitudes. The vibrations recorded on the wall tops prior to chattering showed a maximum of 60mm/s dominated by the transverse wave.

The style of vibrations caused during driving by drop-hammer and vibrodriver were of transient and periodic nature, respectively. The vibrations recorded during the vibrodriver operation showed lower magnitudes than those by drop-hammer.

The attenuation of vibrations recorded by the vibrodriver were more linear with respect to stand-off, while those for the drop-hammer were uniform for 3 and 5m toe depth and non-uniform for 7m toe-depth.

The response of the walls to the ground vibrations comprised some rigid body components, primarily radial displacement and rotation about transverse axis, to-

gether with some little wall deformation. The two types of vibration, transient and periodic, had different effects on walls,

No cracking was observed in the brickwork, either visually or by the demec gauge readings, and none of the attached glass telltales was broken despite the very severe vibrations imposed during the pile driving.

A maximum dynamic strain of 107×10^{-6} was recorded in the brick walls. The strains recorded on wall C, with half brick construction, dpc and some open perpends showed the highest magnitude while those on wall D, with single brick construction, was the lowest.

The tolerance of the brickwork to dynamic strains of some 100×10^{-6} is impressive, especially when compared to measured static strain at failure in four-point bending of only 30×10^{-6}.

The site tests demonstrated the ability of brickwork to withstand dynamic strains due to ground vibration from pile driving without any damage. The substantial reduction in wall strains through the use of the vibrodriver in preference to the drop-hammer is clearly shown, both as a reduced level of ground vibration, and also as a lower strain to ppv ratio.

Further investigations into the dynamic strain capacity of brickwork and of plaster are needed. Tests on a complete domestic house structure in response to piling with measurement of dynamic wall strains would be of considerable value in clarifying the level of risk to structures from pile driving vibrations.

Table (T7-4)

Demec-gauge reading records

Gauge-number	1	2	3	4	5	6	7	8	9	10	11	12	13	14	15	16
Wall (A)																
pile-to-wall	change in demec-gauge readings															
15.0m	+6	-4	+14	-14	—	—	+4	+2	-5	+2	+2	+3	+4	+4	+4	+9
10.0m	-7	-2	+20	—	—	—	+3	+2	+2	-8	+3	-4	+2	-1	+6	-9
5.0m	-6	+5	-11	—	-14	—	+5	+5	+5	+12	+2	+15	0	+2	-1	+9
2.0m	+6	+2	+14	0	+15	—	-2	0	+5	+2	+15	0	+1	-2	+10	-1
Wall (B)																
pile-to-wall	change in demec-gauge readings															
10.0m	-4	-17	-23	-5	-3	-2	-8	+2	-1	+5	-2	0	0	—	0	-10
2.0m	+14	-9	—	+9	-1	+4	-1	—	+10	0	-3	0	0	0	+1	+2
0.5m	+4	+21	+9	+1	-4	+2	-3	+15	0	+3	+2	+2	+1	+3	0	+2
Wall (C)																
pile-t-wall	change in demec-gauge readings															
10.0m	-8	+3	0	-2	-2	+1	0	0	-2	-3	0	-2	-1	0	+1	-6
5.0-0.5m	0	+2	-8	-4	0	+2	-3	+5	+3	+6	0	+2	0	-1	-1	+5
Wall (D)																
pile-to-wall	change in demec-gauge readings															
12.5-0.5m	+2	+3	0	-1	-4	+2	+4	-1	+2	+1	+6	-2	+15	—	+2	+5

One division of *Demec-guage* reading $=19.8 \times 10^{-6}\epsilon$

Table (T7-5), Pile-set records

Wall (A)						
pile-to-wall		15.0m	10.0m	5.0m	2.0m	0.5m
Toe-depth	Drop	pile set per blow (mm)				
3.0m	1.0m	42	80	80	98	64
	0.5m	–	42	35	46	28
5.0m	1.0m	18	24	28	32	34
	0.5m	–	12	15	14	14
7.0m	1.0m	12	11	8	9	14
	0.5m	–	6	3	4	3
Wall (B)						
pile-to-wall		15.0m	10.0m	5.0m	2.0m	0.5m
Toe-depth		pile set in second per 0.5m penetration				
3.0m		11	5	6	30	32
5.0m		93	70	12	25	12
7.0m		277	140	85	210	25
Wall (C)						
pile-to-wall		15.0m	10.0m	5.0m	2.0m	0.5m
Toe-depth	Drop	pile set per blow (mm)				
3.0m	1.0m	–	73	45	62	62
	0.5m	–	28	20	25	32
5.0m	1.0m	–	22	27	25	34
	0.5m	–	11	12	11	11
7.0m	1.0m	–	8	11	9	10
	0.5m	–	3	5	3	5
Wall (D)						
pile-to-wall		12.5m	10.0m	5.0m	2.0m	0.5m
Toe-depth	Drop	pile set per blow (mm)				
3.0m	1.0m	65	83	56	48	58
	0.5m	30	44	25	23	23
5.0m	1.0m	26	24	20	25	23
	0.5m	12	11	9	8	10
7.0m	1.0m	11	14	10	10	9
	0.5m	4	5	4	5	3

Table (T7-6)

Disc No	File No	Date	Wall	Sheet No
PDR2-1	ABC1	17.10.1988	A	1

Pile				
Type	Length	Dimensions	Stand-off	Depth
H-pile	10m	305 × 305 × 89kg.m^{-1}	15.0m	3.0m

Hammer		
Type	Weight	Drop height
Drop	3200kg	1.0m

Ground Vibration Measurements					
Geophone-sets	A	C	B	D	E
Stand-off (m)	16.5	15.0	12.0	7.0	2.0
Peak Particle Velocity ($mm.s^{-1}$)					
Radial	3.60	3.13	5.21	7.13	35.04
Transverse	2.51	2.85	2.09	2.86	28.57
Vertical	2.84	3.19	3.50	5.92	27.44
Resultant	4.26	3.73	5.65	7.84	42.06
Peak Particle Acceleration ($mm.s^{-2}$)					
Radial	750	622	1085	1315	6607
Transverse	387	495	456	557	5190
Vertical	346	411	561	1099	4417
Resultant	799	916	1105	1740	6840
Peak Particle Displacement (mm)					
Radial	0.031	0.015	0.023	0.042	0.226
Transverse	0.014	0.015	0.015	0.023	0.137
Vertical	0.030	0.036	0.047	0.064	0.230
Resultant	0.037	0.039	0.048	0.077	0.328

Table (T7.7)

Disc No	File No	Date	Wall	Sheet No
PDR2-3	ABC4	17.10.1988	A	1

Pile				
Type	Length	Dimensions	Stand-off	Depth
H-pile	10m	305 × 305 × 89kg.m^{-1}	15.0m	5.0m

Hammer		
Type	Weight	Drop height
Drop	3200kg	1.0m

Ground Vibration Measurements					
Geophone-sets	A	C	B	D	E
Stand-off (m)	16.5	15.0	12.0	7.0	2.0
Peak Particle Velocity ($mm.s^{-1}$)					
Radial	13.23	9.12	14.44	26.43	53.57
Transverse	5.95	7.25	4.19	6.18	27.95
Vertical	7.73	7.01	7.81	17.56	26.93
Resultant	15.72	11.17	16.39	31.64	60.62
Peak Particle Acceleration ($mm.s^{-2}$)					
Radial	2137	2020	2304	5186	8317
Transverse	1103	1268	992	1172	6362
Vertical	1222	797	1159	2711	5548
Resultant	2438	2178	2570	5968	8862
Peak Particle Displacement (mm)					
Radial	0.073	0.098	0.095	0.199	0.379
Transverse	0.034	0.036	0.027	0.042	0.156
Vertical	0.069	0.046	0.065	0.128	0.265
Resultant	0.092	0.099	0.101	0.216	0.458

Table (T7.8)

Disc No	File No	Date	Wall	Sheet No
PDR2-1	ABC7	17.10.1988	A	1
Pile				
Type	Length	Dimensions	Stand-off	Depth
H-pile	10m	$305 \times 305 \times 89 kg.m^{-1}$	15.0m	6.70
Hammer				
Type		Weight	Drop height	
Drop		3200kg	1.0m	

Ground Vibration Measurements					
Geophone-sets	A	C	B	D	E
Stand-off (m)	16.5	15.0	12.0	7.0	2.0
Peak Particle Velocity ($mm.s^{-1}$)					
Radial	16.20	14.88	19.65	48.43	29.87
Transverse	8.27	5.61	4.67	5.53	20.09
Vertical	7.53	5.71	7.72	16.93	21.00
Resultant	18.92	15.86	21.27	51.33	36.52
Peak Particle Acceleration ($mm.s^{-2}$)					
Radial	2475	3019	3751	8286	5109
Transverse	1664	1301	1072	1711	5525
Vertical	1324	830	1459	2748	4752
Resultant	3006	3055	4123	8801	5649
Peak Particle Displacement (mm)					
Radial	0.093	0.140	0.138	0.262	0.236
Transverse	0.049	0.041	0.029	0.042	0.091
Vertical	0.065	0.042	0.052	0.109	0.203
Resultant	0.108	0.141	0.142	0.269	0.309

Table (T7-9)

Disc No	File No	Date	Wall	Sheet No
PDR2-3	FHD1	18.10.1988	A	5
Pile				
Type	Length	Dimensions	Stand-off	Depth
H-pile	12m	$305 \times 305 \times 89 kg.m^{-1}$	10.0m	3.0m
Hammer				
Type		Weight	Drop height	
Drop		3200kg	1.0m	

Ground Vibration Measurements					
Geophone-sets	B	A	C	D	E
Stand-off (m)	11.5	10.0[t]	10.0	5.0	2.0
Peak Particle Velocity ($mm.s^{-1}$)					
Radial	3.74	3.60	3.39	10.64	24.43
Transverse	1.91	3.90	3.65	2.86	12.50
Vertical	2.06	1.95	1.89	4.46	14.67
Resultant	3.88	5.17	3.81	10.70	25.74
Peak Particle Acceleration ($mm.s^{-2}$)					
Radial	780	637	891	2330	5532
Transverse	436	638	841	749	3255
Vertical	336	264	365	1346	5360
Resultant	791	735	971	2419	5993
Peak Particle Displacement (mm)					
Radial	0.023	0.030	0.024	0.071	0.175
Transverse	0.014	0.045	0.017	0.014	0.077
Vertical	0.021	0.024	0.026	0.043	0.048
Resultant	0.023	0.055	0.035	0.072	0.182

[t] This set of geophones was placed on the top of the wall.

Table (T7-10)

Disc No	File No	Date	Wall	Sheet No
PDR2-3	FHD2	18.10.1988	A	5

Pile				
Type	Length	Dimensions	Stand-off	Depth
H-pile	12m	$305 \times 305 \times 89 kg.m^{-1}$	10.0m	3.0m

Hammer		
Type	Weight	Drop height
Drop	3200kg	0.5m

Ground Vibration Measurements

Geophone-sets	B	A	C	D	E
Stand-off (m)	11.5	10.0[t]	10.0	5.0	2.0
Peak Particle Velocity ($mm.s^{-1}$)					
Radial	4.48	2.70	3.57	11.91	26.83
Transverse	1.90	2.32	3.54	3.05	9.55
Vertical	2.96	2.05	2.35	6.00	10.55
Resultant	4.55	3.31	4.05	13.19	27.29
Peak Particle Acceleration ($mm.s^{-2}$)					
Radial	1218	431	891	2818	6127
Transverse	397	406	1054	788	2381
Vertical	411	224	343	1251	3726
Resultant	1266	541	1296	3037	6138
Peak Particle Displacement (mm)					
Radial	0.023	0.017	0.022	0.069	0.162
Transverse	0.011	0.015	0.016	0.016	0.043
Vertical	0.017	0.018	0.022	0.033	0.046
Resultant	0.026	0.022	0.031	0.069	0.166

Table (T7-11)

Disc No	File No	Date	Wall	Sheet No
PDR2-3	FHD3	18.10.1988	A	5

Pile				
Type	Length	Dimensions	Stand-off	Depth
H-pile	12m	$305 \times 305 \times 89 kg.m^{-1}$	10.0m	5.0m

Hammer		
Type	Weight	Drop height
Drop	3200kg	1.0m

Ground Vibration Measurements

Geophone-sets	B	A	C	D	E
Stand-off (m)	11.5	10.0[t]	10.0	5.0	2.0
Peak Particle Velocity ($mm.s^{-1}$)					
Radial	15.90	14.76	14.69	35.45	40.11
Transverse	3.24	15.24	9.72	4.71	10.10
Vertical	7.45	6.94	9.71	15.29	19.90
Resultant	16.97	18.21	15.24	36.00	40.73
Peak Particle Acceleration ($mm.s^{-2}$)					
Radial	2608	2006	2818	5280	8086
Transverse	694	2012	3692	1172	2530
Vertical	1328	937	1309	2312	5318
Resultant	2697	2652	3749	5331	8511
Peak Particle Displacement (mm)					
Radial	0.114	0.111	0.117	0.249	0.357
Transverse	0.030	0.140	0.096	0.038	0.053
Vertical	0.076	0.073	0.078	0.101	0.190
Resultant	0.114	0.159	0.126	0.254	0.387

Table (T7-12)

Disc No	File No	Date	Wall	Sheet No
PDR2-3	FHD4	18.10.1988	A	5

Pile				
Type	Length	Dimensions	Stand-off	Depth
H-pile	12m	$305 \times 305 \times 89 kg.m^{-1}$	10.0m	5.0m

Hammer		
Type	Weight	Drop height
Drop	3200kg	0.5m

Ground Vibration Measurements

Geophone-sets	B	A	C	D	E
Stand-off (m)	11.5	10.0[t]	10.0	5.0	2.0
Peak Particle Velocity ($mm.s^{-1}$)					
Radial	18.67	14.67	14.02	38.42	46.74
Transverse	4.00	14.49	11.25	3.69	10.00
Vertical	8.26	6.26	9.54	14.92	17.39
Resultant	19.39	18.21	16.81	39.34	47.81
Peak Particle Acceleration ($mm.s^{-2}$)					
Radial	2856	2231	2921	6295	8355
Transverse	774	1819	3100	1038	2232
Vertical	1590	835	1653	2805	5736
Resultant	2886	2717	3435	6340	8706
Peak Particle Displacement (mm)					
Radial	0.118	0.107	0.128	0.258	0.305
Transverse	0.025	0.130	0.115	0.023	0.058
Vertical	0.072	0.060	0.077	0.112	0.165
Resultant	0.119	0.152	0.135	0.259	0.331

Table (T7-13)

Disc No	File No	Date	Wall	Sheet No
PDR2-3	FHD5	18.10.1988	A	5
Pile				
Type	Length	Dimensions	Stand-off	Depth
H-pile	12m	305 × 305 × 89kg.m^{-1}	10.0m	7.0m
Hammer				
Type		Weight	Drop height	
Drop		3200kg	1.0m	

Ground Vibration Measurements					
Geophone-sets	B	A	C	D	E
Stand-off (m)	11.5	10.0^{t}	10.0	5.0	2.0
Peak Particle Velocity ($mm.s^{-1}$)					
Radial	36.37	40.86	17.82	56.37	42.78
Transverse	8.48	75.89	18.02	5.17	8.75
Vertical	11.94	31.68	11.83	24.93	18.89
Resultant	36.57	83.70	27.13	58.27	44.22
Peak Particle Acceleration ($mm.s^{-2}$)					
Radial	6283	9543	7369	8700	7664
Transverse	1806	10373	5006	1653	2306
Vertical	2245	8170	2317	5005	6071
Resultant	6309	11224	7807	8975	7718
Peak Particle Displacement (mm)					
Radial	0.235	0.325	0.154	0.339	0.231
Transverse	0.051	0.694	0.209	0.022	0.041
Vertical	0.082	0.226	0.104	0.169	0.169
Resultant	0.235	0.711	0.221	0.347	0.275

Table (T7-14)

Disc No	File No	Date	Wall	Sheet No
PDR2-3	FHD6	18.10.1988	A	5
Pile				
Type	Length	Dimensions	Stand-off	Depth
H-pile	12m	$305 \times 305 \times 89 kg.m^{-1}$	10.0m	7.0m
Hammer				
Type		Weight	Drop height	
Drop		3200kg	0.5m	

Ground Vibration Measurements					
Geophone-sets	B	A	C	D	E
Stand-off (m)	11.5	10.0[t]	10.0	5.0	2.0
Peak Particle Velocity ($mm.s^{-1}$)					
Radial	32.99	32.67	17.82	46.81	34.39
Transverse	6.86	68.19	16.72	4.15	8.66
Vertical	9.88	28.36	9.54	22.39	16.68
Resultant	33.10	69.79	25.45	47.75	35.70
Peak Particle Acceleration ($mm.s^{-2}$)					
Radial	5655	8868	6651	8155	7568
Transverse	1588	10489	4944	1172	2251
Vertical	1889	8231	1802	4625	5234
Resultant	5737	11856	6966	8220	7598
Peak Particle Displacement (mm)					
Radial	0.197	0.325	0.166	0.278	0.156
Transverse	0.046	0.581	0.195	0.021	0.036
Vertical	0.067	0.119	0.079	0.138	0.129
Resultant	0.197	0.022	0.219	0.284	0.197

Table (T7-15)

Disc No	File No	Date	Wall	Sheet No
PDR2-2	ABC7	17.10.1988	A	3
Pile				
Type	Length	Dimensions	Distance	Depth
H-pile	12m	305 × 305 × 89kg/m	15m	6.8m
Hammer				
Type		Weight	Drop height	
Drop-hammer		3200kg	1.0m	

Ground Vibration Measurements

PPV (mm/s)

Geophone-set	A	C	B	D	E
Stand-off(m)	16.5	15.0	12.0	7.0	2.0
Radial	16.20	14.89	19.65	48.44	29.87
Transverse	8.27	5.61	4.67	5.54	20.09
Vertical	7.53	5.70	7.72	16.93	21.00
Resultant	18.91	15.86	21.27	51.33	36.52

Strain Gauge Measurement

Sg.n	Ch.n	Strain $\times 10^{-6}$	Sg.n	Ch.n	Strain $\times 10^{-6}$
1	40	1.20	7	46	2.20
2	41	1.00	8	48	3.50
3	42	1.50	9	49	14.70
4	43	1.00	10	50	6.30
5	44	3.70	11	51	4.60
6	45	1.50	12	47	—

Table (T7-16)

Disc No	File No	Date	Wall	Sheet No
PDR2-3	FHD5	18.10.1988	A	5
Pile				
Type	Length	Dimensions	Distance	Depth
H-pile	12m	305 × 305 × 89kg/m	10m	7.0m
Hammer				
Type		Weight	Drop height	
Drop-hammer		3200kg	1.0m	

Ground Vibration Measurements

PPV (mm/s)

Geophone-set	B	A	C	D	E
Stand-off(m)	11.5	10.0[t]	10.0	5.0	2.0
Radial	36.38	40.86	17.82*	56.38	42.78
Transverse	8.48	75.90	18.02*	5.17	8.75
Vertical	11.94	31.69	11.83*	24.93	18.89
Resultant	36.57	83.70	27.13*	58.27	44.22

Strain Gauge Measurement

Sg.n	Ch.n	Strain $\times 10^{-6}$	Sg.n	Ch.n	Strain $\times 10^{-6}$
1	40	2.00	7	46	3.00
2	41	2.00	8	48	10.00
3	42	2.00	9	49	65.00
4	43	3.50	10	50	20.00
5	44	6.00	11	51	10.00
6	45	3.50	12	47	—

* These vibration records were taken by high sensitive geophones Mark-product and the peak values of ppv were cut.

Table (T7-17)

Disc No	File No	Date	Wall	Sheet No
PDR2-4	FD3	18.10.1988	A	6

Pile				
Type	Length	Dimensions	Distance	Depth
H-pile	12m	305 × 305 × 89kg/m	5.0m	7.0m

Hammer		
Type	Weight	Drop height
Drop-hammer	3200kg	1.0m

Ground Vibration Measurements

PPV (mm/s)

Geophone-set	A	B	C	D	E
Stand-off(m)	6.5[t]	6.5	5.0	5.0[t]	2.0
Radial	49.05	68.82	17.82*	38.52	31.62
Transverse	77.20	39.84	18.02*	20.77	11.16
Vertical	49.39	46.43	9.63*	14.47	16.98
Resultant	89.89	70.83	27.10*	41.02	31.69

Strain Gauge Measurement

Sg.n	Ch.n	Strain $\times 10^{-6}$	Sg.n	Ch.n	Strain $\times 10^{-6}$
1	40	2.00	7	46	4.80
2	41	3.00	8	48	21.00
3	42	2.50	9	49	107.00
4	43	2.00	10	50	27.00
5	44	13.50	11	51	11.00
6	45	2.00	12	47	—

Table (T7-18)

Disc No	File No	Date	Wall	Sheet No
PDR2-5	FD10	18.10.1988	A	7
Pile				
Type	Length	Dimensions	Distance	Depth
H-pile	12m	305 × 305 × 89kg/m	2.0m	7.0m
Hammer				
Type		Weight	Drop height	
Drop-hammer		3200kg	1.0m	

Ground Vibration Measurements

PPV (mm/s)

Geophone-set	A	B	D	E
Stand-off(m)	3.5[t]	3.5	2.0[t]	2.0
Radial	49.19	59.59	31.21	22.87
Transverse	62.99	42.98	22.80	15.54
Vertical	66.70	44.00	13.92	16.08
Resultant	70.71	83.30	36.51	29.98

Strain Gauge Measurement

Sg.n	Ch.n	Strain $\times 10^{-6}$	Sg.n	Ch.n	Strain $\times 10^{-6}$
1	40	9.00	7	46	10.00
2	41	14.00	8	48	17.00
3	42	5.00	9	49	88.00
4	43	16.00	10	50	20.00
5	44	16.00	11	51	15.00
6	45	7.00	12	47	—

Table (T7-19)

Disc No	File No	Date	Wall	Sheet No
PDR2-6	FH5	18.10.1988	A	8
Pile				
Type	Length	Dimensions	Distance	Depth
H-pile	12m	305 × 305 × 89kg/m	0.57m	7.0m
Hammer				
Type		Weight	Drop height	
Drop-hammer		3200kg	1.0m	

Ground Vibration Measurements

PPV (mm/s)

Geophone-set	A	B	D	E
Stand-off(m)	2.0[t]	2.0	0.5[t]	0.5
Radial	63.27	40.40	27.06	19.27
Transverse	72.00	57.18	26.49	18.57
Vertical	62.01	49.84	24.84	36.08
Resultant	94.66	74.99	38.21	37.00

Strain Gauge Measurement

Sg.n	Ch.n	Strain $\times 10^{-6}$	Sg.n	Ch.n	Strain $\times 10^{-6}$
1	40	3.00	7	46	4.00
2	41	3.00	8	48	15.00
3	42	2.50	9	49	56.00
4	43	2.50	10	50	11.00
5	44	7.00	11	51	8.00
6	45	3.00	12	47	—

Table (T7-20)

Disc No	File No	Date	Wall	Sheet No
PDR2-8	FV2	18.10.1988	B	9
Pile				
Type	Length	Dimensions	Stand-off	Depth
H-pile	12m	$305 \times 305 \times 89 kg.m^{-1}$	15.0m	5.0m
Hammer				
Type		Model	Max.Energy	
Vibrodriver		PTC-13HF1	3.4kJ/cycle	

Ground Vibration Measurements					
Geophone-sets	B	C	A	D	E
Stand-off (m)	16.5	15.0	10.0	7.0	2.0
Particle Velocity ($mm.s^{-1}$)					
Radial	8.13	16.81	14.13	19.84	22.31
Transverse	2.19	2.55	2.32	5.35	5.09
Vertical	4.31	6.47	4.49	6.73	7.93
Resultant	8.76	17.68	14.45	19.98	23.50
Particle Acceleration ($mm.s^{-2}$)					
Radial	1085	2428	1968	2799	3822
Transverse	297	628	522	1672	1004
Vertical	654	910	753	1213	1172
Resultant	1188	2468	2044	3025	3880
Particle Displacement (mm)					
Radial	0.117	0.389	0.168	0.206	0.284
Transverse	0.024	0.017	0.032	0.036	0.042
Vertical	0.057	0.082	0.070	0.085	0.095
Resultant	0.188	0.433	0.232	0.275	0.399

Table (T7-21)

Disc No	File No	Date	Wall	Sheet No
PDR2-8	FV3	18.10.1988	B	9
Pile				
Type	Length	Dimensions	Stand-off	Depth
H-pile	12m	$305 \times 305 \times 89 kg.m^{-1}$	15.0m	7.0m
Hammer				
Type		Model	Max.Energy	
Vibrodriver		PTC-13HF1	3.4kJ/cycle	

Ground Vibration Measurements					
Geophone-sets	B	C	A	D	E
Stand-off (m)	16.5	15.0	10.0	7.0	2.0
Particle Velocity ($mm.s^{-1}$)					
Radial	4.38	11.63	15.48	18.76	22.68
Transverse	2.57	1.89	2.69	5.54	5.80
Vertical	3.23	4.62	3.81	4.55	10.55
Resultant	4.68	11.89	15.91	19.37	25.49
Particle Acceleration ($mm.s^{-2}$)					
Radial	628	2260	2418	3100	4494
Transverse	377	458	677	1403	1711
Vertical	467	726	713	663	1507
Resultant	735	2377	2458	3130	4847
Particle Displacement (mm)					
Radial	0.038	0.139	0.159	0.161	0.190
Transverse	0.026	0.018	0.037	0.052	0.045
Vertical	0.044	0.063	0.044	0.047	0.126
Resultant	0.078	0.153	0.239	0.292	0.375

Table (T7-22)

Disc No	File No	Date	Wall	Sheet No
PDR2-8	FV5	18.10.1988	B	10
Pile				
Type	Length	Dimensions	Stand-off	Depth
H-pile	12m	305 × 305 × 89kg.m^{-1}	10.0m	3.0m
Hammer				
Type		Model	Max.Energy	
Vibrodriver		PTC-13HF1	3.4kJ/cycle	

Ground Vibration Measurements					
Geophone-sets	B	C	A	D	E
Stand-off (m)	11.5	10.0	10.0^{t}	5.0	2.0
Particle Velocity ($mm.s^{-1}$)					
Radial	4.66	1.80	8.93	13.89	18.62
Transverse	1.71	11.24	2.58	3.05	5.98
Vertical	1.70	3.52	3.64	4.09	8.04
Resultant	4.73	11.36	9.10	14.64	19.63
Particle Acceleration ($mm.s^{-2}$)					
Radial	1028	506	1944	4453	5743
Transverse	416	2767	661	1172	1618
Vertical	392	672	1040	1137	2345
Resultant	1067	2779	2142	4721	5969
Particle Displacement (mm)					
Radial	0.034	0.014	0.056	0.076	0.085
Transverse	0.012	0.072	0.021	0.012	0.020
Vertical	0.012	0.023	0.015	0.026	0.044
Resultant	0.062	0.062	0.051	0.139	0.111

Table (T7-23)

Disc No	File No	Date	Wall	Sheet No
PDR2-8	FV6	18.10.1988	B	10
Pile				
Type	Length	Dimensions	Stand-off	Depth
H-pile	12m	305 × 305 × 89kg.m^{-1}	10.0m	5.0m
Hammer				
Type		Model	Max.Energy	
Vibrodriver		PTC-13HF1	3.4kJ/cycle	

Ground Vibration Measurements					
Geophone-sets	B	C	A	D	E
Stand-off (m)	11.5	10.0	10.0[t]	5.0	2.0
Particle Velocity ($mm.s^{-1}$)					
Radial	4.57	2.97	13.71	21.29	27.38
Transverse	1.62	9.85	1.21	3.05	3.39
Vertical	2.60	4.79	3.55	3.37	4.92
Resultant	4.72	9.94	14.07	21.48	27.52
Particle Acceleration ($mm.s^{-2}$)					
Radial	952	581	3023	5017	5724
Transverse	337	2070	267	788	818
Vertical	523	896	877	1175	963
Resultant	976	2110	3040	5176	5741
Particle Displacement (mm)					
Radial	0.037	0.023	0.175	0.129	0.178
Transverse	0.014	0.062	0.006	0.009	0.014
Vertical	0.016	0.036	0.023	0.026	0.028
Resultant	0.044	0.073	0.240	0.133	0.193

Table (T7-24)

Disc No	File No	Date	Wall	Sheet No
PDR2-9	FV7	18.10.1988	B	10
Pile				
Type	Length	Dimensions	Stand-off	Depth
H-pile	12m	$305 \times 305 \times 89 kg.m^{-1}$	10.0m	7.0m
Hammer				
Type		Model	Max.Energy	
Vibrodriver		PTC-13HF1	3.4kJ/cycle	

Ground Vibration Measurements					
Geophone-sets	B	C	A	D	E
Stand-off (m)	11.5	10.0	10.0^t	5.0	2.0
Particle Velocity ($mm.s^{-1}$)					
Radial	6.21	1.71	17.82	22.91	16.87
Transverse	1.81	11.15	3.41	3.97	3.04
Vertical	3.41	3.62	5.09	3.82	5.73
Resultant	6.43	11.58	18.59	23.01	17.03
Particle Acceleration ($mm.s^{-2}$)					
Radial	1370	506	4237	4134	4014
Transverse	516	3251	841	961	1023
Vertical	654	774	1157	777	1758
Resultant	1519	3279	4258	4203	4126
Particle Displacement (mm)					
Radial	0.055	0.009	0.331	0.149	0.124
Transverse	0.009	0.090	0.021	0.020	0.019
Vertical	0.026	0.030	0.036	0.022	0.021
Resultant	0.103	0.113	0.400	0.281	0.111

Table (T7-25)

Disc No	File No	Date	Wall	Sheet No
PDR2-8	FV3	18.10.1988	B	9

Pile				
Type	Length	Dimensions	Distance	Depth
H-pile	12m	305 × 305 × 89kg/m	15m	7.0m

Hammer		
Type	Model	Max.Energy
Vibrodriver	PTC-13HF1	3.4kJ/cycle

Ground Vibration Measurements

PPV (mm/s)

Geophone-set	B	C	A	D	E
Stand-off(m)	16.5	15.0	10.0	7.0	2.0
Radial	4.39	11.63	15.48	18.76	22.68
Transverse	2.57	1.89	2.69	5.54	5.80
Vertical	3.23	4.63	3.81	4.55	10.55
Resultant	4.68	11.89	15.91	19.37	25.40

Strain Gauge Measurement

Sg.n	Ch.n	Strain $\times 10^{-6}$	Sg.n	Ch.n	Strain $\times 10^{-6}$
1	40	1.00	7	46	4.00
2	41	2.00	8	48	2.00
3	42	7.00	9	49	9.00
4	43	2.50	10	50	2.00
5	44	8.00	11	51	7.00
6	45	1.50	12	47	—

Table (T7-26)

Disc No	File No	Date	Wall	Sheet No
PDR2-9	FV7	18.10.1988	B	10

Pile				
Type	Length	Dimensions	Distance	Depth
H-pile	12m	305 × 305 × 89kg/m	10m	7.0m

Hammer		
Type	Model	Max.Energy
Vibrodriver	PTC-13HF1	3.4kJ/cycle

Ground Vibration Measurements

PPV (mm/s)

Geophone-set	B	C	A	D	E
Stand-off(m)	11.5	10.0	10.0[t]	5.0	2.0
Radial	6.22	17.82	1.71	22.91	16.87
Transverse	1.81	3.41	11.15	3.97	3.04
Vertical	3.41	5.09	3.62	3.82	5.73
Resultant	6.43	18.59	11.58	23.01	17.03

Strain Gauge Measurement

Sg.n	Ch.n	Strain $\times 10^{-6}$	Sg.n	Ch.n	Strain $\times 10^{-6}$
1	40	1.50	7	46	3.20
2	41	2.00	8	48	2.00
3	42	2.00	9	49	3.50
4	43	2.50	10	50	3.00
5	44	3.50	11	51	5.00
6	45	2.00	12	47	—

Table (T7-27)

Disc No	File No	Date	Wall	Sheet No
PDR2-9	FV12	18.10.1988	B	11

Pile				
Type	Length	Dimensions	Distance	Depth
H-pile	12m	305 × 305 × 89kg/m	5.0m	7.0m

Hammer		
Type	Model	Max.Energy
Vibrodriver	PTC-13HF1	3.4kJ/cycle

Ground Vibration Measurements

PPV (mm/s)

Geophone-set	B	A	C	D	E
Stand-off(m)	6.5	6.5[t]	5.0	5.0[t]	2.0
Radial	15.30	31.44	17.82	30.22	22.49
Transverse	3.99	44.69	11.36	12.83	9.10
Vertical	4.20	6.82	8.30	11.10	7.24
Resultant	15.39	46.62	21.15	32.33	22.52

Strain Gauge Measurement

Sg.n	Ch.n	Strain $\times 10^{-6}$	Sg.n	Ch.n	Strain $\times 10^{-6}$
1	40	1.50	7	46	6.00
2	41	1.00	8	48	4.00
3	42	2.30	9	49	5.00
4	43	2.50	10	50	7.00
5	44	9.00	11	51	5.00
6	45	1.70	12	47	—

Table (T7-28)

Disc No	File No	Date	Wall	Sheet No
PDR2-10	FV16	19.10.1988	B	12

Pile				
Type	Length	Dimensions	Distance	Depth
H-pile	12m	305 × 305 × 89kg/m	2.0m	7.0m

Hammer		
Type	Model	Max.Energy
Vibrodriver	PTC-13HF1	3.4kJ/cycle

Ground Vibration Measurements

PPV (mm/s)

Geophone-set	B	A	E	D
Stand-off(m)	3.5	3.5^t	2.0	2.0^t
Radial	19.38	9.09	18.26	7.13
Transverse	6.48	18.49	6.43	7.38
Vertical	8.53	13.20	3.92	7.37
Resultant	20.45	20.46	18.42	10.96

Strain Gauge Measurement

Sg.n	Ch.n	Strain $\times 10^{-6}$	Sg.n	Ch.n	Strain $\times 10^{-6}$
1	40	1.00	7	46	5.00
2	41	1.00	8	48	4.00
3	42	2.50	9	49	5.00
4	43	2.00	10	50	7.00
5	44	13.00	11	51	7.50
6	45	2.00	12	47	—

Table (T7-29)

Disc No	File No	Date	Wall	Sheet No
PDR2-11	FV20	19.10.1988	B	13

Pile				
Type	Length	Dimensions	Distance	Depth
H-pile	12m	305 × 305 × 89kg/m	0.53m	7.0m

Hammer		
Type	Model	Max.Energy
Vibrodriver	PTC-13HF1	3.4kJ/cycle

Ground Vibration Measurements

PPV (mm/s)

Geophone-set	B	A	E	D
Stand-off(m)	2.0	2.0^t	0.5	0.5^t
Radial	8.87	3.42	14.11	4.33
Transverse	4.10	8.18	5.09	10.34
Vertical	3.05	5.28	12.76	6.55
Resultant	9.09	8.62	15.62	10.47

Strain Gauge Measurement

Sg.n	Ch.n	Strain $\times 10^{-6}$	Sg.n	Ch.n	Strain $\times 10^{-6}$
1	40	1.00	7	46	4.00
2	41	1.00	8	48	3.00
3	42	2.50	9	49	5.00
4	43	1.00	10	50	7.00
5	44	6.20	11	51	5.80
6	45	1.00	12	47	—

Table (T7-30)

Disc No	File No	Date	Wall	Sheet No
PDR2-12	FCD5	19.10.1988	C	14
Pile				
Type	Length	Dimensions	Distance	Depth
H-pile	12m	305 × 305 × 89kg/m	10m	7.0m
Hammer				
Type		Weight	Drop height	
Drop-hammer		3200kg	1.0m	

Ground Vibration Measurements

PPV (mm/s)

Geophone-set	A	B	D	E
Stand-off(m)	11.5	10.0	5.0	2.0
Radial	22.48	36.99	43.39	14.75
Transverse	5.34	15.24	13.20	10.63
Vertical	6.11	6.26	8.19	12.46
Resultant	23.75	40.05	44.57	18.67

Strain Gauge Measurement

Sg.n	Ch.n	Strain $\times 10^{-6}$	Sg.n	Ch.n	Strain $\times 10^{-6}$
1	40	1.50	7	46	19.80
2	41	5.00	8	48	25.50
3	42	25.00	9	49	25.00
4	43	81.00	10	50	16.70
5	44	29.00	11	51	3.00
6	45	2.50	12	47	—

Table (T7-31)

Disc No	File No	Date	Wall	Sheet No
PDR2-13	FCD9	19.10.1988	C	15

Pile				
Type	Length	Dimensions	Distance	Depth
H-pile	12m	305 × 305 × 89kg/m	5.0m	7.0m

Hammer		
Type	Weight	Drop height
Drop-hammer	3200kg	1.0m

Ground Vibration Measurements

PPV (mm/s)

Geophone-set	B	A	D	E
Stand-off(m)	6.5	5.0	5.0[t]	2.0
Radial	33.73	36.18	33.46	37.80
Transverse	6.39	14.40	22.24	37.95
Vertical	7.09	7.73	19.23	37.59
Resultant	34.41	39.22	38.53	61.65

Strain Gauge Measurement

Sg.n	Ch.n	Strain $\times 10^{-6}$	Sg.n	Ch.n	Strain $\times 10^{-6}$
1	40	1.00	7	46	27.00
2	41	6.00	8	48	32.00
3	42	26.00	9	49	31.00
4	43	90.00	10	50	5.30
5	44	37.00	11	51	3.00
6	45	2.50	12	47	—

Table (T7-32)

Disc No	File No	Date	Wall	Sheet No
PDR2-14	FCD17	19.10.1988	C	16

Pile				
Type	Length	Dimensions	Distance	Depth
H-pile	12m	305 × 305 × 89kg/m	2.0m	7.0m

Hammer		
Type	Weight	Drop height
Drop-hammer	3200kg	1.0m

Ground Vibration Measurements

PPV (mm/s)

Geophone-set	A	B	D	E
Stand-off(m)	3.5^{t}	3.5	2.0^{t}	2.0
Radial	49.86	25.96	31.93	70.81
Transverse	129.69	15.72	26.12	67.60
Vertical	52.62	8.17	71.16	79.29
Resultant	133.93	27.72	72.40	122.94

Strain Gauge Measurement

Sg.n	Ch.n	Strain $\times 10^{-6}$	Sg.n	Ch.n	Strain $\times 10^{-6}$
1	40	1.00	7	46	29.80
2	41	4.00	8	48	20.00
3	42	20.00	9	49	42.00
4	43	67.00	10	50	31.30
5	44	44.00	11	51	3.00
6	45	2.50	12	47	—

Table (T7-33)

Disc No	File No	Date	Wall	Sheet No
PDR2-16	FCD25	19.10.1988	C	17

Pile				
Type	Length	Dimensions	Distance	Depth
H-pile	12m	305 × 305 × 89kg/m	0.54m	7.0m

Hammer		
Type	Weight	Drop height
Drop-hammer	3200kg	1.0m

Ground Vibration Measurements

PPV (mm/s)

Geophone-set	A	B	D	E
Stand-off(m)	2.0[t]	2.0	0.5[t]	0.5
Radial	24.93	20.02	23.18	74.31
Transverse	92.06	13.63	27.87	76.62
Vertical	27.97	18.68	27.62	70.55
Resultant	93.89	29.75	30.53	123.91

Strain Gauge Measurement

Sg.n	Ch.n	Strain $\times 10^{-6}$	Sg.n	Ch.n	Strain $\times 10^{-6}$
1	40	1.00	7	46	24.00
2	41	4.60	8	48	12.50
3	42	8.00	9	49	38.00
4	43	45.00	10	50	32.50
5	44	37.20	11	51	3.00
6	45	2.50	12	47	—

Table (T7-34)

Disc No	File No	Date	Wall	Sheet No
PDR2-17	FDD5	20.10.1988	D	18
Pile				
Type	Length	Dimensions	Distance	Depth
H-pile	12m	305 × 305 × 89kg/m	12.5m	7.0m
Hammer				
Type		Weight	Drop height	
Drop-hammer		3200kg	1.0m	

Ground Vibration Measurements

PPV (mm/s)

Geophone-set	B	A	C	D	E
Stand-off(m)	14.0	12.5	10.5	5.0	2.0
Radial	14.35	32.13	17.82	28.23	18.26
Transverse	4.29	5.67	16.16	7.75	6.52
Vertical	5.84	6.45	5.75	11.56	13.57
Resultant	15.02	32.20	18.98	31.09	21.24

Strain Gauge Measurement

Sg.n	Ch.n	Strain $\times 10^{-6}$	Sg.n	Ch.n	Strain $\times 10^{-6}$
1	40	1.00	7	46	10.00
2	41	2.00	8	48	17.60
12	42	1.00	9	49	18.00
4	43	4.50	10	50	3.00
5	44	4.00	11	51	2.00
6	45	3.60	3	47	—

Table (T7-35)

Disc No	File No	Date	Wall	Sheet No
PDR2-18	FDD5	20.10.1988	D	19

Pile				
Type	Length	Dimensions	Distance	Depth
H-pile	12m	305 × 305 × 89kg/m	10.0m	7.0m

Hammer		
Type	Weight	Drop height
Drop	3200kg	1.0m

Ground Vibration Measurements

PPV (mm/s)

Geophone-set	B	A	C	D	E
Stand-off(m)	11.5	10.0	8.0	5.0	2.0
Radial	18.65	39.06	17.82	44.11	18.16
Transverse	5.05	5.11	18.01	9.97	8.93
Vertical	7.27	8.02	6.17	8.55	23.62
Resultant	19.55	39.17	24.53	45.29	24.03

Strain Gauge Measurement

Sg.n	Ch.n	Strain $\times 10^{-6}$	Sg.n	Ch.n	Strain $\times 10^{-6}$
1	40	1.00	7	46	11.00
2	41	2.50	8	48	22.00
12	42	2.00	9	49	22.00
4	43	3.50	10	50	2.50
5	44	4.00	11	51	2.50
6	45	6.00	3	47	—

Table (T7-36)

Disc No	File No	Date	Wall	Sheet No
PDR2-19	FDD19	20.10.1988	D	20
Pile				
Type	Length	Dimensions	Distance	Depth
H-pile	12m	305 × 305 × 89kg/m	5.0m	7.0m
Hammer				
Type		Weight	Drop height	
Drop-hammer		3200kg	1.0m	

Ground Vibration Measurements

PPV (mm/s)

Geophone-set	B	A	D	E
Stand-off(m)	6.5	5.0	5.0[t]	2.0
Radial	31.53	46.62	32.47	12.72
Transverse	13.72	11.24	14.68	7.77
Vertical	6.38	17.11	14.10	13.07
Resultant	31.99	47.12	35.06	17.72

Strain Gauge Measurement

Sg.n	Ch.n	Strain $\times 10^{-6}$	Sg.n	Ch.n	Strain $\times 10^{-6}$
1	40	2.00	7	46	16.20
2	41	4.40	8	48	32.60
12	42	2.00	9	49	32.00
4	43	3.50	10	50	2.00
5	44	4.00	11	51	3.00
6	45	7.20	3	47	—

Table (T7-37)

Disc No	File No	Date	Wall	Sheet No
PDR2-20	FDD26	20.10.1988	D	21

Pile				
Type	Length	Dimensions	Distance	Depth
H-pile	12m	305 × 305 × 89kg/m	2.0m	7.0m

Hammer		
Type	Weight	Drop height
Drop-hammer	3200kg	1.0m

Ground Vibration Measurements

PPV (mm/s)

Geophone-set	B	A	D	E
Stand-off(m)	3.5	3.5[t]	2.0[t]	2.0
Radial	21.57	24.48	27.51	18.72
Transverse	14.87	24.25	15.14	8.57
Vertical	7.72	11.83	15.11	20.60
Resultant	23.60	32.68	31.82	22.93

Strain Gauge Measurement

Sg.n	Ch.n	Strain $\times 10^{-6}$	Sg.n	Ch.n	Strain $\times 10^{-6}$
1	40	1.50	7	46	12.00
2	41	3.60	8	48	23.60
12	42	1.00	9	49	33.00
4	43	2.50	10	50	2.00
5	44	3.00	11	51	2.00
6	45	3.80	3	47	—

Table (T7-38)

Disc No	File No	Date	Wall	Sheet No
PDR2-21	FDD33	20.10.1988	D	22
Pile				
Type	Length	Dimensions	Distance	Depth
H-pile	12m	305 × 305 × 89kg/m	0.5m	7.0m
Hammer				
Type		Weight	Drop height	
Drop-hammer		3200kg	1.0m	

Ground Vibration Measurements

PPV (mm/s)

Geophone-set	B	A	D	E
Stand-off(m)	2.0	2.0^t	0.5^t	0.5
Radial	14.90	16.38	14.43	40.38
Transverse	15.72	34.65	21.97	128.32
Vertical	16.34	22.89	16.83	81.91
Resultant	21.32	35.80	27.73	143.32

Strain Gauge Measurement

Sg.n	Ch.n	Strain $\times 10^{-6}$	Sg.n	Ch.n	Strain $\times 10^{-6}$
1	40	1.50	7	46	27.00
2	41	2.00	8	48	13.60
12	42	2.50	9	49	36.00
4	43	1.50	10	50	5.00
5	44	12.00	11	51	3.00
6	45	3.80	3	47	—

Table (T7-39)

Disc No	File No	Date	Wall	Sheet No
PDR2-22	FDD39	21.10.1988	D	24
Pile				
Type	Length	Dimensions	Distance	Depth
Sheet-pile	10m	Frodingham (3N)	9.82m	5.0m
Hammer				
Type		Weight	Drop height	
Drop-hammer		3200kg	1.0m	

Ground Vibration Measurements

PPV (mm/s)

Geophone-set	B	A	D	E
Stand-off(m)	11.32	9.82	5.32	2.32
Radial	14.26	26.82	27.51	25.82
Transverse	4.38	4.92	11.45	8.93
Vertical	12.12	9.49	8.74	19.10
Resultant	18.17	28.62	28.41	28.74

Strain Gauge Measurement

Sg.n	Ch.n	Strain $\times 10^{-6}$	Sg.n	Ch.n	Strain $\times 10^{-6}$
1	40	1.50	7	46	13.00
2	41	2.00	8	48	10.60
12	42	2.50	9	49	16.20
4	43	1.50	10	50	5.00
5	44	6.00	11	51	3.00
6	45	2.80	3	47	—

Table (T7-40)

Disc No	File No	Date	Wall	Sheet No
PDR2-23	FDD45	21.10.1988	D	25
Pile				
Type	Length	Dimensions	Distance	Depth
Sheet-pile	10m	Frodingham (3N)	5.0m	5.0m
Hammer				
Type		Weight	Drop height	
Drop-hammer		3200kg	1.0m	

Ground Vibration Measurements

PPV (mm/s)

Geophone-set	B	A	D	E
Stand-off(m)	6.5	5.0	5.0[t]	3.0
Radial	24.49	47.97	34.55	31.62
Transverse	10.77	10.54	38.49	12.95
Vertical	11.76	13.49	13.19	15.47
Resultant	29.02	48.34	46.54	35.54

Strain Gauge Measurement

Sg.n	Ch.n	Strain $\times 10^{-6}$	Sg.n	Ch.n	Strain $\times 10^{-6}$
1	40	1.00	7	46	35.00
2	41	2.00	8	48	19.60
12	42	2.20	9	49	25.20
4	43	3.00	10	50	4.20
5	44	7.00	11	51	3.50
6	45	4.00	3	47	—

Table (T7-41)

Disc No	File No	Date	Wall	Sheet No
PDR2-24	FDD50	21.10.1988	D	26
Pile				
Type	Length	Dimensions	Distance	Depth
Sheet-pile	10m	Frodingham (3N)	2.0m	5.0m
Hammer				
Type		Weight	Drop height	
Drop-hammer		3200kg	1.0m	

Ground Vibration Measurements

PPV (mm/s)

Geophone-set	B	A	D	E
Stand-off(m)	3.5	3.5^t	2.0^t	2.0
Radial	26.51	19.89	17.77	24.89
Transverse	15.63	42.73	34.98	32.95
Vertical	8.44	10.66	10.83	18.99
Resultant				

Strain Gauge Measurement

Sg.n	Ch.n	Strain $\times 10^{-6}$	Sg.n	Ch.n	Strain $\times 10^{-6}$
1	40	1.50	7	46	30.00
2	41	2.00	8	48	10.60
12	42	2.50	9	49	11.20
4	43	5.00	10	50	6.00
5	44	8.00	11	51	2.00
6	45	5.00	3	47	—

Table (T7-42)

Disc No	File No	Date	Wall	Sheet No
PDR2-25	FDD56	21.10.1988	D	27
Pile				
Type	Length	Dimensions	Distance	Depth
Sheet-pile	10m	Frodingham (3N)	0.25m	5.0m
Hammer				
Type		Weight	Drop height	
Drop-hammer		3200kg	1.0m	

Ground Vibration Measurements

PPV (mm/s)

Geophone-set	B	A	D	E
Stand-off(m)	1.75	1.75[t]	0.25[t]	0.25
Radial	29.89	11.88	12.54	14.19
Transverse	28.30	37.11	22.24	32.50
Vertical	17.06	32.66	23.66	26.03
Resultant				

Strain Gauge Measurement

Sg.n	Ch.n	Strain $\times 10^{-6}$	Sg.n	Ch.n	Strain $\times 10^{-6}$
1	40	1.50	7	46	36.00
2	41	2.00	8	48	15.60
12	42	2.50	9	49	68.00
4	43	6.00	10	50	6.00
5	44	14.00	11	51	2.00
6	45	3.80	3	47	—

Table (T7-43)

Disc No	File No	Date	Wall	Sheet No
PDR2-26	FCD62	21.10.1988	C	28
Pile				
Type	Length	Dimensions	Distance	Depth
Sheet-pile	10m	Frodingham (3N)	0.40m	5.0m
Hammer				
Type		Weight	Drop height	
Drop-hammer		3200kg	1.0m	

Ground Vibration Measurements

PPV (mm/s)

Geophone-set	B	A	D	E
Stand-off(m)	1.90	1.90[t]	0.40[t]	0.40
Radial	30.16	34.20	33.55	19.73
Transverse	39.07	79.71	31.18	47.77
Vertical	16.07	28.07	25.84	27.13
Resultant				

Strain Gauge Measurement

Sg.n	Ch.n	Strain $\times 10^{-6}$	Sg.n	Ch.n	Strain $\times 10^{-6}$
1	40	1.50	7	46	38.00
2	41	6.00	8	48	27.60
12	42	37.00	9	49	38.00
4	43	143.0	10	50	46.00
5	44	44.00	11	51	2.00
6	45	5.00	3	47	—

	Toe-depth=3m					Toe-depth=5m					Toe-depth=7m				
		D=1.0m		D=0.5m			D=1.0m		D=0.5m			D=1.0m		D=0.5m	
S	r	$\sqrt{W}/r$	ppv	$\sqrt{W}/r$	ppv	r	$\sqrt{W}/r$	ppv	$\sqrt{W}/r$	ppv	r	$\sqrt{W}/r$	ppv	$\sqrt{W}/r$	ppv
2.0	3.61	49.08	25.74	34.71	27.29	5.36	33.06	40.73	23.37	47.81	7.28	24.34	44.22	17.21	35.70
5.0	5.83	30.39	10.70	21.49	13.19	7.07	25.06	36.00	17.72	39.31	8.60	20.60	58.27	14.57	47.75
10.0	10.44	16.97	3.81	12.00	4.05	11.18	15.85	15.24	11.21	16.81	12.21	14.51	27.13	10.26	25.45
11.5	11.88	14.92	3.88	10.55	4.55	12.54	14.13	16.97	9.99	18.21	13.46	13.16	36.57	9.31	33.10

Pile stands 10m from wall A

H-pile, Drop-hammer

Table (T7-44) Summary of vibration records taken at different depths with different drop-heights

$W_{0.5}$: hammer energy with 0.5m drop 15.7kJ

$W_{1.0}$: hammer energy with 1.0m drop 31.4kJ

ppv : peak particle velocity resultant $(mm.s^{-1})$

D : hammer drop height (m)

S : horizontal distance between geophone and pile (m)

r : radial distance between geophone and pile-toe (m)

S	Toe-depth=3m			Toe-depth=5m			Toe-depth=7m		
		W=3.4kJ/cycle			W=3.4kJ/cycle			W=3.4kJ/cycle	
	r	$\sqrt{W}/r$	ppv	r	$\sqrt{W}/r$	ppv	r	$\sqrt{W}/r$	ppv
2.0	3.61	16.15	19.63	5.36	10.88	27.52	7.28	8.01	17.03
5.0	5.83	10.00	14.64	7.07	8.25	21.48	8.60	6.78	23.01
10.0	10.44	5.58	11.36	11.18	5.22	9.94	12.21	4.77	11.58
11.5	11.88	4.91	4.73	12.54	4.65	4.72	13.46	4.33	6.43

Pile stands 10m from wall B

H-pile, Vibrodriver

Table (T7-45) Summary of vibration records taken at different depths with different drop-heights

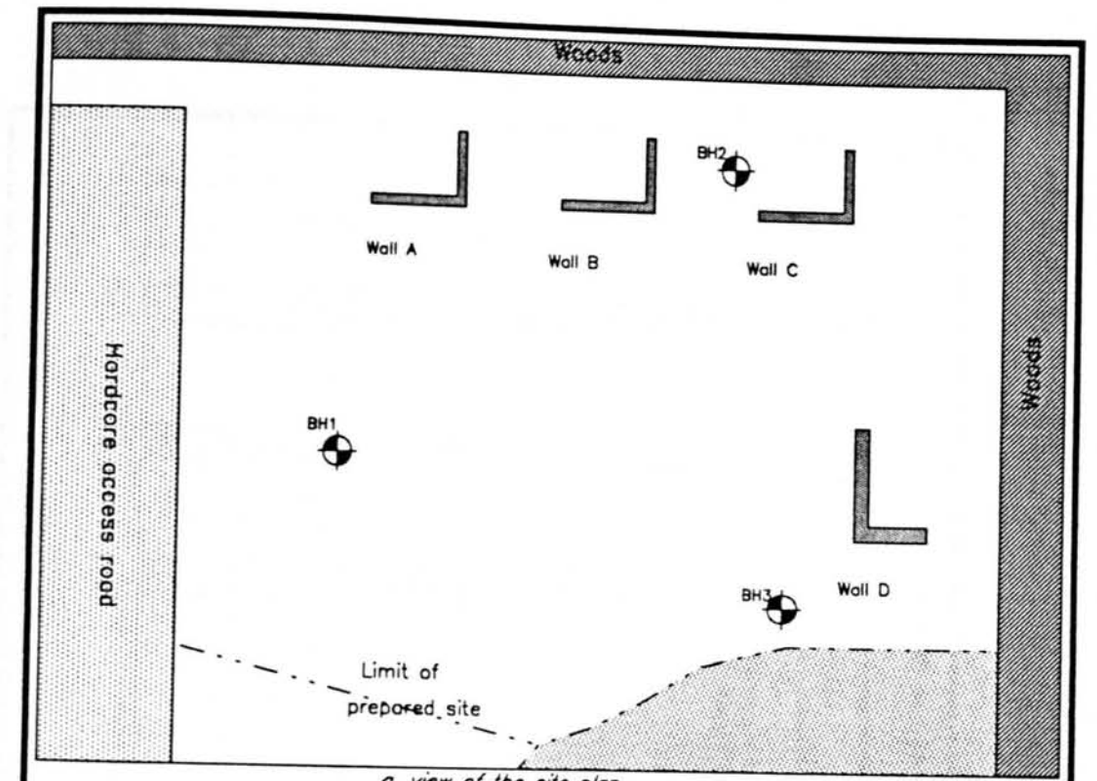

a. view of the site plan

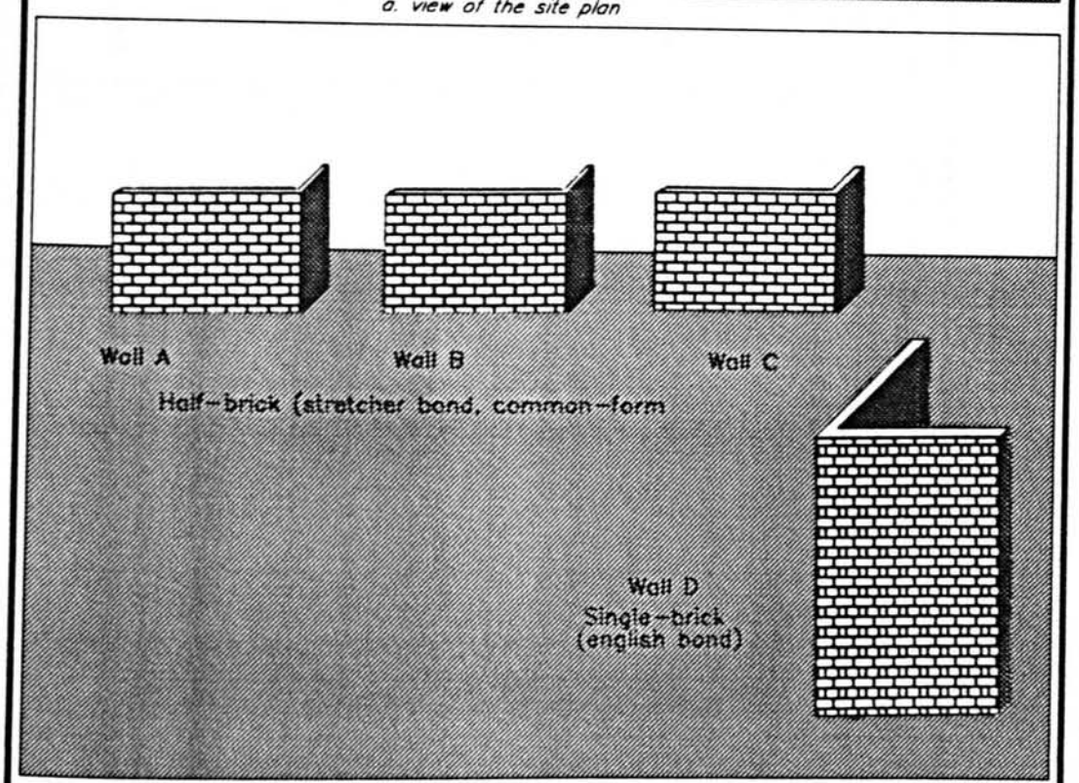

b. illustration of the wall constructions

Figure (7.1) A schematic layout of the Flitwick site

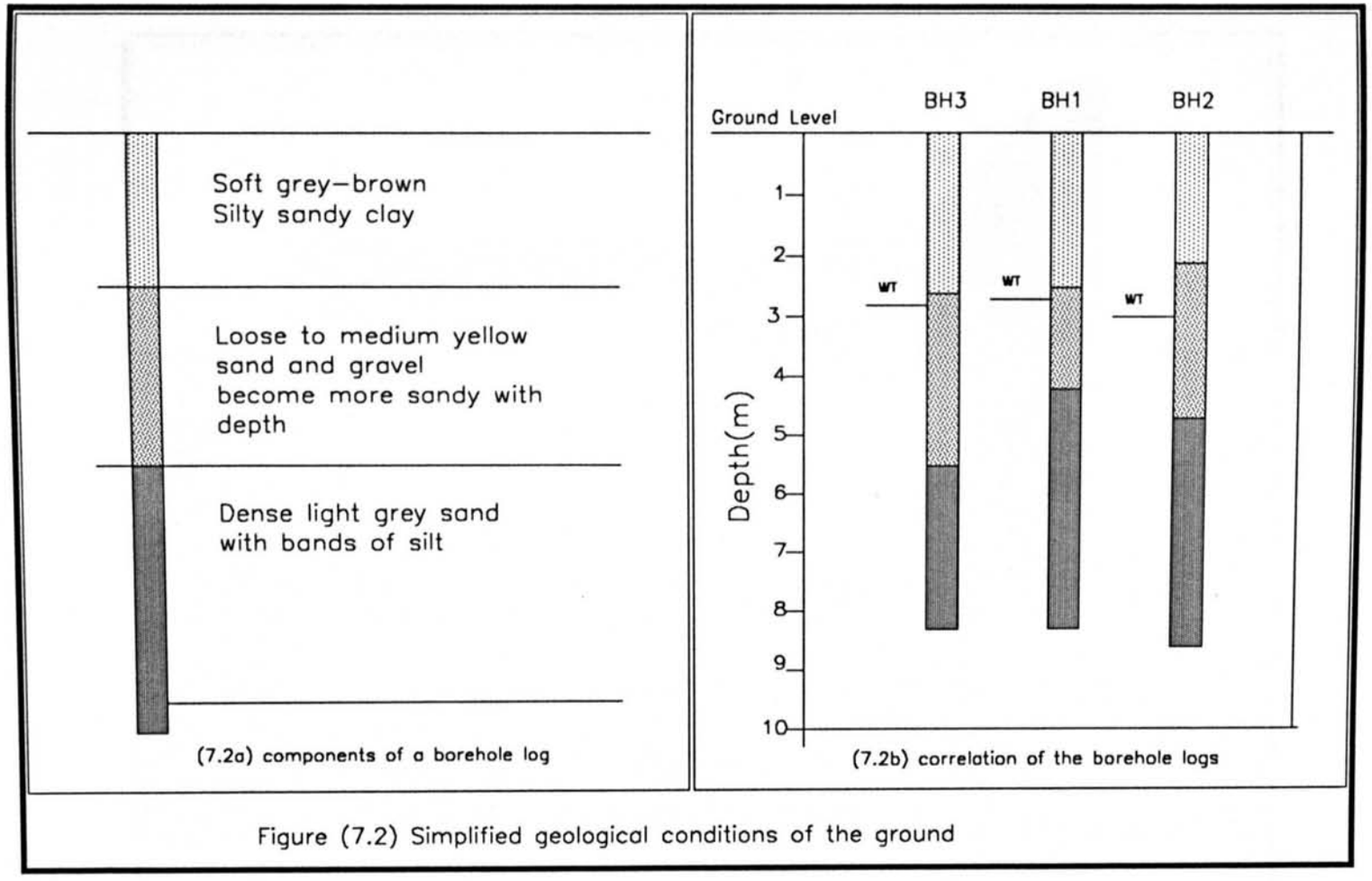

Figure (7.2) Simplified geological conditions of the ground

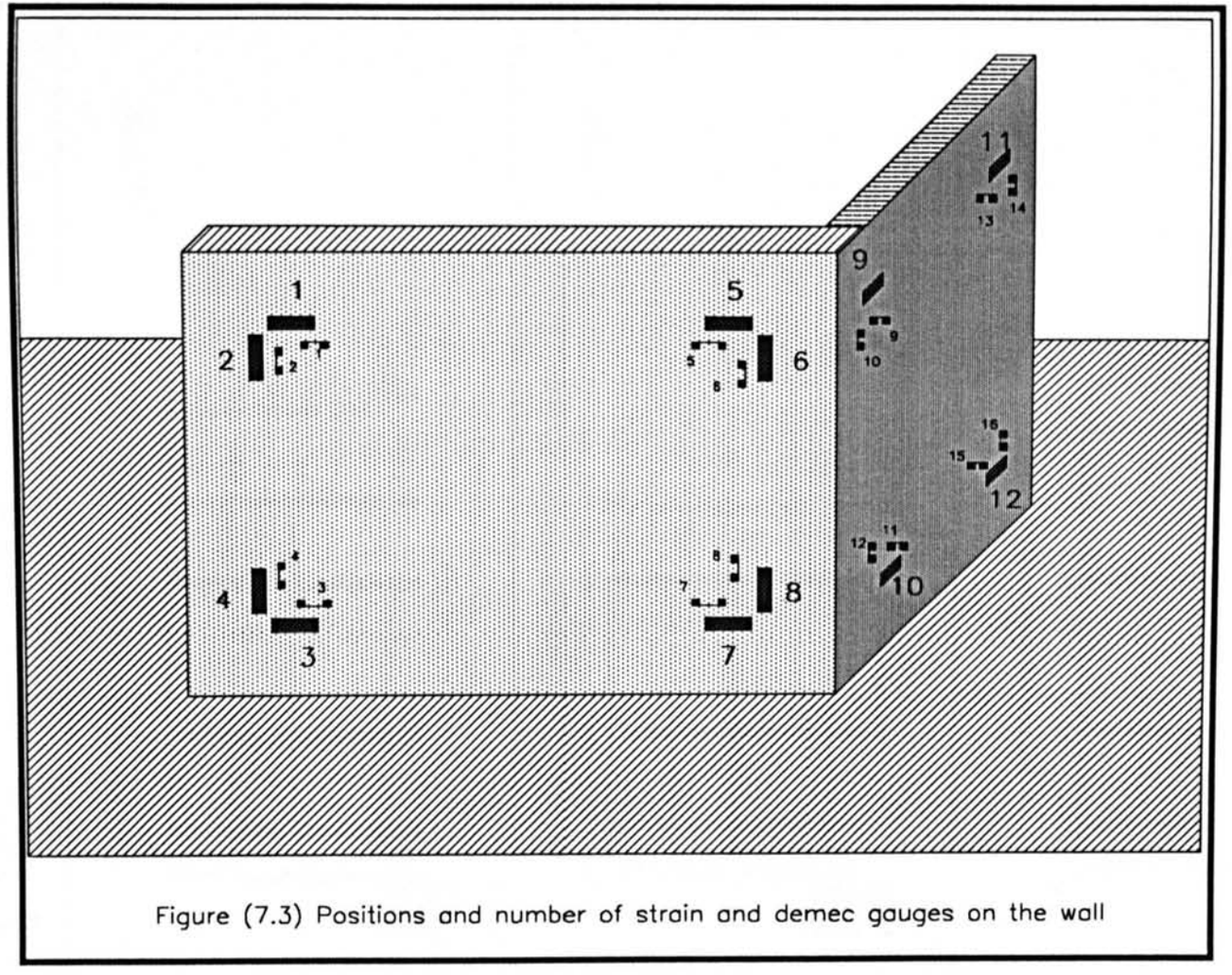

Figure (7.3) Positions and number of strain and demec gauges on the wall

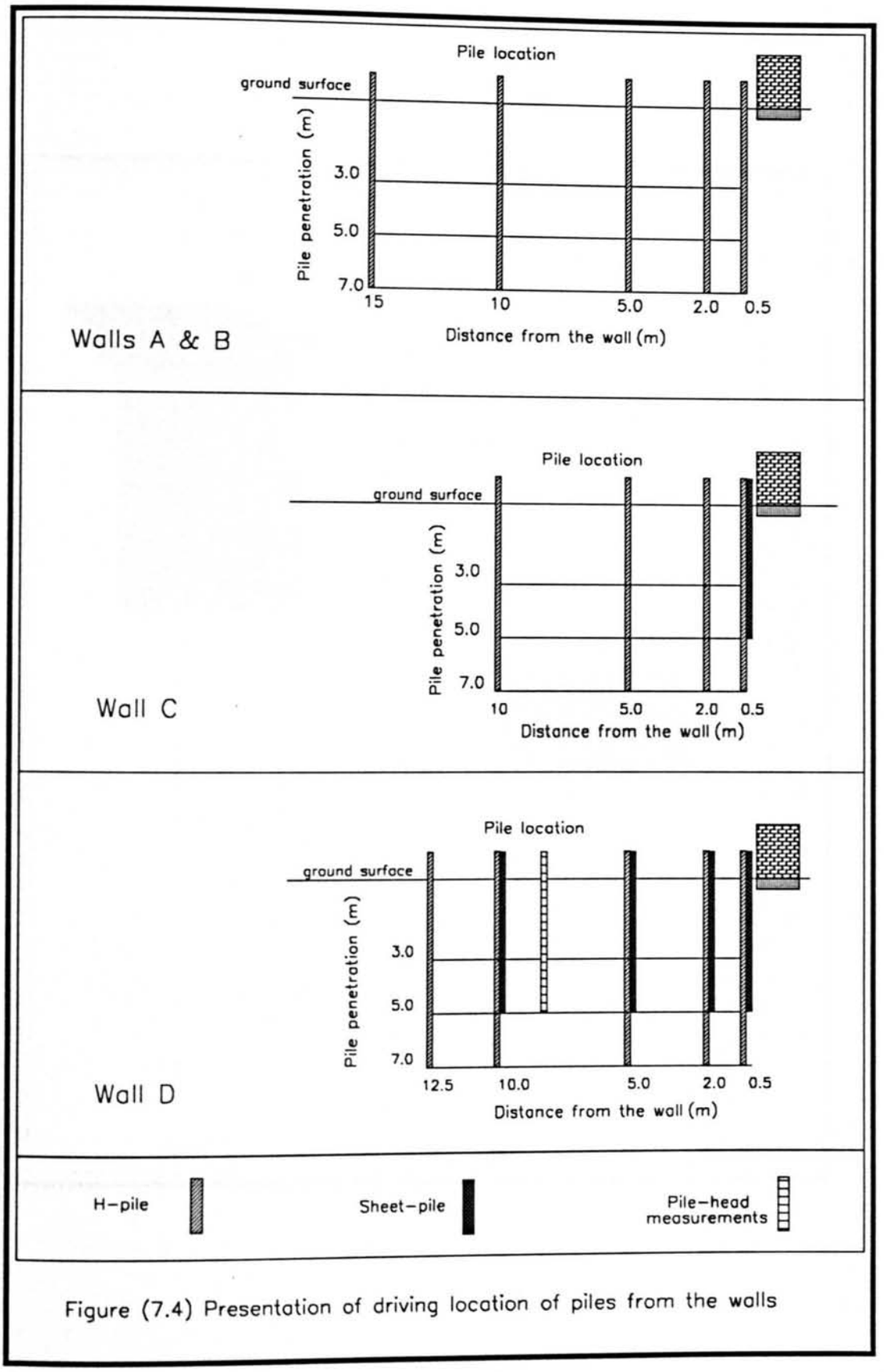

Figure (7.4) Presentation of driving location of piles from the walls

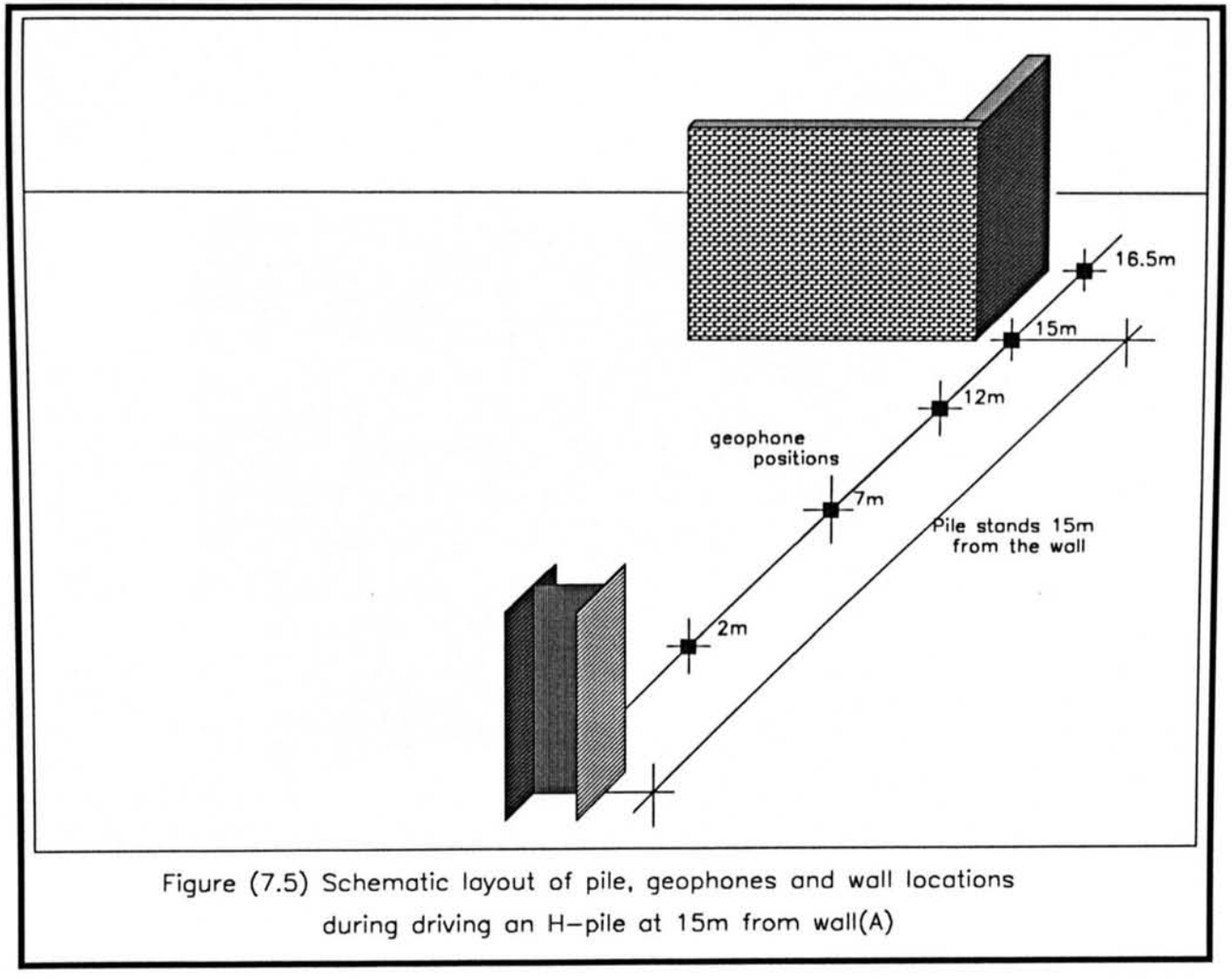

Figure (7.5) Schematic layout of pile, geophones and wall locations during driving an H–pile at 15m from wall(A)

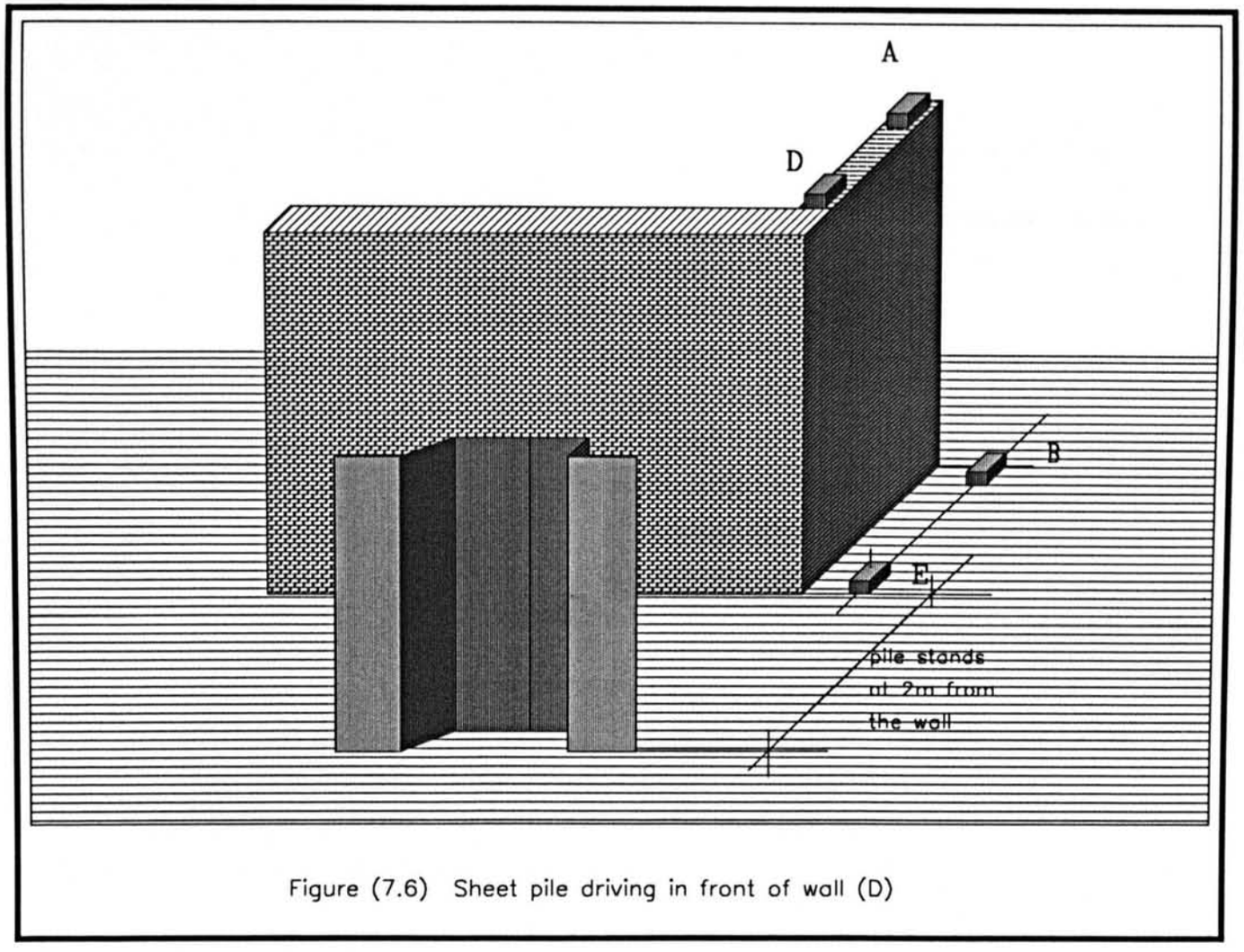

Figure (7.6) Sheet pile driving in front of wall (D)

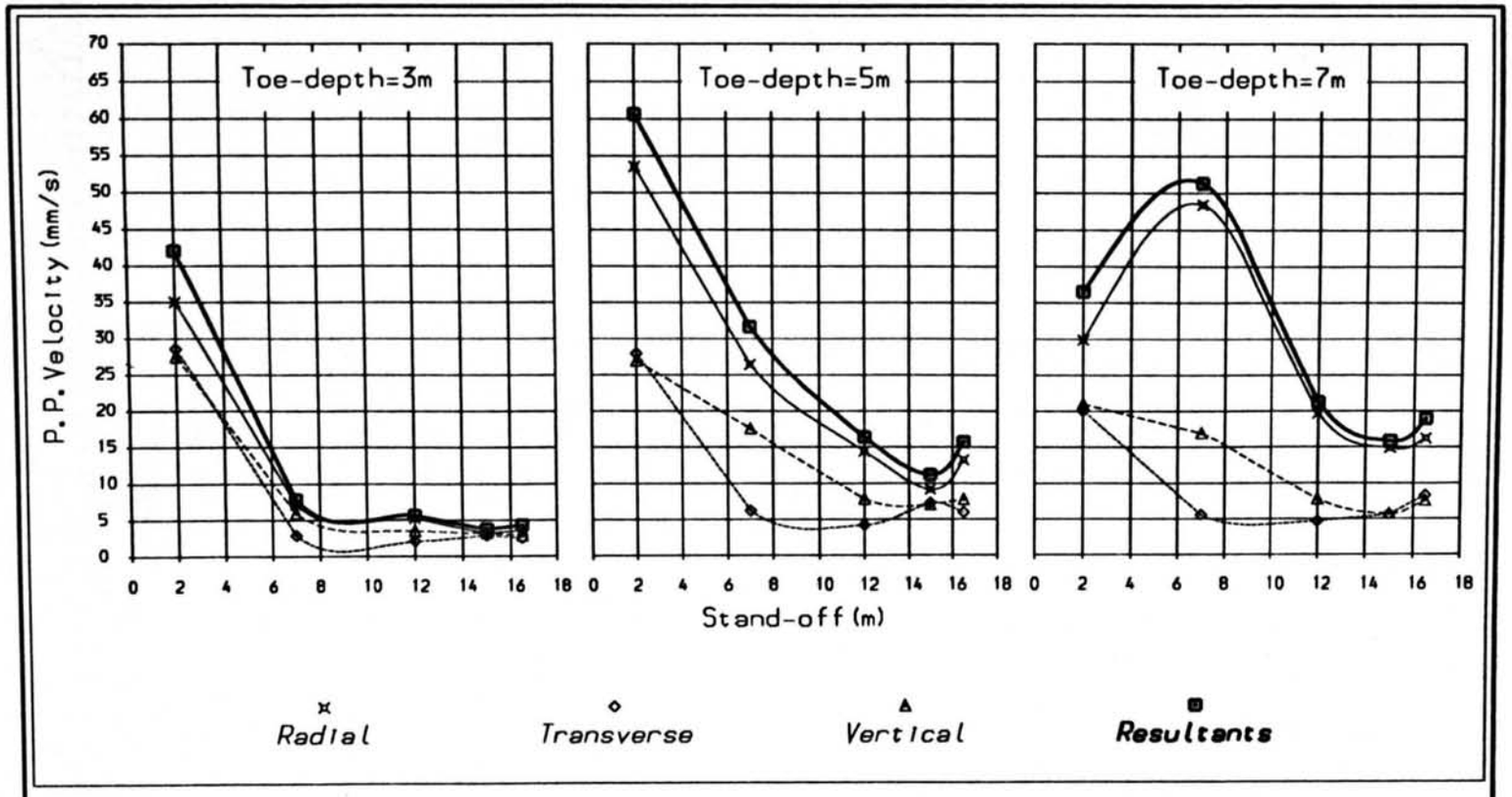

Figure (7.8) Vibration Attenuation for different toe depths
Wall A, pile-to-wall=15m

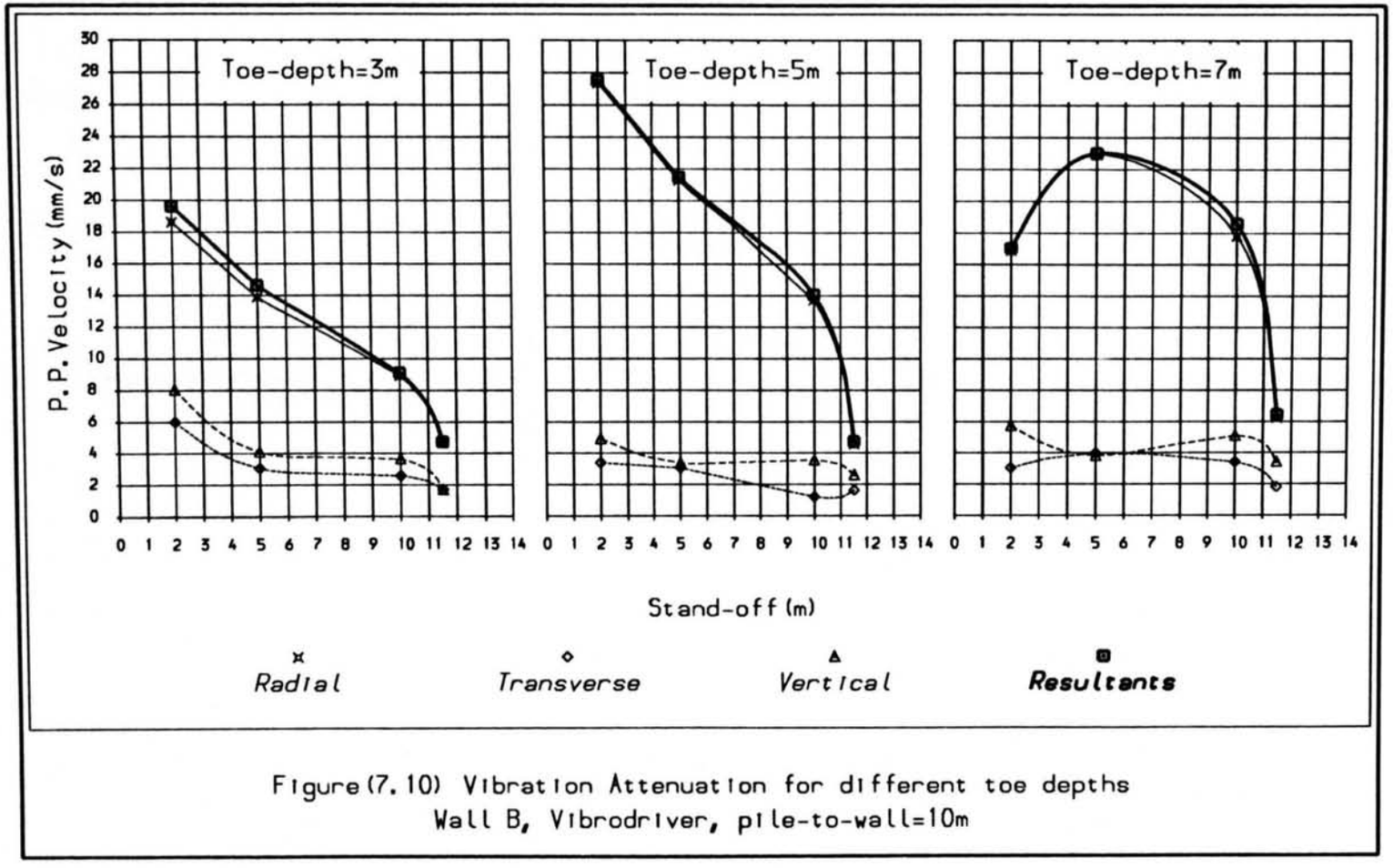

Figure (7.10) Vibration Attenuation for different toe depths
Wall B, Vibrodriver, pile-to-wall=10m

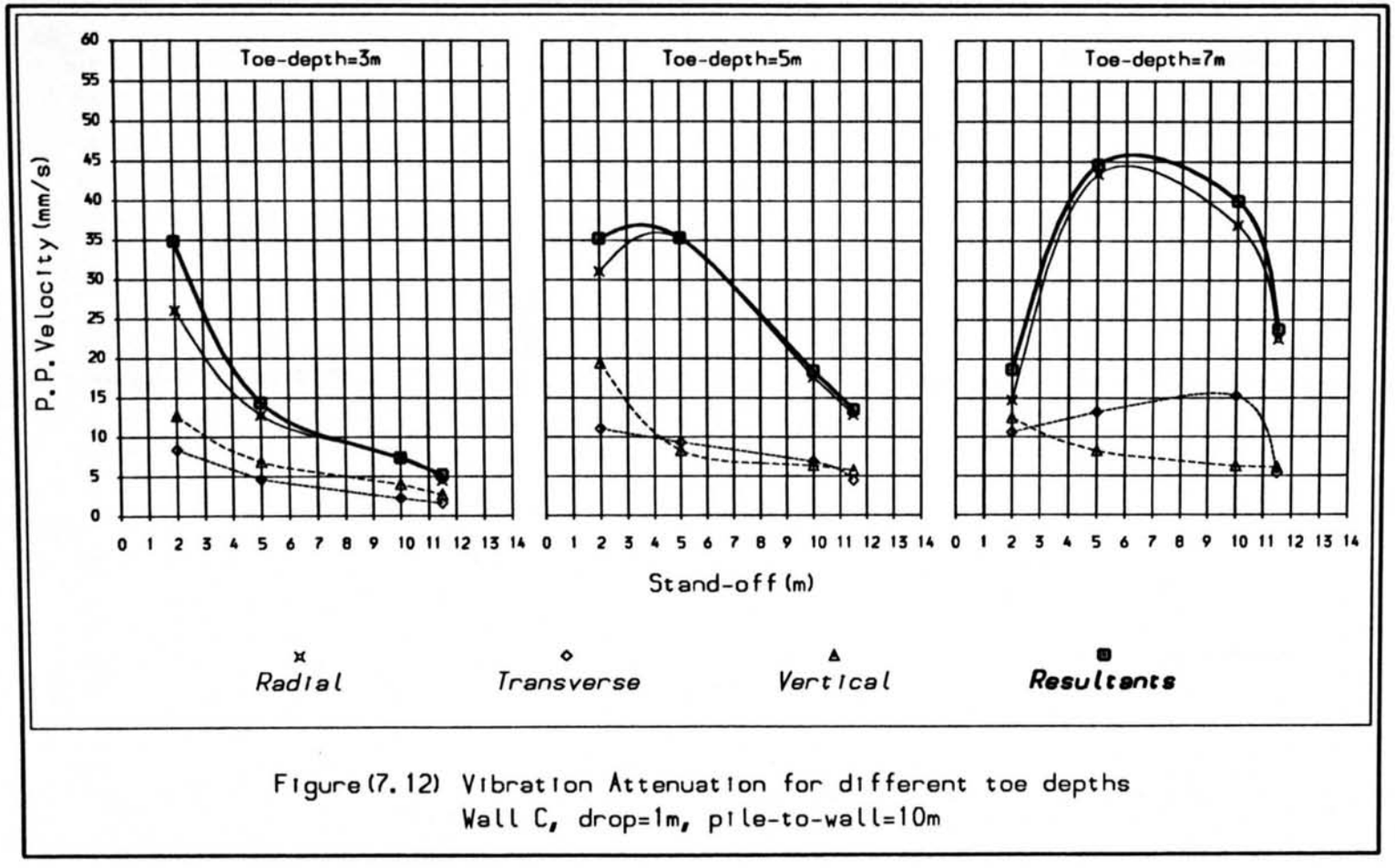

Figure (7.12) Vibration Attenuation for different toe depths
Wall C, drop=1m, pile-to-wall=10m

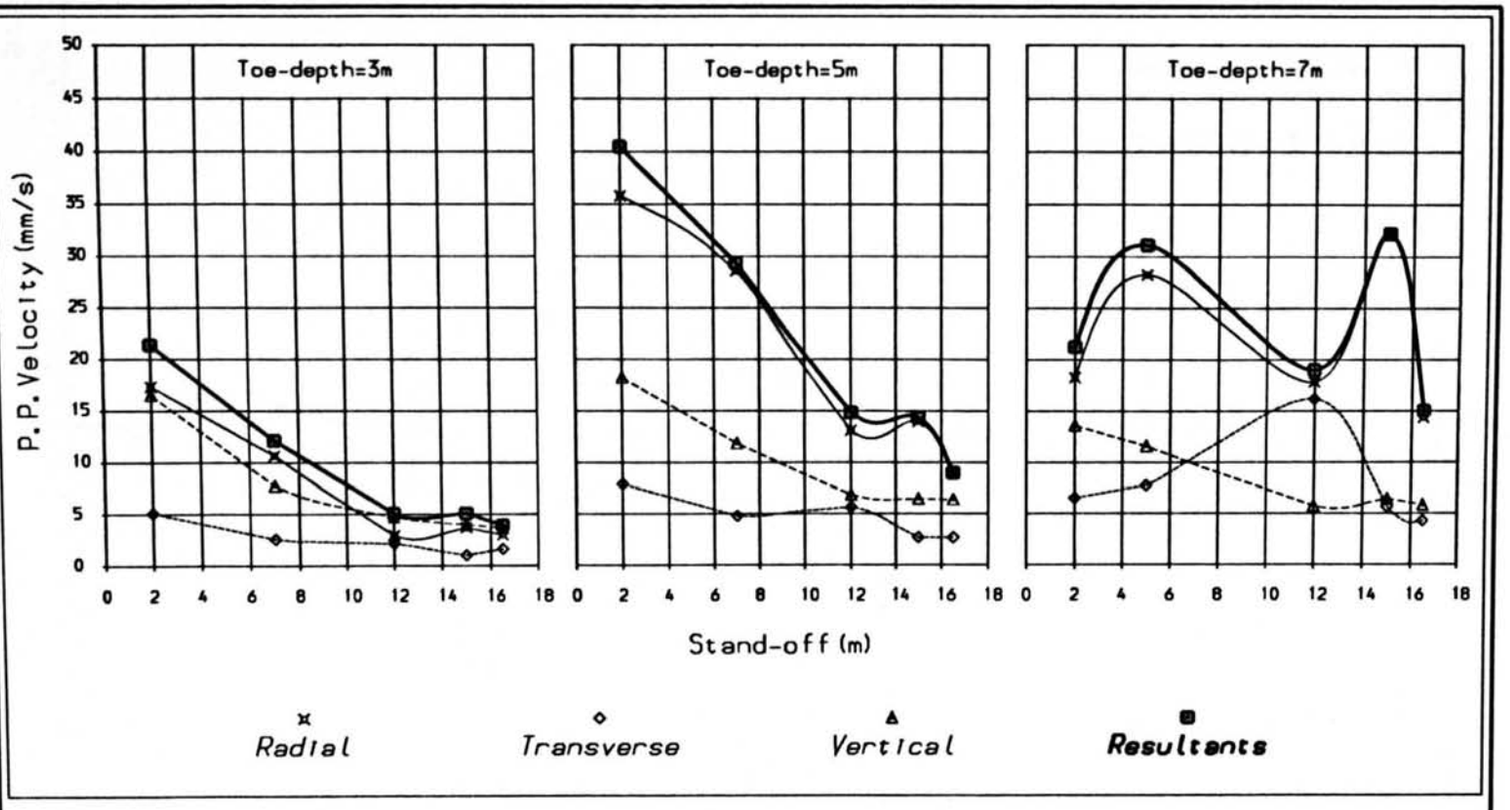

Figure (7.15) Vibration Attenuation for different toe depths
Wall D, Drop=1m, pile-to-wall=12.5m

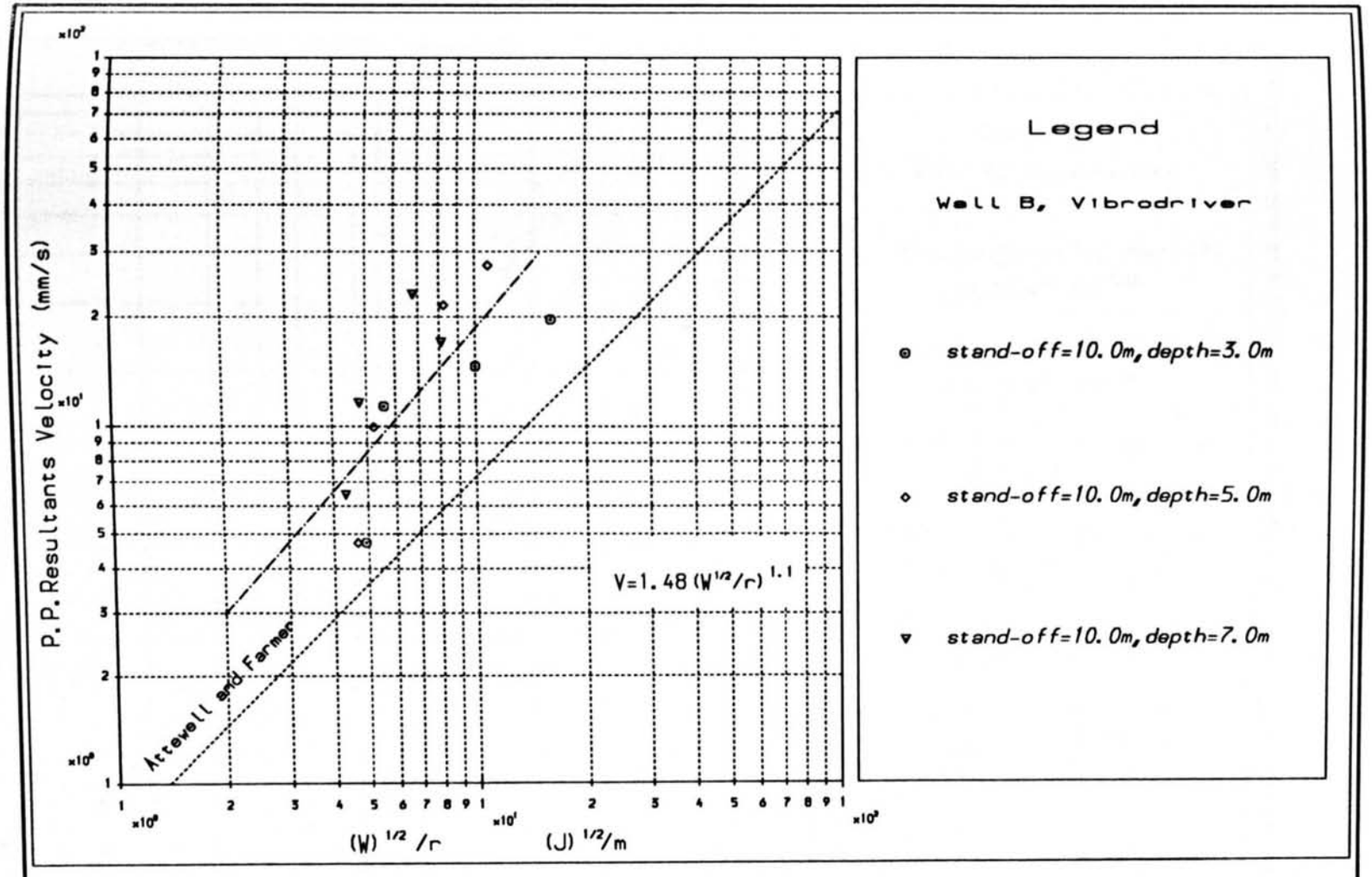

Figure (7.17) Vibration attenuation analysis, Vibrodriver

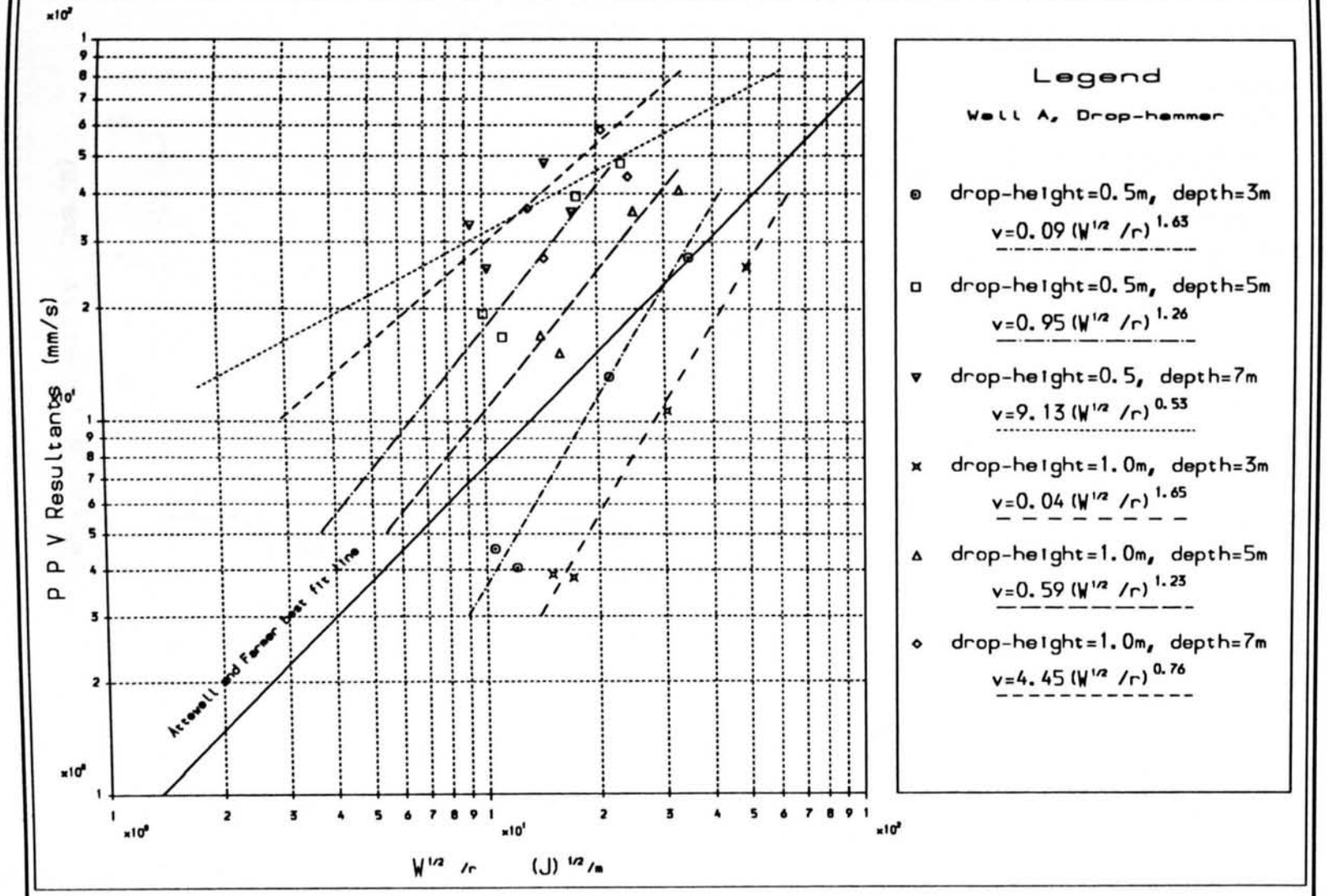

Figure (7.18) Vibration attenuation analysis, Drop-hammer

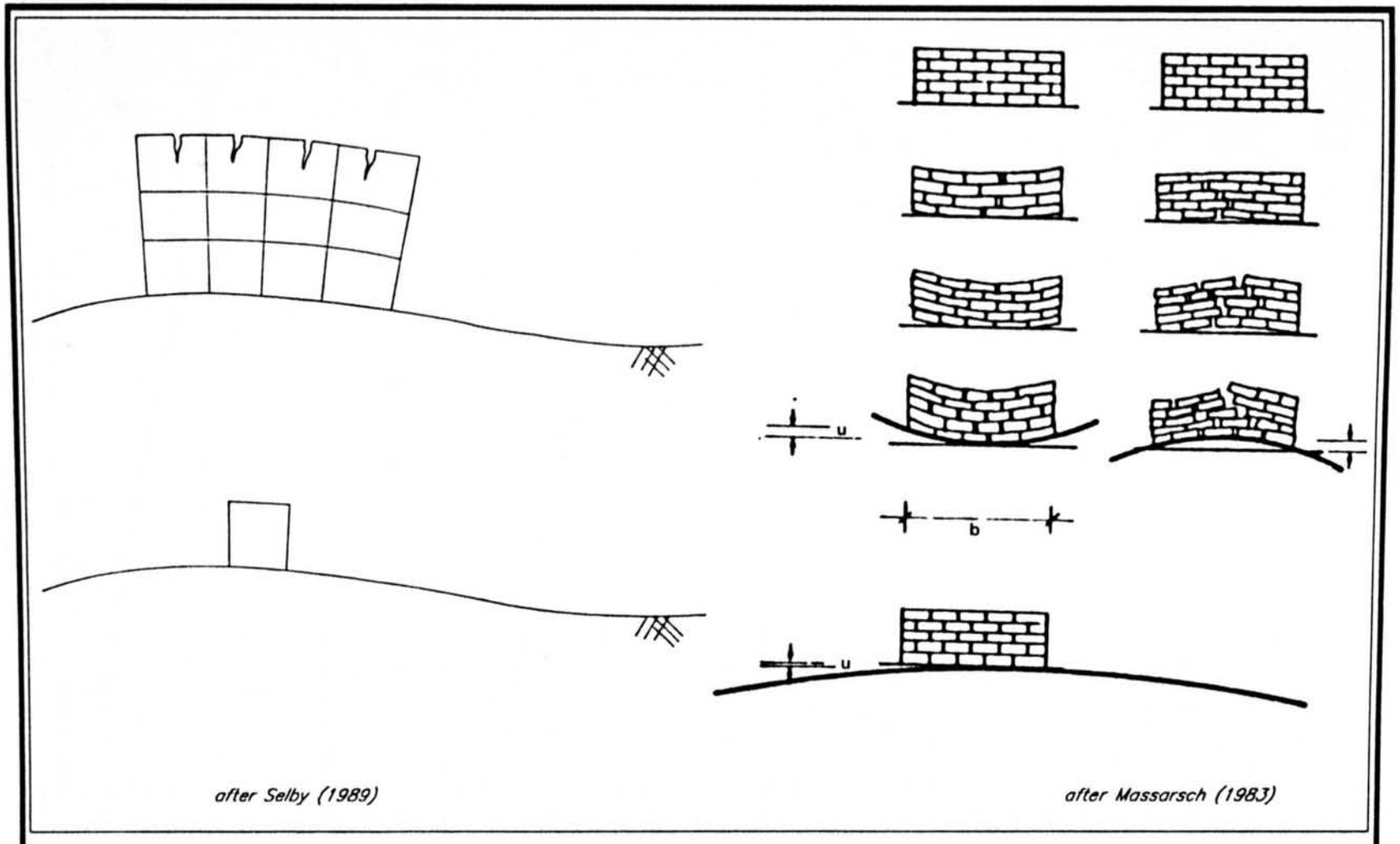

Figure (7.21) Effects of wave–length on structure sides

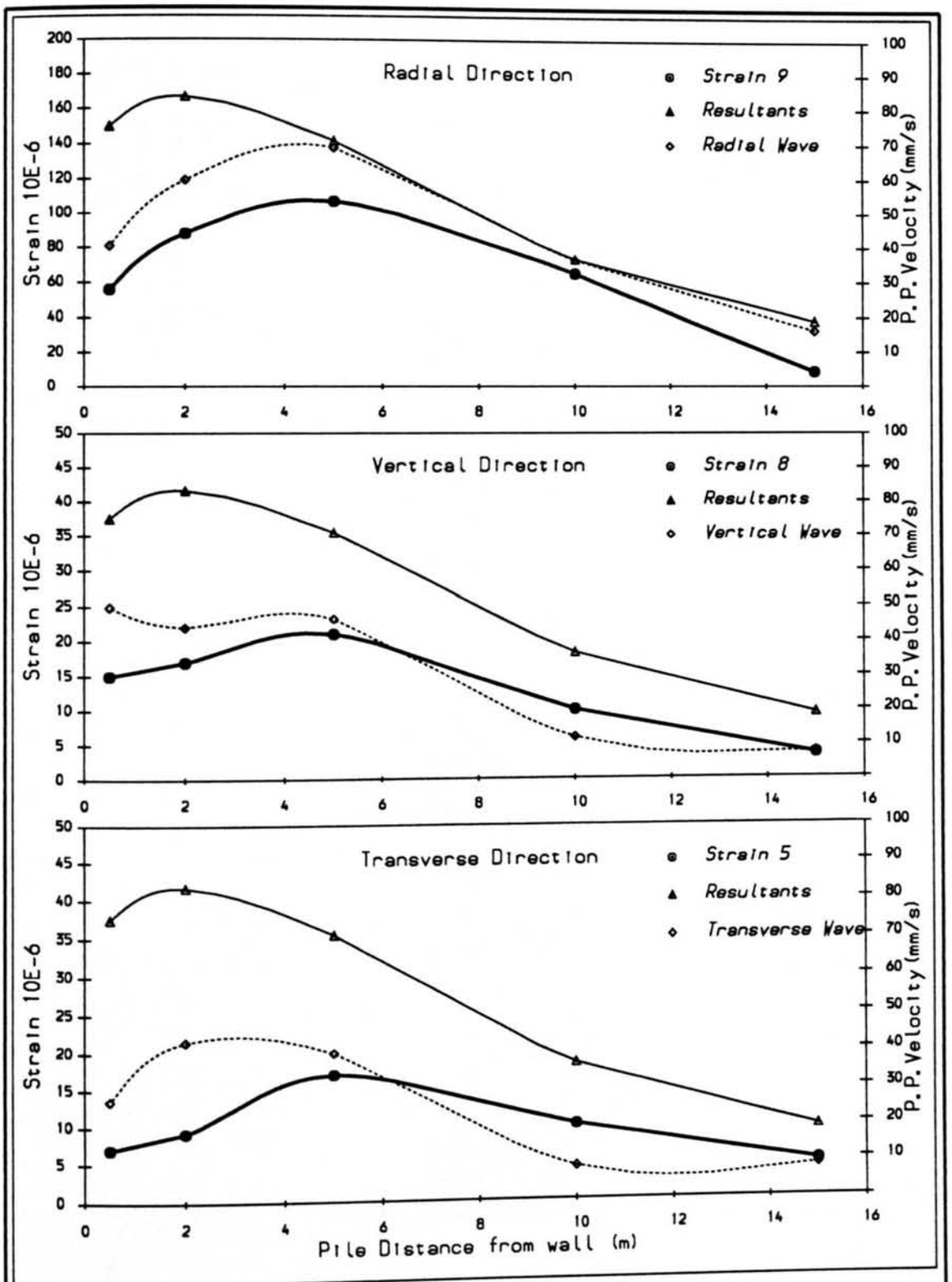

Figure (7.22) Comparison of wall strain and ground vibration
Wall A, drop-hammer

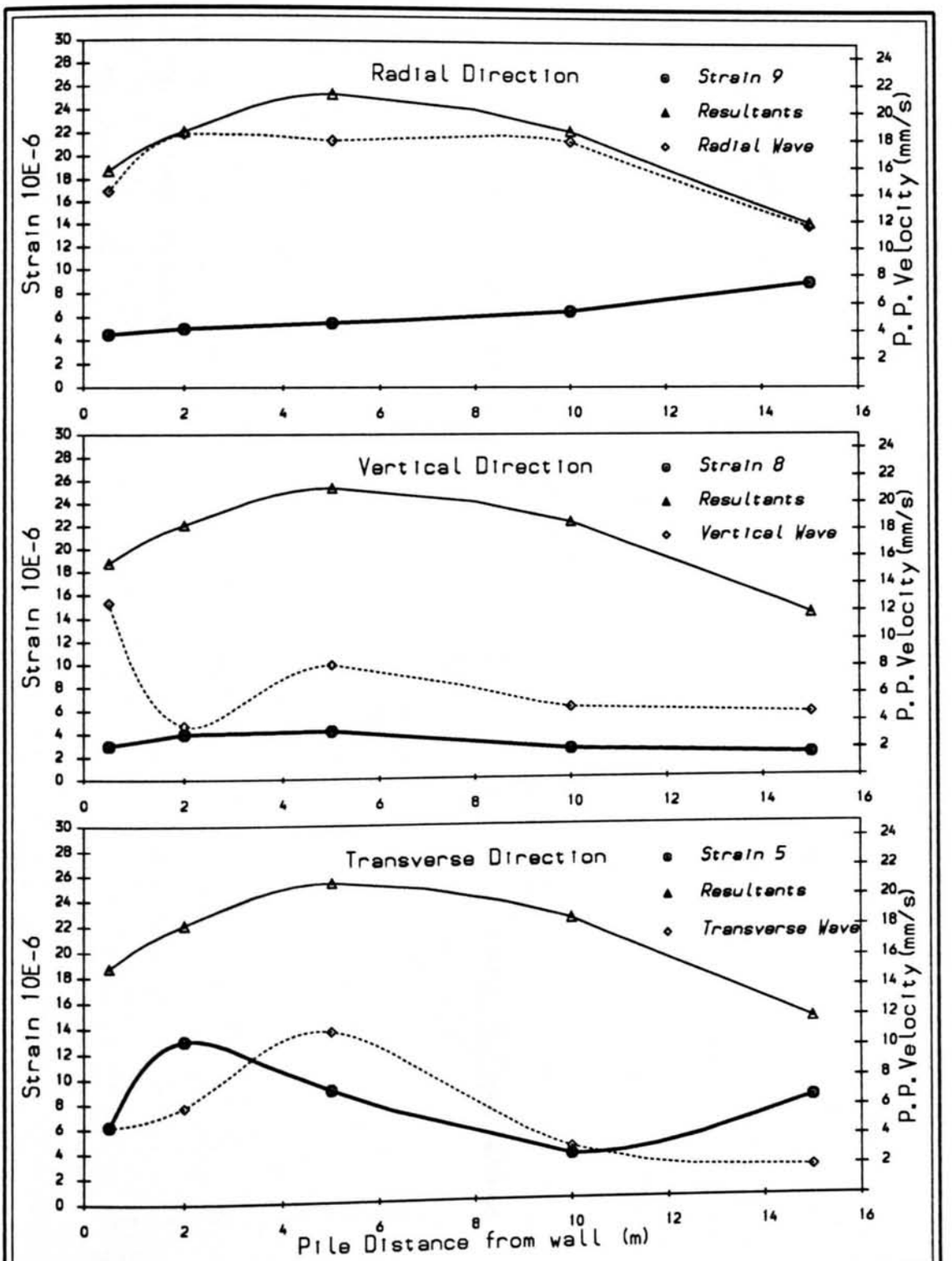

Figure (7.24) Comparison of wall strain and ground vibration
Wall B, Vibrodriver

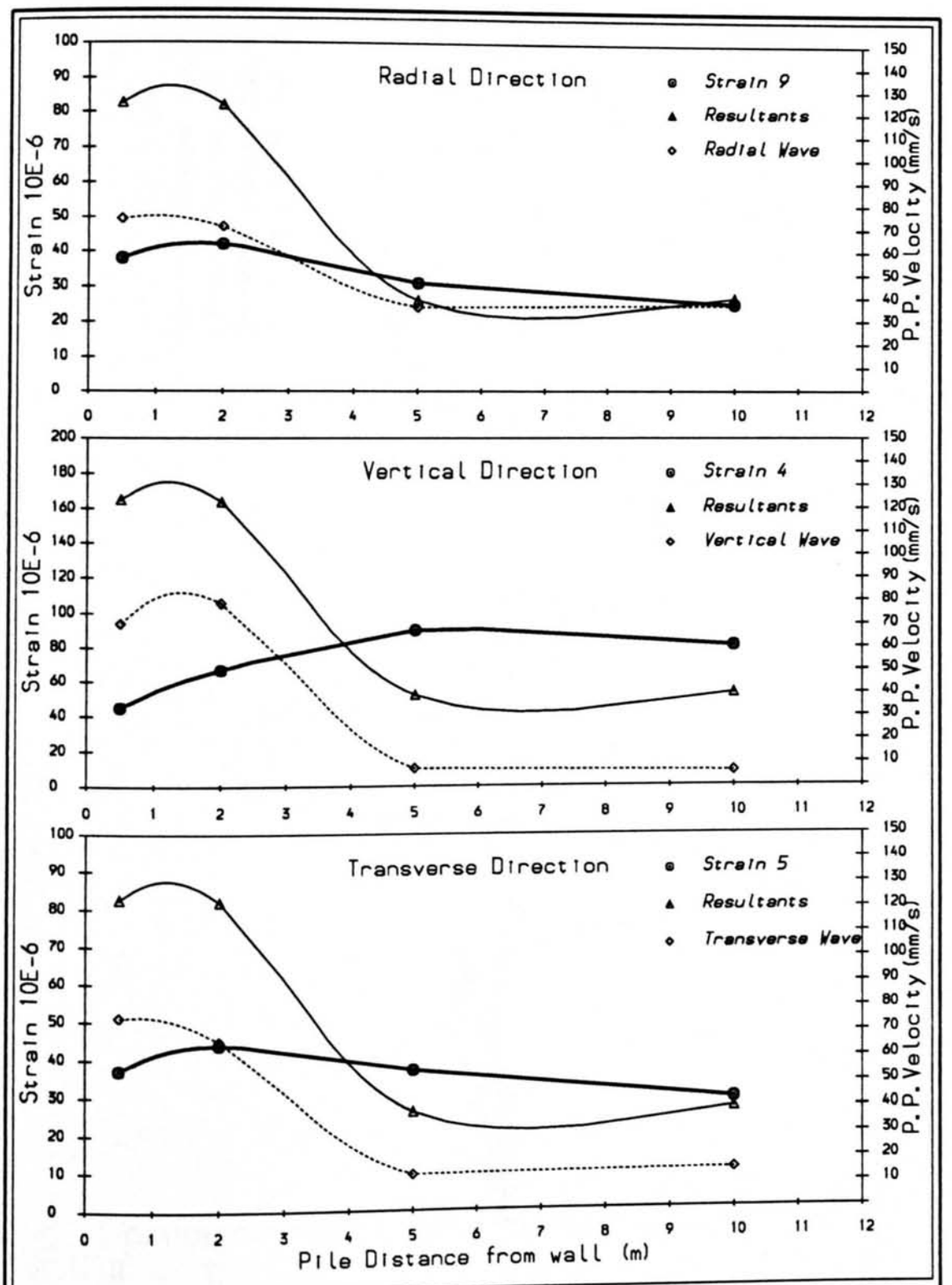

Figure (7.26) Comparison of wall strain and ground vibration
Wall C, drop-hammer

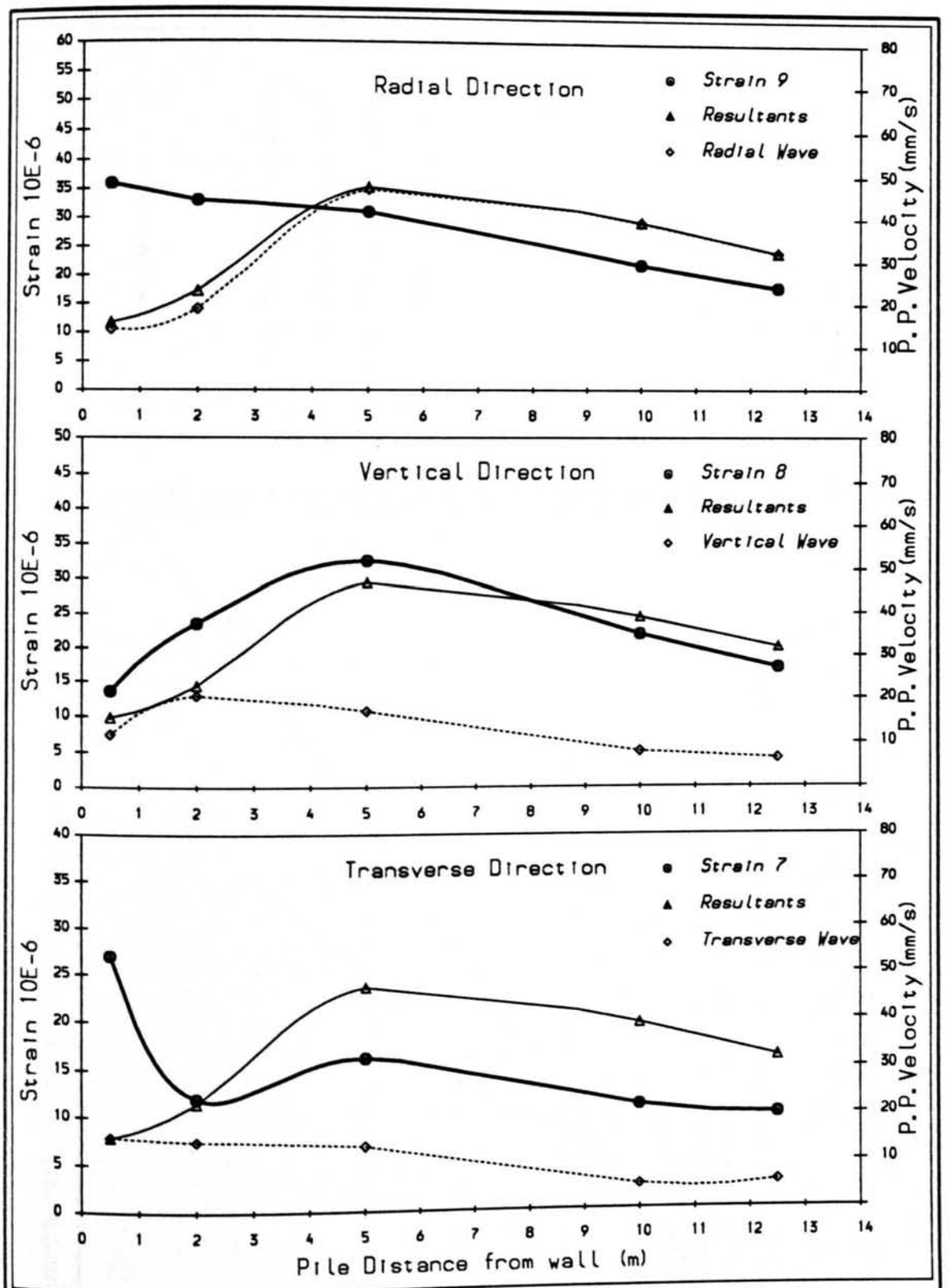

Figure (7.28) Comparison of wall strain and ground vibration
Wall D, drop-hammer

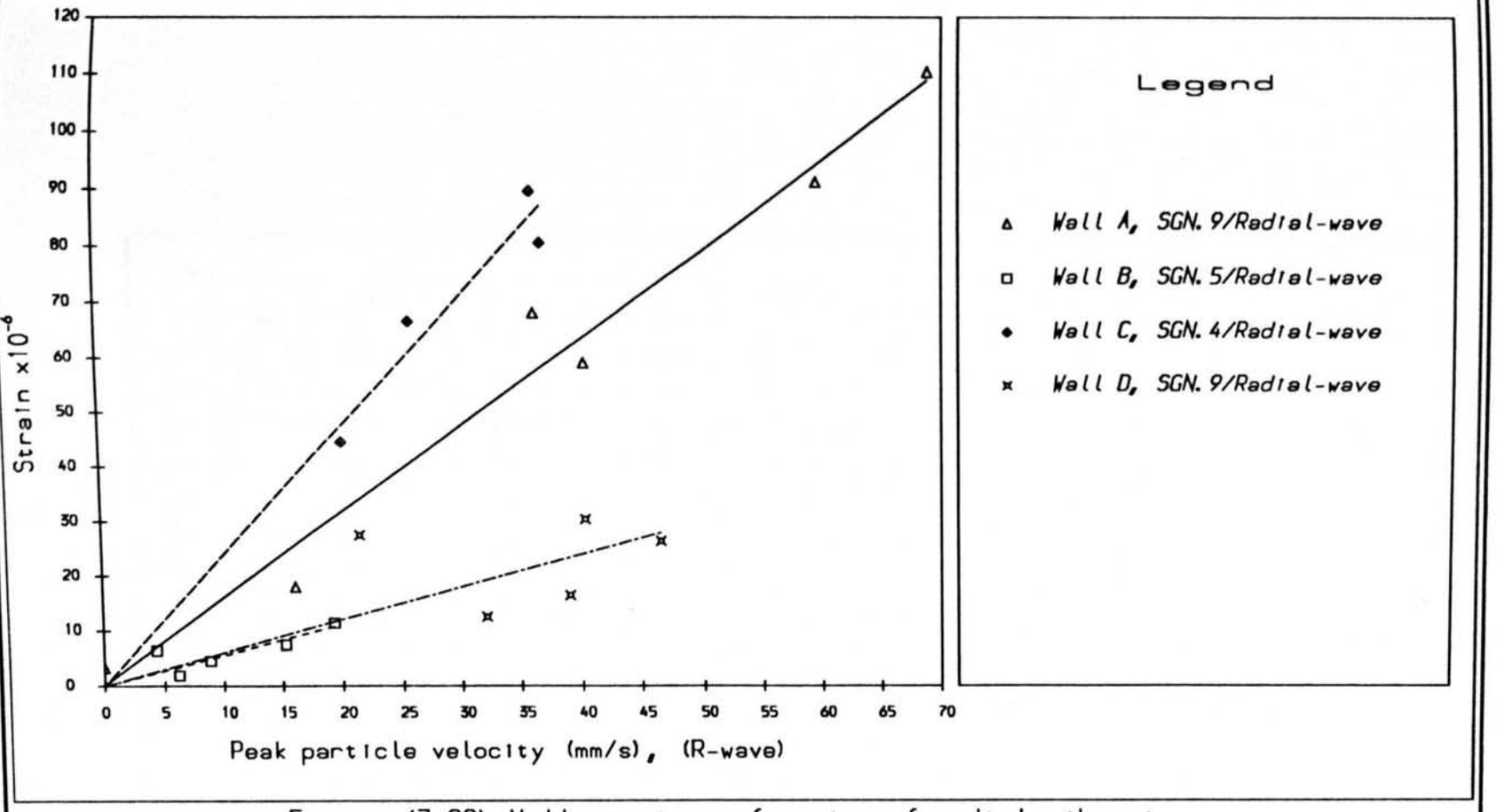

Figure (7.29) Wall strain as function of radial vibration

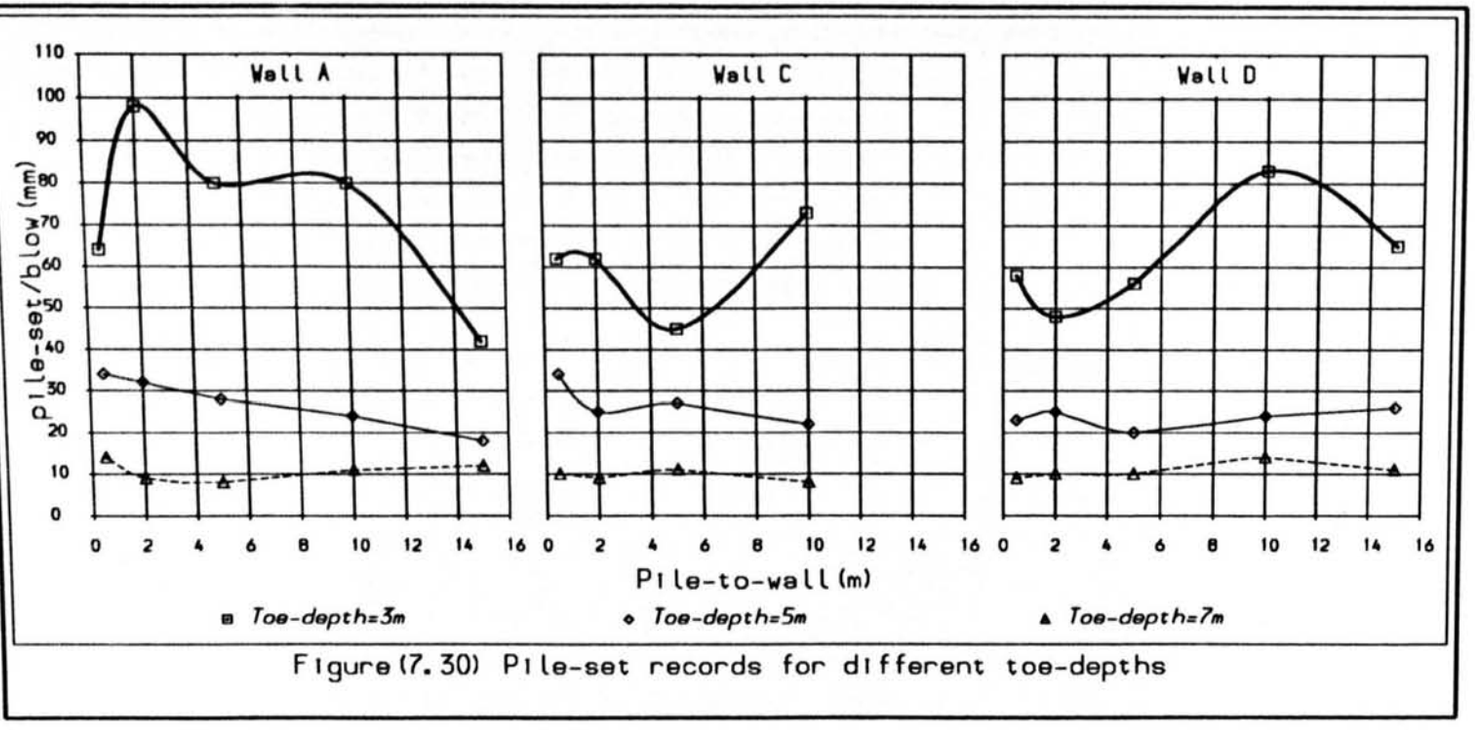

Figure (7.30) Pile-set records for different toe-depths

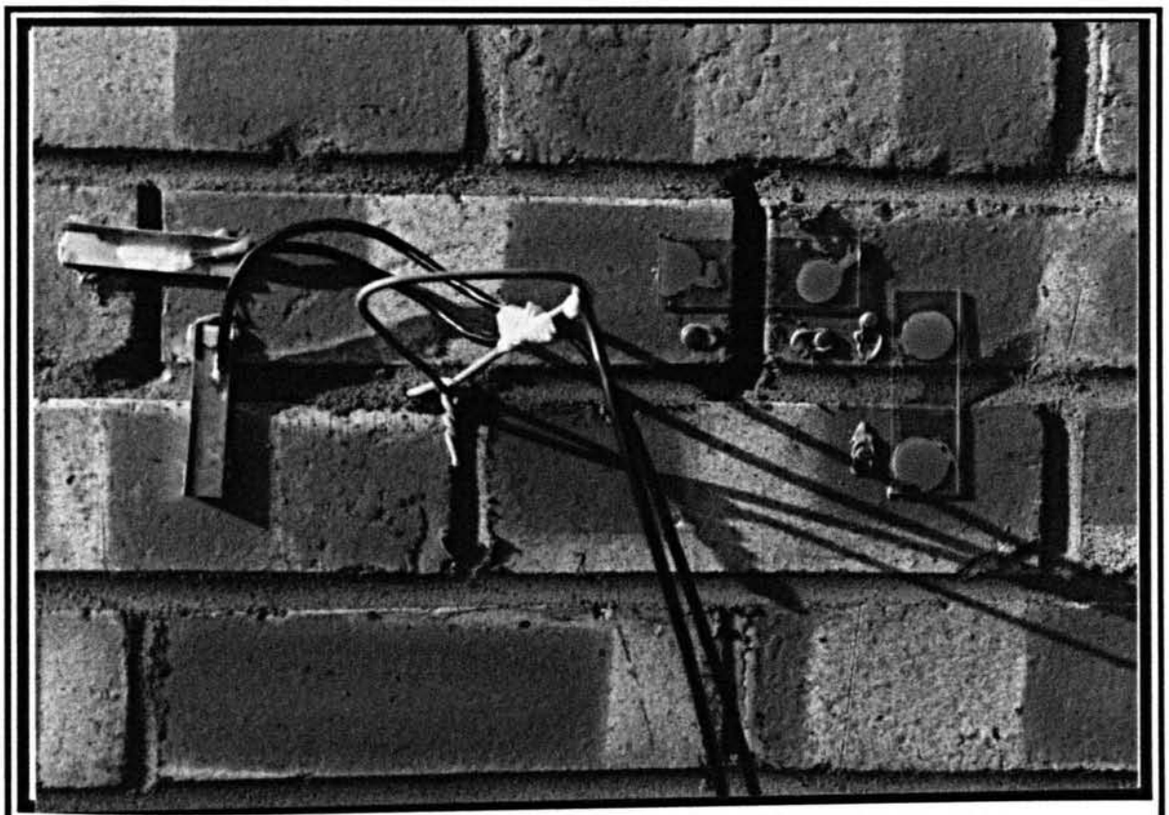

Plate (7–1) Location of measuring instruments on the wall

Flitwick, 1988

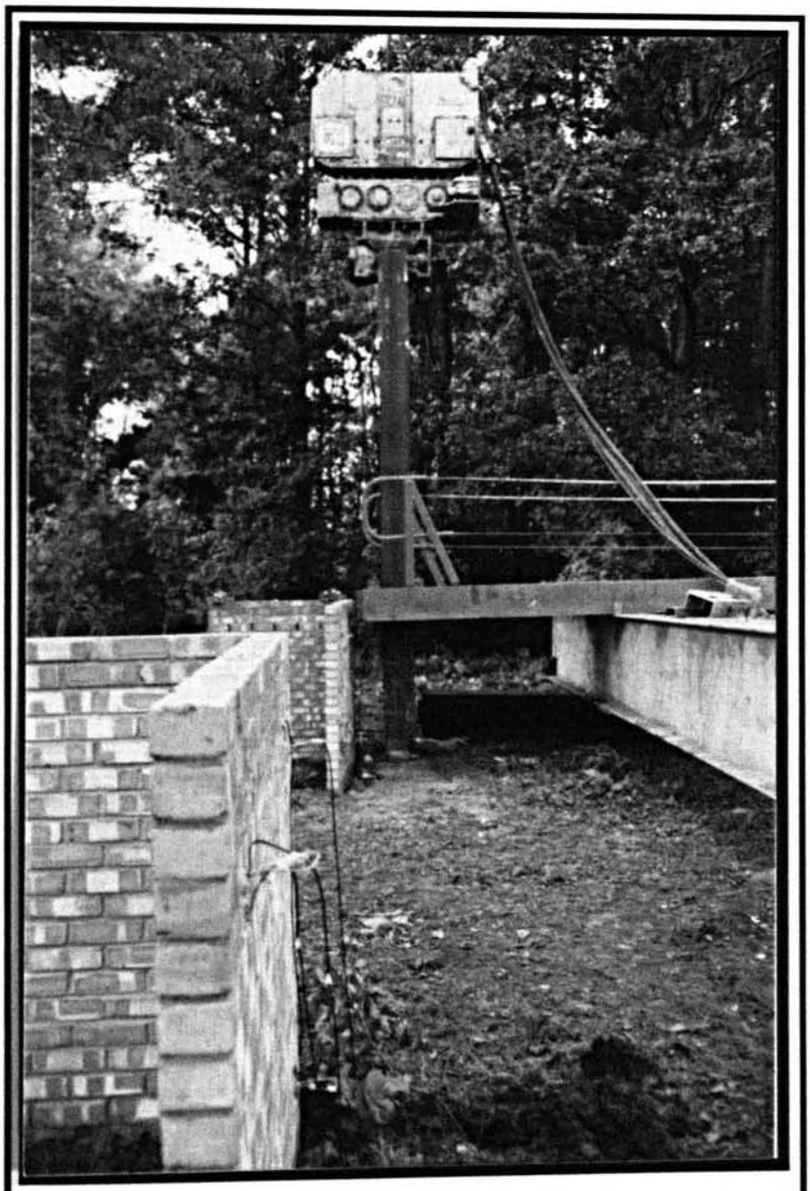

Plate (7–2)
Driving H–pile by Vibrodriver 0.5m from wall [c]

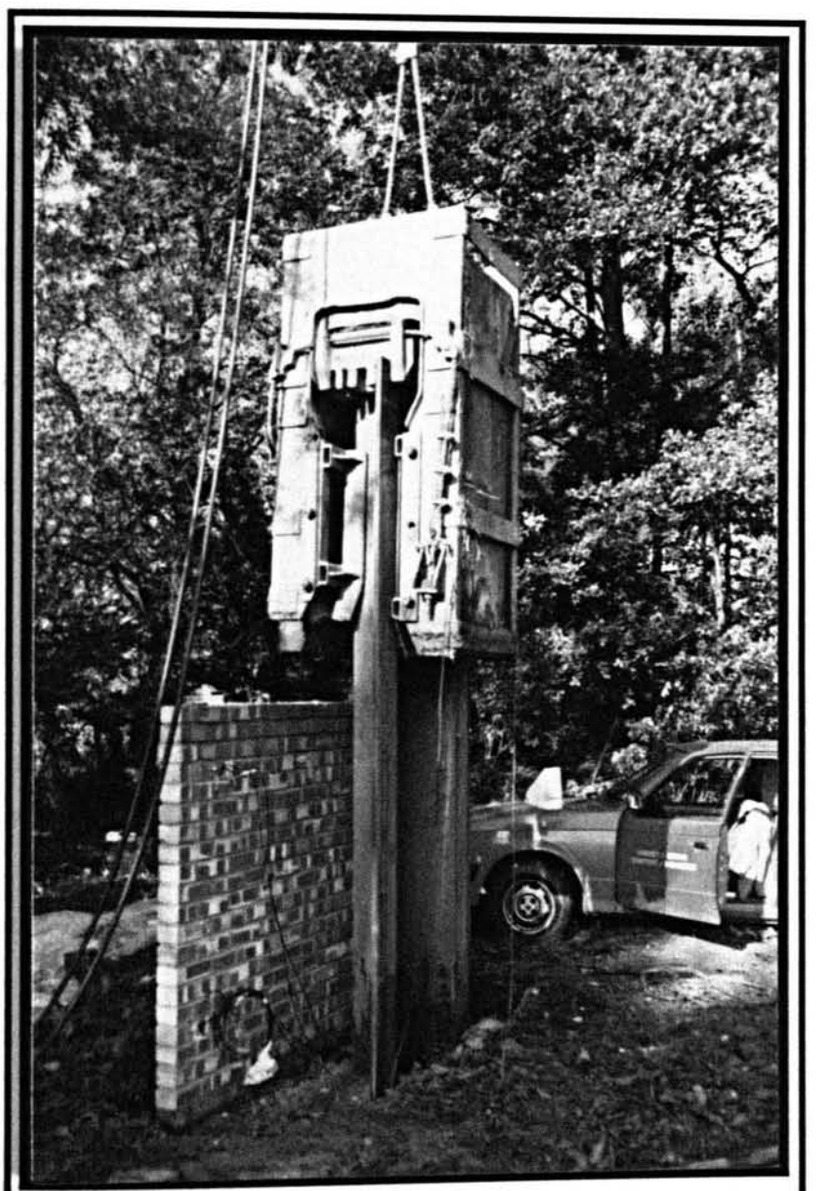

Plate (7–3)
Driving Sheet–pile by Drop–hammer next to Wall [D]

Chapter Eight
8. Conclusions and Recommendations

8.1 Introduction

This thesis has described a programme of measuring and analysing ground vibrations caused by different sources, including rail and road traffic, blasting and pile driving. The main emphasis was focused on studying and analysing the ground vibrations associated with pile driving activities in order to evaluate the amplitude and attenuation of the induced vibrations caused by different types of hammer driving various configurations of piles in different types of ground. The results of these investigations can be used to assist in estimating levels of vibration likely to be imposed at any site having conditions similar to a site on which records were taken. The project involved a large number of visits to different sites around Britain in order to experience a wide range of pile driving situations.

8.2 Conclusions

A brief guide to some of the current knowledge concerning human and structural response to vibration is reviewed in Chapter One. It was observed that there is no British Standard which gives guidance on permissible levels of vibration in buildings for avoidance of structural damage. Several existing international standards offer information on safe levels of vibration for commercial, domestic and other sensitive structures. However, the recommendations for safe limits vary considerably.

The mechanisms of wave propagation and the interference of discrete waves at the ground surface were discussed in Chapter Two. Three types of wave generated in the ground during pile driving were identified. These included waves transmitted directly along ground surface (surface wave), and body waves from around the pile-shaft and from the pile-toe. The "surface wave" motions may dominate the vibration close to a pile depending on the depth of pile-toe. Expansion (divergence) of vertically polarized shear waves from the pile-shaft as a wave front takes the form of

a narrow inverted cone. The transmission of the body-waves from the pile-toe show spherical propagation outwards into the surrounding medium. A primary study of the vibration records showed that most of the transmitted wave motion from the toe appearing at the ground surface have the character of a P-wave.

Installation of driven piles causes dynamic stress changes in the surrounding ground, these changes inducing temporary but sometimes partially irrecoverable movements. The magnitude of the dynamic forces applied to the ground from pile driving is dependent on three primary variables, which include pile type, hammer type and ground conditions.

The vibration amplitude at the ground surface was measured simultaneously in three orthogonal directions and at different stand-off distances from the pile using 15 geophones. The geophone signals were recorded digitally, using a purpose built recorder, allowing detailed signal analysis by micro-computer. The primary processing allowed time based vector resultants of each geophone set, frequency analysis and integration and differentation to give particle displacement and acceleration, respectively. Full details of the equipment are given in Chapter Four.

The effect of different environmental conditions on the ground vibration measurements were examined through a number of visits to different sites. These conditions include the variation of vibration sources, for example, blasting, traffic and driving hammers of different types, the type of driven pile and the geology of the ground. A review of all site visits is presented in Chapter Five.

In Chapter Six, the recorded vibration data were used to study the relationships between the magnitude of the input energy and the level of vibration at any distance from the source for a particular set of conditions. Because of the complex mixture of ground vibration sources and transmission, and the variability of the piling operations, it is difficult, and unrealistic, to make clear recommendations of predictive equations. However, using the well-established scaled-distance law that can readily be used by industrialists, several attenuation equations for different types of hammer, pile toe-depths and ground conditions are suggested below for average values of peak particle velocity:

vibrodriver, sheet-pile, toe-depth=6-10m

$$v = 79\left(\frac{r}{\sqrt{W_o}}\right)^{-1.95}$$

impact-hammers, sheet-pile, toe-depth=6-14m

$$v = 33\left(\frac{r}{\sqrt{W_o}}\right)^{-1.47}$$

hydraulic-hammer, H-pile, medium dense soil, toe-depth=10-17m

$$v = 51\left(\frac{r}{\sqrt{W_o}}\right)^{-1.55}$$

hydraulic-hammer, H-pile, medium dense soil, toe-depth=19-24m

$$v = 249\left(\frac{r}{\sqrt{W_o}}\right)^{-2.27}$$

hydraulic-hammer, H-pile, very dense soil, toe-depth=20-30m

$$v = 15\left(\frac{r}{\sqrt{W_o}}\right)^{-0.41}$$

diesel-hammer, H-pile, loose to medium dense soil, toe-depth=6-10m

$$v = 39\left(\frac{r}{\sqrt{W_o}}\right)^{-1.80}$$

diesel-hammer, H-pile, medium dense to dense soil, toe-depth=17-27m

$$v = 13\left(\frac{r}{\sqrt{W_o}}\right)^{-0.59}$$

drop-hammer, end-bearing-pile, toe-depth=7-12m

$$v = 38\left(\frac{r}{\sqrt{W_o}}\right)^{-1.97}$$

vibrodriver, end-bearing-pile, toe-depth=10-16m

$$v = 87\left(\frac{r}{\sqrt{W_o}}\right)^{-1.63}$$

where v is peak particle velocity (mm/s), r is radial distance from the pile-toe in (m), and W_o is the nominal hammer energy in kJ.

In comparison to the original Attewell and Farmer best fit line equation ($v = 15\left(\frac{r}{\sqrt{W_o}}\right)^{-0.87}$), the regression analysis of the ground vibration data presented in the above equations shows relatively steeper attenuation gradients except for a case when an impact hammer was used to drive an end-bearing pile deep into a very dense soil. The graphical presentation of the above equations are included in Appendix (A6).

Several general trends of behaviour have emerged. It was observed that an increase in hammer nominal energy caused an increase in vibration amplitudes, but the rate of increase was not linear, and was rather dependent on the ground conditions of the site. The results also show that for driving in similar conditions, the use of a vibrodriver especially a high frequency type, normally causes smaller vibrations than when an impact hammer is used. The results have indicated that the rate of vibration attenuation increased with pile toe depth. However, the detailed observations of vibration attenuation have shown that the linear regression of log(velocity) against log(distance) did not describe the results accurately in many cases. In particular, when a pile was driven by an impact hammer deep into dense soils, the levels of vibration recorded at the ground surface (especially those recorded in the radial direction) showed a non-uniform attenuation with an increase of distance from the pile. A method has been proposed for interpreting the above form of attenuation based on calculation of the arrival times of the wave-fronts of the body-wave and surface-wave from the toe and from the shaft of the pile. These calculations have shown that when these two arrival times coincide at one position a maximum vibration amplitude could be expected at that location.

The topography and the features of the ground surface where the geophones are placed also have influence on the measured amplitude of vibration. Pile driving causes compaction in loose granular soil creating a high vibration amplitude, especially in the vertical direction. Furthermore, loose soil on the surface of a slope may show unexpectedly high vibration amplitudes.

The drop-height of an impact-hammer has a relatively small effect on vibration amplitudes measured at the ground surface when the pile is driven in soft or loose soils. However, in dense ground with deep toe penetration, the amplitude of the vibration increases more substantially with an increase in the input energy of the hammer.

In most cases, the ground vibrations recorded in the radial and vertical directions have shown a higher amplitude than those recorded in the transverse direction. When the source of vibration was clearly non-axi-symmetric, the chosen orientation of line of geophones influenced the relative magnitudes of the radial to transverse components of motion.

When the amplitudes of different sources of vibration were plotted against the horizontal transmission distance using the scaled-distance law, the highest levels of vibration generated from the different sources were ranked in order of severity as follows:

1.blasting, 2.pile driving, 3.rail traffic & 4.road traffic

With respect to piling, the operation of an air-hammer generally caused the lowest vibrations while the hydraulic-hammer and the diesel-hammer showed the largest.

The amplitude of the dominant frequency of the induced vibration is a function both of the type of operating hammer and the type of ground. A high frequency was recorded from the fast driving hammmers, such as a high frequency vibrodriver and a double acting air-hammer. Also, a higher dominant frequency was recorded during impact driving in dense sand and stiff clay compared with the frequency in loose and soft soils.

Use of the hemispherical projection technique for displaying the time-dependent vector directions of ground vibration has provided an useful method of interpreting the recorded data. With respect to the directional sense of the vibration components, projection of the periodic vibration data from a vibrodriver can easily be discerned from upper and lower hemisphere projection, but the projection of the transient vibration from an impact hammer has demonstrated more complexity.

The method can be applied to the ground-structure vibration problem, and it can be suggested that the effect of any vibration component is greatest when an element of a building lies at right angles to the direction of wave propagation. For example, the vertical wave has a strong influence on the roof and floors while the transverse and the radial waves act more directly on the walls of the building. The effect of a travelling wave on a building is controlled by the composition of the vibration frequency and the associated wavelength in the context of length and stiffness of critical structural components.

From a review of results obtained from the Flitwick site it is concluded that a wall having a full brick construction has shown a lower response to incident ground vibrations than has a similar wall of half brick construction. The amplitude of dynamic wall strain recorded during the action of a vibrodriver was much less than that recorded from the use of a drop-hammer, both in absolute terms and also as a ratio of peak structural strain to foundation peak particle velocity.

8.3 Recommendation for further work

It is suggested that it would be advantageous to employ a larger number of velocity transducers for the measurement of ground vibration over a greater range of stand-off distances, especially when a pile is driven to a depth of more than 20m, in order to establish a more complete definition of vibration attenuation and to use one set at some 50m horizontal distance from the pile.

A full study of the structural response to typical applied ground vibrations from different sources is needed in order to estimate the risk of damage to particular buildings. This type of study should logically be reinforced by controlled tests on a fully instrumented structure.

If the design of a new data recorder/processor unit is considered, the new unit should be of a smaller size, be lighter, and be compatible with any IBM system and use 3.5 inch floppy disks rather the present 5.25 inch disks.

List of References

Ambraseys N, and Jackson J, (1984), *Seismic movements*, chapter 12, in Ground movements and their effects on structures edited by Attewell P B and Taylor R, Surrey University Press, pp 353-355.

Attewell P B, and Farmer I, (1973), *Attenuation of ground vibration from pile driving*, Ground Engineering, June, No.4, pp 26-29.

Attewell P B, and Farmer I, (1976), *Principles of engineering geology*, Chapman & Hall, London.

Attewell P B, (1985), *Estimation of ground vibration caused by driven piling in soil*, Proc. 12th Int. Conf. Soil Mech., San Francisco, pp 1-10.

Attewell P B, (1986), *Noise and vibration in civil engineering*, Mun.Eng 3, pp 139-158

Attewell P B, Selby A R, and Wilson J M, (1988), *Low amplitude mechanical vibration and structures*, Proc. Int. Symp. in *The engineering geology of ancient works, monuments and historical sites*, edited by Marinos P & Koukis G., Vol.3, pp 1189-1205, Athens, Balkema.

Attewell P B, Selby A R, and Uromeihy A, (1989), *Appraisal of ground vibration from civil engineering construction*, Int. J. Min.& Geo. Eng. July, pp.183-208, London.

Attewell P B, Oliver A and Selby A R, (1990), *Database management and analysis of piling-induced ground vibration records*, AMSE Confer. "Signals & Systems", Vol. 2, pp 115-126, Rabat, Moracco.

Beverstock P D, (1980), *Vibration from piling*, DoE/CIRIA piling development group report PG9, edited by Weltman A, PSA Civil Engineering Technical Guide No.32, London.

Bornitz, G, (1931), *Uber die ausberitung der von groszkolbenmaschinen erzeugten bodenschwingungen in die tiefe*, J. Springer, Berlin.

BS 6472, (1984), *Evaluation of human exposure to vibration in building (1-*

80Hz), 12p, British Standard Institution, London.

BS 8004, (1986), *British standard code of practice for foundations*, pp 84-108, British Standard Institution, London.

BS 5228:4, (1986), *Noise control on construction and open sites*, Part 4, 'Code of practice for noise control applicable to piling operations', British Standard Institution, London.

BS 6841, (1987), *British standard guide to measurement and evaluation of human exposure to whole-body mechanical vibration and repeated shock*, p22, British Standard Institution, London.

BS 6955, (1988), *Calibration of vibration and shock pick-up*, pp12, British Standard Institution, London.

BS 5607, (1988), *Safe use of explosives in the construction industry*, British Standard Institution, London.

British Standard Piling, (1986), *Hydraulic BSP357 hammer*, BSP International Foundations Ltd., Ipswich IP6 0JD England.

British Standard Piling, (1986), *Double-acting air-hammers*, BSP International Foundations Ltd., Ipswich IP6 0JD England.

British Steel Corporation, (1985), *Steel Piling Products*, Report No. BSC S-781b, BSC Sections, UK.

British Steel Corporation, (1986), *The rosenstock shock blasting process for piling*, Report No. BSC S-808, BSC Sections, UK.

Bullen and Partners, (1986), *N.W.B. Trial piling survey*, Report B-01, Blaydon Bridge, Neville Cross, Durham.

Cahm J M, (1986), *Pile driving and ground vibration*, M.Sc. University of Durham, UK.

Chellis R D, (1961), *Pile foundation*, 2nd edition, McGraw-Hill, New York.

Correns C W, (1969), *Introduction to minerology* 2nd edition, Georg Allen & Unwin Ltd. London.

Das B M, (1983), *Fundamentals of soil dynamics*, Elsevier, Amsterdam, 399p.

Das B M, (1984), *Principles of foundation engineering*, Brooks/Cole, Engineering Division, California.

Davis G H, (1984), *Structural geology for rocks and regions*, 5th edition, pp 361-384, John Wiley & Sons, New York.

Delmag (1988), *Diesel pile hammers*, Technical data of DELMAG construction machinery and equipment, Reinhold Dornfeld GmbH+Co, W.Germany.

Dowding C, (1985), *Blast vibration monitoring and control*, Prentice-Hall, New Jersy, USA, 297pp.

Fleming W, Weltman A, Randolph M, and Elson W, (1985), *Piling engineering*, Surrey University Press, London.

Fugro Ltd., (1986), *Geotechnical computer programs*, Technical notes, FUGRO Ltd., 18 Frogmore Rd. Hertfords, HP3 9RT, UK.

Goble G, and Rausche F, (1979), *Pile drivability predictions by CAPWAP*, Pro. In. Conf. on Numerical methods in off-shore piling, ICE, London, pp.29-36.

Goodman R E, (1980), *Introduction to rock mechanics*, Wiley, New York.

Gravare C, Goble G, and Rausche F, (1980), *Pile driving construction control by Case method*, Ground Engineering, Balken Piling Ltd. UK.

Griffin M J, (1982), *Human response to vibration*, Chapter 31, in Noise and Vibration, edited by White R C & Walker J G, Ellis Horwood Publishers, UK.

Grose W E, (1986), *Driving piles adjacent to vibration sensitive structures*, Ground Engineering, May, pp 23-28, London.

Hanna T, (1985), *Field instrumentation in geotechnical engineering*, Trans Tech Publications, USA.

Harris F, (1983), *Ground engineering equipment and methods*, Granada.

Herceg E, (1976), *Handbook of measurement and control*, Schaevitz Engineering, Pennsauken, N.J.

Heurelen A V, (1986), *Physics, A general introduction*, 2nd edition, Little,

Brown & Company, Canada.

Hiley A, (1925), *A rational pile driving formula and its application in piling practice explained*, Engineering, No.119, pp 657 and 721, London.

Hoek E, and Bray J, (1981), *Rock slope engineering*, 3rd edn. Institution of Mining and Metallurgy, London, pp.402.

Hoek E, and Brown E, (1980), *Underground excavations in rock*, Institution of Mining and Metallurgy, London, pp.527.

Hunter C, (1988), *Determination of principal accelerations, forces and stresses caused by pile driving vibrations*, M.Sc. Unversity of Durham, UK.

Jaeger J, and Cook N, (1979), *Fundamentals of rock mechanics*, Chapman Hall, London.

Jeffrey N, (1980), *Three case histories*, DoE/CIRIA piling development group report PG9, edited by Weltman A, PSA Civil Engineering Technical Guide No.32, London.

Jones S, Pearcy M, and Attewell P B, (1987), *A Graphical presentation of three-dimensional joint mobility*, Clinical Biomechanics 2, pp 14-21, London.

Kightley M L, (1980), *Tapping in to driving data*, reprint from Contract Journal, September 25, Balken Piling Ltd. Derbyshire, UK.

Knight T, (1975), *Illustrated introduction to brickwork design*, BDA Technical notes, the Brick Development Association, Windsor, UK.

Massarsch K, (1983). *Vibration problems in soft soils*, Int. Conf. on Recent Developments in Laboratory and Field Tests and Analysis of Geotechnical Problems, Bangkok. edited by Balasubramaniam *et al*, Asian Institute of Technology, Bangkok.

Miller G, and Pursey H, (1955), *On the partition of energy between elatic waves in a semi-infinite solid*, Proceding of the Royal Society of London, Series A, Mathematical and Physical Scieneces, Vol. 233, No. 1192, pp.55-69.

New B M, (1984), *Explosively-induced ground vibration in civil engineering construction*, PhD thesis, Durham University.

New B M, (1986), *Ground vibration caused by civil engineering works*, TRRL Research Report 53, 19p.

Oliver A, (1989), *An introduction to the use of a database program*, Internal report, Applied mechanics group, SEAS, University of Durham.

Oliver A, (1989), *Discussion of proposed relationships to compute predicted ground vibration data*, Internal report, Applied mechanics group, SEAS, University of Durham.

Palmer D, (1983), *Ground-borne vibrations arising from piling*, Construction Industry Research and Information Association, Final draft report 106/2 on contract RP 299, London.

Papoulis A, (1962), *The fourier integral and its application*, McGraw-Hill, New York, USA.

Paterson S, (1985), *A portable digital seismic data recorder for measurement of vibrations during piling.* MSc, University of Durham.

Phillips F C, (1983), *The use of stereographic projection in structural geology*, 3rd edition, Edward Arnold, London.

Prakash S, (1981), *Soil dynamics*, McGraw-Hill, USA.

Prakash S and Gupta M, (1970), *Report on dynamic properties of soil for diesel power house, Nakodar*, Earthquake Engineering Studies, University of Roorkee, India.

Priest S, (1985), *Hemispherical projection methods in rock mechanics*, Allen & Unwin, London 124p.

PTC Vibrofonceur, (1986), *Vibratory hammers catalogue*, supplied by Watson & Hillhouse Ltd, Whitehouse Rd., Ipswich, IP1 5NT, Suffolk, UK.

Rausche F, and Goble G, (1979), *Determination of pile damage by top measurements*, Special Technical Publication no.670, American Society for Testing and Material, Philadelphia, USA.

Redhead D, (1986), *Pile Driving equipment developments*, Civil Engineering 5, pp 21-29, London.

Richart F, and Woods R, (1987), *Vibrations*, section 17, in *Ground Engineer's Reference Book*, edited by Bell F, pp 17/3-17/15, Butterworths, London.

Richart F, Hall J, and Woods R, (1970), *Vibrations of soils and foundations*, Prentice-Hall, Englewood Cliffs, N J.

Selby A, 1989, *Acquisition by microcomputer of some ground vibration data during pile driving*, Proc. Int. Symp. on *computer and physical modelling in geotechnical engineering*, Dec. 1986, edited by Balasubramanian *eta A.A*, Balkema, Rotterdam pp 133-147.

Selby A R, (1988), *Ground vibration caused by pile driving*, British Steel Seminar, Sheffield, UK.

Selby A R, (1989), *Strains in brickwork due to ground vibration caused by pile driving*, Internal report, SEAS, Durham University.

Selby A R, (1990), personal communication.

Selby A R, and Swift J, (1989), *Recording and processing ground vibrations caused by pile driving*, Proceeding Intern. AMSE Conference "Signals & Systems", Vol.6,p.101-113, Brighton, UK.

Sensor, (1985), *Geosource geophone SM-6*, Exploration Products Division, Norwich NR6 6JB, Norfolk, England.

Skipp B, (1984), *Dynamic ground movements, man-made vibrations*, chapter 13 in Ground movements and their effects on structures edited by Attewell P B, & Taylor R, Surrey University Press, pp 382-395.

Smith E A, (1960), *Pile driving analysis by wave equation*, J. Soil Mechanics and Foundations Division, ASCE, Vol.86, pp. 35-61.

Spivak M, (1967), *Calculus*, W.A.Benjamin, Inc., California, USA.

Steffens R, (1974), *Structural vibration and damage*, BRE Report, London.

Storey R and Ellery G (1985), *A comparison of efficiency and driveability of*

drop and diesel hammers on varing pile types, 2nd International Conference on *Application of stress-wave theory on piles*, Stockholm, Edited by Holm G, Bredenberg H & Gravare C.

Timoshenko S, and Goodier J, (1984), *Theory of elasticity*, 3rd edition, McGraw-Hill, New York.

Tomlinson M J, (1977), *Pile design and construction practice*, Viewpoint Publication, London.

Uromeihy A, 1988, *A Convenient device for hemispherical projection plotting in rock mechanics*, Int. J. Min. & Geo. Eng. 6, pp 163-168, London.

Waller R, (1969), *Building on springs*, Pergamon Press, 88p, Oxford, UK.

Waltham M A, (1980), *SR-4 strain gauge handbook*, BLH Electronic HDBK 103 USA.

Walton C, (1990), *A database of ground borne vibration and structural damage cases-description of the database and initial analyses of data*, Building Research Establishment Report, BRE/84/7/2, SD/BRE/GD224, N6/90, UK.

Watkins L H, (1980), *Some research into the environmental impact of roads and traffic*, TRRL supplementary report no.539, pp 1-13, London.

Weisflog W, (1967), *Vibratory pile driving*, Rolba limited, Sussex, UK.

Wellington A M, (1888), *Piles and pile driving*, Engineering News Publication Co., New York, USA.

Whitaker T, (1976), *The design of piled foundations* 2nd ed. Pergamon Press, 218p, Oxford, UK.

White R G, (1982), *Vibration testing* Chapter 27, in Noise and Vibration, edited by White R & Walker J, Ellis Horwood Publishers, UK.

Winney M, (1989), *Dutch hammer into hydraulic piling*, Ground Engineering 4, pp 19-20, London.

Wiss J, (1981), *Construction vibrations: state of the art*, J. of the Geotechnical Engineering Division, ASCE, Vol. 107, No. GT2, February, pp 167-181.

Appendices

Appendix A1

A1.1 Derivation of Wave Equations

Derivation of the body-wave propagation equations in one and three dimensions is reviewed in the following sections. The detailed information on these equations is covered in several rock and soil dynamics textbooks, for example, see Jaeger and Cook (1979), Timoshenko and Goodier (1984), Prakash (1981) and Das (1983).

A1.1.1 One-dimensional Solution

When a load is applied impulsively to an elastic rod, the applied load transfers to the other parts of the rod as a propagated wave. If the applied load is axial, it then generates a longitudinal wave and if it is torsional, it generates a shear wave in the rod.

a. Compressional Wave

Consider a thin uniform rod, having constant cross-sectional area A, elastic modulus E and density ρ to be under a uniform force in the x-direction. It is assumed that the stress remains uniform over the cross-section area, and the cross-section remains plane during the motion. Also consider an element in this rod of length Δx, as shown in figure (A1.1a). The applied stress on plane (x) is (σ_x) and applied stress on plane $(x + \Delta x)$ is $\left(\sigma_x + \frac{\partial \sigma_x}{\partial x}\Delta x\right)$. The application of the stresses causes positive propagation of the wave in a compressive sense and negative propagation in a tensile sense. According to *Newton's second law*

$$\text{Sum of forces} = \text{mass} \times \text{acceleration}$$

$$\Sigma F = ma$$

$$-\sigma_x A + (\sigma_x + \frac{\partial \sigma_x}{\partial x}\Delta x)A = \Delta x A \rho \frac{\partial^2 u}{\partial t^2} \qquad 1.1$$

Eq(1.1) can be written;

$$\frac{\partial \sigma_x}{\partial x} = \rho \frac{\partial^2 u}{\partial t^2} \qquad 1.2$$

Since $\epsilon = \frac{\partial u}{\partial x}$, and $\sigma = E\epsilon$, then;

$$\sigma_x = E\frac{\partial u_x}{\partial x} \qquad 1.3$$

Differentiating Eq(1.3) respect to x;

$$\frac{\partial \sigma_x}{\partial x} = E\frac{\partial^2 u}{\partial x^2}$$

Eq(1.2) can be written;

$$\frac{\partial^2 u}{\partial t^2} = \frac{E}{\rho}\frac{\partial^2 u}{\partial x^2}$$

$$\frac{\partial x^2}{\partial t^2} = \frac{E}{\rho}$$

and

$$c_p = \sqrt{\frac{E}{\rho}} \qquad 1.4$$

where c_p is defined as the longitudinal wave propagation velocity in the rod and is a function of material (ground) properties.

Consider figure (A1.1b). When the load is applied at one end of the rod, at time (∂t), there will be some displacement (∂u) in the rod. If $(\partial u/\partial t = v_t)$ which is particle velocity, then (v_t) can be related to the wave velocity (c_p) by the following equations

$$\text{particle velocity} = \frac{\partial u}{\partial t} \qquad \textit{and} \qquad \text{wave velocity} = \frac{\partial x}{\partial t}$$

or

$$\partial u = v_t \times \partial t \qquad \textit{and} \qquad \partial x = v_p \times \partial t$$

Since $(\epsilon_x = \partial u/\partial x)$ and $(\epsilon = \sigma_x/E)$, then

$$v_t = \frac{\sigma}{E}c_p \qquad \textit{or} \qquad v_t = \epsilon c_p \qquad 1.5$$

It can be concluded that the particle velocity depends on the intensity of the applied stress or strain, while the wave velocity is a function of the material (ground) properties.

b. Shear Waves

The one-dimensional shear-wave propagation velocity can be related to the solution of the torsional vibration equation in the rod using *Hooke's law*

$$G = \tau/\gamma \qquad 1.6$$

where G is shear modulus, τ is shear stress and γ is shear strain. Since

$$\tau = T/I_p \qquad and \qquad \gamma = \partial\theta/\partial x$$

where T is the torque force, I_p is polar moment of inertia of the cross-sectional area of the rod, and $\partial\theta$ is the angle of torsion at any length ∂x. Eq(1.6) can be represented by

$$T = I_p G \frac{\partial\theta}{\partial x} \qquad 1.7$$

The applied torque at distance x is T and at distance $x + \Delta x$ is $T + (\partial T/\partial x)\Delta x$. Applying *Newton's second law*

$$-T + \left(T + \frac{\partial T}{\partial x}\Delta x\right) = \rho I_p \Delta x \frac{\partial^2\theta}{\partial t^2} \qquad 1.8$$

Substitution of Eq(1.6) into Eq(1.7) results in

$$\frac{\partial^2\theta}{\partial t^2} = \frac{G}{\rho}\frac{\partial^2\theta}{\partial x^2}$$

$$\frac{\partial^2 x}{\partial t^2} = \frac{G}{\rho}$$

$$c_s = \sqrt{\frac{G}{\rho}} \qquad 1.9$$

where c_s is the shear velocity in the rod, which has similar form to that for the compressional wave velocity.

A1.1.2 Three-dimensional Solution

It is possible to establish the propagation of stress waves through an elastic medium in three dimensions using Hooke's law.

Consider a small cube element of soil illustrated in figure (A1.2), the sides of which are defined as dx, dy and dz. Two types of external forces (body forces &

surface forces) can act on that element. According to Newton's second law, the application of three orthogonal normal forces on planes x, y and z results in the following stresses;

$$plane\ x, \quad \sigma_x, \tau_{yx}, \tau_{zx}$$

$$plane\ y, \quad \sigma_y, \tau_{xy}, \tau_{zy}$$

$$plane\ z, \quad \sigma_z, \tau_{xz}, \tau_{yz}$$

Thus, on plane x, σ_x is the normal stress and τ_{yx}, τ_{zx} are the shear stresses acting normal to planes y and z, respectively. Correspondingly, the same explanation can be applied for plane y and plane z.

The sum of the forces on the soil element in the x, y and z directions are;

$$\frac{\partial \sigma_x}{\partial x} + \frac{\partial \tau_{yx}}{\partial y} + \frac{\partial \tau_{zx}}{\partial z} = \rho \frac{\partial^2 u}{\partial t^2} \qquad 1.10$$

$$\frac{\partial \sigma_y}{\partial y} + \frac{\partial \tau_{xy}}{\partial x} + \frac{\partial \tau_{zy}}{\partial z} = \rho \frac{\partial^2 v}{\partial t^2} \qquad 1.11$$

$$\frac{\partial \sigma_z}{\partial z} + \frac{\partial \tau_{xz}}{\partial x} + \frac{\partial \tau_{yz}}{\partial y} = \rho \frac{\partial^2 w}{\partial t^2} \qquad 1.12$$

where ρ is the density of the soil, and u, v and w are the components of displacement in x, y and z directions, respectively.

If the element undergoes some deformation under the action of stress, then the equation defining strain and rotation of the element in terms of displacement can be written as

Strain:

$$\epsilon_x = \frac{\partial u}{\partial x} \qquad \gamma_{xy} = \frac{\partial v}{\partial x} + \frac{\partial u}{\partial y} \qquad 1.13$$

$$\epsilon_y = \frac{\partial v}{\partial y} \qquad \gamma_{yz} = \frac{\partial w}{\partial y} + \frac{\partial v}{\partial z} \qquad 1.14$$

$$\epsilon_z = \frac{\partial w}{\partial z} \qquad \gamma_{zx} = \frac{\partial u}{\partial z} + \frac{\partial w}{\partial x} \qquad 1.15$$

Rotation:

$$\hat{w}_x = \frac{1}{2}\left(\frac{\partial w}{\partial y} - \frac{\partial v}{\partial z}\right) \qquad 1.16$$

$$\widehat{w}_y = \frac{1}{2}\left(\frac{\partial u}{\partial z} - \frac{\partial w}{\partial x}\right) \qquad 1.17$$

$$\widehat{w}_z = \frac{1}{2}\left(\frac{\partial v}{\partial x} - \frac{\partial u}{\partial y}\right) \qquad 1.18$$

The quantities of ϵ_x, ϵ_y and ϵ_z and γ_{xy}, γ_{yz} and γ_{zx} which determine the deformation of a body are called components of strain, where ϵ is the normal strain and γ is shear strain, and $\widehat{w}_x, \widehat{w}_y$ and $\widehat{w}_z$ are the components of rotation about the x, y and z axes, respectively.

For an elastic medium, the normal strains and stresses can be related by the following equations:

$$\epsilon_x = (1/E)[\sigma_x - \nu(\sigma_y + \sigma_z)] \qquad 1.19$$

$$\epsilon_y = (1/E)[\sigma_y - \nu(\sigma_x + \sigma_z)] \qquad 1.20$$

$$\epsilon_z = (1/E)[\sigma_z - \nu(\sigma_x + \sigma_y)] \qquad 1.21$$

where E is the elastic modulus $(= \sigma/\epsilon)$, and ν is the Poissons ratio$^{\oplus}$. Also, normal stresses and strains can be related to shear stresses and shear strains by the following equations:

$$\sigma_x = \lambda\Delta + 2G\epsilon_x \qquad \tau_{xy} = \tau_{yx} = G\gamma_{xy}$$

$$\sigma_y = \lambda\Delta + 2G\epsilon_y \qquad \tau_{yz} = \tau_{zy} = G\gamma_{yz}$$

$$\sigma_z = \lambda\Delta + 2G\epsilon_z \qquad \tau_{zx} = \tau_{xz} = G\gamma_{zx}$$

where G and λ are elastic constants, termed Lame's constants, G also known as the shear modulus and Δ is the dilation.

$$G = \frac{E}{2(1+\nu)}$$

$$\lambda = \frac{\nu E}{[(1+\nu)(1-2\nu)]}$$

$$\Delta = (\epsilon_x + \epsilon_y + \epsilon_z) \qquad 1.22$$

$^{\oplus}$ Poissons ratio (ν) is the ratio of induced strain in lateral direction to the strain in axial direction and lies within the limit $0 < \nu < 0.5$.

Also the Poisson's ratio(ν) can expressed as;

$$\nu = \frac{\lambda}{2(\lambda + G)}$$

Substitution of above quantities in Eq(1.10), (1.11) & (1.12), gives:

$$\rho\frac{\partial^2 u}{\partial t^2} = (\lambda + G)\frac{\partial \Delta}{\partial x} + G\,\nabla^2 u \qquad 1.23$$

$$\rho\frac{\partial^2 v}{\partial t^2} = (\lambda + G)\frac{\partial \Delta}{\partial y} + G\,\nabla^2 v \qquad 1.24$$

$$\rho\frac{\partial^2 w}{\partial t^2} = (\lambda + G)\frac{\partial \Delta}{\partial z} + G\,\nabla^2 w \qquad 1.25$$

Where ∇^2 is defined as

$$\nabla^2 = \left(\frac{\partial^2}{\partial x^2} + \frac{\partial^2}{\partial y^2} + \frac{\partial^2}{\partial z^2}\right) \qquad 1.26$$

There are two solutions for Eq(1.23), (1.24) & (1.25). One determines the propagation of longtitudinal waves while the other describes the propagation of shear waves.

a. Compressional Waves

The longitudinal wave propagation velocity can be obtained by differentiating Eqs(1.23), (1.24) & (1.25) with respect to x, y & z, respectively, and adding all three expressions together, giving

$$\rho\frac{\partial^2}{\partial t^2}\left(\frac{\partial u}{\partial x} + \frac{\partial v}{\partial y} + \frac{\partial w}{\partial z}\right) = (\lambda + G)\left(\frac{\partial^2 \Delta}{\partial x^2} + \frac{\partial^2 \Delta}{\partial y^2} + \frac{\partial^2 \Delta}{\partial z^2}\right) + G\,\nabla^2\left(\frac{\partial u}{\partial x} + \frac{\partial v}{\partial y} + \frac{\partial w}{\partial z}\right)$$

or

$$\rho\frac{\partial^2 \Delta}{\partial t^2} = (\lambda + G)(\nabla^2\Delta) + G(\nabla^2\Delta) = (\lambda + 2G)\,\nabla^2\,\Delta$$

Therefore

$$\rho\frac{\partial^2 \Delta}{\partial t^2} = (\lambda + 2G)\,\nabla^2\,\Delta = c_p^2\,\nabla^2\,\Delta$$

Then

$$c_p = \sqrt{\frac{\lambda + 2G}{\rho}} \qquad 1.27$$

where c_p is the compression wave propagation velocity in an infinite elastic medium.

b. Shear waves

The other solution for Eq(1.23),(1.24) and (1.25) can be achieved by differentiating Eq(1.24) with respect to z and Eq(1.25) with respect to y

$$\rho\frac{\partial^2}{\partial t^2}\left(\frac{\partial v}{\partial z}\right) = (\lambda + G)\frac{\partial \Delta}{(\partial y)(\partial z)} + G\,\nabla^2\,\frac{\partial v}{\partial z} \qquad 1.28$$

$$\rho\frac{\partial^2}{\partial t^2}\left(\frac{\partial w}{\partial y}\right) = (\lambda + G)\frac{\partial \Delta}{(\partial y)(\partial z)} + G\,\nabla^2\,\frac{\partial w}{\partial y} \qquad 1.29$$

Subtracting Eq(1.29) from Eq(1.28), gives

$$\rho\frac{\partial^2}{\partial t^2}\left(\frac{\partial w}{\partial y} - \frac{\partial v}{\partial z}\right) = (\lambda + G)\left(\frac{\partial w}{\partial y} - \frac{\partial v}{\partial z}\right) \qquad 1.30$$

Substitute the expression of rotation from Eq(1.16) to Eq(1.30), results

$$\rho\frac{\partial^2 \widehat{w}_x}{\partial t^2} = G\,\nabla^2\,\widehat{w}_x$$

$$\frac{\partial^2 \widehat{w}_x}{\partial t^2} = \frac{G}{\rho}\,\nabla^2\,\widehat{w}_x = c_s^2\,\nabla^2\,\widehat{w}_x \qquad 1.31$$

Therefore

$$c_s = \sqrt{\frac{G}{\rho}} \qquad 1.32$$

Eq(1.31) is the equation of distortional waves, and Eq(1.32) defines the shear wave propagation velocity. Similar processes can be used for Eq(1.23) to (1.25) to obtain two more distortional equations around y and z axes:

$$\frac{\partial^2 \widehat{w}_y}{\partial t^2} = c_s^2\,\nabla^2\,\widehat{w}_y$$

$$\frac{\partial^2 \widehat{w}_z}{\partial t^2} = c_s^2\,\nabla^2\,\widehat{w}_z$$

A1.2 Wave Transmissions

A1.2.1 Wave Reflection

When a wave is incident on a boundary between two media that have different acoustic impedance (ρc) properties, part of the wave is reflected. The directions of the incident and the reflected waves are shown in figure (A1.3). The incident ray makes an angle θ_i with the normal line (which is perpendicular to the boundary surface), and the reflected ray makes an angle θ_r with respect to the normal. According to the *law of reflection*

$$\theta_i = \theta_r \qquad 1.33$$

The incident and reflected rays are on opposite sides of the normal line and in the same plane with it.

A1.2.2 Wave Refraction

As has been mentioned above, part of the incident wave will refract into the new medium. Refraction is caused by the change in speed of a wave as it passes from one medium to another of different acoustic impedance, causing changes in wave direction.

Considering figure (A1.4), the direction of the incident wave is indicated by angle θ_1, and θ_2 represents the direction of the refracted wave (both angles relative to the normal line). If a wave enters a medium in which its speed decreases, its direction bends toward the normal line. However, if the speed increases, the refraction direction bends away from the normal line.

To derive an equation for calculating the expected change in direction, refer to the wavefront shown in figure (A1.5a) as it approaches the boundary between two media. Point B on the wavefront requires a time t to move forward to the boundary. Since the wave speed in medium 1 is v_1, point B moves the distance $v_1 t$ during that time to reach the boundary. Point A which has just entered medium 2 moves

a distance v_2t during that same time. If v_2 is less than v_1♣, then point A moves a shorter distance than point B, and the wave refracts toward the normal line. If v_2 is greater than v_1, point A moves a greater distance than point B and the wave refracts away from the normal line (see figure (A1.5b)).

The change in wave direction can be calculated by comparing the triangles shown in figure (A1.5c)

$$sin\theta_1 = \frac{v_1 t}{L} \qquad sin\theta_2 = \frac{v_2 t}{L}$$

$$\frac{sin\theta_1}{sin\theta_2} = \frac{v_1 t/L}{v_2 t/L} = \frac{v_1}{v_2}$$

$$\frac{sin\theta_1}{v_1} = \frac{sin\theta_2}{v_2} \qquad 1.34$$

This equation, known as *Snell's law*, was introduced in 1621†.

The transmission of a wave from the pile toe in an uniform and homogeneous ground follows a straight path towards the ground surface, while in a non-uniform ground with different acoustic impedance, (ρc), the wave will be refracted towards the pile or away from the pile as the ρc decreases or increases towards the ground surface, respectively. The refraction path of the transmitted wave in the ground is shown in figure (A1.6).

A1.2.3 Reflection and Refraction of Body Waves

As has been discussed in section 2.3, the direction of a body wave can be parallel to the direction of propagation as in a *radial sense*(`P-wave`), and it can be perpendicular to the direction of propagation as in *shear*(`S-wave`). Shear waves can either be *vertical*(S_v`-wave`) or *horizontal*(S_h`-wave`).

If a P-wave reaches the boundary between two layers as shown in figure (A1.7a), there are two reflected waves (P_1, S_{v1}) in layer one, and two refracted waves (P_2, S_{v2}) in layer two. According to the reflection law;

$$\alpha_1 = \alpha_2$$

♣ The speed of a wave in a medium is mainly controlled by its acoustic impedance (ρc)

† See Heurelen (1986)

Using Snell's law:

$$\frac{sin\alpha_1}{v_{p1}} = \frac{sin\alpha_2}{v_{p1}} = \frac{sin\beta_2}{v_{s1}} = \frac{sin\alpha_3}{v_{p2}} = \frac{sin\beta_3}{v_{s2}} \qquad 1.35$$

where v_{p1} and v_{p2} are the velocities of P-waves in layers 1 and 2, respectively and v_{s1} and v_{s2} are the S_v-wave velocities in layers 1 and 2, respectively.

If an S_h-wave reaches the boundary between two layers, as shown in figure (A1.7b), there is only one reflected wave (S_{h1}-wave) and one refracted wave (S_{h2}-wave).

$$\beta_1 = \beta_2$$

$$\frac{sin\beta_1}{v_{s1}} = \frac{sin\beta_3}{v_{s2}} \qquad 1.36$$

Finally, if an S_v-wave reaches the boundary between two layers, as shown in figure(A1.7c), this results in two reflected waves (S_{v1}, P_1) and two refracted waves (S_{v2}, P_2).

$$\frac{sin\beta_1}{v_{s1}} = \frac{sin\beta_2}{v_{s1}} = \frac{sin\alpha_2}{v_{p1}} = \frac{sin\beta_3}{v_{s2}} = \frac{sin\alpha_3}{v_{p2}} \qquad 1.37$$

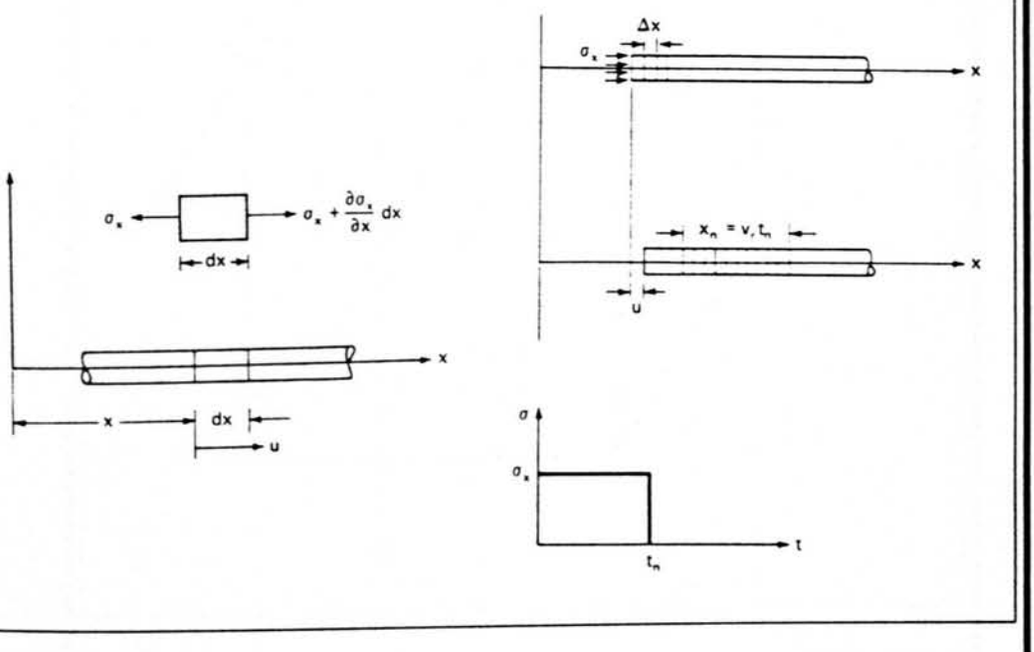

Figure (A1.1) Propagation of P–wave in one–dimensional rod

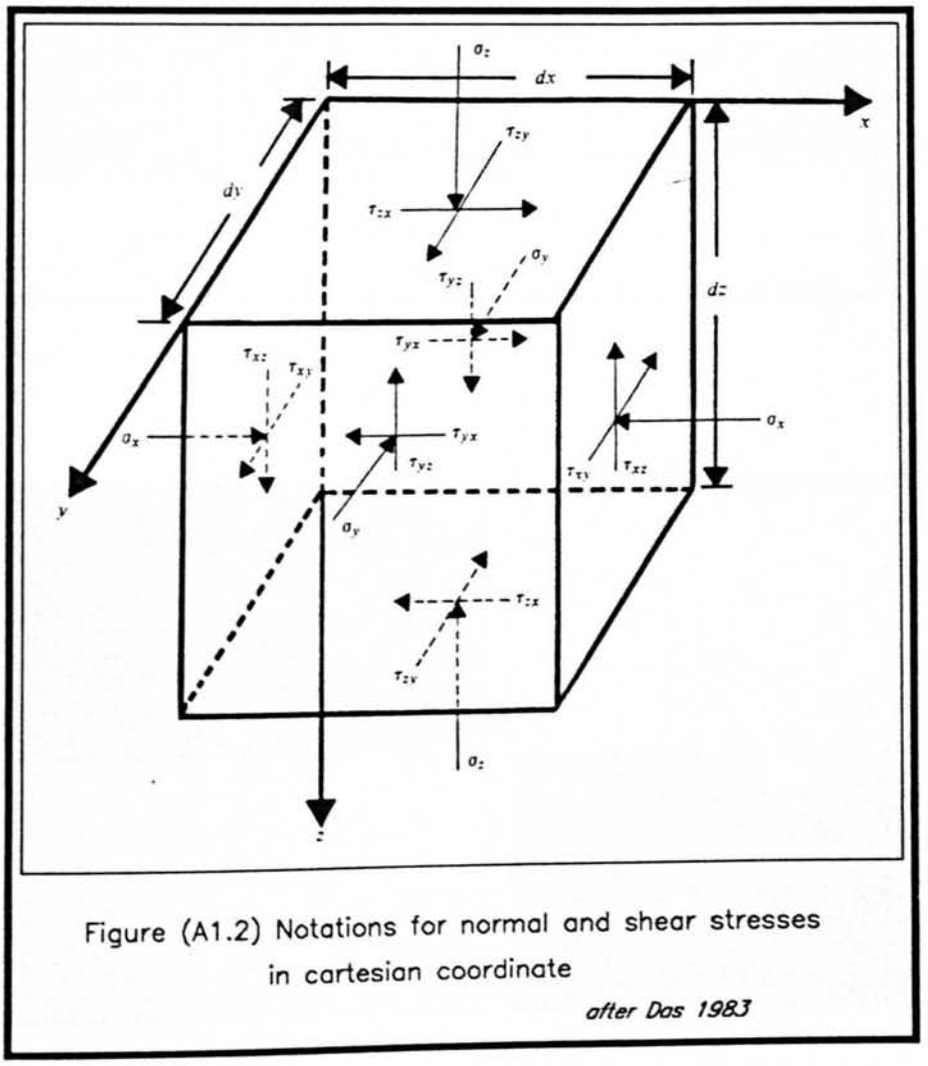

Figure (A1.2) Notations for normal and shear stresses in cartesian coordinate

after Das 1983

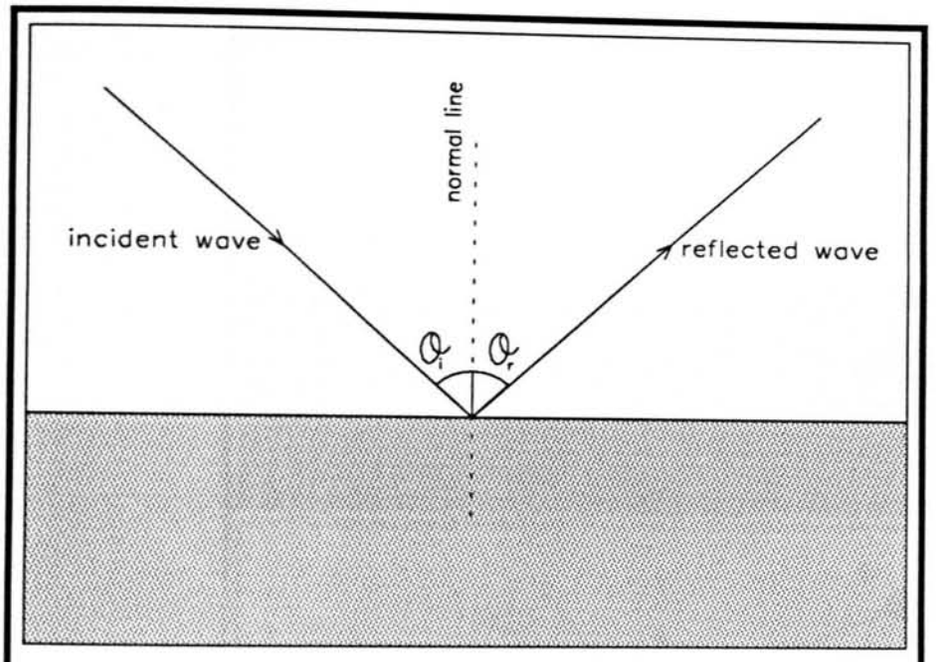

Figure (A1.3) The mechanism of wave reflection

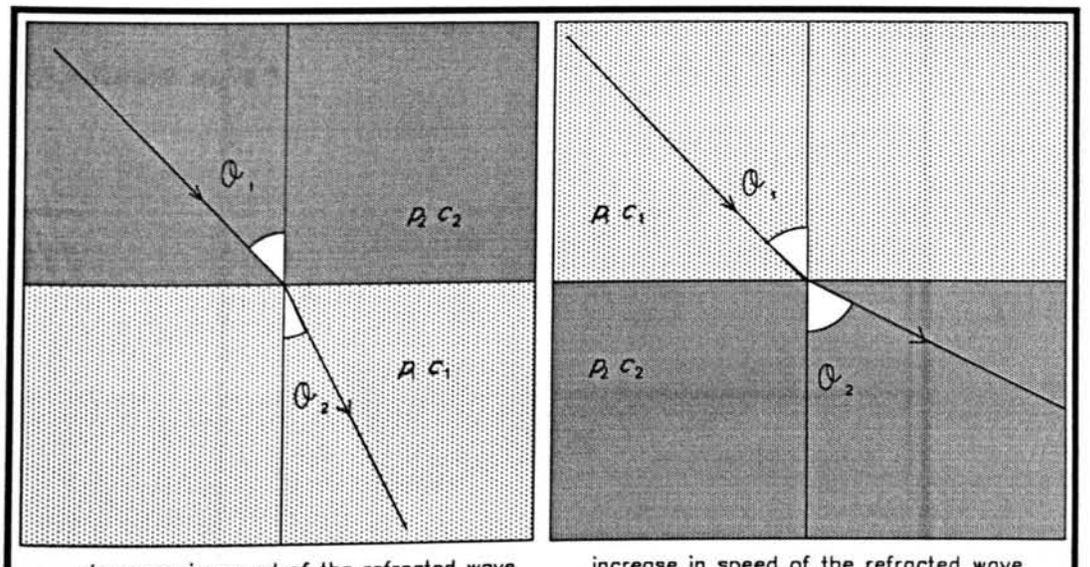

decrease in speed of the refracted wave

increase in speed of the refracted wave

$\rho_2 c_2 > \rho_1 c_1$

Figure (A1.4) The behaviour of a refracted wave

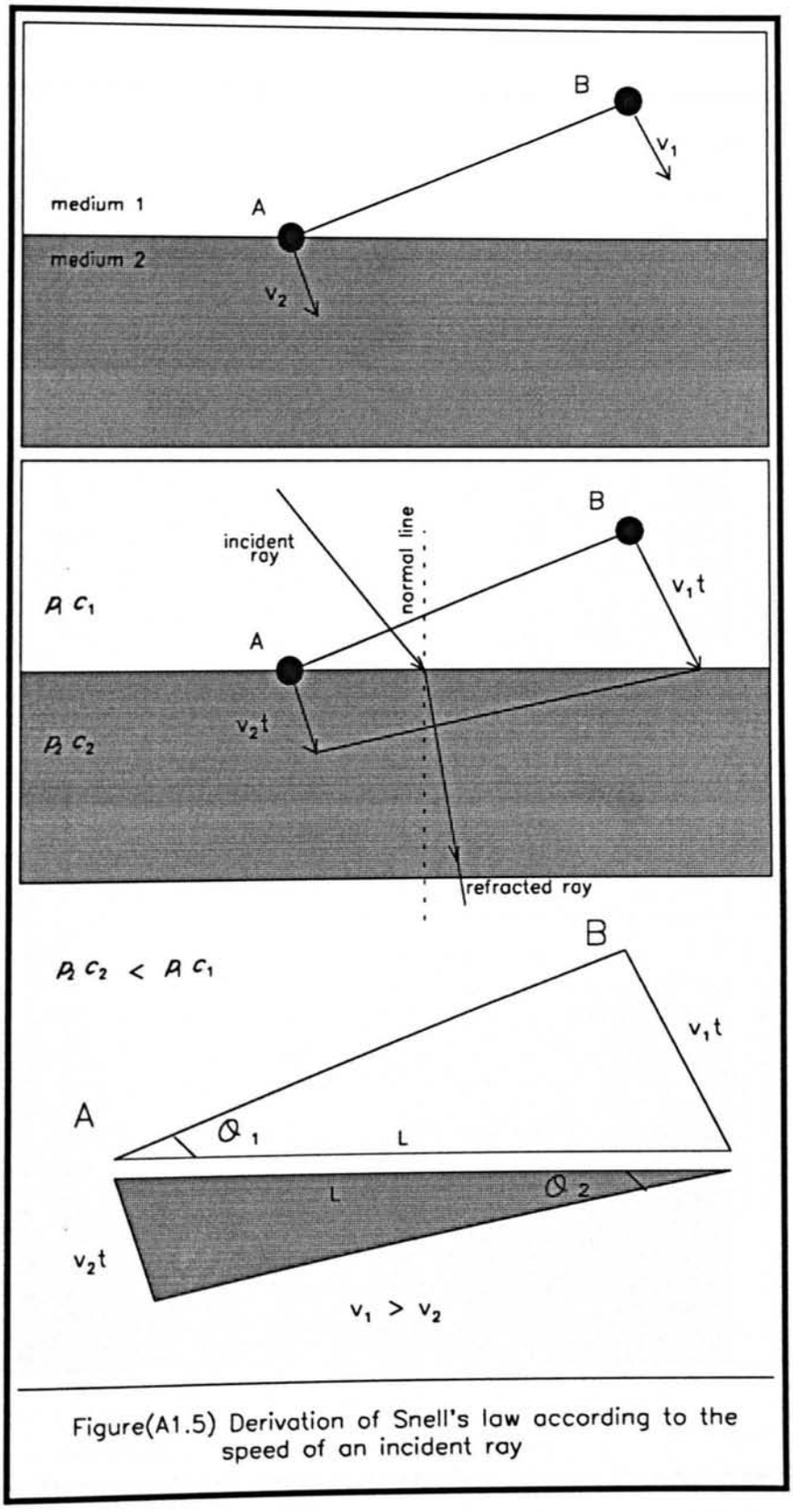

Figure(A1.5) Derivation of Snell's law according to the speed of an incident ray

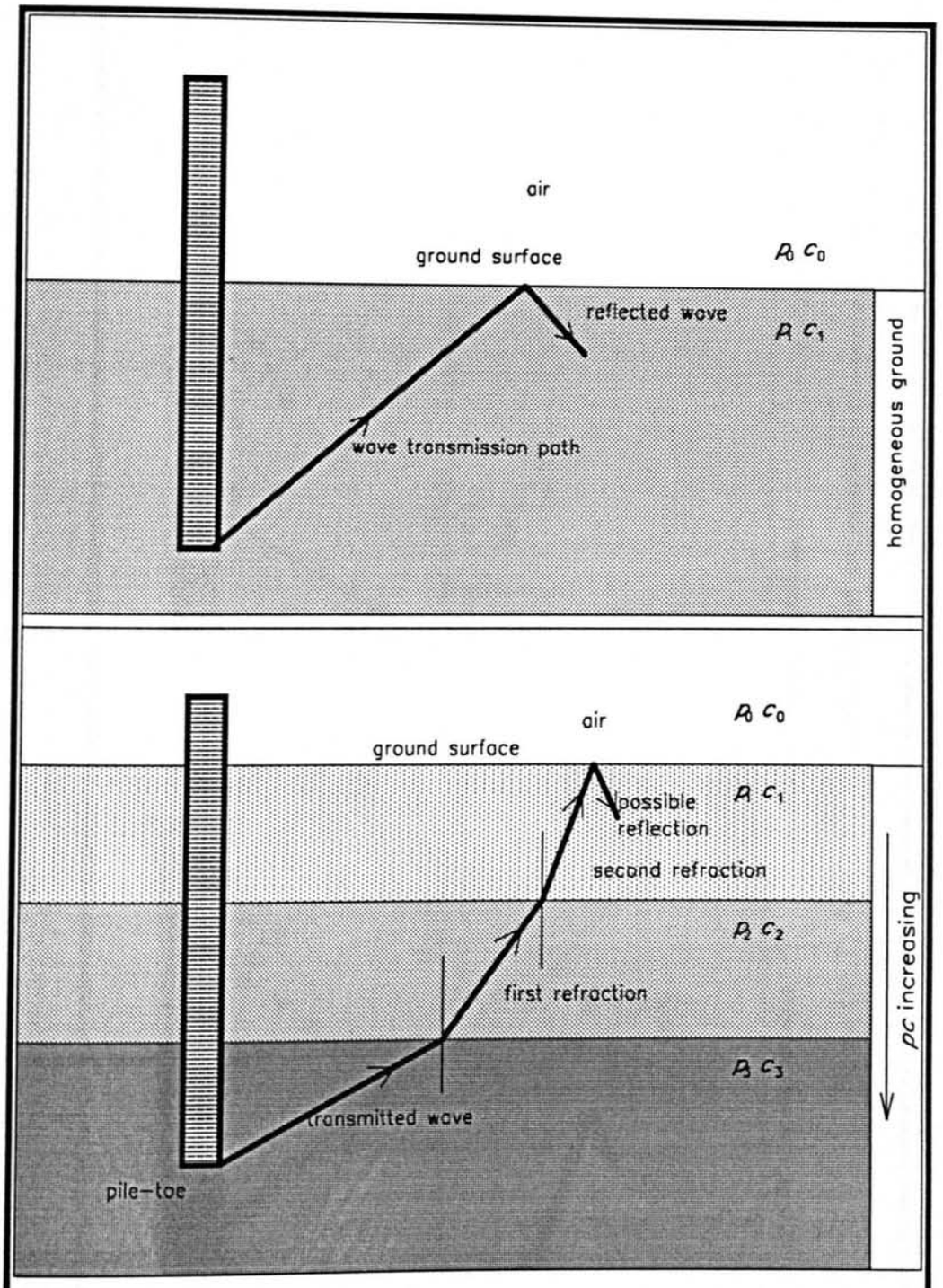

Figure (A1.6) Refraction path of a transmitted wave from pile-toe in a homogeneous and non-homogeneous ground

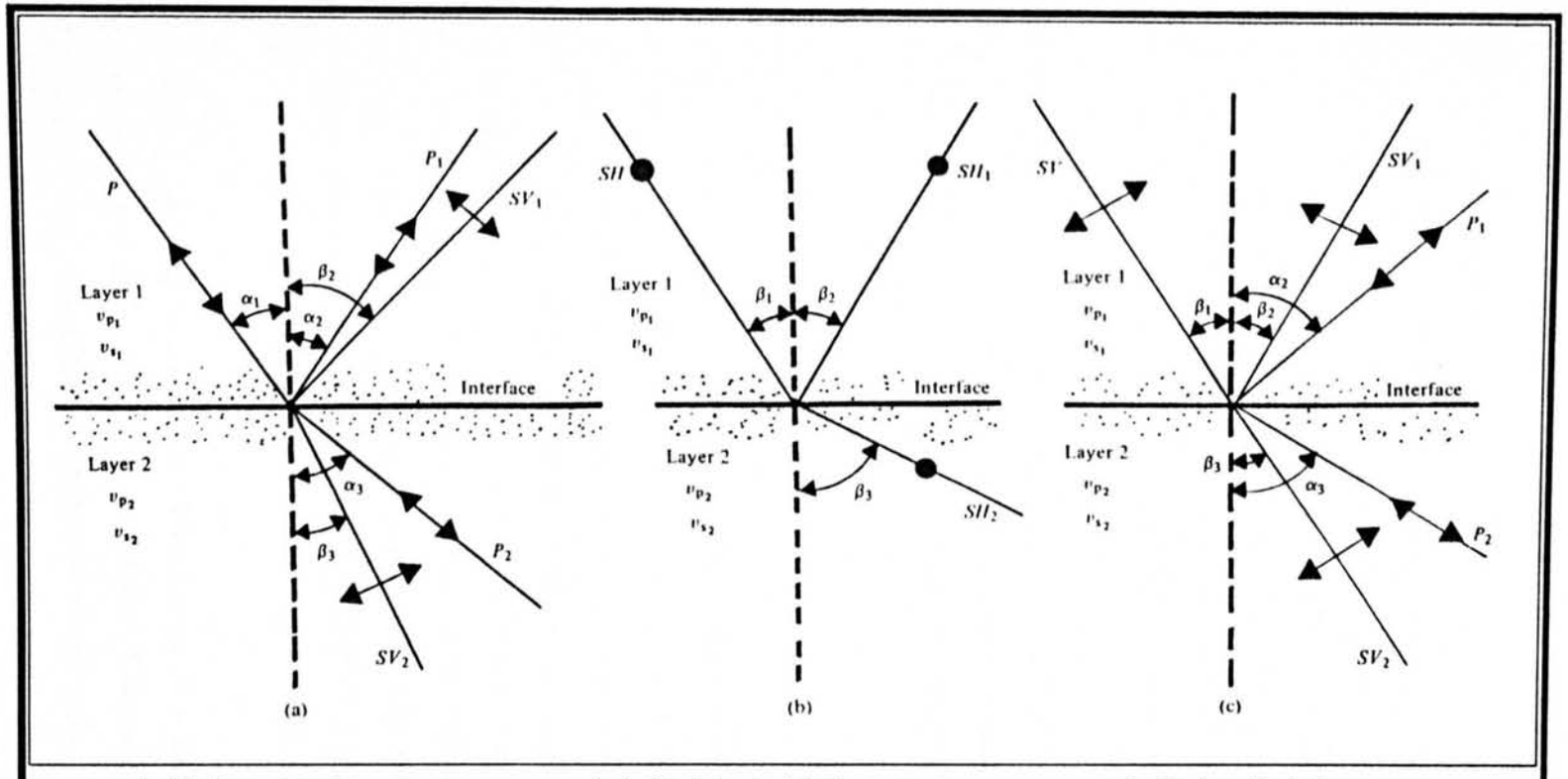

a. incident compression–wave b. incident horzontal shear–wave c. incident vertical shear–wave

Figure (A1.7) Reflection and refraction of an incident body–wave

after Das 1983

Appendix A2

A2. Variation of Pile Material

A summary of different classifications of pile is reviewed in Chapter (3). The pile may be made of either steel, concrete, timber or a combination of more than one material. The choice of a particular type of pile for construction is mainly controlled by the economics, the environmental conditions of that particular site (for example, the geological conditions of the ground and the depth of water table), and the construction design (for example, the use of piles for temporary or permanent works).

This appendix gives a brief classification of piles according to their material components. More details of pile classification can be found in several text books, for example, Tomlinson (1977), Fleming *et al* (1985) and British Standard BS 8004 (1986).

A2.1 Steel Piles

Steel piles are commonly used in both permanent works (for example, as earth retaining walls and structural foundation) and temporary works (for example, for supporting the ground during cofferdam construction). Steel piles provide many advantages; for example their ability to withstand hard driving and their capability of carrying a high load capacity for deeper penetration in hard deposits and rock. Their length can easily be extended or reduced if required by welding or cutting to cope with the driving conditions of the site, they cause smaller soil displacements, so reducing the effect of compaction in cohesionless soil and ground heave in cohesive soil, and finally steel piles are robust and stable during handling, lifting, pitching and driving.

Steel piles may be affected by corrosion. The degree of corrosion in steel is dependent on the conditions of the working environment. Corrosion in a steel pile below the ground water level is negligible. Above the water table, the pile may be

protected by different methods of coating[⊖]. A summary of the degree of corrosion in steel piles with respect to different environmental conditions is listed in table (A2-1)[⊙].

Steel piles can be classified according to their functions as *sheet piles* and *bearing piles.*

A2.1.1. Sheet piles

Sheet piles are widely used for retaining or containing soil or water, and consequently the loads acting on the pile are primarily horizontal. They may also be used as bearing piles to carry applied vertical loads. Sheet piles can be employed either for temporary works such as cofferdams and retaining walls (dock and harbour works), or in permanent structures, for example piled foundations, land reclamation and sea defence works.

The standard sheet pile sections available in the UK, are either the U-section or *Larssen pile*, or the Z-section or *Frodingham pile.* Frodingham piles are normally supplied in interlocked pairs, while Larssen piles are supplied as single piles. The sections and the interlock facilities are designed to provide the maximum strength and durability to resist applied loads during pitching and driving and also in their working condition. The cross sections of the above piles and other relevant information are displayed in figure (A2.1).

A wide range of different section sizes and weights is available in various grades of steel to suit the nature and requirements of most construction activities. The wider sections are slightly harder to drive, as resistance to penetration is partly dependent on width as well as on interlock friction, and in such cases a heavier hammer may be needed.

Heavier sections are appropriate for use in permanent structures where the ap-

---

⊖ Information on mechanism of corrosion and method of protection can be found in standard texts, for example, see British Steel reports.

⊙ The information of this table are extracted from the BSC report edited by Morley J (1979)

plied stresses are very high, and the tops of the piles can then be cut-off, trimmed and capped with a concrete beam to form a permanent steel wall from a series of interlocked sheet piles. Where piles form temporary works, they can be extracted easily and without distortion for re-use.

Steel sheet piling is generally available in lengths up to 30m. The maximum driveable length for each piling section depends upon the type of ground, the penetration required and the type of construction for which the piling is designed. Where it is necessary to increase the pile length during driving, fishplated or site-welded joints can be used.

The Frodingham and Larssen piles include a special range of sections to be used in different types of construction; for example *corner* or *junction piles* are usually used in cofferdam constructions. Different parts of sheet piles can be jointed together to form *box piles*, and also they can be welded to bearing piles to produce *high modulus* piles. Examples of the above piles are shown in figure (A2.1).

A2.1.2. Bearing Piles

Steel bearing piles are used to transmit predominantly vertical loads into the ground. They are usually driven vertically but when large horizontal forces are to be carried, piles can be driven to a rake. Common applications include foundations for bridges and buildings, jetties and dolphins.

There are three main types of steel bearing piles: *H-pile, tube-pile* and *box-pile.* Universal bearing piles are a rolled steel H-section of approximately equal depth and width and having flanges and web of equal thickness, thus providing uniform resistance to driving forces and any possible corrosion. A typical example of an H-section steel pile is indicated in figure (A2.1). The pile is available in a wide range of sizes and weights to allow driving in different ground conditions. They are widely used for driving in hard stratum or to rock because they show a high base resistance, and also they can be driven close to existing structures since they cause little displacement in the surrounding soil.

Both tube and box piles are usually driven into the ground with their ends

open. When fitted with a shoe or when driven into soils likely to cause plugging, they become displacement piles and may cause ground heave. Occasionally tube or box piles are filled with concrete after driving and although this does not greatly increase the load bearing capacity, the filling may reduce internal corrosion.

In general, the H-pile is effective for use in foundations, while tube and box piles are more advantageous where the piles project above bed level, as in marine constructions.

A2.2 Concrete Piles

Concrete piles are economical and can be used in most types of soil. They are very widely used in Sweden, Holland and North America. Usually concrete piles act as friction piles in which most of the applied load is transferred to the surrounding soil through shaft friction. Concrete piles may be classified into two groups, *precast concrete* and *cast-in-place concrete* piles.

A2.2.1. Precast Concrete Piles

This type of pile is available in a range of cross-sections including triangular, square, circular and hexagonal. They are reinforced with three, four or six steel bars in the corners of the relevant types. The presence of the reinforcement bars is to enable the pile to resist axial loads and bending moments developed during transportation and driving, and also to withstand vertical loads and bending moments caused by lateral loading. Concrete piles can be easily spliced by proprietary joints to get longer piles up to 100m. The length of each section is typically of the order of 12m and the diameter is usually between 20-40cm.

Precast concrete piles may be *prestressed* or *reinforced.* The prestressed pile has advantages of light weight, good bending strength and drivability, while the reinforced pile may have a higher bearing capacity.

A2.2.2. Cast-in-place Concrete Piles

There are several methods available for installation of cast-in-place concrete piles. These methods are fully explained by Chellis (1961), Tomlinson (1977) and Fleming *et al* (1985). Below a brief classification of different installation techniques

is reviewed.

The cast-in-place concrete piles can behave either as *displacement piles* or *non-displacement piles*

Displacement pile: these piles can be formed using the following two ways of installation:

1. by driving a temporary tube pile into the ground (the tube is usually locked from its toe end by using a flat steel plate shoe), and then filling with concrete as the tube is withdrawn. The tube can be driven either by an external impact hammer as in *Alpha* (now superseded) and *Delta* piles (see figure (A2.2a)), or by an internal drop hammer as in *Franki* and *Dowsett* piles (see figure (A2.2b)). see also the *shell-pile* method (figure (A2.3b)).
2. in the other method, a tube is driven into the ground by mean of a hammer to form a permanent casing (again, the tube end can be closed by means of different shoes, see the above refrencess) and then can be filled with concrete as in *West shell*, *Raymond shell*, *position shell* piles, etc (see figure (A2.2c)).

Non-displacement piles: to install this type of pile, the soil is removed from specified location of the ground by means of auger or drill machine to form a hole which will then be filled with concrete, as shown in figure (A2.3a).

The cast-in-place concrete piles may be reinforced by using steel bar or steel cages. The pile offers the advantages that the length of pile can be adjusted to fit the elevation of the foundation without cutting or splicing.

A2.3 Timber Piles

Timber piles are tree trunks that have had their branches carefully trimmed off. The maximum length of most timber piles is 10-20m. In order to qualify for use as a pile, the timber should be straight, sound, and without any major defect. The diameter of pile tip should not be less than 150mm.

Timber piles cannot withstand hard driving stress, which limits the pile capacity to about 250kN. A steel shoe may be used to avoid damage at the pile tip. The tops

of timber piles may also be damaged during the driving operation. The crushing of the wood fibres caused by the impact of the hammer is referred to as *brooming*. To avoid damage to the pile top, a metal band or a cap may be used. Timber piles can easily be cut to the desired length and are cheaper than other types of piles.

Timber piles can stay undamaged indefinitely if they are surrounded by saturated soil, and they can be protected above the permanent ground water level with arsenic salt and creosote oil. However, in a marine environment timber piles are subject to attack by various organisms and can be extensively damaged in a few months. When located above the water table, the piles are subject to attack by insects.

A2.4 Composite Piles

In special locations it may be necessary to construct composite piles in which the upper and lower parts are made of different materials. For example, in marine structures a composite pile can be made of steel in the lower part and cast insitu concrete in the upper part to reduce the effect of sea water on steel corrosion (see figure (A2.3c)). Also, a composite pile may consist of timber in the lower portion below the permanent water table and concrete in the upper part to overcome the decay problem of the timber above the ground water level. In either case, it is difficult to form a good joint between dissimilar materials, and for that reason, composite piles are not widely used.

Table (A2-1)

Corrosion in Steel Piles

Environment	Degree of Corrosion	Coating
underground corrosion	0.01 mm/year	not required
atmospheric corrosion	0.10 mm/year	required
corrosion in fresh water	0.05 mm/year	required
corrosion in marine environment		
below the mud line	0.02 mm/year	not required
sea water immersion zone	0.08 mm/year	required
intertidal zone	0.08 mm/year	required
splash & atmospheric zone	0.1- 0.25 mm/year	required

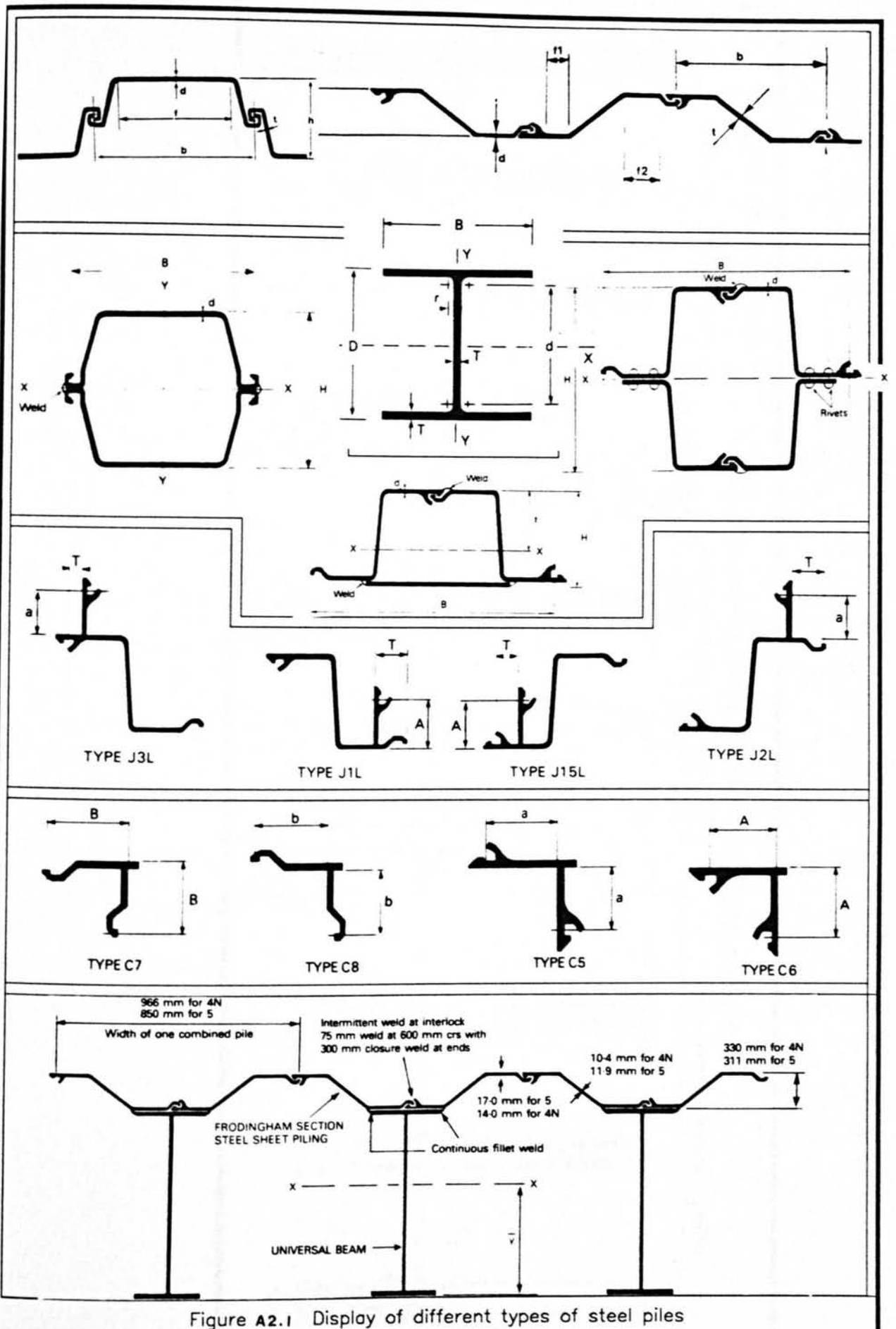

Figure A2.1 Display of different types of steel piles

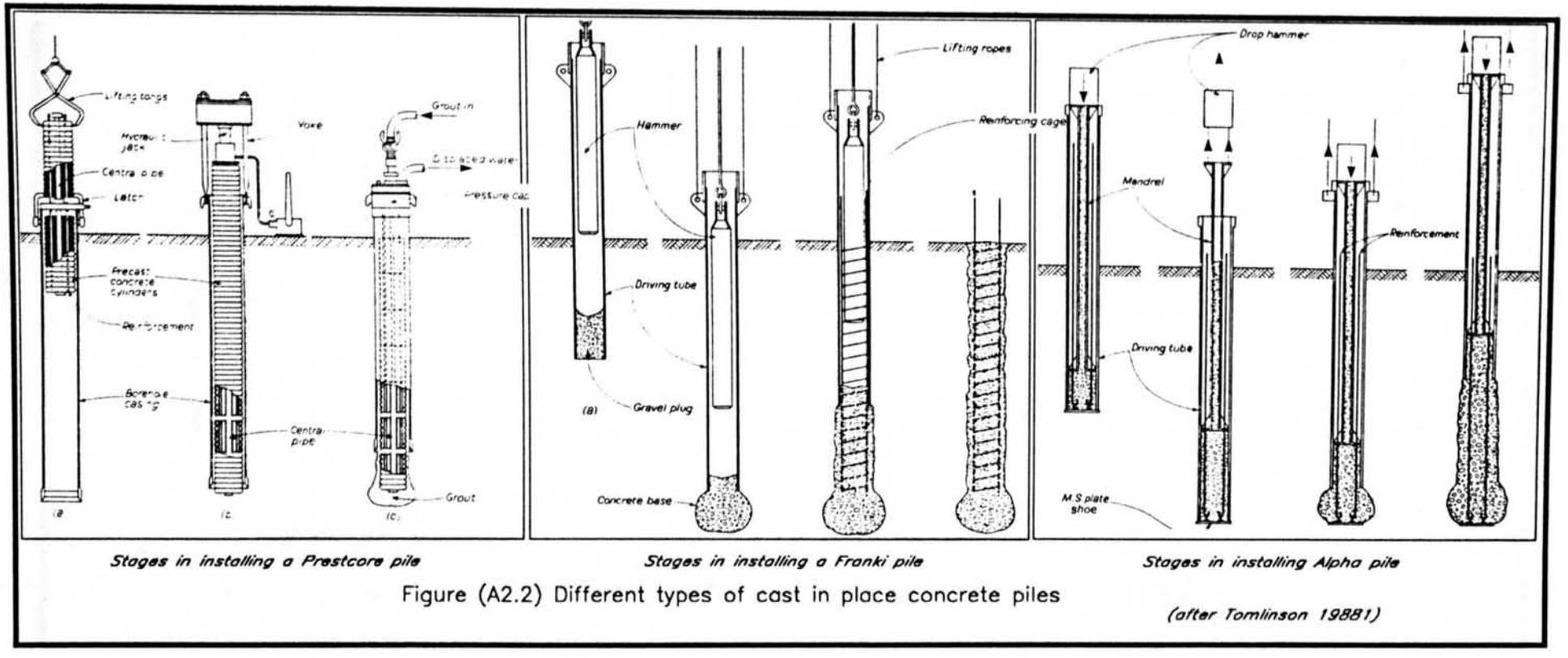

Figure (A2.2) Different types of cast in place concrete piles

(after Tomlinson 19881)

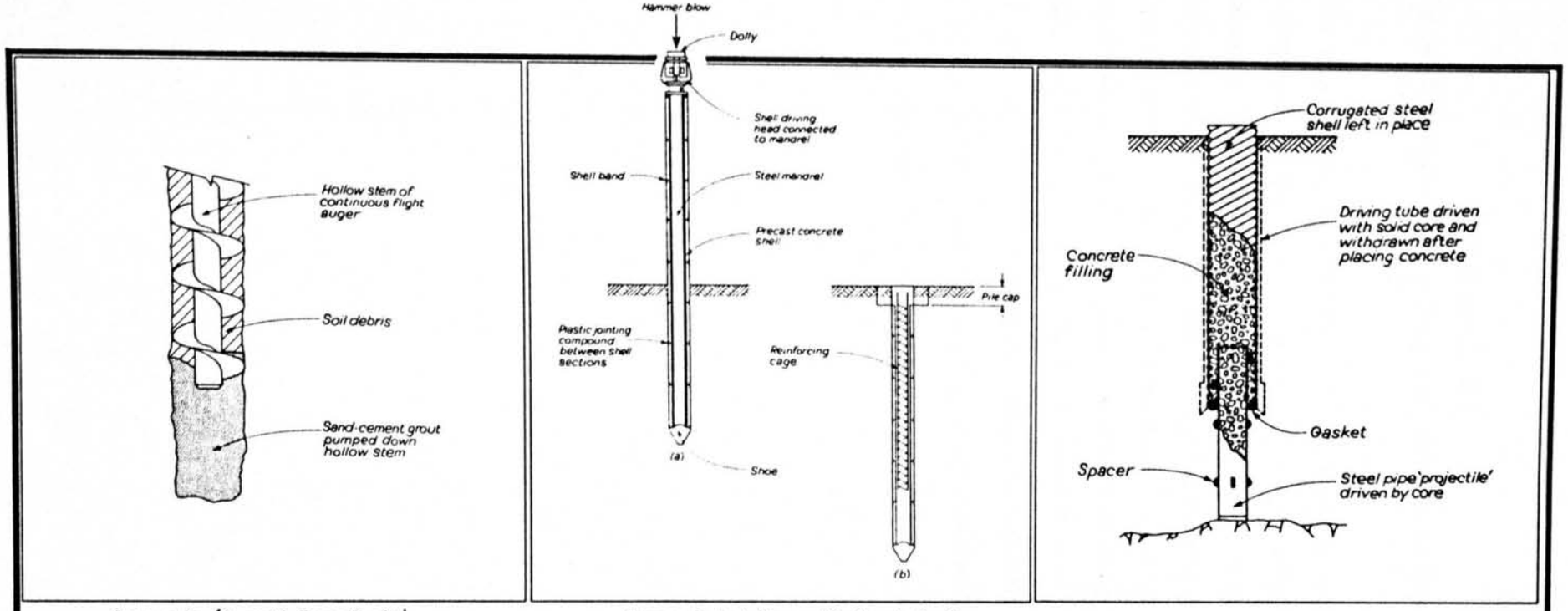

Screw pile (Dowsett Prepakt pile)

Stages in installing a West's shell pile

Composite shell and steel pile

Figure (A2.3) Different methods for installation cast–in–place concrete piles

(after Tomlinson 19881)

Appendix A3

A3. Specifications of Recording and Measuring Equipment

This Appendix explains the main features of the equipmrnt used in the ground vibration measurements throughout this project. The appendix also provides an simplified manual for operating both the PDR-1 and PDR-2 units. The programs used in recording and processing the ground vibration data include a number of commands, options and parameters. Their applications and operation are explained in detail in the following sections. A number of examples are given to simplify their sequence usage. The Appendix contains three sections as follows:

. *Appendix (A3.1)* describes and reviews the programs used with the PDR-1 unit.

. *Appendix (A3.2)* describes and reviews the programs used with the PDR-2 unit.

. *Appendix (A3.3)* displays the main specifications of the velocity transducers.

Appendix A3

A3.1. Recording and Processing Programs of the PDR-1 Unit

Introduction

The specification and other general features of the PDR1 unit have been described in section (4.3.1). The application of the unit's programs and their uses is detailed in the following sections.

After the unit is switched on, insert a pre-formatted and pre-programmed disc into the disc-drive and turn the drive on (turn the lever clockwise downwards), after about 15 seconds (during this waiting time, three clicks can be heard), the following message will display on the screen:

enter main option number

which shows the unit is ready to receive the user commands. If nothing is displayed, turn the disc-drive off and press the RESET button and repeat the procedure. At the same time check the connection plug and cable and check the light indicators on the side of the disc-drive. It is necessary for each blank floppy disc first to be formatted on a DUET-16 microcomputer where the recording program can then be copied from the original disc to this newly formatted disc. Also the loaded file can be checked and compared to the original program.

A3.1.1 Recording Procedure

The recording program contains seven main user options where option one contains 31 parameters. These options and parameters which are listed in table (T4-2) and (T4-3), are described in the following sections.

option 1

This option is used to modify and up-date the set-up configuration data to suit the particular conditions of the site. To run this option, follow the sequence below:

PDR1 display	user input

enter main option number press 1, then A
Edit par. no

The user can enter any listed parameter number to be modified (excluding 11, 12& 13), the following message will display:

old 0000 new —

a new figure can be inserted which will display after new. By pressing [A], the inserted figure will be stored in the memory and the display reverts to:

Edit par. no.

and by pressing [A] again, the option 1 mode will terminate. The parameter within option one controls different functions:

parameters 0, 1 & 2

these parameters control the input trigger levels for the first three channels attached to the PDR1 unit. The trigger levels are entered in terms of the PDR1 units where (2048 $unit = \pm 5$ $volts$). The geophones corresponding to these channels should be placed close to the vibration source.

parameter 3

This parameter controls the number of sampling points within a limit of time. The length of sampling depends on the number of recording channels, sampling time, sampling points before trigger and the capacity of the recorder's memory.

parameter 4

This parameter controls the number of sample points before triggering which allows capture of pre-trigger data. The pre-trigger length should be longer for impact hammers (eg. 20 units) and shorter for vibrodrivers (eg. 1 unit), since the vibration event is repeated in a very short of period time.

parameter 5

This controls the time interval between sampling points in 10 microseconds units (time between sampling points), and it is limited by the number of recording

channels.

parameters 6, 7, 8 & 9

These parameters control the general information such as date, time, direction, etc. and it is not essential to enter any figures.

parameter 10

This controls the number of channels to be sampled, independent of how many geophones are connected to the PDR1 unit.

parameter 11, 12 & 13

These parameters are not used.

parameter 14

This parameter controls the number of data sets recorded by the unit.

parameter 15

This controls the time of monitoring the signals of the geophones that are connected to the three first channels of the recorder.

parameters 16-31

These parameters control the order of the user channels corresponding to the connected geophones to the PDR1 unit. Usually parameters 16-31 are put in the same order of channels 0-14.

Typical set-up configuration data for ground vibration measurement is shown table (A3-1)

Table (A3-1)

Configuration of the set-up data PDR-1 unit						
parameter no.	set-up data		parameter no	set-up data	parameter no.	set-up data
	V_h	I_h				
0	1	30	7	—	14	3
1	1	30	8	—	15	2
2	1	30	9	—	16	0
3	500	500	10	15	17	1
4	20	20	11	—	18	2
5	60	60	12	—	.	.
6	—	—	13	—	30	14

V_h : vibratory-hammers

I_h : impact-hammers

option 2

This is used to load an existing configuration set-up from the disc into the memory of the unit. It is essential to load the unit's memory with a configuration data prior to any recording either by the use of this option or by entering a new set-up using option one.

option 3

This option is used to write the modified configuration data into a disc.

option 4

This option is used to store the captured data (by option 6) on a disc. The number of stored data is limited by the capacity of the disc, the number of recorded channels, the number of data sets and the sampling frequency. Typically a maximum of 18 files can be stored on a double density disc during the measurement of the ground vibration.

option 5

This option is used to clear the memory of the unit of all existing data. It is essential to use this parameter before the recording takes place.

option 6

This option is used to record the vibration signals. The number of recording data set is shown on the unit's LCD screen (e.g. 1,2,3...) indicating the unit is receiving data. When the memory is filled with the captured data, the screen returns to display the main operating system message. The number of data sets is related to the set up of the configuration data defined by parameters 0-5 and 14 of option one (see table **(A3-1)**.

option 7

This option is used to display the maximum vibration signals received from the first three channels in terms of the PDR1 units. The displayed information has the following form:

```
00325 00514 00267
```

For an immediate estimate of peak particle velocity(mm/s) of the connected geophone, the displayed figures should be multiplied by the calibration figure of the corresponding geophone, for example:

for geosource geophone,

$$peak\ particle\ velocity = 0.09 \times display\ figure$$

and Mark geophone,

$$peak\ particle\ velocity = 0.009 \times display\ figure$$

The period of time in which the figures are displayed can be controlled by parameter 15 of option 1.

Example 1: Sequences of recording procedure

First switch the unit on, insert a proper disc, turn the disc-drive on and wait for the main menu to be displayed on the screen. Then follows the sequence below to record and save data on the inserted disc.

unit displays	**user input**
enter main option number	[2]. then [A]
Turn disc on. hit A	do so. file will be loaded
Turn disc off. hit A	do so. return to main menu
entermain option number	[5]. then [A]
	(*above procedure will be repeated*)
enter main option number	[6]. then [A]
	(*above procedure will be repeated*)
enter main option number	[4]. then [A]
enter file number	e.g. [12]. then [A]
Turn disc on. hit A	do so.
Writing to the disk	(*the disc indicator turns on*)
Turn disc off. hit A	do so. return to main menu

A3.1.2 Analysing Procedure

The process of analysing the recorded data by the PDR1 unit can be achieved by the use of the analysing program which includes two sub-programs. They can only be used with a (DUET-16 SDC) micro-computer. These programs provide the following functions:

1. MAIN16 : *transfers data from* PDR *disc to* DUET *disc*
2. CAL16 : *processes the loaded data on the* DUET *disc*

The MS-DOS(8086) operating system program available within the DUET unit, helps to create, edit, delete, etc.. files during the process of data analysis.

a. MAIN16

This program is used to transfer the collected data from a PDR1 formatted disc to a DUET-16 formatted disc. To run the program, insert the DUET system disc into drive "A" (the Duet disc should already be loaded with the MAIN-16 program), and PDR field data disc into drive "B" *(drive A on the left and drive B on the right side of the* DUET *unit)* and type in:

MAIN16 *(return)*

A graphic cursor will appear at the bottom of the screen, by pressing any key a list of MAIN16 commands will display. The functions of these commands are explained in the following sections.

1. READHOME

This accesses the Home Block Content⊙ from the PDR formatted data disc which must be in drive "A".

2. DISPHOME

This command displays the home block content mentioned above on the screen, and it is a non-essential option.

⊙ Home Block Content is a set of configuration parameters saved on the disc while running option 1 of the recording program

3. FILEREAD n

This loads a file specified by (n) from the disc to the memory. The file number (n) is the number which is given to the file (e.g. 1-18) during the used option 4 of the recording program.

4. FILEWRIT fn

This saves the loaded file from the memory into a DUET-16 formatted disc with a file-name (fn) supplied by the user. The file-name usually has three characters and a number, such as WSH5, which represent a data file number 5, recorded in Waltham-cross, using sheet-pile and hydraulic-hammer.

5. EXIT

This command leaves the current program and returns to MS-DOS operating system.

6. USE

This calls a specially created file (for example, by EDLIN) to run the sequences of commands instead of using the keyboard (see example 3).

The above commands can be represented by the eight function keys on the DUET unit by creating a BATCH file using the EDLIN command from the MS-DOS operating system of the DUET unit.

Example 2 Creation of a BATCH file

While the MS-DOS is operating, type in the following commands and then press return.

```
EDLIN MAIN.BAT
type 1I, and insert the following text:
1:*FKEY F1='MAIN16'
```

```
2:*FKEY F2='READHOME'
3:*FKEY F3='FILEREAD'
4:*FKEY F4='FILEWRIT'
5:*FKEY F5='EXIT'
6:*Ctr+Z
```

the last line terminates the insert mode. Then type E to exit from the Edlin mode. Now by typing in MAIN.BAT the function keys will be activated, so by pressing the function key F1 the MAIN16 will be loaded and F2 will call the READHOME commands and so on.

Example 3 Creation of a USE file

Also the MAIN-16 commands can be written in a single file which then can be used with USE command while running the MAIN-16. First create a file MAIN.CAL using the EDLIN command. For example;

```
EDLIN MAIN.CAL
```

type 1I, and insert the sequences of the commands

```
1:* READHOME
2:* FILEREAD
3:* FILEWRIT
4:* EXIT
5:* Ctr+Z,   followed by E.
```

Then, while running the MAIN16 program, call the USE commands and then return (see below),

```
USE MAIN.CAL
```

the list of the loaded commands on the file will be called and displayed automatically.

b. CAL16

This program analyses the transferred data. The output result can be displayed

graphically on the screen as particle velocities versus time. Also the values of peak particle velocity for each channel or group of channels can be calculated and displayed on the screen. These results can be plotted and printed to get permanent copies if required. The program has the *fast fourier transform* FFT subroutine for frequency spectra calculation on both natural and logarithmic bases.

To run the program, insert a programed disc into disc-drive "A", turn the drive on and type in;

`CAL16` *(return)*

A graphic cursor will appear on the screen; press any key and a list of `CAL16` commands will display. A list of the commands and a brief description of their functions is given below:

READFILE (fn)

This reads a file-name (fn) from the disc and loads it into the memory.

GETSET n

This reads the data-set defined by (n) from the loaded file. The number of data-set can be controlled by *option 1* from the recording program (see section D2.1).

Draw (y-scale)

This draws the uncalibrated (raw) data traces on the screen. The y-scale should first be specified otherwise the default scale of 3000 screen unit will be drawn.

GETCAL

This loads the calibration file from the inserted disc into the memory. The file containing the calibration factors must be loaded to the disc before the process of analysis. The list of geophone calibration factors is shown in table `(T4-1)` in section (4.2.1). First a trial file should be created using `EDLIN` command, then the calibration factors can be inserted for each geophone, see section (4.3.2.3) for more

details.

DISPNUM n

This controls the number(n) of channels to be displayed.

DRAWCAL (y-scale)

This draws the calibrated data on the screen for 15 channels, and the y-axis shows the velocity magnitude which can be controlled by selecting a value for the y-scale, otherwise the defualt scale of 3000 will be drawn. The number of displayed channels can be controlled using `DISPNUM` command.

SETDCHAN n m

This sets the current channel number (n) to user channel number (m). For example, if the channel number 9 is to be replaced by the current channel (e.g. n=2), type in `(SETDCHAN 2 9)`, or if only the five vertical channels of the loaded file is required to be displayed, follow the sequence below:

```
SETDCHAN 0 2
SETDCHAN 1 5
SETDCHAN 2 8
SETDCHAN 3 11
SETDCHAN 4 14
```

SETCOL n c

This sets user channel number(n) to specified colour number(c)[⊘], for example; `SETCOL 9 3`, displays channel 9 in colour 3.

COPY n

⊘ The unit colour numbers are; 1.blue, 2.red, 3.magenta, 4.green, 5.yelow, 6.cyan & 7.white

This copies a single channel specified by (n) from the loaded file to be registered in the memory.

RGCLEAR

This clears the register array.

EXIT

This termites the CAL-16 program and returns to the MS-DOS operating system. If plotter or printer are needed to be used with the system, the following text should be typed in before running the CAL16 program.

```
MODE AUX: BP=96 ST=2
```

then while running the CAL16 program, use the following commands to send the displayed information to the printer or to the plotter:

SCDUMP

This transfers the graphic display to the printer. Y-scale can be supplied by the user.

HPDRAW

This transfers the graphic display to the plotter. Y-scale can be supplied by the user.

TITLE

A title of 60 characters can be plotted by the use of this command. The title should be inserted immediately after the y-scale figure.(see example below):

```
HPDRAW 20 Newark H-pile Drop-hammer 24.09.1988
```

The following commands are used to calculate the peak particle velocity and the resultant for a channel or group of channels.

CALMAX

This calculates the peak particle velocity for all channels of the loaded file.

DISPMAX

This displays the peak particle velocities value on the screen in mm/s.

Example 4 obtain a print out of p.p.velocities

While running the CAL16 program, enter the following commands to obtain a hard copy of the calculated results. The DUET should already be connected to a printer.

```
PRINT AUX: =0
CALMAX
DISPMAX
```

the system will respond

```
copy to printer?  (Y/N)
```
(type y)

then type:

```
NOPRINT
```
to send to printer

Example 5 *Calculation of resultant p.p.velocities*

The following sequence of commands is used to calculate the resultants of peak particle velocity for three orthogonally positioned geophones represnted by channels 1, 2 & 3 for a registered file in the memory:

```
SUMSQ 1
SUMSQ 2
SUMSQ 3
ROOT
REGMAX
DISPREG
```

Example 6 *Frequency calculation*

To display frequency spectrum in both natural and logarithmic bases for any channel, use the following sequence of commands:

```
REGCLEAR
COPY n (n= the channel number)
SPECTRUM or LOGSPEC (normal base, or log.  base respectively)
DISPSPEC (displays the FFT output)
```

The x-axis of the graphic display is divided into 130 screen units. The scale of the spectrum output will be indicated on the top of the screen (e.g. `MAX FREQUENCY = 500Hz`, which means the maximum scale is 500Hz. Therefore `1 screen unit = 500/130 Hz`. The location of peak frequency can be indicated by moving the cursor to that point where its location will be displayed on the right bottom corner of the screen as (`x=62  y=0`). So the accurate frequency can be calculated in the following form:

$$62 \times 500/130 = 238.5\text{Hz}$$

Example 7 *Application of the* `USE` *command*

As mentioned in the previous section a trial file (in this example called `PLOT.CAL`) should first be created by `EDLIN` command of the `MS-DOS` operating system in which the following commands can be inserted:

```
EDLIN PLOT.CAL
type 1I to insert
1:*READFILE (e.g.  DATA1)
2:*GETSET 1
3:*GETCAL (e.g.  DATA.CAL)
4:*DISPNUM 3
5:*DRAWCAL 20
6:*HPDRAW 20 file 1, ground vibration measurements
```

Then while running the `CAL16` program, type in:

```
USE PLOT.CAL
```

The sequence of the commands will be loaded without using the keyboard. This command is very useful when a series of files is to be processed in which a sequence of commands will be repeated. By little modification to the original file, the file can be loaded to different discs and can be used for the processing of different sets of data files.

More examples can be found in dissertations by S.Paterson (1985) and J.Cahm (1986).

Appendix A3

A3.2. Recording and Processing Programs of the PDR-2 Unit

The general description of the PDR2 unit is given in section (4.3.2). As mentioned in that section, there are three programs available within the unit, which are listed below:

1. Monitor Disc Program
2. Recording Program (pdr2)
3. Analysing Program (DANA3)

Each of the above programs contains a number of commands which are listed in tables (T4-6), (T4-7) and (T4-8), respectively. A full description of the commands is given in this Appendix for use as a guide manual for the PDR2 unit operation.

A3.2.1 Monitor Disc Program

This program is stored on the processor board ROM during the manufacture of the PDR2 unit. The program includes the basic commands for formatting and displaying disc-drive information on the screen similar to the MS-DOS operating program. Details of some of the more frequently used commands are given below:

drive : *change drive number*
dir : *list directory of the disc*
del : *delete file name*
mkdir : *clear all disc file*
load : *load file to the memory*
save : *save file to the disc*
run : *begins program*
go : *resume program*
history : *list last 20 commands*
help : *list commands name*
format : *format disc*

dcopy : *copy from one disc to another*

Note: The commands should be inserted as lowercase characters during operation.

1. drive n

This command can be used to change the current disc drive number. The disc drive number "n" can either be 0 or 1. The default number is set to 0. Disc drive 0 is the closer to the screen and drive 1 closer to the keyboard.

2. dir

This lists the files on the currently selected drive. Also information about the size of the disc and remaining free space will be given. To use this command, insert a disc into the disc drive and turn it on. Type in the command and press return, and the following message will display;

```
Disk name:
next available block: 2
disc size 737280 bytes
available space: 695897
pdr5   41383   0×400      0×400
```

After each file name is listed, the following column indicates the size(bytes), load address (hex) and execution start adress (hex) respectively.

3. del (file name)

This command removes the file named from the directory. The use of this command will not free any space in the disc.

4. mkdir

This command writes an empty directory on the disc in the currently selected drive. Since the run of this command would result in loss of any files already stored on the disc, the below message will appear on the screen;

```
old directory will be overwritten. ok? (y/n)
```

Type "y" to confirm, otherwise no.

5. load (file name)

This command loads an existing file from the disc to the memory. If the optional load address (in hex) is given, the file is loaded, starting at that address, otherwise the load address found in the directory is used.

6. save (file name)

This command is used to save a file from the memory to the disc in a currently selected disc drive. If a name already in the disc is used, the existing file will be deleted and the new file will overwrite the old one.

7. run

This command is used to start a program which has been loaded with its symbol table. When "start" symbol is found, the program will be loaded into the register set and then the exceution begins. If not, the following error message will display;

```
cannot find start address for run
```

8. go

The command is usually used during debugging to continue running the interrupted program. eg. after using `Reset` or `Abort` keys. When these two keys are used the program will interrupt and returns to the main operating system. If the *go* command is used after the use of `reset`, the operation will go back to the start of the listing and if it is used after `abort`, the operation will go back to where the program is interrupted.

9. history

This command lists the last 20 commands which were entered. If "!!"(return) is entered the last command will be repeated, if (return) is pressed the command will terminate.

10. help

When this command is used, a list of available commands will display on the screen as;

help available on these topics:

help	commands	syntax	history	expressions	show
host	bklen	delete	dir	drive	dshow
load	save	mkdir	format	bbc	duet
other	ipl	mode	cache	regiters	$registers
$copy	$set	size	byte	word	long
go	continue	start	run	dump	mem
put	symbols	ctrace	break	bclear	trace
tjump	set	unset	assign	serset	S2
sload	progstat	softreset	copy	fill	monvars
adresses					

Enter: help topic(return) for help on a topic

The list contains 55 commands although some of them are not directly relevant to the user. Further information about each individual command can be obtained by typing "help" followed by the name of the command required.

11. format

This command formats a blank disc to either DUET or IBM system. The command is stored on a disc and the command should first be loaded into the memory. On running the command the following message will display;

Which D R I V E? (0 or 1) or (A or B): (eg.0)
Which F O R M A T? D U E T(D) or I B M(I): (eg.D)
D U E T F O R M A T D I S K F O R M A T T E R
80 track MFM, 512 bytes/sector, 9 sectors/track, 2 sides

After defining the disc drive number(eg. 0) and the formatting sysytem (D) *(usually duet format is used)* and the (CR) pressed, this message will appear;

Insert disk into DRIVE 0
press CR when ready
starting format operation
++.++.++. etc.

FORMATTING DONE. CHCKING
++.++.++. etc.

When the formatting is finished the program returns to monitor, and the *mkdir* command will clear the disc. The available space on an empty double densety disc is;

$$512 \times 9 \times 80 \times 2 = 737280 \quad bytes$$

12. dcopy

This command copies the contents of one disc to another. The command should be loaded into the memory and then by running the command the following information will display;

DISK COPY UTILITY
Which format? DUET(D) or IBM(I)

Insert SOURCE disk into drive 0
Insert DESTINATION disk into the drive 1
Ready? (Y)

When "Y" is entered the light on disc drive 0 and then 1 will alternately go on and off while the following information displays on the screen.

READING SOURCE DISK. Please wait
WRITING DESTINATION DISK. Please wait

When copying is finished the program returns to monitor and the content of the copied disc can be checked using *dir* command.

Example 1 Running monitor disc commands

To format a blank disc, first insert the format disc which is indicated as system disc into disc-drive (0 or 1), turn the drive on (turn the lever clockwise downwards) and type in the following commands then return:

```
load format
run
```

Insert a blank disc into the disc-drive and follow the procedure explained in `format section`. When the formating is completed, use the `mkdir` command to write an empty directory on the disc. It is essential to use this command before loading any file to the disc.

To copy files from disc [A] to disc [B], either use the **dcopy** command in which the whole contents of disc [A] will be copied into disc [B] (see the **dcopy section**) or follow the sequence below in which each individual file should first be loaded to the PDR2 memory and then saved to the other disc, the procedure of copying file (e.g. pdr5) is shown below:

1. insert disc [A] into drive [0], turn the drive on.
2. type in "load pdr5" then return.
3. wait until the loading is completed, turn drive[0] off.
4. insert disc [B] into drive [1], turn the drive on.
5. type in "drive 1" to activate drive [1].
6. type in "save pdr5", the file will be loaded into disc [B]
7. type in "dir", press return, the list of files will display

Appendix A3

A3.2.2 Recording Program (pdr)

The **pdr** program is used to record vibration data sent to the PDR2 unit via transducers. The program can store, display and save the captured data. Also the program can monitor the level of ground vibration while the vibration source is active. The use of the **pdr** program is explained in the following section.

The latest version of the modified recording program is **pdr5** and it must be loaded to the user disc. To run the program, switch the PDR2 on, insert the disc into the disc-drive and turn the drive on. Then type in the following commands:

```
load pdr5

run
```

On running the **pdr5**, the menu below will display on the screen.

```
0 Change configuration data
1 Set default configuration
2 Clear memory
3 Collect data
4 Go to plotting menu
5 Save configuration
6 Reload configuration
7 Save data
8 Reload data
9 Set drive number
10 Write a duit format file on drive 1
11 Monitor max. and min. values
12 Return to DUMCBUG
13 Display Power Supply voltage
```

The menu contains 14 options which provide different functions. The use of these options can be achieved by typing the required option number followed by pressing the return key. The use of each option is reviewed in the following sections.

Option 0

This option changes the default configuration data to a new configuration to satisfy the conditions of the recording site. Option "0" contains 9 parameters where each parameter controls a different item within the configuration file. By running option "0" the list of the parameters will display:

```
type NUM(ret) to change a parameter, 0(ret) to exit this menu
1.Channels per ADC : 8 8 2 2
2.Channel list by ADC :
        ADC0 0 1 2 3 4 5 6 7
        ADC1 0 1 2 3 4 5 6 7
        ADC2 0 1
        ADC3 0 1
3.Scan Rate (microseconds) : 30
4.Channels per scan clock : 2
5.Points before trigger : 200
6.Points after trigger : 200
7.Channel map list :
        0 1 2 3 4 5 6 7 10 11 12 13 14 15 16 17 20 21 30 31
        f0 f0 f0 f0 f0 f0 f0 f0 f0 f0 f0 f0 f0 f0 f0 f0 f0 f0 f0 f0
        f0 f0 f0 f0 f0 f0 f0 f0 f0 f0 f0 f0 f0 f0 f0 f0 f0 f0 f0 f0
        f0 f0 f0 f0
8.Number of triggers : 4
9.Channels and trigger levels :
        0 200 1 200 2 200 3 200
```

This menu is orginally supplied with a set of default numbers which should be changed according to the conditions of the site. Below, the function of each option is described:

Parameters (1) and (2) display the number of channel per ADC and the list of channel per ADC. ADC stands for *Analogue to Digital Convertor.* The analogue data is converted into digital data after passing first through a *multiplexer* and then through a *converter.* The number of analogue channels entering the multiplexer controls the speed of the output data to the convertor. As the number is decreased the output data speeds up and goes to the convertor. The above menu shows that there are two standard ADCs each with eight channels input and two fast ADCs with two channels input. So 16 channels (0-15) are specified for velocity recording through the standard geophones and 4 channels (16-19) are specified for fast recording through accelerometers or strain gauges.

parameter (3) controls the rate of scanning; when a larger scan rate is chosen, the sampling rate will be slower. An example shown in figure (A3.1) demonstrates the above procedure. The default figure is 30, but for recording ground vibrations from pile driving, 180 microsecond should be used.

parameter (4) controls the scan clock per channel which means that with a bigger scan clock setting a shorter sampling rate occurs, see the example shown in figure (A3.2). The default figure, 2, should be used.

parameter (5) adjusts the sampling points before trigger. The default is 200 points but 20 points should be used for impact hammers and 1 point for vibrodriver.

parameter (6) adjusts the sampling points after trigger. If more sampling points after trigger are used a longer sampling time is taken (see figure (A3.3)). Default is 200 points, but 500 points should normally be used.

The signal duration can be calculated using the following equation:

$$\text{Sample time} = \frac{\text{Channel per ADC} \times \text{Scan rate}}{\text{Scan clock}} \times \text{No.sampling point}$$

Using the set up configuration data used before, the sampling time is:

$$\text{Sample time (t)} = \frac{8 \times 180}{2} \times 520$$

$$t = 0.3744\text{sec}$$

parameter (8) selects the number of channels to be triggered, which defaults to 4. The displayed message is:

enter number of trigger channels :

parameter (9) sets the trigger channels in the order of the connections of geophones into the unit. The range of trigger levels can first be seen on the screen using option 11. Multiply that figure by about three and then insert it to the menu. The following message will display:

OPTION : 9
enter list position, user channel and level

The following example explains the use of this option. If channel 5 is the first trigger channel and trigger level is 30, then insert the above figure in the following sequence:

0 5 30

The inserted figures will be displayed. Any channel can be used as trigger channel. The trigger channels usually belong to the set of geophones which are placed close to the source of vibration. When the modification of the configuration set up is completed, type in 0 then return to leave this mode.

Option 1

This option loads the default configuration set up into the memory.

Option 2

Type 2 then return and the displayed message is:

Clear memory option, type c to confirm :

Type c to confirm and return, and the memory will be cleared. This option must be used before every record takes place, as when the memory is full no more data can be collected.

Option 3

The data can be recorded by using option 3. This message will display on the top of the screen:

Collecting data, Maximum number of set 3
waiting for set 1

The number of data sets is dependent on the arrangement of the configuration setup. Data capturing starts when one of the trigger levels of the selected channels is exceeded. When trigger levels are higher than the data received then the process is not activated and no data will be recorded. If the return key is pressed while the logger is waiting for a data set, the recording sequence will interrupt and return to the main menu.

Option 4

This option displays the captured data on the screen, which a is very important facility for checking the recorded data on the site. When this option is used this message will display on the top of the screen:

0:clear 1:plot 2:return 3:range 4:pskip 5:pplot 6:nset

When any of these parameters are used, the messages are;

1: enter user channel to plot
3: enter range
4: enter percentage per skip
5: enter percentage to plot
6: enter number of set to plot

No message will be shown when options 0 and 2 are used. Option 0 clears the screen and option 2 will return to main menu. Option 3 changes the Y-scale of plotting (default is 3000), any part of the existing plot can be skipped by using option 4, and the plot can be magnified using option 5.

Option 5

This saves the set up configuration data edited by option 0. Also it saves any other configuration setupfile from other discs (after reloading using option 6). Type 5 then return and the message is:

Enter file name for configuration data:

Option 6

This reloads a configuration data from any disc to the memory. The message is:

Enter file name for configuration data :

Option 7

Stores the data recorded by option 3; the prompt is;

Enter file name for file data :

A meaningful prefix should be chosen for the file name. Usually three characters and a number is used. The three characters refer to the name of the site, name of the hammer and name of the pile. The number indicates the file sequence, for example *ndh5* means *Newark Drop-hammer H-pile* and file number five. Remember that the maximum space for restoring data on a double density disc is six files. If additional files are offered, the following error message will display on top of the screen above the list of the menu;

Error writing to file code : 50331648

Option 8

This reads a previously loaded data file from disc for display with option 4; the message is;

Enter file name for file data :

Option 9

The use of disc drive (0 or 1) can be selected by this option. The message is;

Enter drive number :

Option 10

This option is used when recorded data is to be used with a `DUET 16` using the same programs is used to run the `PDR1` data. The displayed message is;

Enter duet configuration number and file number :

`DUET-16` configuration number is 10 and any number can be entered for file.

Option 11

This option displays the maximum and minimum amplitudes of vibration for each individual connected transducer (represented by a channel number), in terms of `"PDR-2 units"`, where `2048 units = 5 volts`. When the option is called, the following message will display on the screen.

number of scans to average over :

The selection of the number defines the period of time in seconds for data to be sampled and displayed. The displayed information has the form:

Channel	0 max	12	min	-8	Channel	1 max	3	min	-4
Channel	2 max	9	min	-11	Channel	3 max	18	min	-23

From the above information, an approximate calculation of the particle velocity can be achieved by multiplying the displayed figure to the calibration factor of geophone of the particular channel.

$$unit \quad value \times 0.09 = velocity(mm/s) \quad geosource$$

$$unit \quad value \times 0.009 = velocity(mm/s) \quad Mark \quad geophone$$

Option 12

This ends the operation of the `pdr` program and returns to the operating system menu. The message is;

Type c to confirm return to DUMCBUG :

Option 13

This option helps to check whether or not the transformer is supplying the correct output voltage to the unit.

```
Internal Power Supply Voltage

average   =5.11    pp error   =-0.1  , 0.1
average   =14.88   pp error   =-0.1  , 0.3
average   =-15.17  pp error   =-0.3  , 0.2
press any key to continue
```

Example 1 *Set-up Configuration Data File*

The following example shows the set-up of configuration file for ground vibration data taken during driving of a 20m long H-pile, using an impact hammer of 5 tonnes, into a silty clay soil. First insert a pre-formatted disc into disc-drive(0) while running the `pdr5` on the `PDR2` unit. Call option(0) by typing in `0` then `return`, and the following default menu will display on the screen:

```
type NUM(ret) to change a parameter, 0(ret) to exit this menu
1.Channels per ADC : 8 8 2 2
2.Channel list by ADC :
        ADC0 0 1 2 3 4 5 6 7
        ADC1 0 1 2 3 4 5 6 7
        ADC2 0 1
        ADC3 0 1
3.Scan Rate (microseconds) : 30
4.Channels per scan clock : 2
5.Points before trigger : 200
6.Points after trigger : 200
7.Channel map list :
        0 1 2 3 4 5 6 7 10 11 12 13 14 15 16 17 20 21 30 31
        f0 f0 f0 f0 f0 f0 f0 f0 f0 f0 f0 f0 f0 f0 f0 f0 f0 f0 f0 f0
        f0 f0 f0 f0 f0 f0 f0 f0 f0 f0 f0 f0 f0 f0 f0 f0 f0 f0 f0 f0
        f0 f0 f0 f0
8.Number of triggers : 4
9.Channels and trigger levels :
        0 200 1 200 2 200 3 200
```

The more frequently changed parameters are 3, 5, 6, 8 & 9. To change any of these parameters, use the following sequence:

option no.	PDR2 displays	user input	press
3	enter scan rate (microseconds)	180	return
5	enter points before trigger	20	return
6	enter points after trigger	500	return
8	enter number of trigger channels	3	return
9	enter list position, user channel and level	0 0 30	return
9	enter list position, user channel and level	1 1 30	return
9	enter list position, user channel and level	2 2 30	return

The first three channels (0, 1 & 2) are chosen in this example as trigger channels

and usually they should be placed closest to the source of the vibration. When the new set -up of the configuration file is completed, press (0) then return, the screen will return to the main options menu and the file can be stored using option (5).

Example 2 *The stages of the recording procedure*

Having a suitable set of configuration data loaded into the PDR2 memory either by using option(1) or loading a configuration file from the disc to the memory using option(6), the following sequence is used to record a file data into the disc.

enter	press	PDR2 responds
2	return	Clear memory option, type c to confirm
c	return	returns to the main menu
3	return	Collecting data, Maximum number of set 3
		waiting for set 1, 2, ...
7	return	Enter file name for file data
bhh3		return returns to the main menu

Note: the user disc must first be formatted prior to the procedure of recording, and the disc should be inserted into disc-drive(0) (the default disc-drive) unless the other disc-drive is defined by option(9). The file name bhh3 in the above example stands for *Blaydon, Hydraulic-hammer, H-pile* and 3 represents the file number which is usually a function of pile depth.

Appendix A3

A3.2.3 Analysing Program (DANA)

The main features of the analysing program DANA3 are briefly explained in section(4.3.3). The program contains some 78 commands which are listed in tables (T4-9). The use of the commands and their application is fully described in the following sections.

Before running the program, the PDR2 unit might be connected to a plotter, printer or VDU terminal if required. When it is connected to an external VDU, only the text information will display on the VDU screen while the graphic output will display on the PDR2's screen. Having the terminal connected to the PDR2 unit by means of serial cable, insert the following commands to link the terminal to the unit and to activate the terminal's keyboard:

```
. ass con line 0
```

To run the DANA3 program, insert the pre-programed disc into the disc-drive, turn the drive on and follow the procedure below:

input user	press	PDR2 response
load DANA3	return	start address: 0 × 400
run	return	(see below)

On running the program, a list of a default calibration file will display on the screen, and below that the following message will display on the screen:

```
FACTOR = 1
calling gdef(1)
V D U connected?  Y or N (cr):
P L O T T E R connected?  Y or N (cr):
P R I N T E R connected?  Y or N (cr):
```

By replacing a proper answer to the above lines, the promp >> 0 – 0 >> will appear

on the screen indicating the program is ready for operation. Type in HELP then press return, and a list of commands will display. According to their operational application, the commands are classified into nine main functional groups as follows:

a. Screen Control Commands

b. Calibration Array Commands

c. Data Control Commands

d. Data Display Commands

e. Register Calculation Commands

f. Plotting Control Commands

g. Legend Control Commands

h. The Use Control Commands

i. The Communication Commands

Each group of the above commands includes a number of sub-commands which are listed in table (T4-9) from section (4.3.3). There are certain conventions for the first letters of some commands names, such as;

S show : *show the information on the screen*

D display : *display or plot graphic information*

P print : *send the information to the printer*

E edit : *display information in edit mode*

In the following section each of these functional groups will be discussed in detail.

a. Screen Control Commands

The following commands control the disc drive and the screen:

HELP : *displays list of commands on the screen*

DRV : *changes the current disc drive*

DIR : *lists the files of the disc in the current drive*

CS : *clears the screen*

EXIT : *terminates the running program*

1. HELP

This command displays the list of the commands available within the DANA3 program. The user may check the spelling of the command before use while they are displayed on the screen.

2. DRV n

This command changes the current disc-drive number. The drive number is specified by [n] which can be either [0] or [1]. The default disc-drive is [0] and the prompt on the screen is >> 0 – 0 >>. When disc drive [1] is selected, the prompt will change to >> 1 – 0 >>. The second figure in the prompt refers to the data set number (see DTSET command).

3. DIR

This command lists the directory of the loaded disc on the current disc drive. When this command is used the current drive should be turned on.

4. CS

This command clears the screen of all information (either text or graphic display). The command is frequently used to have an empty screen for displaying new data.

5. EXIT

This command terminates the running DANA program and returns to the monitor disc program system.

Note; the use of the EXIT command differs from the **reset** and **abort** push button in completely interrupting the running program. The program should be loaded again to be run, while the other two, temporarily interrupt the running program and the program can be run again by using **run** or **go** commands from the monitor disc program.

b. Calibration Array Commands

SCALBR : *shows the calibration data on the screen*

LOADCAL : *loads calibration figures from the disk*

EDITCAL : *edits calibration data*

SAVECAL : *saves calibration data on the disk*

DEFCAL : *loads default calibration data*

PCALBR : *sends the calibration data to the printer*

1. SCALBR

This command displays the default calibration array on the screen unless the register is loaded with a calibration file. The calibration array will display in three columns representing the list of channel numbers, offset coefficient followed by calibration factor (see `EDITCAL` command for more detail).

2. LOADCAL

This command loads a calibration file from the disc into the register. First insert a disc file into the disc-drive, turn the drive on and type in:

`LOADCAL` then press return

A list of files and other related information will display as:

```
Disk name:
next available block: 1070
disc size 737280 bytes
available space: 188928

pdr5        41383    0×400   0×400
ghh         512      0×0     0×0
mhh1        100864   0×0     0×0
mhh2        100864   0×0     0×0
...         ...      ...     ...
...         ...      ...     ...
mhh.cal     512      0×0     0×0

Enter file name for calibration data:
```

Usually all calibration data files name have (.cal) suffix. For example; file *mhh.cal* is a calibration data file for field data files `mhh`)†. By loading this file,

† Files recorded in Blaydon (Metro Center), during driving H-piles by a Hydraulic-hammer

the calibration array for all channels will display on the screen.

3. EDITCAL

This command enables the user to edit the loaded calibration file in which any individual channels can be edited. By typing in the command, a list of calibrations will display on the screen, and the user can select any channel and replace the current figure. As mentioned above, the calibration array is represented in three columns, so the replaced figures should also represent these columns, see the example below in which only channels 12, 13 & 14 are shown:

channel no.	offset coef.	calibration factor
12	0	0.0922
13	-5	0.0893
14	2	0.1005

The *channel number* is the list of channels in sequence. The first 17 channels (0-16) represent the geophone transducers, channels number 17-20 the accelerometers and channels 40-51 the strain gauges.

Offset coefficient refers to the zero-value position of the displayed graph on the screen. If the transducer is well balanced during the data recording, the graph will display centred on the zero line so the offset coefficient is 0. However the graph will display either above the zero (central) line or below it if the transducer has a small zero offset; this is common for very sensitive transducers such as the *strain gauges.* In this case, the offset coefficient will be either [+] when the graph is displayed above the zero line or [-] when below the zero line. To correct a zero offset figure, measure the position of the displayed graph in relation to the y-axis scale. If the y-axis is scaled to 100mm/s, 2mm on the screen equals to 100 unit of the offset number. It is obvious that when the scaling increases the offset number decreases. It is essential to balance the output graph before any further data processing.

Calibration factor is the figure obtained during calibrating the transducers (see section 4.2.1.3). The calibration factors for all strain gauges is 1 and the calibration factor for each individual geophone is shown in table (T4.1). The calibration factor

for each geophone should be entered to comply with the connections of the geophones to the PDR2 unit.

After editing, the modified calibration will display on the screen replacing the old figure after pressing the return key. The edit loop can be terminated by pressing any non-numeric key followed by the CR. The final modified calibration data are then displayed and edit mode terminated.

4. SAVECAL

The loaded calibration data can be saved using this command. A name for a file should be entered after the following message is displayed;

Enter file name for calibration data :

5. DEFCAL

The default calibration data for all channels which is set to 0.0 (offset) and 1.0 (scale) can be used for display of uncalibrated data.

6. PCALBR

This command is used to print the calibration file via a printer. The printer should first be connected to the PDR2 unit.

c. Data Control Commands

LOADDATA: *loads data to the memory*
LOADCON : *loads the configuration data*
SCON : *displays the configuration data*
PCON : *prints the configuration data*
DTSET : *sets the user data set number*
WIN : *shows the window information*
WINS : *sets the window screen*
WINR : *resets the window screen*
FACT : *draws magnified y-scale graph*

KOL : *controls the output axes and colour*

KLIP : *smoothes the out put graph*

FILTER : *filters a spikey signal*

1. LOADDATA

This command loads the file data from the disc to the register. First insert a file disc into the disc-drive, turn the drive on and type in the command then press return, a list of files will display on the screen as follows:

```
Disk name:
next available block: 1070
disc size 737280 bytes
available space: 188928
pdr5        41383     0×400   0×400
ghh         512       0×0     0×0
mhh1        100864    0×0     0×0
mhh2        100864    0×0     0×0
...         ...       ...     ...
...         ...       ...     ...
mhh.cal     512       0×0     0×0
Enter file name for file data:
```

Enter the file data name and press return and the file will be loaded to the register. When the loading is completed a list of configuration set up data at the time of recording will display on the screen.

It can be noticed that the file data name is followed by three columns representing the space size occupied by the data (in the above example 100864 bytes), ram top and ram bottom addresses of the board processor. Since the file data is stored on the floppy disc, no **RAM** address is registered in the memory.

The name of a data file usually has three characters and a figure. For example **mhh2**, **sdh5**, etc.. which refers to name of the site, hammer type and pile type. The figure refers to the number of files within a disc, and in many cases this figure is a function of the pile depth.

2. LOADCON

This command loads the configuration data file from the disc into the register of the **PDR2** unit as in the example below:

```
type NUM(ret) to change a parameter, 0(ret) to exit this menu
```

```
1.Channels per ADC : 8 8 2 2
2.Channel list by ADC :
        ADC0 0 1 2 3 4 5 6 7
        ADC1 0 1 2 3 4 5 6 7
        ADC2 0 1
        ADC3 0 1
3.Scan Rate (microseconds) : 180
4.Channels per scan clock : 2
5.Points before trigger : 20
6.Points after trigger : 500
7.Channel map list :
        0 1 2 3 4 5 6 7 10 11 12 13 14 15 16 17 20 21 30 31
        f0 f0 f0 f0 f0 f0 f0 f0 f0 f0 f0 f0 f0 f0 f0 f0 f0 f0 f0 f0
        f0 f0 f0 f0 f0 f0 f0 f0 f0 f0 f0 f0 f0 f0 f0 f0 f0 f0 f0 f0
        f0 f0 f0 f0
8.Number of triggers : 3
9.Channels and trigger levels :
        0 30 1 30 2 30
```

4. PCON

This command prints the displayed configuration data.

5. DTSET n

This command sets a data set number specified [n] into the memory. The data set number refers to the configuration set arrangement at the time of data recording. If the scan rate time is longer more data set could be obtained, for more detail see section `(4.2.3.option 0)`. The default data set is zero which is indicated on the screen as `>> 0 – 0 >>`. When set number (n=1) is selected and `(CR)` key is pressed then this information will display:

DATA SET set to 1

The prompt on the screen will be `>> 0 – 1 >>`.

6. WIN

This display information of window setting of the screen as;

DATA WINDOW SET TO 0 and 100%

START TIME : 0 s
END TIME : 0.37368 s

7. WINS

By this command a selected part of the displayed graph can be shown. The following information can be seen on the screen after the command is used;

```
Cursor movement
d    ...  1    step right
s    ...  1    step left
D    ...  10   step right
S    ...  10   step left
CR ..          Terminate setting
Setting the START of the data window (CR)
Setting the END of the eindow (CR)

DATA WINDOW set to 0 and 50.2%

START Time : 0 s
END Time : 0.1872 s
```

8. WINR

This resets the window to the default figure. Display information is;

```
DATA WINDOW set to 0 and 100%
```

9. FACT n

The display graph may be magnified by the use of this command. For example, if n=1 the real output will display which is the default set, but when n=5 the y-scale output is multiplied by five.

10. KOL c a

This command allows the x-y axis to be withdrawn from the output if they are not required to be shown (see example 5). The command also controls the number of colour to be used for plotting the output graph.

[a] controls the axes and can either be 0 or 1: If (a=0) then no x-y axis will be plotted otherwise when (a=1) which is the default figure the x-y axis will be plotted.

[c] controls the colour number of the pen and can be 1-7 depending on the type of the connected plotter. This command is very useful when velocity, acceleration and displacement are plotted on a single graph (see example 6).

11. KLIP

This command smoothes the output graphic display data from any noise effect. The below information will appear on the screen when the command is used;

```
in    mv-y-kurs      100    100
in    mv-y-kurs      -100   -100
      Clipping limit set to -10.000000 10.000000
```

The above first line will limit the upper band of the graph and the second line will limit the lower band. This can be done by moving the cursor up or down using "d" or "s" (for one step movement) and "D" or "S" (for 10 step movement). The (CR) key should be pressed after defining each line and then the bottom line information display.

12. FILTER n

This command should be used immediately after KLIP which will filter the graphical output to a set number of "n". Then a series of similar error messages will display on the screen which have to be ignored:

UNABLE TO FILTER SPIKES

When the display of the above messages is completed, use CS then DREG command to display the filtered and smothed graphical output on the screen.

d. Display Data Commands

The following commands deal with displaying the calibrated data.

EDC : *edit display channel list*
SDC : *show display channel list*
DISPNUM : *set number of channel to be displayed*
SETDCHAN : *set display list of channel to user channel*
SETCOL : *set colour associated with display channel*
DCAL : *display a single x-axis calibrated data*
DCALM : *display multiple x-axis calibrated data*
DRAW : *draws uncalibrated data on the screen*
SSS : *set skip step*

1. EDC n

This command edits the number of displayed channel or channels. The number of channels can be specified by [n]. On the screen four columns of information will display representing array number, channel number, colour number and y-scale

poistion. The user can edit the required channel number and other information by typing in four figures corresponding to the above columns, see example below, where three orthogonal channels (3, 4 & 5) are edited and shown on the screen:

Array	Channel no.	Colour no.	Y-position
0	3	1	60
1	4	2	0
2	5	3	-60

Channel no. refers to the user channel, (e.g. 3, 4 & 5 are used in this example to represent R, T & V waves, respectively, from the second set of geophones).

Colour no. 1,2,3 are the colour numbers which are indicated on the plotter. The following colours are chosen to represent the *R, T & V* waves:

1. Pink *Radial*
2. Red *Transverse*
3. Green *Vertical*

Y-position (n) controls the position of the displayed channel where (n) can either be 0 or in a range between +200 and -200. If [n=0] the channel will display on the midline and if [n=±200] the channel will display either above or below the midline. This is very useful in separating the displayed channels for comparison, (see **DCALM** command for more details).

After each line is entered the updated list will display on the screen. The editing loop continues until it is terminated by pressing any alphabetic key followed by return. The final version of the modified list will be displayed and the edit mode will terminate.

Example 1 *editing of five channels using EDC*

Five vertical waves representing channels 2, 5, 8, 11 & 14 to be edited using the above command:

```
EDC 5
```

screen displays				user input				press
0	0	0	0	0	2	1	120	return
1	1	1	0	1	5	2	60	return
2	2	2	0	2	8	3	0	return
3	3	3	0	3	11	4	-60	return
4	4	4	0	4	14	5	-120	return

2. SDC

This command displays the latest version of the displayed channels mentioned above on the screen.

3. DISPNUM n

This command controls the number of channels to be displayed which can be specified by [n].

4. SETDCHAN n m

This sets the displayed channel "n" to user channel "m". For example `SETDCHAN 3 8` means that, channel 8 will display instead of channel 3.

5. SETCOL n c

This sets the colour number "c" to represent the displayed channel "n". For example `SETCOL 2 3` means that, channel 2 will be plotted by colour number 3 of the plotter.

6. DCAL n

This will display the selected channel from *EDC* on the screen. "n" controls the y-scale magnitude. When this command is used, all channels will display on the zero y-axis whatever Y-postion is chosen on `EDC` arrangement.

7. DCALM n

The selected channels will display on the screen on different levels of y-axis according to the EDC arrangement of the y-position. The midline of the Y-axis is the zero line, the maximum and minimum scale are +200 and −200 respectively. This command is very useful for comparing a group of waves. The scale of drawing can be controlled by [n].

8. DRAW n

This draws uncalibrated data for all 15 channel on the graphics screen. The y-scale may be defined by [n].

9. SSS n

This command controls the set of skip steps of the displayed channel or channels. The user can select the number of steps by [n]. When [n=1] a smoother curve will display, and as the magnitude of [n] is increased a sharper broken curve will result. The default setting of skip step is 1. Some examples for different set up skip (n=1,10,20) are shown on figure (A3.4).

Example 2 *display data procedure*

The following sequence may be used to load a file to the register and display the results on the screen:

```
1.  LOADDATA          loads data file to the register
2.  LOADCAL           loads calibration file to register
3.  SCON              displays the configuration data
4.  DTSET 1           sets data set number 1
or  DTSET 2           sets data sets number 2
5.  DISPNUM 3         sets 3 channels for display
6.  SETDCHAN 0 6      replace channel 0 to 6 for display
7.  SETDCHAN 1 7      replace channel 1 to 7 for display
9.  SETDCHAN 2 8      replace channel 2 to 8 for display
8.  SETCOL 6 1        sets colour 1 for channel 6
10. SETCOL 7 2        sets colour 2 for channel 7
11. SETCOL 8 3        sets colour 3 for channel 8
12. DCAL 20           draws the registered channels
or
5.  EDC 3             see the edc command
6.  DCALM 20          draws multi-axis of the reg. chan.
```

e. Data Calculation Commands

The following commands manipulate the register calibrated data into further required analyses such as integration, differentiation and other calculations from the original input data.

COPY : *copy calibrated channel into register*
DREG : *plot the register array*
PREG : *print the register array*
CALMAX : *calculate the MPV for specified channel*
VMAX : *calculate the MPV for 15 channels*
AMAX : *calculate the MPA for 15 channels*
DMAX : *calculate the MPD for 15 channels*
SMAX : *show the max. array on the screen*
PMAX : *print the max. register data*
DISPMAX : *display the max. array on the screen*
REGPMAX : *calculate and display the max. reg.*
REGCLEAR : *clears the register*
ACCEL2 : *differentiate register data*
BINTEG : *integrate the register data*
SUMSQ : *add square register data*
SUBSQ : *subtract square register data*
SUMCH : *sum channels register data*
SUBCH : *subtract channel register data*
INV : *invert the register array*
ROOT : *squares root the register data*
VECT : *calculate the velocity vector*
VACC : *calculate the acceleration vector*
VDISP : *calculate the displacement vector*
LOGSPEC : *calculate the log. fourier analysis*
SPECTRUM : *calculate the FFT value*
DISPEC : *plot the FFT graph*
PSPEC : *print the FFT values*

1. COPY n

Loads a channel defined by [n] into the register array. It then displays the register contents on the sreen as graphic curve in terms of particle velocity in a default y-scale of ±3000 mm/s. The graph may be redrawn with smaller scale by using the DREG command. When this command is used the new input register channel will override any existing data in the register.

2. DREG n

Displays the register data on graphics screen with a defined y-scale by [n]. If the y-scale is not specified, the automatic scaling of the register will be performed. The data in the register might be velocity, acceleration, displacement, or their resultant(vector).

3. PREG

Prints the content of the register array via a printer. The data will be printed in the same manner as they are stored in the register and will be represented in seven columns where the first column indicates the sequence of the registered array, second column shows the time interval and columns 3 to 7 represent the magnitude of the registered data in 0.6 microsecond time interval. Each row should be read from left to right and continued to the second row. An example of the output print is illustrated below:

```
<0000   0        >-8.3518  11.9312  8.94841  -6.9598  12.5278
<0005   0.0036   >50.1111  150.332  25.0556  12.5279  -87.694
```

4. CALMAX

This command calculates peak particle velocities of the loaded file in the register and then displays the results on the screen. The number of channels may be specified by two pairs of figures following the command. For example if the peak particle velocity for only one channel (eg. 5) is to be displayed then type:

CALMAX 5 5 (return)

But if the peak particle velocity for channels number 0-15, 40-46 and 48-51 is required to be calculated, then type in:

CALMAX 0 15 40 46 48 51 (return)

If no number is specified then a default calculation of channels 0-14 will be carried out.

5. VMAX

Calculates the peak particle velocities ($mm.s^{-1}$) of 15 channels and displays the results on the screen.

6. AMAX

Differentiates the calibrated registered data, finds the peak particle acceleration ($mm.s^{-2}$) for all 15 channels and then displays the results on the screen.

7. DMAX

Integrates the calibrated registered array as peak particle displacement(mm) and then displays the results on the screen.

8. SMAX

Displays the registered data on the screen.

9. PMAX

Sends the registered data to the printer.

10. DISPMAX

Displays the registered data on the screen.

11. REGMAX

Displays the peak value of the registered data on the screen.

Example 3 *peak particle calculation*

First load a file into the register (see example 2) then follow the procedure below to calculate the peak particle velocity, acceleration and displacement for a number of channels:

1.	`LOADDATA`	loads data file to the register
2.	`LOADCAL`	loads calibration file to the register
3.	`COPY 2`	copys channel 2 to the register
4.	`CS`	clears screen
5.	`VMAX`	calculates p.p.velocity for 15 chan.
or	`AMAX`	calculates p.p.acceleration for 15 chan.
or	`DMAX`	calculates p.p.displacement for 15 chan.
or	`CALMAX 1 5`	calculates p.p.velocity for chan 1 to 5
6.	`PMAX`	prints the registered calculation
7.	`SMAX`	displays the registered calculation

12. REGCLEAR

Clears the register array of any stored data.

13. ACCEL2

Diffrentiates any individual channel specified by `COPY` command and displays the results on the graphic screen using automatic scale. The peak value of the registered channel in $(mm.s^{-2})$ may be obtained using `REGMAX` command. Also `DREG` can be used to adjust the out put y-scale. The `ACCEL2` is modified from the original version `ACCEL`, and gives a much smoother displayed output.

Example 4 *acceleration calculation*

Having a file loaded to the register, use the following sequence to get the acceleration measurement of the loaded data:

1.	`COPY 2`	copies channel 2 to the register
2.	`ACCEL2`	differentiates the registered data
3.	`CS`	clears screen
4.	`REGMAX`	displays the peak registered data
5.	`DREG 2000`	draws the registered data
6.	`PREG`	prints the registered data

14. BINTEG

Integrates the data currently in the register and displays the integration result as graphic output on the screen. During the process of integration, the program will ask to specify the left and right limit of the displayed velocity to be integrated, and this can be done by pressing the "s" and "d" keys for one step movement of the cursor to the left and right respectively or "S" and "D" for ten step movement. The (CR) key should be pressed after defining each limit. Finally the graphical displacement output will display with an automatic scale on the screen. The **DREG** command can be used to obtain a desirable scale. A summary of the screen messages during the integration process is listed below;

```
setting START of the CYCLE (define the left limit)
time=0s reg.value=-0.402 x=0
setting the END of the CYCLE (define the right limit)
time=0.37368s reg.value=-0.603 x=519
Performing automatic Y-scaling
FACTOR 1
Y-scale=0.2
```

The maximum registered displacement can be obtained using **REGMAX** command. The **BINTEG** program is modified from the older version **INTEG** program.

Example 5 *displacement calculation*

First load a file data into the register (see example 2) then use the following sequence of commands to obtain the displacement measurement of the loaded data:

1.	**COPY 2**	copies channel 2 to the register
2.	**BINTEG**	integrates the registered data
3.	**CS**	clears screen
4.	**REGMAX**	displays the peak registered data
5.	**DREG 0.2**	draws the registered data
6.	**PREG**	prints the registered data

15. SUMSQ n

Adds the squared calibrated data channel defined by "n" into the register array.

16. SUBSQ n

Subtracts the square calibrated channel from the register array.

17. SUMCH

adds the calibrated channel to the register array.

18. SUBCH

Subtracts the calibrated channel from the register array.

19. INV

Inverts the sign of the register array data.

20. ROOT

Finds square root of the register array.

Example 6 *resultants calculation*

First load a file data into the register (see example 2) then use the following sequence of commands to obtain the peak particle resultant for three orthogonal channels (for example channels 3, 4, & 5) which may be repeated for other channels.

1.	`SUMSQ 3`	sums the square of channel 3
2.	`SUMSQ 4`	sums the square of channel 4
3.	`SUMSQ 5`	sums the square of channel 5
4.	`ROOT`	squares root the registered data
5.	`CS`	clears screen
6.	`REGMAX`	displays the peak registered data
7.	`DREG 40`	draws the registered data
8.	`PREG`	prints the registered data

21. VECT $n_1 n_2 n_3$

This command calculates the resultant with respect to time of three orthogonal channels (*radial, transverse* and *vertical*) of the registered data by adding together the square root of channel numbers specified by "n_1, n_2, n_3"

$$R_{vt} = \sqrt{R^2 + T^2 + V^2}$$

The graphical out put then will be displayed on the screen together with the maximum registered figure.

22. VACC n_1, n_2, n_3

Differentiates and calculates the vector of the registered calibrated channels specified by "n_1, n_2, n_3" and then displays the maximum register value and the corresponded ouput on the screen.

23. VDISP n_1, n_2, n_3, l, r

Integrates and calculates the vector of the registered channels specified by n_1, n_2, n_3. The left and right limit of the output data can be controlled by l and r for the process of the integration. For an ordinary loaded file $l = 20$ and $r = 519$.

Example 7 *vector calculation*

First load a file data into the register (see example 2) then use the following sequence of commands to obtain the vector of three orthogonal channels (for example channels 3, 4, & 5) which may be repeated for other channels.

1.	`VECT 1 2 3`	velocity vector for channels 1,2,3
or	`VACC 1 2 3`	acceleration vector for chan. 1,2,3
or	`VDISP 1 2 3 20 519`	displacement vector for chan. 1,2 3
2.	`CS`	clears screen
3.	`REGMAX`	displays the max. registered vector
4.	`DREG n`	draws the registered vector
5.	`PREG`	prints the registered vector

24. SPECTRUM

Calculates the frequency spectrum for the channel in the register and displays the graphical output and the maximum frequency(`Hz`) on the screen. The *fast fourier transform* analysis `FFT` is used for this calculation.

25. LOGSPEC

Calculates the logarithmic spectrum for the channel in the register and displays the result on the screen.

26. DSPEC

Draws the spectrum data in the register on the screen or when the plotter is on, plots the result.

27. PSPEC

Prints the output spectrum result through the printer.

Example 8 *frequency calculation*

First load a file of data into the register (see example 2) then use the following sequence of commands to obtain the vibration frequency of a loaded channel:

1.	`REGCLEAR`	clears the register
2.	`COPY 2`	loads channel 2 to the register
3.	`SPECTRUM`	calculates the frequency
4.	`CS`	clear screen
5.	`DSPEC`	draws the frequency output
6.	`PSPEC`	prints the frequency output

f. Plotting Control Commands

These commands control the route of the graphical information in which the output information can either be displayed on the screen or sent to the plotter for permanent record of display. The commands in this group are;

PL : *toggle the ploton/plotoff*

PLOT : *toggle the ploton/plotoff*

PLOTON : *direct graphic output to the plotter*

PLOTOFF : *direct graphic output to the screen*

HPTST : *plot a test frame*

1. PL

This command is used to change the direction of the output information to the other destination. The result of these changes can then be shown on the screen as either;

```
>> 0.0 >> PL (return)
PLOTTER ON
```

When the plotter is on, all the drawing commands which start with "D" can activate the plotter and draw the output result on the plotter. When in plotter mode, PL will redirect to the screen.

```
>> 0.0 >> PL (return)
SCREEN ON
```

2. PLOT

This command has same function as PL command.

3. PLOTON

This command directs the graphical output to the plotter.

4. PLOTOFF

This command activates the screen. Usually PLOTOFF is used while the plot mode is on and PLOTON is used when the screen mode is on.

5. HPTST

Due to an unresolved problem in the software, the first time that information is sent to the plotter it will not be plotted, and it is necessary to use HPTST immediately after loading and running the DANA3 program. Nothing will display on the screen and the cursor will blink. Use the RESET botton and run the DANA3 program again. This time the information will be plotted once the PL is used.

Example 9 *plotting procedure*

First load a file data into the register (see example 2), then follow the sequence below to plot the calculated result obtained from examples 3,4,5,6 & 7:

```
1.  PL          activates the plotter
2.  DCAL 20     draws single x-axis graph
or  DCALM 20    draws multi-x-axis graph
or  DREG 20     draws the registered data
3.              if the plotter did not activate, press
4.  reset       then type run or go, press return
```

or	`abort`	then type run or go, press return
5.		the plotter starts to plot
6.	`PL`	activates the screen

g. Legend Commands

This series of commands deals with putting the legend on the plot. The commands in this group are;

TITLE : *enter a line of title text*

DATE : *enter date for the plot*

CAHR : *control the size of characters*

TXT : *enter text at any position wanted*

TEXT : *enter text on the top of the output*

BOX : *draw frame and plot the legend text*

XLBL : *enter the x-axis text*

YLBL : *enter the y-axis text*

SLEG : *display the above text on the screen*

1. TITLE

This command writes one line of title for the plot to the lower left side of the the graph. The size of the characters is fixed and is in uppercase mode.

2. DATE

Writes the required date on lower right side of the graph.

3. CHAR w h c x y f

This command controls the size and the orientation of the characters. Suitable figures should be replaced for the width [w], height [h], colour [c], x-axis [x], y-axis [y] and the font shape [f] to obtaine the required character. Below is an example of information arrangement used for this command;

horizontal display

width	height	colour	x	y	font
22	19	1	1	0	0.20

vertical display

width	height	colour	x	y	font
22	19	1	0	1	0.20

The orientation of the text can be adjusted to any required direction by selecting proper values for x and y. The font of the character is normal when the value is zero and as the decimal point is increased the angle of italic increases. When the input values for the **CHAR** command are inserted, press return and the following information will display;

txt-run=1.000 txt-rise=000

4. TXT x y c

This command controls the position and the colour of the text to be inserted through the selected values for *x, y &c*. The command is usually used in connection with **CHAR** command. The colour number in this command unlike the **EDC** command, is the same as in the plotter pen numbers. After the command is typed in and return key pressed, a required text can be entered (in one line or multiple lines), and then the mode can be terminated by pressing simultaneously **Ctrl+Z** keys. Below is an example of running this command;

TXT 1700 1400 6 (return)

Stand-off=10.0m
from the pile
(Ctrl+Z)

After **(Ctrl+Z)** is pressed, the modified text will display, and below that the following message will display twice;

char size 22 19 , char colour: 2, rotation: 1 0
ok ? (Y/N)

If the correct information displayed type *y* and then (return), the plotter will activate and plot the text. If *n* is used the **TXT** will terminate.

5. TEXT

This command writes a fixed size character text on the top of the output paper. The colour and the position of the character can not be changed.

6. BOX

This command draws a border for the output and plots the information supplied by `TITLE, DATE & TEXT` commands. The plotter chooses colour number one for plotting these commands.

7. XLBL (text)

A label can be entered for the x-axis by using this command. The label in this command can only be inserted as upper case characters. If lower case characters are needed, it is better to leave `XLBL` empty and the `TXT` command can be used to enter the desired label. The default text for `XLBL` is `XLBL(ABC)`.

8. YLBL (text)

This command inserts the y-label in a similar manner to x-label. The orientation of the text is in the horizontal direction. Often it is better to use empty text for this command and to use the `TXT` command facilities.

9. SLEG

This command shows the legend content on the screen.

h. The Use Commands

The following commands are used in connection with *USE*

USE : *loads a file written by the* `lcded` *program*

PAUSE : *pauses the program from running*

WT : *keeps the program waiting*

lcded : *is a multiple command program*

1. USE

This command loads a *lcded file* into the memory while the DANA3 program is on run, see lcded program for more details.

2. PAUSE & WT

These two commands have a similar function of temporarily freezing a running program. They are of use within the file of `lcded` program.

3. lcded

The program name stands for `LCD screen EDIT`. The `lcded` program is stored in a floppy disc and has similar applications to the `EDLIN` program available in most `MS-DOS` operating system. This command is very useful when a series of commands is to be repeated during the analysis of data. A sequence of commands can be written in a single file and the file will run the commands automatically. The use of commands within the `lcded` program is given below:

I. *insert:* used to insert lines to a file. If the number of line is not specified a new file will be opened. If the number is specified the insertion will start from the specified line. Use `(Ctrl+Z)` to terminate this mode.

D. *delete:* used to delete line or lines. If the line number is specified that line will be deleted. If two numbers with a comma between is used (eg. 2,18) lines 2 and 18 will be deleted. When two numbers with gap between is used (eg. 5 15), all lines between 5 and 15 will be deleted.

W. *write:* this writes a supplied name for a file. The disc drive should be turned on, (see example 10).

R. *read:* this reads a specified file name from the disc and displays the file on the screen.

L. *list:* this lists the currently used file on the screen.

E. *exit* this terminates the `lcded` program and returns to the main operating system program. A message will display on the screen, type `Q!` to confirm, (see example 10). The use of the command is explained in the following example:

Example 10 *running the lcded program*

```
1.  load lcded
```

2. `run`

By running the program, the prompt < 1 > will appear. Type `I` to insert a sequence of command, and when the inserting is finished press `(Ctrl+Z)` to terminate this mode. A list of inserted commands will be shown on the screen, (see example below):

3. < 1 > `I`
4. 0001> `loaddata`
5. 0002> `loadcal`
6. 0003> `copy 2`
7. 0004> `cs`
8. 0005> `dreg 30`
9. 0006> `vmax`
10. 0007> `pmax`
11. 0008> `cs`
12. 0009> `vect 0 1 2`
13. 00010> `wt`
14. 00011> `vect 3 4 5`
15. 00012> `wt`
16. 00013> `Ctrl+Z`

To write the inserted command into the disc as a file, use the `W` command followed by file name `(eg.ABC)`, then turn the disc-drive on and press return:

17. < 13 > `W ABC`

It is advisable to write the `lcded` file in the same file data disc to give easy access to the file during the processing.

To exit from this mode type `E`, press return, and then type `Q!`:

18. < 14 > `E`

`NO WRITE SINCE LAST CHANGE: (Q! overrides): Q!`

The program will return to the monitor system. Now by loading and running the **DANA** program the **USE** command can be used.

```
>> 0.0 >> USE
ENTER file name to USE:
```

When the file name (eg.ABC) is entered, the sequence of commands will display and the procedure can be repeated for the new file.

i. The Communication Commands

This includes the following commands;

SNDCHAN *send a specified channel to PC unit*

SNDCONF *send a configuration file to PC unit*

These two commands are within the DANA program. They are used to transfer data to any external personal computer for further analyses such as stereonet plotting using the SENT program. The PDR2 unit should be connected to the PC unit by a parallel cable with one end in the printer socket of the PDR2 unit and the other end in the serial port of the PC unit. To enable effective communications the rate at which the PDR2 unit sends out information must be slowed down. This can be done by typing the following line on the operating system of the PDR2 operating system prompt (immediately after switching on and before loading the DANA program).

```
. serset line1 2400
```

The procomm program must first be run on the PC unit. Press (Alt+P) to bring up a parameter table, selecting option 5 and then press return, the correct speed line will replace into the current line on the top of the creen. Esc will return to the main screen. Load and run DANA on the PDR2 unit and load a file of data to the memory. The PC unit should be on procomm mode. Press Pg Dn key. Select option 7 from the menu and give the name of the file to be stored on the PC unit. Now the PC is ready to receive the transferred data. On the PDR2, type in SNDCHAN command followed by a channel number and wait until the transfer is completed. Now press ESC on the PC and then Pg Dn again to set up for next channel transfer. The SNDCONF command is used to transfer the configuration file and it can be done in a similar way to the above command and needs to be used once with each group of channels. For more details see Hunter (1988).

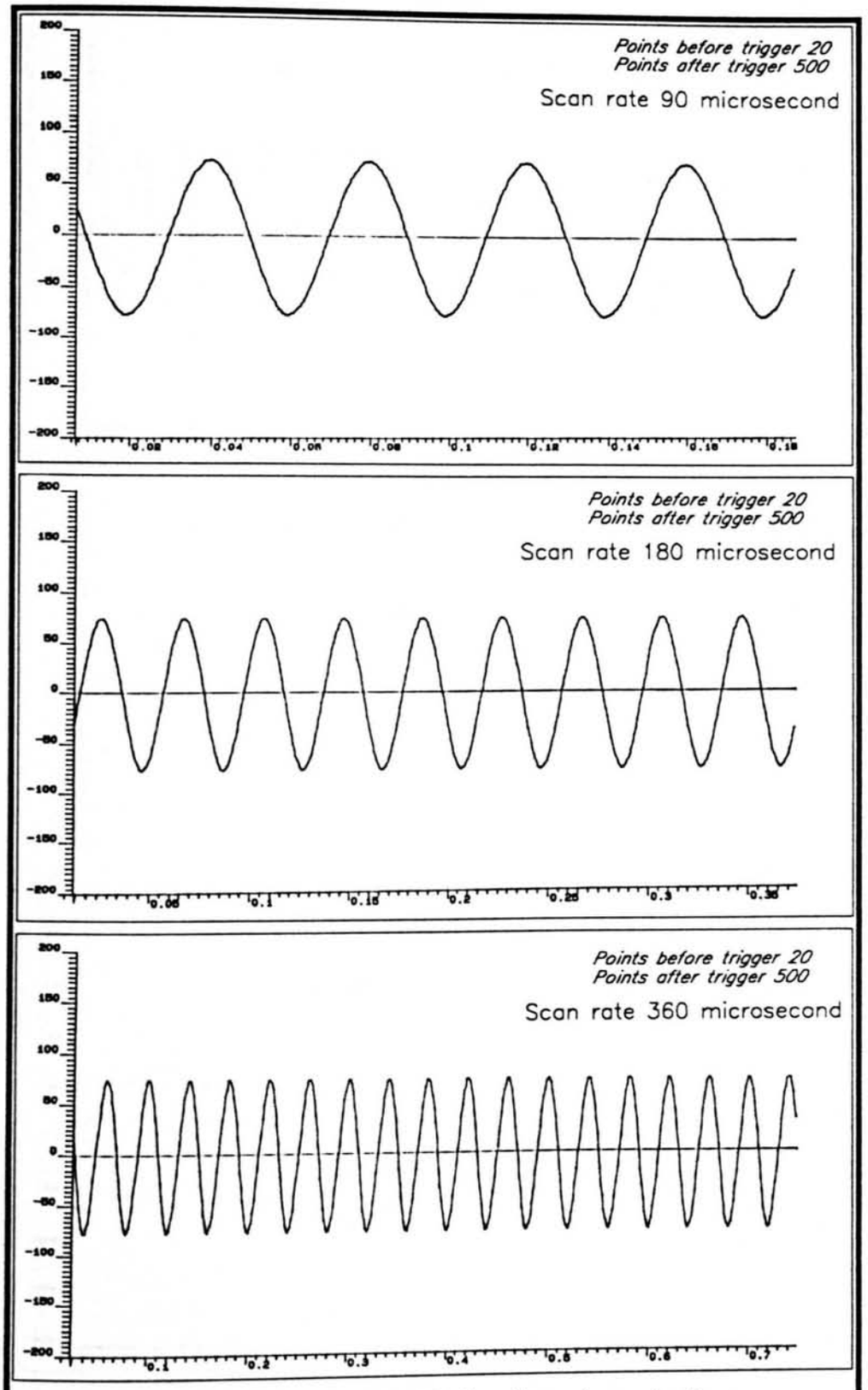

Figure (A3.1) The effect of Option three in controlling the output vibration traces

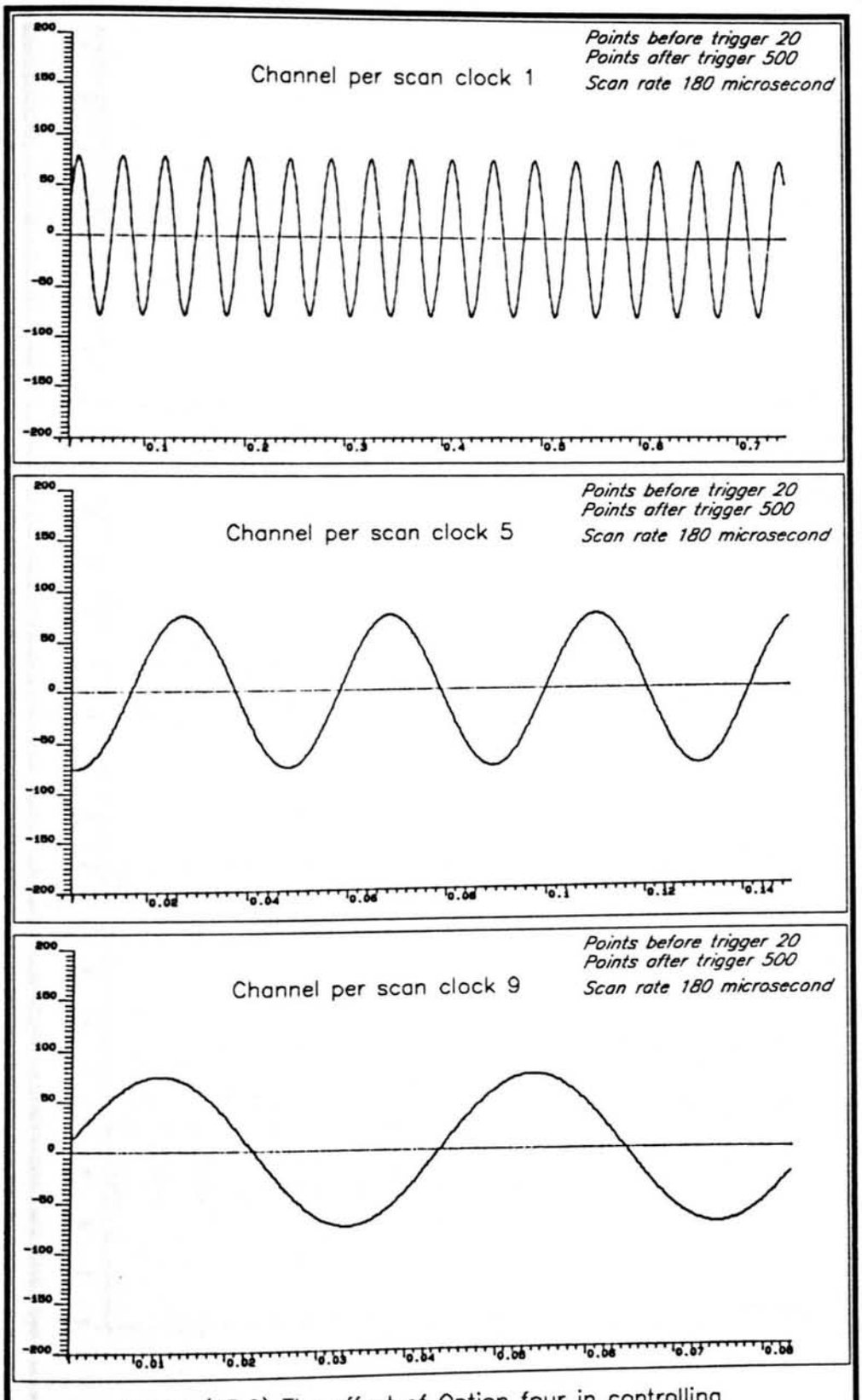

Figure (A3.2) The effect of Option four in controlling the output vibration traces

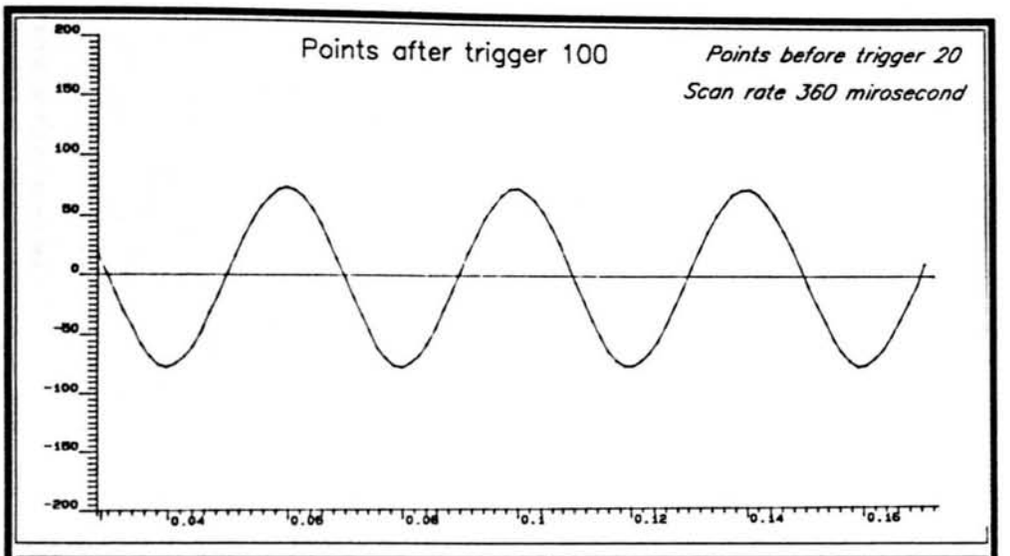

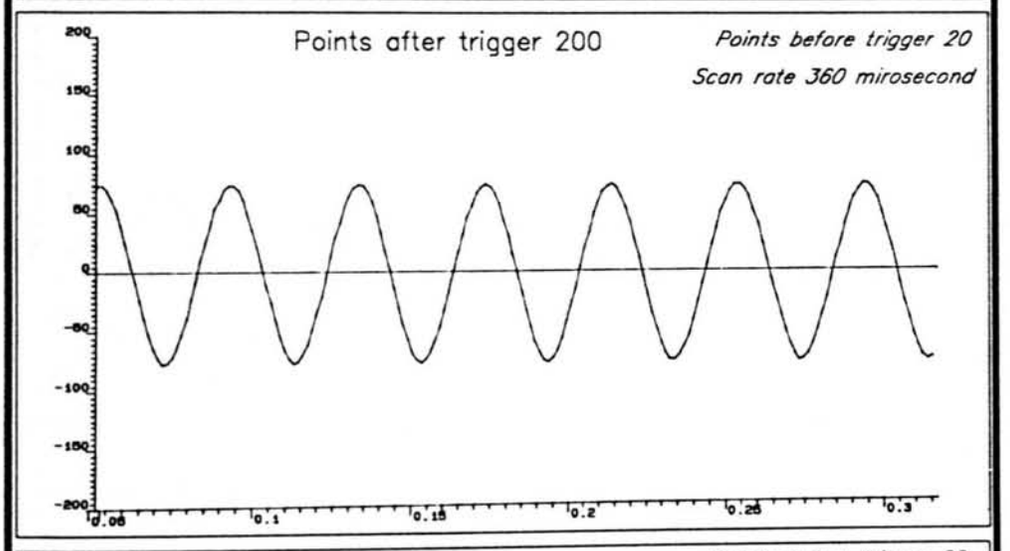

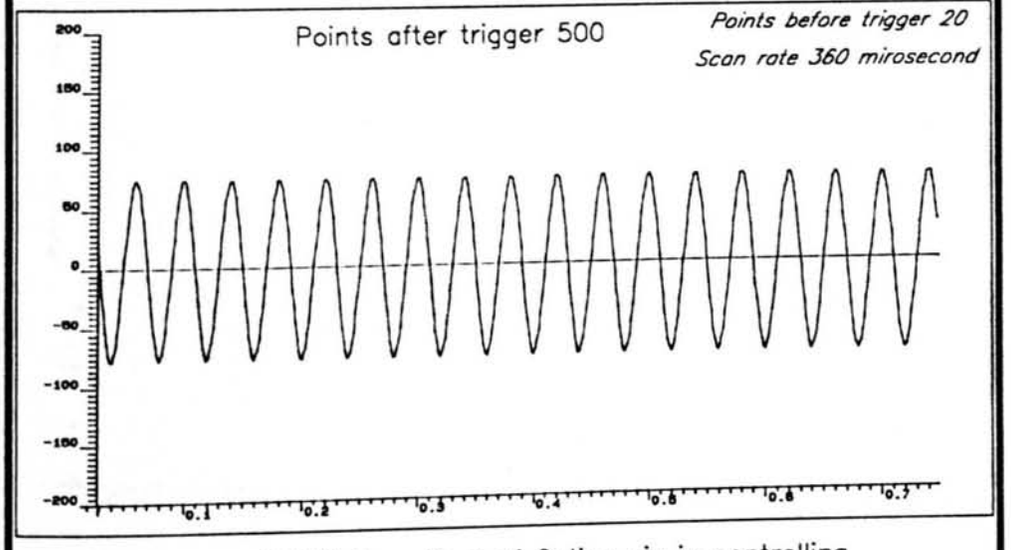

Figure (A3.3) The effect of Option six in controlling the output vibration traces

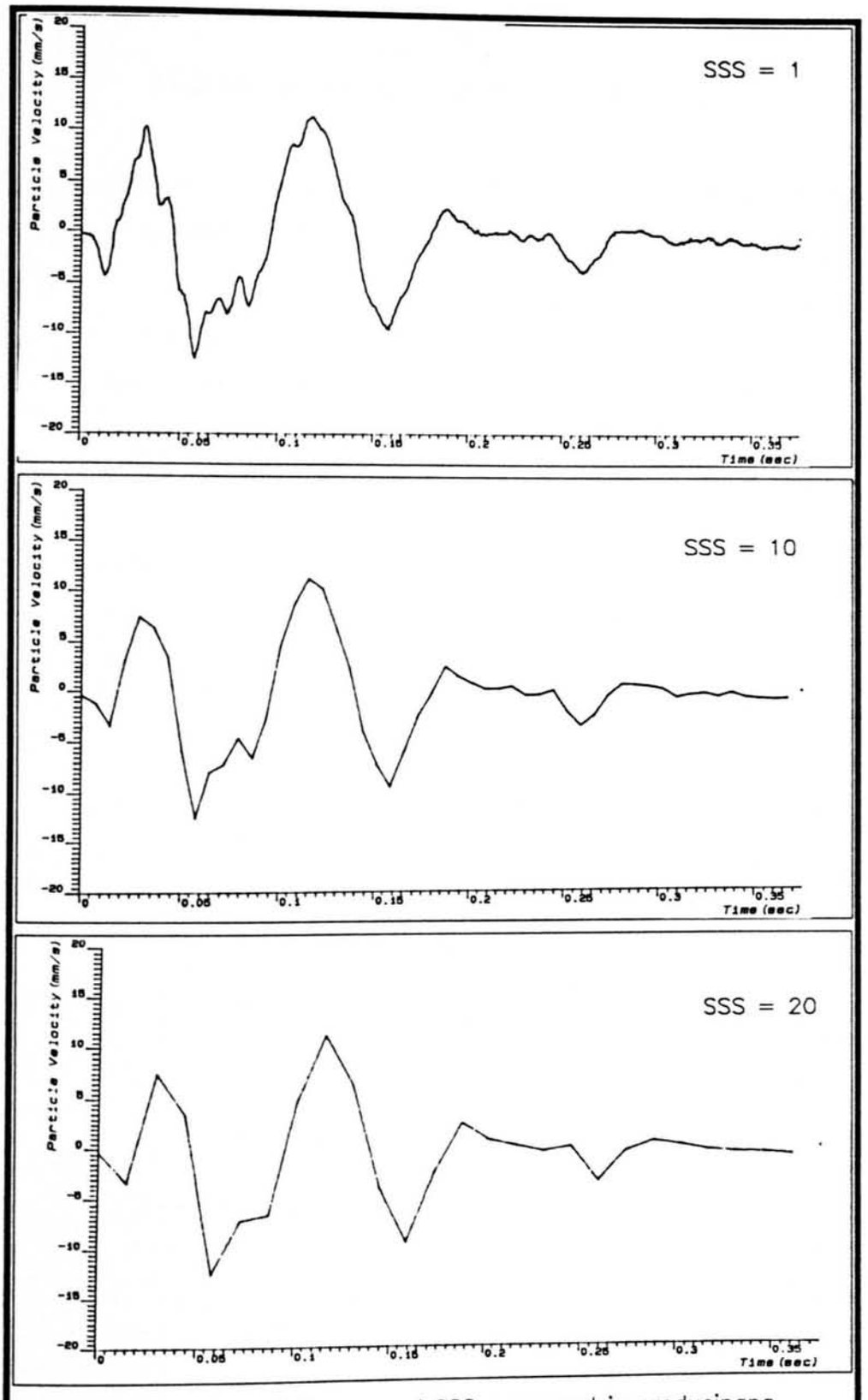

Figure (A3.4) The use of SSS command in producingng the output vibration

Appendix A3

A3.3 Specifications of the Velocity Transducers

This Appendix presents the details of the specifications and features of the two types of geophones employed in this project. It is noted that the models of the devices used are:

1. Geosource geophone, type SM-6, model A.
2. Mark product geophone, type L-4C, 1Hz frequency.

SPECIFICATIONS FOR SM-6 GEOPHONES

Parameters	Symbol	Unit	Geophone Model				
			A	B	B	B	B
Frequency							
Natural Frequency	Fn	Hz	4.5 ± 0.5 Hz	4.5 ± 0.5 Hz	8.0 ± 0.5 Hz	10.0 ± 5%	14.0 ± 5%
Frequency Tolerance			-	-	20	25	25
Maximum tilt angle for specified Fn (vertical units only)		DEG	-	-	150	170	190
Typical spurious frequency		Hz					
Distortion							
Distortion with 0.7 in/s pp coil to case movement			< 0.3%	< 0.3%	< 0.2%	< 0.2%	< 0.2%
Distortion measured at frequency of		Hz	12	12	12	12	14
Maximum tilt angle for distortion specification (vertical units only)		DEG	-	-	15	20	20
Damping							
Open circuit damping for 375 ohm coil	Bo		0.265	0.560	0.315	0.250	0.180
Shunt resistance used for damping calibration with 375 ohm coil	Rs	Ohm	-	-	2257	1339	645
Damping with shunt for 375 ohm coil	Bt		-	-	0.60	0.60	0.60
Damping tolerance			± 5%	± 5%	± 5%	± 5%	± 5%

Standard coil resistance (other values available	Rc	375 ± 5%	Ohm
Sensitivity for Model 'A'		28.0 ± 5%	V/m/s
		0.71	V/in/s
Sensitivity for Model 'B'		28.8 ± 5%	V/m/s
		0.73	V/in/s
RtBcFn for Model 'A'		3875	Ohm Hz
RtBcFn for Model 'B'		6000	Ohm Hz

Physical Specifications	Basic unit (element)	PE-4 case	PE-5 case	HPE-case
Length	-	40.0 mm (1.57 in)	40.0 mm (1.57 in)	57 mm (2.24 in)
Width	-	35.0 mm (1.38 in)	35.0 mm (1.38 in)	45 mm (1.77 in)
Diameter	25.4 mm (1.00 in)	-	-	-
Height	36.0 mm (1.42 in)	56.0 mm (2.20 in)	62.0 mm (2.44 in)	35.0 mm (1.38 in)
Weight	81.0 g (2.86 oz)	183 g (6.46 oz)	141 g (4.97 oz)	192.5 g (6.79 oz)
Guarantee with normal use*	2 years	1½ years	1½ years	1½ years

4.5 Hz model guaranteed for one year
Normal use excludes damage caused by high voltage and physical damage to case

Sensor reserves the right to alter specifications to offer the best possible product.

Suspended mass Model 'A' 16.1 g
Model 'B' 11.1 g
Total DC to case movement 4 mm (0.16 in)
Operating temperature range +40° C to +100° C
+40° F to +212° F
All parameters specified at 20° C

KEY
Sensitivity G
Natural frequency Fn
Open circuit damping Bo
Coil current damping Bc = Rtbc/Rc - 5%
Coil resistance Rc
Shunt resistance Rs
Total damping Bt = Bc + Bs
Total resistance Rt = Rc x Rs/Rs + Rc
RtBcFn Model 'A' = 1.73 Rc
Model 'B' = 1.6 Rc
Transduction constant
Model 'A' G = 0.036 Rc v/in/sec 5%
Model 'B' G = 0.037 Rc v/in/sec 5%

The SM-6 is a digital grade, miniature geophone based on the popular SM-4 design.
Engineered for consistent performance over a long life.
Advanced computerized testing, manufacturing techniques and quality control are used in the production process to provide both the uniform parameters and the rugged qualities necessary in modern geophones.

Features of the SM-6

- Available coil movement of 4 mm (0.16 in) which makes it suitable in a vertical mode and high tilt for lower natural frequencies and for industrial purposes where the force of one G is exceeded.
- In the horizontal mode the large coil excursion of the 10 Hz model makes it suitable for shear wave detection with planting faults of up to 20 degrees without resorting to cumbersome leveling devices.
- Symmetrical rotating dual coil construction minimizing the force on the spring arms.
- Use of precious metals ensures optimum electrical contact and long operating life.
- The unbreakable and lightweight PE-4, PE-5 and HPE case provide for easy access to the element in the field.
- Sensor's UV stabilized rubber sleeved gasket minimizes cable fatigue and has excellent watersealing capabilities.

SM-6 FREQUENCY RESPONSE CURVES

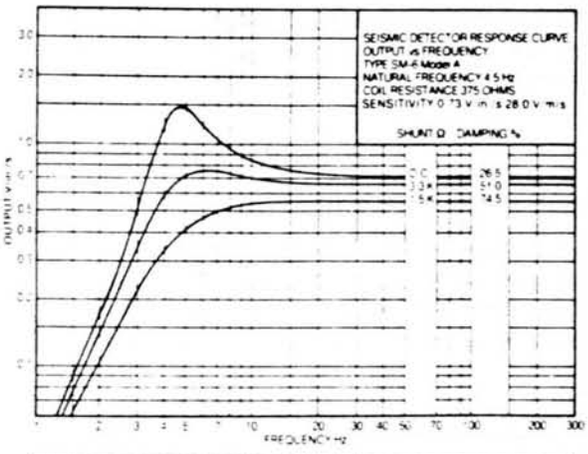

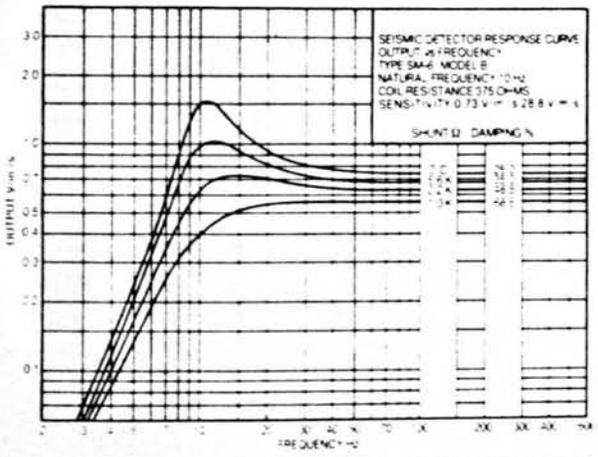

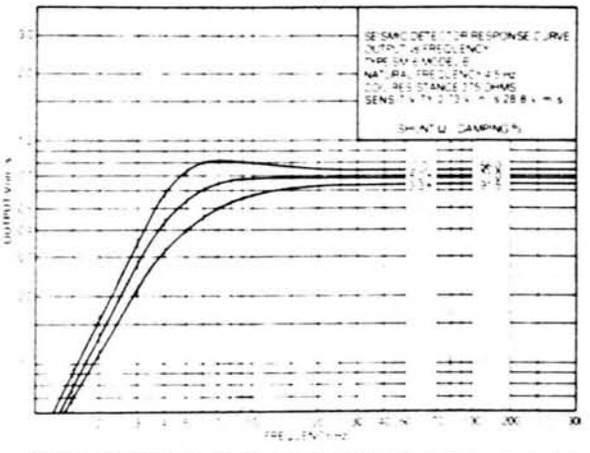

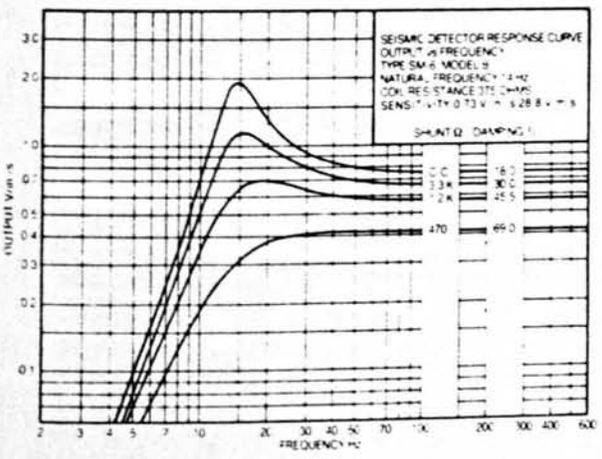

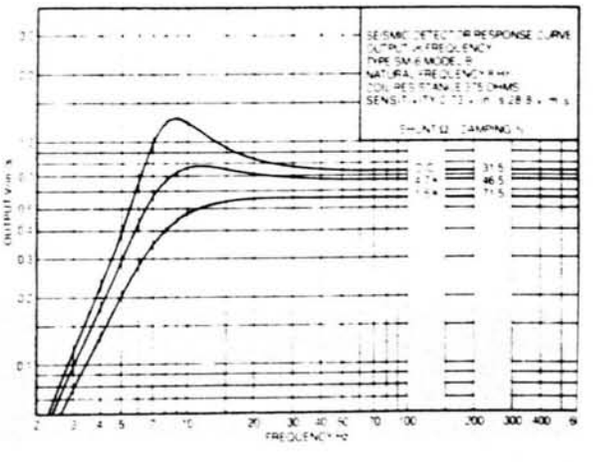

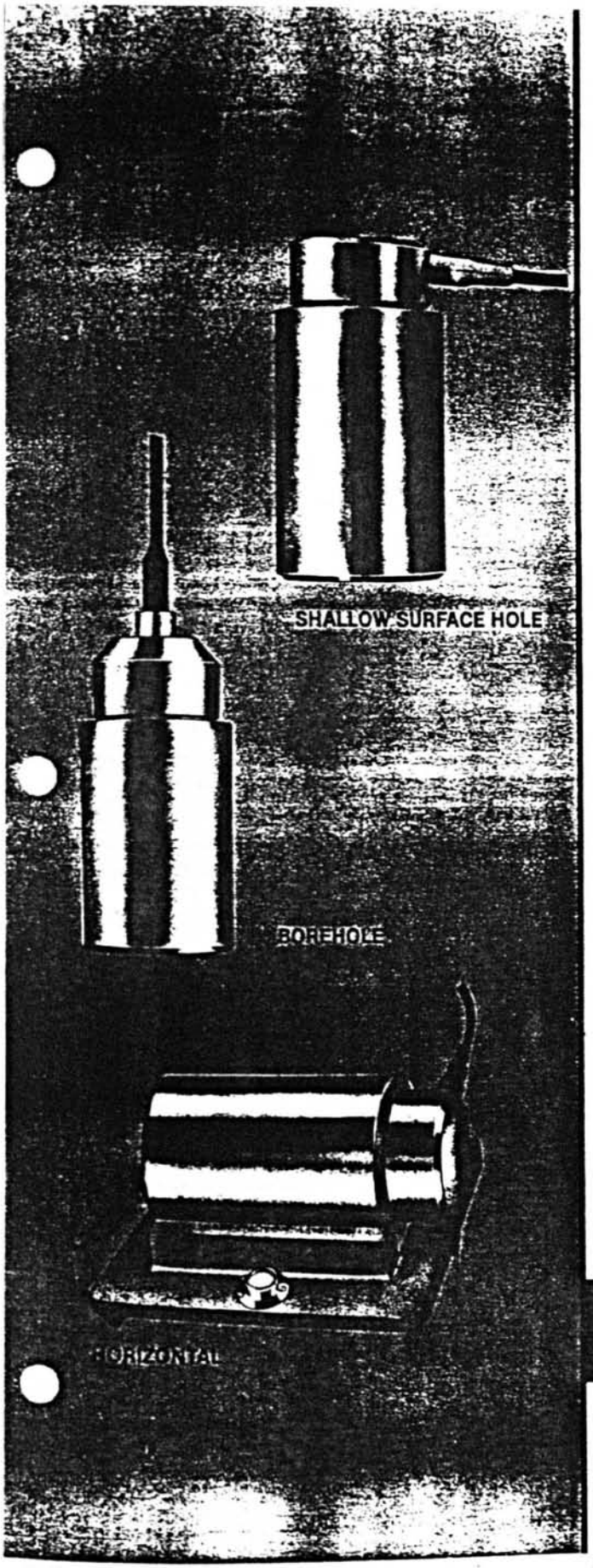

The L-4 is an INSTRUMENT QUALITY ONE Hz or TWO Hz multi-purpose geophone, that is small, light, and economical. It is designed to yield the performance needed for scientific studies, yet has the ruggedness required for petroleum exploration work.

The L-4 design ELIMINATES the usual causes of FAILURE in VERY LOW FREQUENCY geophones, such as SPRING FATIGUE, OVER-STRESS and INSTABILITY. This geophone maintains a close frequency tolerance with tilt and temperature, and is TRANSPORTED WITHOUT CLAMPING the moving element.

The L-4 is available with or without calibration coils and may be obtained as VERTICAL OR HORIZONTAL elements. A variety of fittings are available for custom application.

FEATURES

STABLE NATURAL FREQUENCY

LOWEST DISTORTION

INSTRUMENT QUALITY

HUMBUCK CONSTRUCTION

VERY HIGH OUTPUT

NO SPRING SAG

U.S. PATENT 3,451,040
FRENCH PATENT 1,598,454

1.0 Hz AND 2.0 Hz LAND OR BOREHOLE GEOPHONE

Basic unit is guaranteed for six months, external voltage and highline damage not included on warranty.

Warranty is subject to the terms and conditions listed on our General Warranty page in this catalog.

	L-4C 1.0 Hz GEOPHONE	L-4A 2.0 Hz GEOPHONE
TYPE	Moving dual coil, humbuck wound	Moving dual coil, humbuck wound
FREQUENCY	1.0 ± 0.05 Hz measured on 200 pound weight at 0.09 inches/second	2.0 ± 0.25 Hz measured on 200 pound weight at 0.09 inches/second
FREQUENCY CHANGE WITH TILT	Less than 0.05 Hz at 5° from vertical	less than 0.10 Hz at 10° from vertical
FREQUENCY CHANGE WITH EXCITATION	Less than 0.05 Hz from 0 to 0.09 inches/second	Less than 0.10 Hz from 0 to 0.18 inches/second
SUSPENDED MASS	1000 grams	500 grams
STANDARD COIL RESISTANCES	500, 2000, 5500	500, 2000, 5500
LEAKAGE TO CASE	100 megohm minimum at 500 volts	100 megohm minimum at 500 volts
TRANSDUCTION POWER	$8.8\ 10^{-3}$ watts/inch/second or 13.6 watts/meter/second	$8.8\ 10^{-3}$ watts/inch/second or 13.6 watts/meter/second
OPEN CIRCUIT DAMPING	(bo) = 0.28 critical	(bo) = 0.28 critical
CURRENT DAMPING	$(bc) = \frac{1.1\ Rc}{Rs + Rc}$	$(bc) = \frac{1.1\ Rc}{Rs + Rc}$
COIL INDUCTANCE	Lc = 0.0011 Rc Lc in henries	Lc = 0.0011 Rc Lc in henries
ELECTRIC ANALOG OF CAPACITY	$Cc = \frac{73,500}{Rc}$ (microfarads)	$Cc = \frac{36,500}{Rc}$ (microfarads)
ELECTRIC ANALOG OF INDUCTANCE	Lm = 0.345Rc (henries)	Lm = 0.17Rc (henries)
CASE HEIGHT	5¼ inches—13 cm.	5¼ inches—13 cm.
CASE DIAMETER	3 inches—7.6 cm.	3 inches—7.6 cm.
TOTAL DENSITY	3.7 grams/cm³	2.9 grams/cm³
TOTAL WEIGHT	4¾ pounds—2.15 kilograms	3¾ pounds—1.7 kilograms
OPERATING TEMPERATURE	Range: −20° to 140°F or −29° to 60°C	Range: −20° to 140°F or −29° to 60°C

	L-4C 1.0 Hz GEOPHONE			L-4A 2.0 Hz GEOPHONE		
COIL RESISTANCE, OHMS	500	2000	5500	500	2000	5500
TRANSDUCTION, VOLTS/IN/SEC	2.12	4.23	7.02	2.12	4.23	7.02
COIL INDUCTANCE, HENRIES	0.55	2.20	6.05	0.55	2.20	6.05
ANALOG CAPACITANCE, MICROFARADS	147	36.8	13.4	73.0	18.3	6.64
ANALOG INDUCTANCE, HENRIES	173	690	1900	85.0	340	935
SHUNT FOR 0.70 DAMPING, OHM	810	3238	8905	810	3238	8905

Open Circuit Damping (b_o) = 0.28 Critical Coil Current Damping (b_c) = $\frac{1.1\ Rc}{Rc + Rs}$, Total Damping (b_t) = $b_o + b_c$

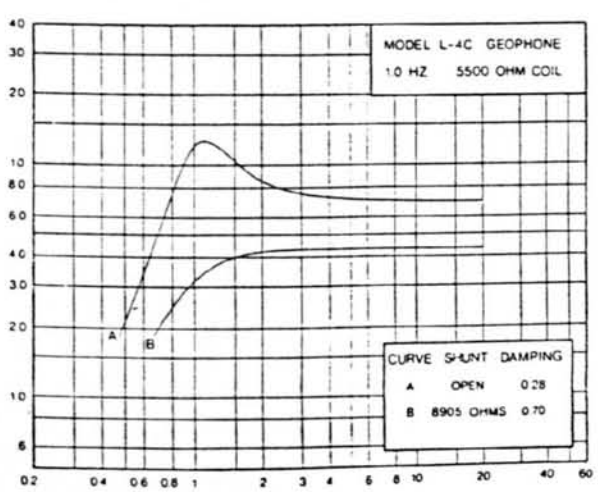

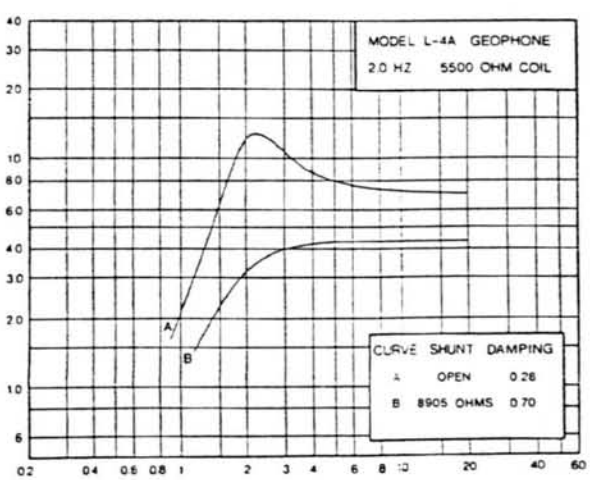

MARK PRODUCTS U.S., INC.
Area 713/498-0600
10507 Kinghurst Dr.
Houston, Texas 77099
Telex 76-2069

MARK PRODUCTS, LTD.
Area 403/275-3544
1108 55th Ave. N.E.
P.O. Box 73, Station M
Calgary, Alberta T2P-2G9
® Canada

Appendix A4

A4. Hemispherical Projection of Ground Vibration Vectors

The use of computer program for plotting stereogrphically, the ground vibration vectors on upper and lower hemispheres is presented in this Appendix. The program is written in `Fortran-77` using a software package `GHOST-80` for the drawing procedure. The above package is available within the `DUR.MTS` network.

A list of the program is given in the following pages. To create a file and run the program see the `GHOST-80` manual.

A4. Stereographic projection of Vibration vectors

```
C
      DATA PI /3.141592654/
C
      CALL PAPER(1)
      CALL FILNAM('GRSHAP')
      CALL MAP(-1.0,1.0,-1.0,1.0)
      CALL PSPACE(0.20,0.60,0.20,0.60)
      CALL CTRMAG(15)
      CALL PCSCEN(0.0,0.0,'+')
      CALL CTRMAG(12)
      CALL THICK(2)
      CALL PCSCEN(0.945,0.0,'R')
      CALL PCSCEN(-0.955,0.0,'-R')
      CALL PCSCEN(0.0,-0.96,'-T')
      CALL PCSCEN(0.0,0.94,'T')
      CALL THICK(1)
      CALL POSITN(0.0,0.0)
      CALL CIRCLE(0.9)
      CALL CTRMAG(10)
C
      CALL AA10(PI,J)
      CALL DOILY(PI,RAD,I)
      CALL PPVS(J)
C
      CALL FRAME
      CALL GREND
      STOP
      END
C
      SUBROUTINE AA10(PI,N)
      COMMON/C/ R(100), T(100), V(100)
      DIMENSION DIR(100), DIP(100), RE(100)
      READ(*,*)N
      DO 10 I=1,N
      READ(*,*) R(I), T(I), V(I)
      RE(I)=SQRT((R(I)**2)+(T(I)**2))
      IF (V(I).GT.0) GOTO 50
      IF (V(I).LT.0) GOTO 60
 50   DIP(I)=ATAN(V(I)/RE(I))
      CN=0.9*TAN(DIP(I))
      RD=0.9/COS(DIP(I))
      CALL CTRMAG(10)
      CALL LINCOL(4)
      IF (R(I).GT.0.AND.T(I).GT.0) GOTO 100
      IF (R(I).GT.0.AND.T(I).LT.0) GOTO 200
      IF (R(I).LT.0.AND.T(I).LT.0) GOTO 300
      IF (R(I).LT.0.AND.T(I).GT.0) GOTO 400
 100  DIR(I)=ATAN(T(I)/R(I))
      ALPA=(DIR(I))
      GAMA=PI/2-(ALPA)
      BETA=2*ATAN(0.9/CN)
      X1=CN*COS(ALPA)
      Y1=CN*SIN(ALPA)
      X2=0.9*COS(GAMA)
      Y2=0.9*SIN(GAMA)
      X3=(RD-CN)*COS(ALPA)
```

A4. Stereographic projection of Vibration vectors

```
            Y3=(RD-CN)*SIN(ALPA)
            CALL POSITN(-X1,-Y1)
C           CALL ARC(X2,-Y2,(BETA*180/PI))
            CALL PTPLOT(X3,Y3,1,1,245)
            CALL PLOTNI(X3+0.13,Y3,I+45)
            GOTO 10
  200       DIR(I)=2*PI-ATAN(T(I)/R(I))
            ALPA=(DIR(I))
            GAMA=(PI/2-(ALPA))
            BETA=2*ATAN(0.9/CN)
            X1=CN*COS(ALPA)
            Y1=CN*SIN(ALPA)
            X2=0.9*COS(GAMA)
            Y2=0.9*SIN(GAMA)
            X3=(RD-CN)*COS(ALPA)
            Y3=(RD-CN)*SIN(ALPA)
            CALL POSITN(-X1,Y1)
C           CALL ARC(-X2,-Y2,(BETA*180/PI))
            CALL PTPLOT(X3,-Y3,1,1,245)
            CALL PLOTNI(X3+0.13,-Y3,I+45)
C           CALL JOIN((X3-I),(Y3-I))
            GOTO 10
  300       DIR(I)=2*PI+ATAN(T(I)/R(I))
            ALPA=(DIR(I))
            GAMA=(PI/2-(ALPA))
            BETA=2*ATAN(0.9/CN)
            X1=CN*COS(ALPA)
            Y1=CN*SIN(ALPA)
            X2=0.9*COS(GAMA)
            Y2=0.9*SIN(GAMA)
            X3=(RD-CN)*COS(ALPA)
            Y3=(RD-CN)*SIN(ALPA)
            CALL POSITN(X1,Y1)
C           CALL ARC(-X2,Y2,(BETA*180/PI))
            CALL PTPLOT(-X3,-Y3,1,1,245)
            CALL PLOTNI(-X3+0.13,-Y3,I+45)
C           CALL JOIN((X3-I),(Y3-I))
            GOTO10
  400       DIR(I)=2*PI-ATAN(T(I)/R(I))
            ALPA=(DIR(I))
            GAMA=(PI/2-(ALPA))
            BETA=2*ATAN(0.9/CN)
            X1=CN*COS(ALPA)
            Y1=CN*SIN(ALPA)
            X2=0.9*COS(GAMA)
            Y2=0.9*SIN(GAMA)
            X3=(RD-CN)*COS(ALPA)
            Y3=(RD-CN)*SIN(ALPA)
            CALL POSITN(X1,-Y1)
C           CALL ARC(X2,Y2,(BETA*180/PI))
            CALL PTPLOT(-X3,Y3,1,1,245)
            CALL PLOTNI(-X3+0.13,Y3,I+45)
C           CALL JOIN((X3-I),(Y3-I))
            GOTO 10
C
  60        DIP(I)=PI+ATAN(V(I)/RE(I))
```

A4. Stereographic projection of Vibration vectors

```
      CN=0.9*TAN(DIP(I))
      RD=0.9/COS(DIP(I))
      CALL LINCOL(3)
      CALL BROKEN(8,5,8,5)
      IF (R(I).GT.0.AND.T(I).GT.0) GOTO 110
      IF (R(I).GT.0.AND.T(I).LT.0) GOTO 220
      IF (R(I).LT.0.AND.T(I).LT.0) GOTO 330
      IF (R(I).LT.0.AND.T(I).GT.0) GOTO 440
110   DIR(I)=ATAN(T(I)/R(I))
      ALPA=PI+(DIR(I))
      GAMA=PI/2-(ALPA)
      BETA=2*ATAN(0.9/CN)
      X1=CN*COS(ALPA)
      Y1=CN*SIN(ALPA)
      X2=0.9*COS(GAMA)
      Y2=0.9*SIN(GAMA)
      X3=(RD-CN)*COS(ALPA)
      Y3=(RD-CN)*SIN(ALPA)
      CALL POSITN(X1,Y1)
C     CALL ARC(-X2,Y2,(BETA*180/PI))
      CALL PTPLOT(X3,Y3,1,1,255)
      CALL PLOTNI(X3+0.13,Y3,I+45)
      GOTO 10
220   DIR(I)=2*PI-ATAN(T(I)/R(I))
      ALPA=PI+(DIR(I))
      GAMA=(PI/2-(ALPA))
      BETA=2*ATAN(0.9/CN)
      X1=CN*COS(ALPA)
      Y1=CN*SIN(ALPA)
      X2=0.9*COS(GAMA)
      Y2=0.9*SIN(GAMA)
      X3=(RD-CN)*COS(ALPA)
      Y3=(RD-CN)*SIN(ALPA)
      CALL POSITN(X1,-Y1)
C     CALL ARC(X2,Y2,(BETA*180/PI))
      CALL PTPLOT(X3,-Y3,1,1,255)
      CALL PLOTNI(X3+0.13,-Y3,I+45)
      GOTO 10
330   DIR(I)=2*PI+ATAN(T(I)/R(I))
      ALPA=PI+(DIR(I))
      GAMA=(PI/2-(ALPA))
      BETA=2*ATAN(0.9/CN)
      X1=CN*COS(ALPA)
      Y1=CN*SIN(ALPA)
      X2=0.9*COS(GAMA)
      Y2=0.9*SIN(GAMA)
      X3=(RD-CN)*COS(ALPA)
      Y3=(RD-CN)*SIN(ALPA)
      CALL POSITN(-X1,-Y1)
C     CALL ARC(X2,-Y2,(BETA*180/PI))
      CALL PTPLOT(-X3,-Y3,1,1,255)
      CALL PLOTNI(-X3+0.13,-Y3,I+45)
      GOTO10
440   DIR(I)=2*PI-ATAN(T(I)/R(I))
      ALPA=PI+(DIR(I))
      GAMA=(PI/2-(ALPA))
```

A4. Stereographic projection of Vibration vectors

```
      BETA=2*ATAN(0.9/CN)
      X1=CN*COS(ALPA)
      Y1=CN*SIN(ALPA)
      X2=0.9*COS(GAMA)
      Y2=0.9*SIN(GAMA)
      X3=(RD-CN)*COS(ALPA)
      Y3=(RD-CN)*SIN(ALPA)
      CALL POSITN(-X1,Y1)
C     CALL ARC(-X2,-Y2,(BETA*180/PI))
      CALL PTPLOT(-X3,Y3,1,1,255)
      CALL PLOTNI(-X3+0.13,Y3,I+45)
      GOTO 10
 10   CONTINUE
      RETURN
      END
C
      SUBROUTINE DOILY(PI,RAD,I)
C
      DO 20 I=1,4
      THETA=2*PI*I/4
      X=0.9*COS(THETA)
      Y=0.9*SIN(THETA)
      CALL FULL
      CALL POSITN(0.89*X,0.89*Y)
      CALL JOIN(X,Y)
 20   CONTINUE
      RETURN
      END
C
      SUBROUTINE PPVS(N)
      COMMON/C/ R(100), T(100), V(100)
      CALL THICK(2)
      CALL PLOTCS(1.14,1.0,'SET      R        T        V')
      CALL THICK(1)
      DO 30 I=1,N
      CALL PLOTNI(1.25,0.9-I*0.1,I+45)
      CALL PLOTNF(1.5,0.9-I*0.1,R(I),2)
      CALL PLOTNF(1.9,0.9-I*0.1,T(I),2)
      CALL PLOTNF(2.3,0.9-I*0.1,V(I),2)
 30   CONTINUE
      RETURN
      END
      END
```

Appendix A5
A5. Laboratory tets on the soil and brickwork of the Flitwick site

This Appendix includes information of the Flitwick site in the following terms:

A5.1 Borehole Logs

A5.2 Soil mechanics tests

- A5.2.1 Moisture contents
- A5.2.2 Particle size distribution
- A5.2.3 Shear box tests
- A5.2.4 Quick undrained triaxial tests

A5.3 Brick panel tests

Location	Flitwick	**Ground Level**	10.0 nom.
Carried out for	Durham University	**Diameter**	150mm
Borehole No.	one	**Date**	06.08.1988

DESCRIPTION	REDUCED LEVEL	LEGEND	SAMPLE	DEPTH	THICKNESS	
Soft grey-brown silty sandy clay	7.50		B U4 J	0.5 1.0-1.45 1.5	2.50	
Medium dense yellow sandy gravel with flints and cobbles	6.30		B CPT	3.0 3.0-3.45	1.20	CPT 57 blows
Yellow sand	5.80		B	4.0	0.50	
Dense light grey sand with silty bands			SPT	6.10-6.55		SPT 113 blows/270 mm
			B	7.0	4.10	
			SPT	7.90-8.35		SPT 28 blows - base of b.h. liquefied
End of b.h.	1.60					
Water strike 2.70 m depth, rising to 1.70 m						

Appendix A5.1.1 Borehole log information, BH-1

Location	Flitwick	Ground Level	10.0 nom.
Carried out for	Durham University	Diameter	150mm
Borehole No.	two	Date	06.08.1988

DESCRIPTION	REDUCED LEVEL	LEGEND	SAMPLE	DEPTH	THICKNESS	
Soft grey brown silty sandy clay with some peat	7.90		B U4 J	0.5 1.0-1.4 1.5	2.10	
Loose yellow clayey sand and gravel	7.00		B CPT	2.5 3.0-3.45	0.90	CPT 32 blows
Loose yellow sand gravel and flints	6.20		B	3.4	0.80	
Loose yellow sand	5.10		B	4.3	1.10	
Dense light grey sand with silty bands			SPT B SPT	6.0-6.45 7.0 8.2-8.65	3.70	SPT 80 blows SPT 90 blows
End of b.h.	1.35					
Water strike at 3.00 m depth, rising to 1.40 m						

Appendix A5.1.2 Borehole log information, BH-2

Location	Flitwick	**Ground Level**	10.0 nom.
Carried out for	Durham University	**Diameter**	150mm
Borehole No.	three	**Date**	06.08.1988

DESCRIPTION	REDUCED LEVEL	LEGEND	SAMPLE	DEPTH	THICKNESS	
Soft grey brown silty sandy clay with peat	7.40		B U4 J	0.6 1.0-1.45 1.5		
Loose to medium yellow sand gravel and flints	5.60		B CPT B	2.8 3.0-3.45 3.7		CPT 39 blows
Loose light grey sand	4.50					
Dense light grey sand with silty bands			SPT B SPT	6.0-6.45 6.7 7.90- 8.35		SPT 77 blows SPT 47 blows (some liquefaction)
End of b.h.	1.65					
Water strike at 2.80 m depth, rising to 1.30 m						

Appendix A5.1.3 Borehole log information, BH-3

Appendix A5.2.1

Results of the Moisture Content Tests

Borehole no.	Sample no.	Depth (m)	U100 or Bag	Moisture Content (%)
1	2	1.0-1.45	U100	22.7
	4	2.5-3.7	Bag	7.1
	4	2.8-3.7	Bag	10.2
	5	3.7-4.7	Bag	22.0
	7	4.2-7.9	Bag	27.6
2	2	1.0-1.45	U100	18.3
	4	2.0-3.0	Bag	14.3
	5	3.0-3.8	Bag	8.9
	6	3.8-4.9	Bag	17.8
	7	4.9-6.0	Bag	22.1
	9	6.0-8.2	Bag	23.3
3	2	1.0-1.45	U100	33.0
	4	2.6-3.0	Bag	11.9
	5	3.0-4.4	Bag	10.2
	6	4.4-5.5	Bag	23.6
	8	5.5-7.9	Bag	21.8

Appendix A5.2.2

Results of the Particle Size Distributions

Borehole no.	Sample no.	Depth (m)	$< 60\mu m$ %	$60\mu m - 2mm$ %	$2mm - 60mm$ %	$60mm >$ %
1	4	2.5-3.7	2	38	60	0
	4	2.8-3.7	3	51	46	0
	5	3.7-4.7	6	91	3	0
	7	4.2-7.9	5	94	1	0
2	4	2.0-3.0	9	49	42	0
	5	3.0-3.8	2	54	44	0
	6	3.8-4.9	1	98	1	0
	7	4.9-6.0	5	91	4	0
	9	6.0-8.2	6	92	2	0
3	2	1.0-1.45	26	64	10	0
	4	2.6-3.0	11	45	44	0
	5	3.0-4.4	5	39	56	0
	6	4.4-5.5	2	95	3	0
	8	5.5-7.9	5	94	1	0

Appendix A5.2.3

Results of the Shear Box Tests

Borehole No.	Sample No.	Depth (m)	c (kN/m^2)	ϕ degrees	% passing 2mm
1	4	2.5-3.7	0	44°	40
	4	2.8-3.7	—	—	—
	5	3.7-4.2	0	37°	97
	7	4.2-7.9	0	38°	99
2	4	2.0-3.0	0	41°	58
	5	3.0-3.8	0	42°	56
	6	3.8-4.9	0	37°	99
	7	4.9-6.0	0	38°	96
	9	6.0-8.2	0	39.5°	98
3	4	2.6-3.0	—	—	—
	5	3.0-4.4	0	36°	44
	6	4.4-5.5	0	40°	97
	8	5.5-7.9	0	35°	99

Titles	Borehole [1] sample 2, depth 1.0-1.45m				Borehole [2] sample 2, depth 1.0-1.45m			Borehole [3] sample 2, depth 1.0-1.45m			
Normal Pressure ($kN.m^{-2}$)	70	115	140	210	70	140	210	70	115	140	210
Moisture Content (%)	22.7				18.3			33.0			
Bulk Desity ($kg.m^{-3}$)	2139	1954	2015	1994	2132	2222	2158	1930	1712	1947	1612
Stress ot Failure ($kN.m^{-2}$)	44	38	38	36	60	70	68	27	17	31	19
Strain at Failure	7	20	20	20	20	20	20	20	20	18	20
Final M.C. (%)	19.7	26.8	24.4	25.8	17.3	15.0	16.3	19.8	45.6	27.1	44.7
Cohesion (c) ($kN.m^{-2}$)	34.0				19.0			15.0			
Friction (ϕ^o)	0^o				0^o			0^o			

Appendix A5.2.4 Quick Undrained Triaxial Tests

Appendix A5.3

Brick Panel Tests

A small brickwork panel some 510mm wide, 210mm (three course) high, and 100mm (half brick) in thickness, was tested for bending strain, broadly in accordance with Appendix 3 of BS-5628:part 1,(1978). The panel was cast into steel channels with extensions so that a four point test bend test could be carried out over a 700mm span.

The moment/tensile strain curve shows failure at a strain approximately 30×10^{-6}, static test. The dynamic strain capacity would be expected to be higher.

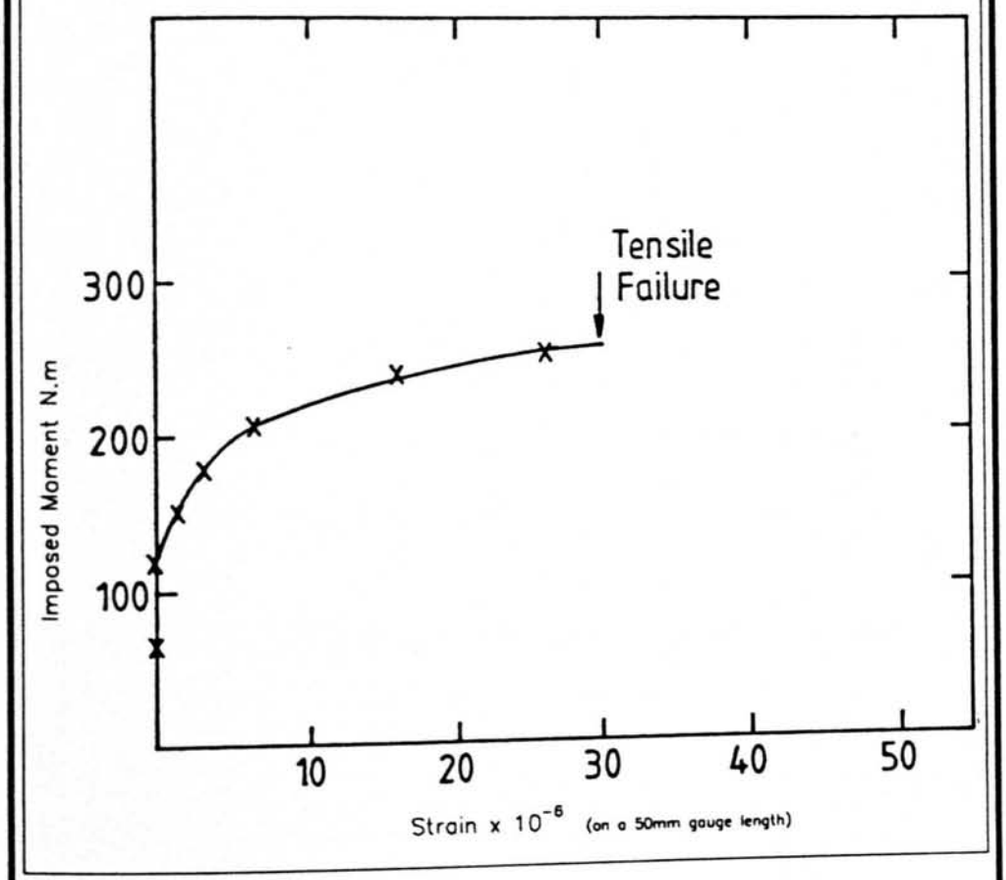

Figure (A5.3.1) Moment–surface strain behaviour of brickwork tested to bending failure *after Selby (1989)*

Appendix A6

A6. Graphical Presentation of Attenuation Records

This Appendix present graphically the attenuation equations given in Chapter eight. With respect to different types of hammers, piles, ground conditions and pile toe-depths, the vibration records are plotted in nine different figures.

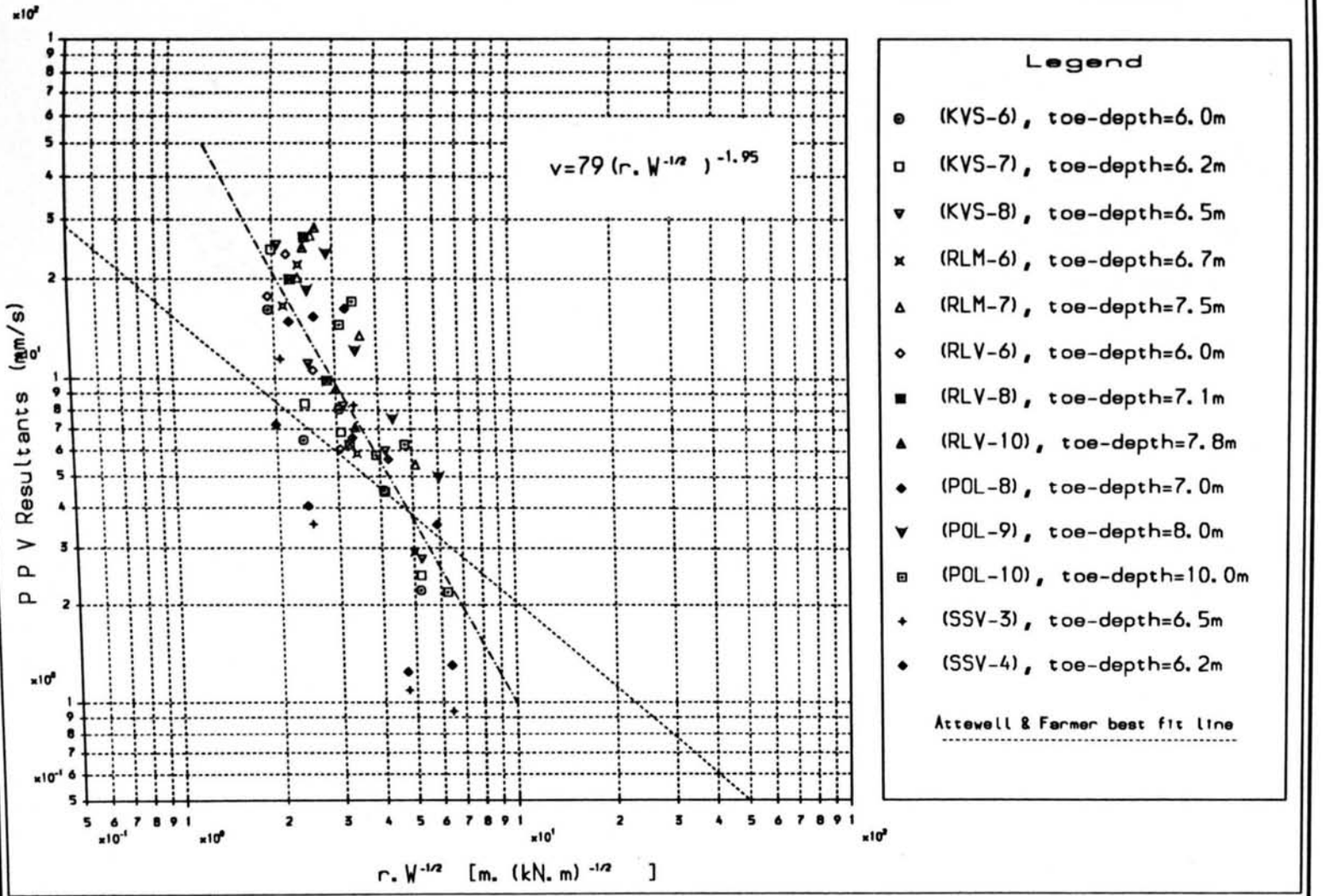

Figure (A6. 1) Vibrodriver, Sheet-pile, Depth=6-10m

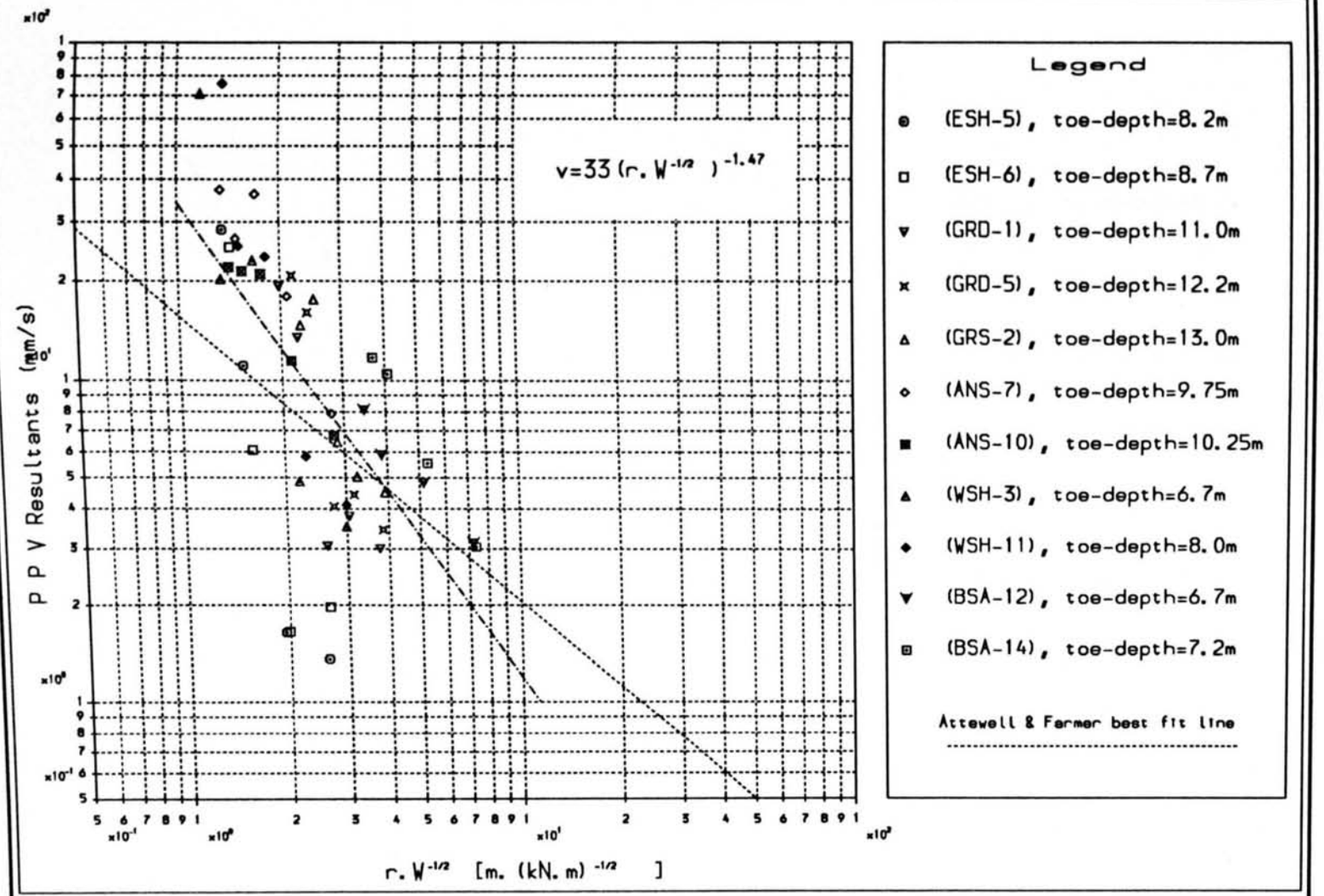

Figure (A6.2) Impact-hammers, Sheet-pile, Depth=6-10m

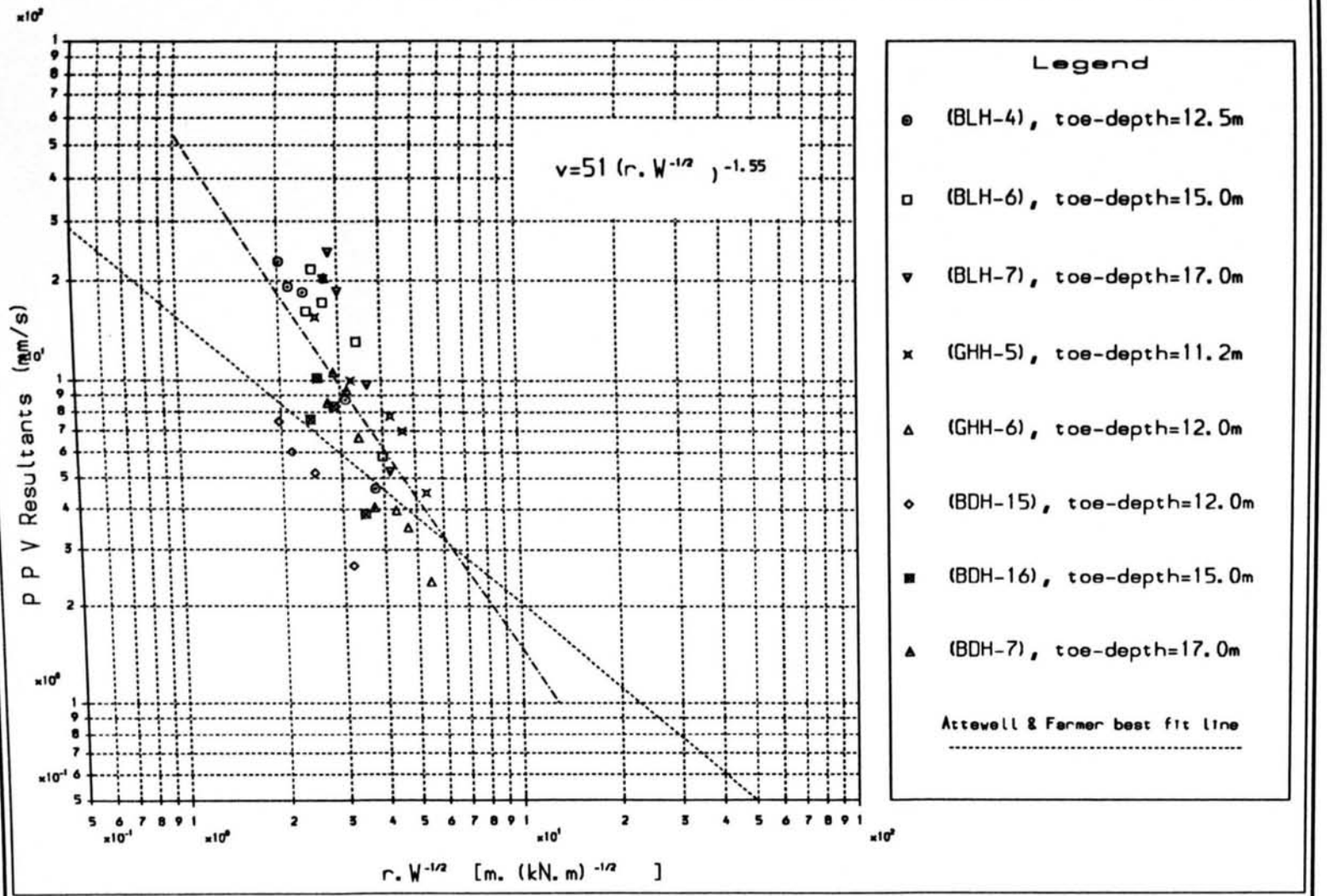

Figure (A6.3) Hydraulic-hammer, H-pile, Depth=10-17m

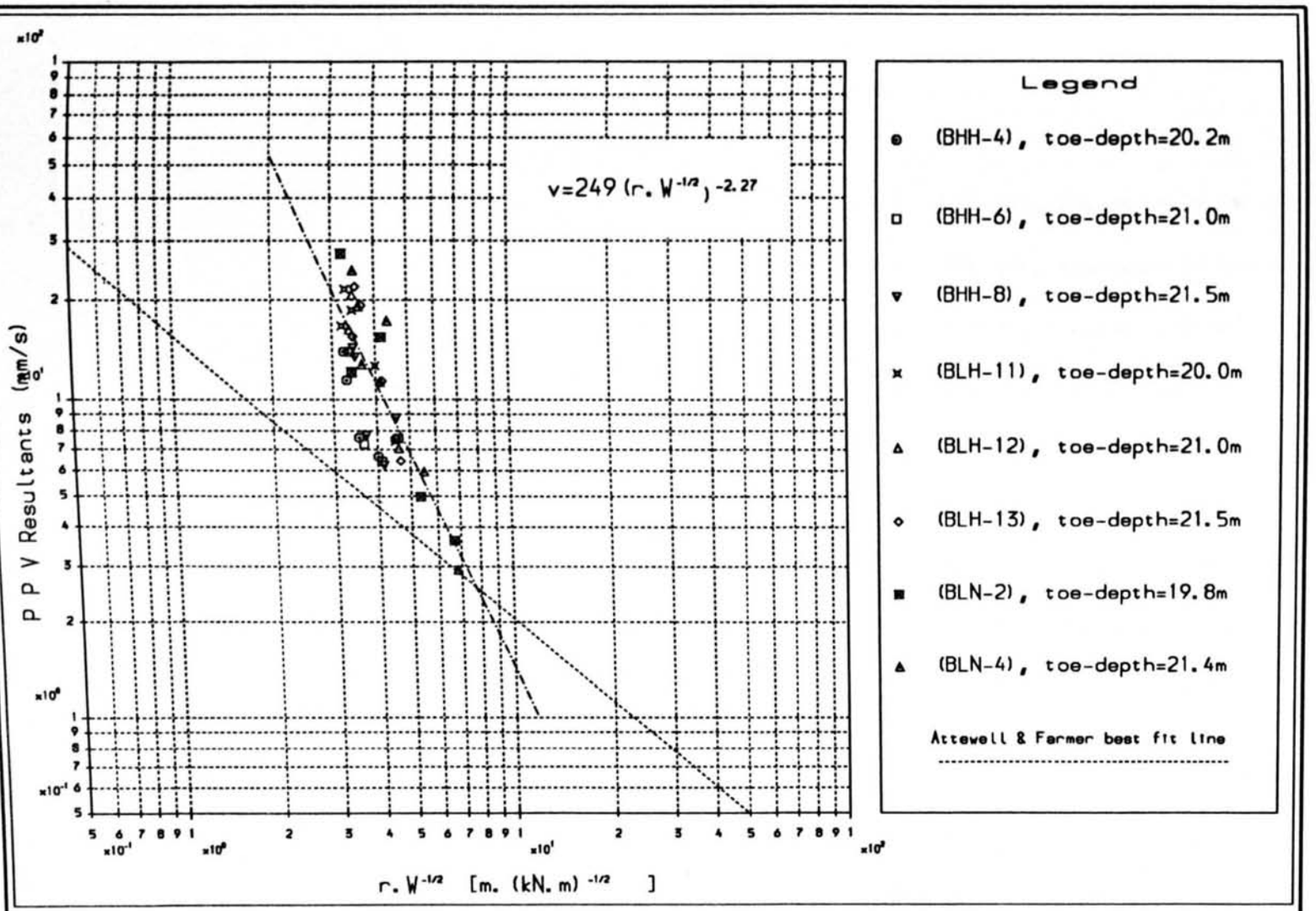

Figure (A6.4) Hydraulic-hammer, H-pile, Depth=19-24m

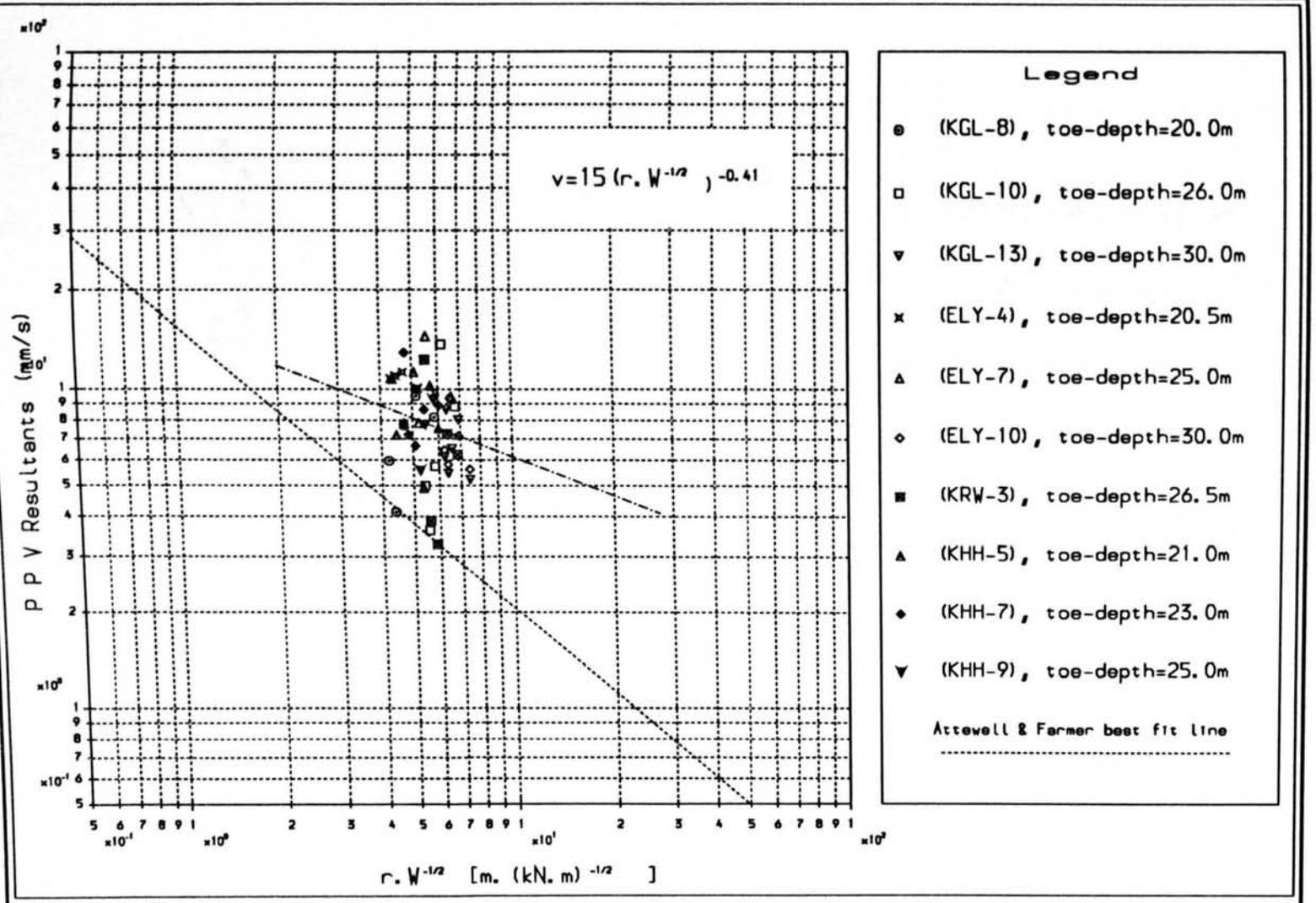

Figure (A6.5) Hydraulic-hammer, H-pile, Depth=20-30m

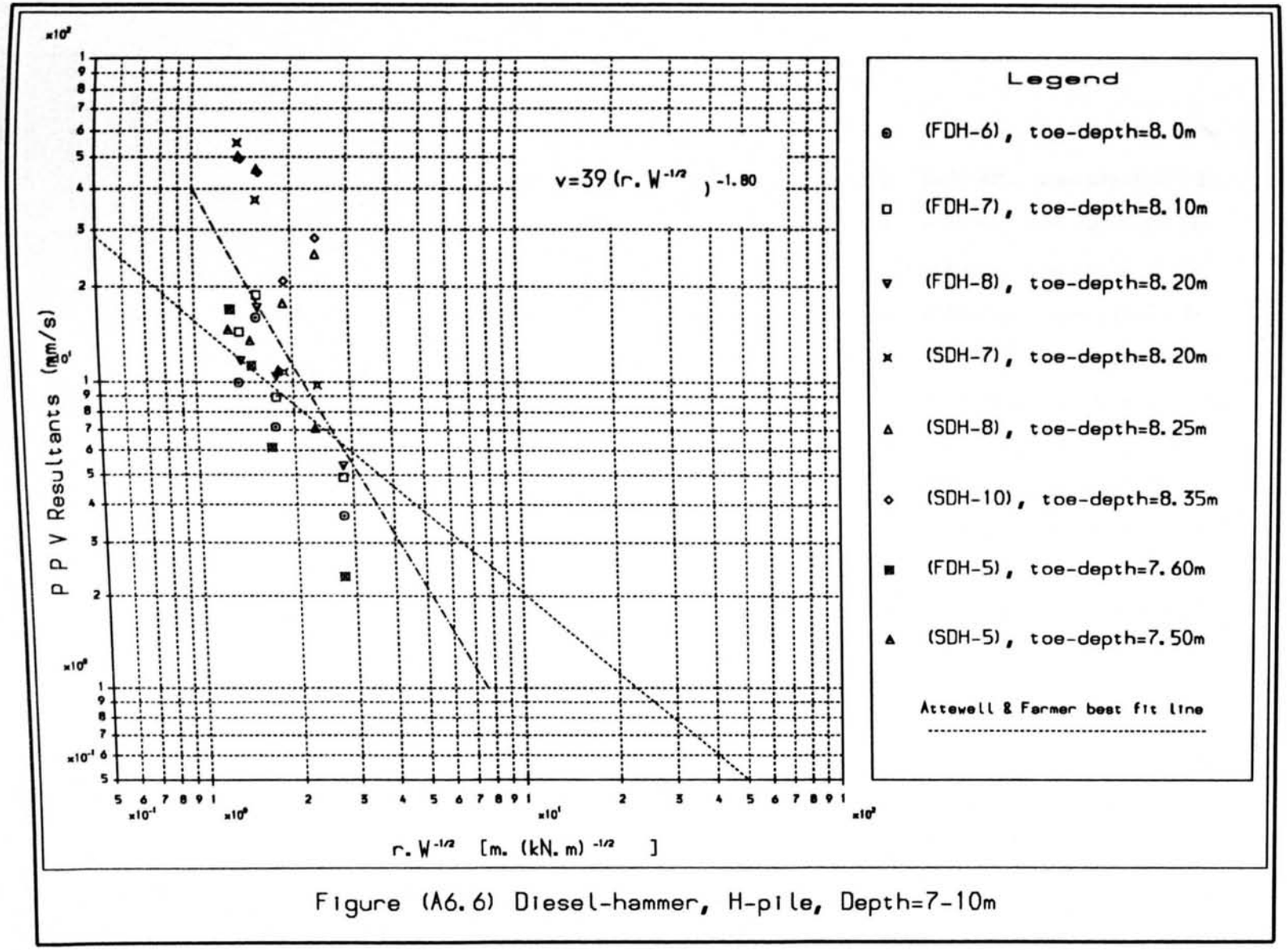

Figure (A6.6) Diesel-hammer, H-pile, Depth=7-10m

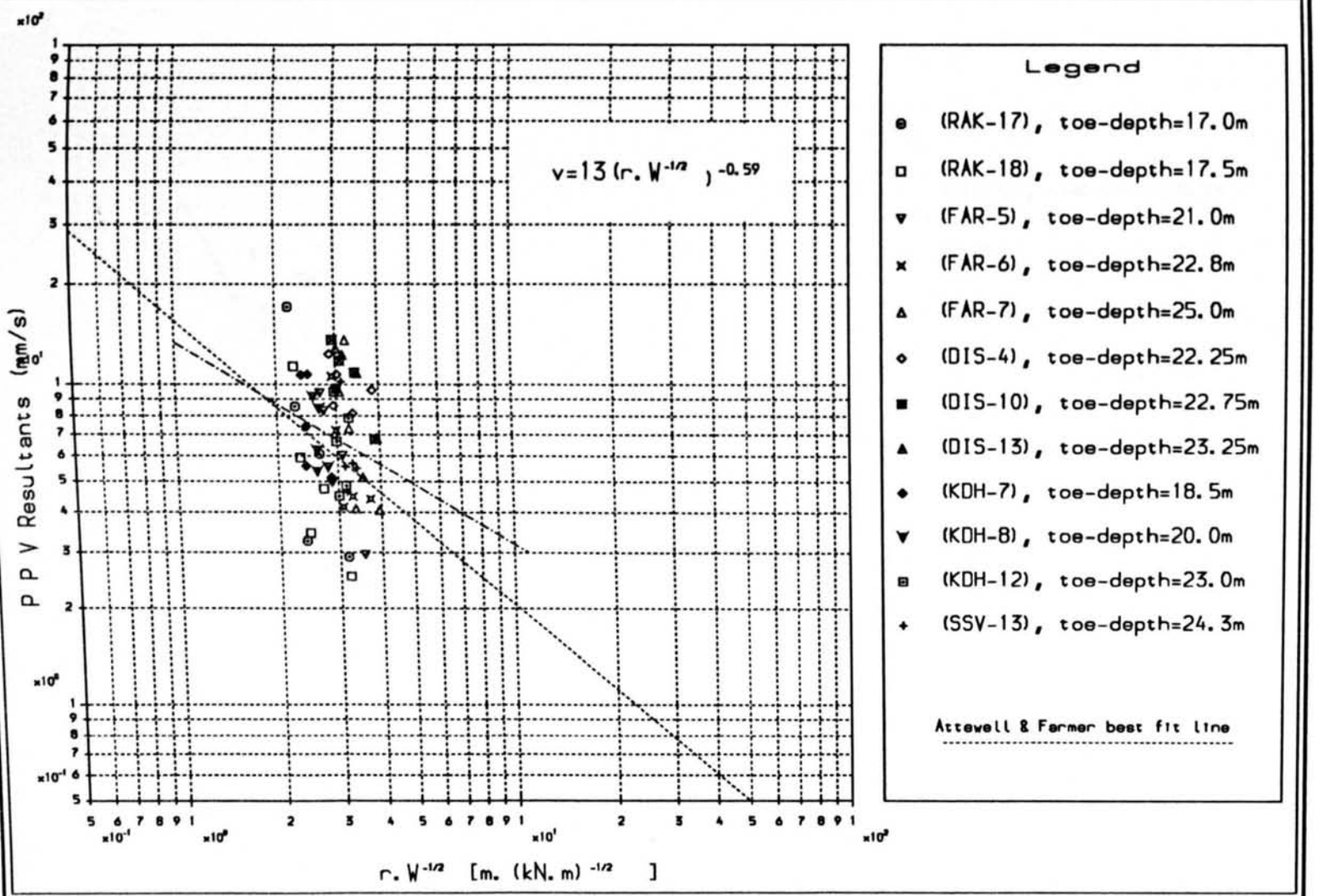

Figure (A6.7) Diesel-hammer, H-pile, Depth=15-25m

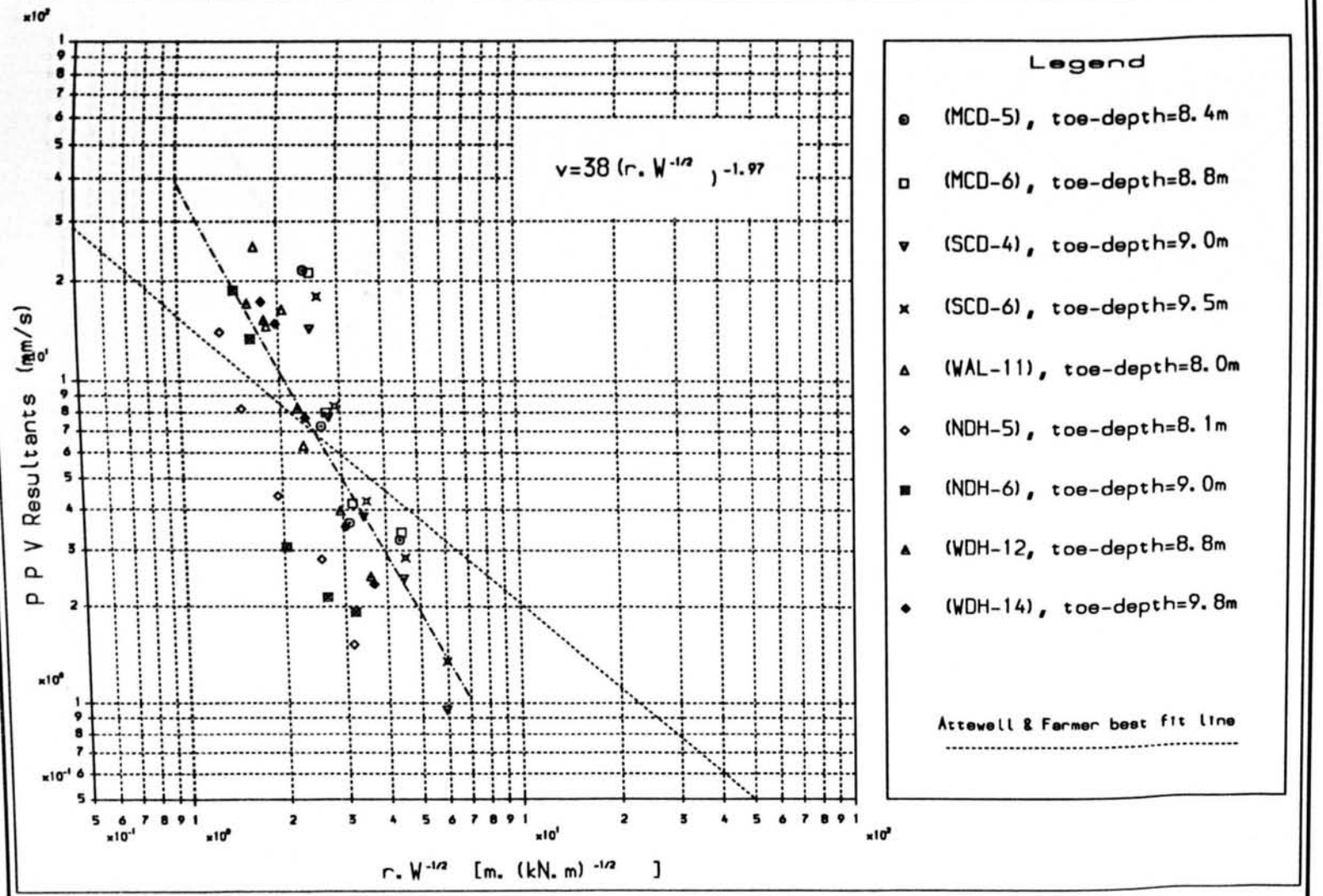

Figure (A6.8) Drop-hammer, End-bearing-piles, Depth=7-10m

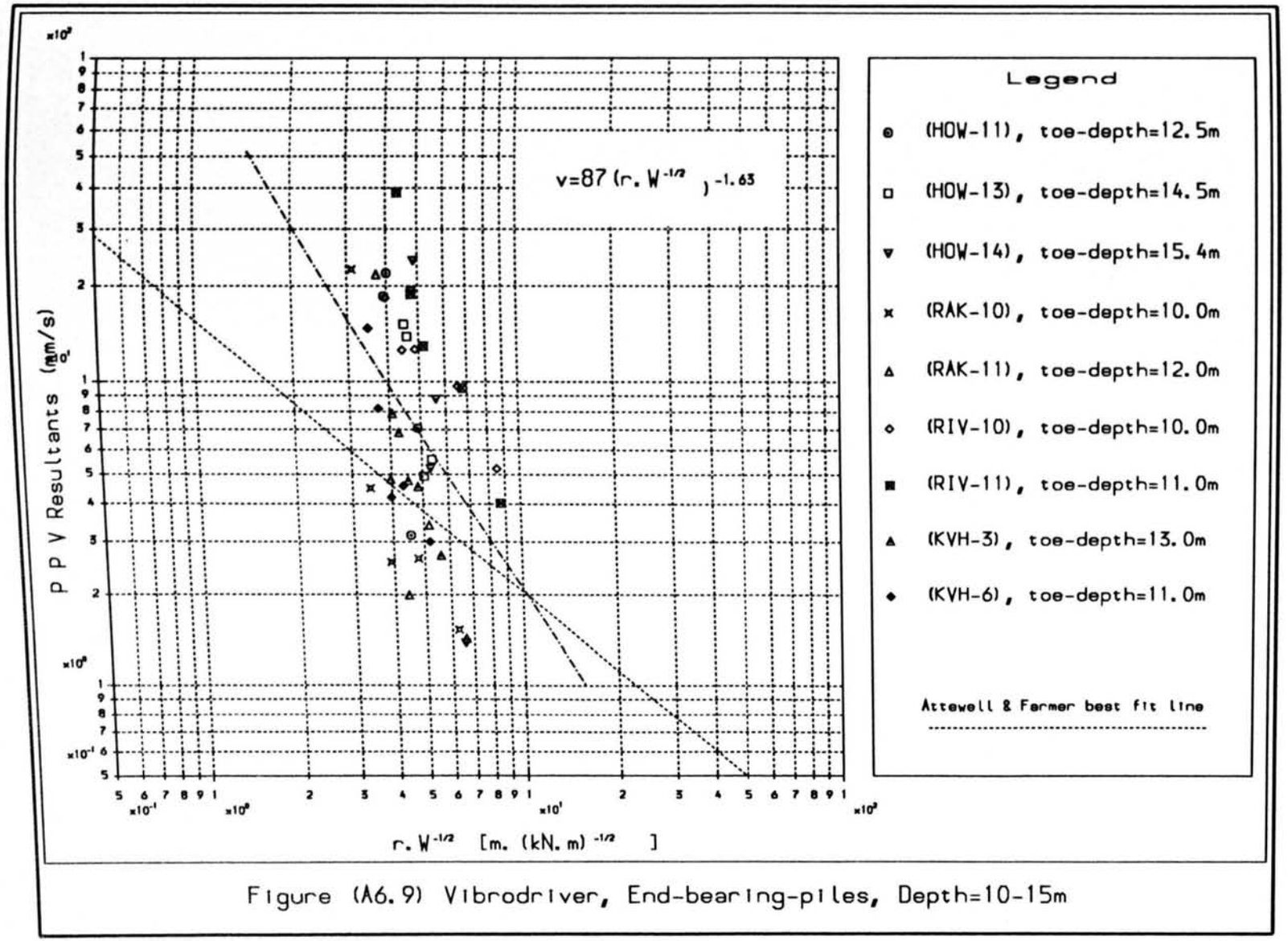

Figure (A6.9) Vibrodriver, End-bearing-piles, Depth=10-15m